Al-Mustansiriya University

COLLEGE OF SCIENCE

AL - MUSTANSIRIYA JOURNAL OF SCIENCE

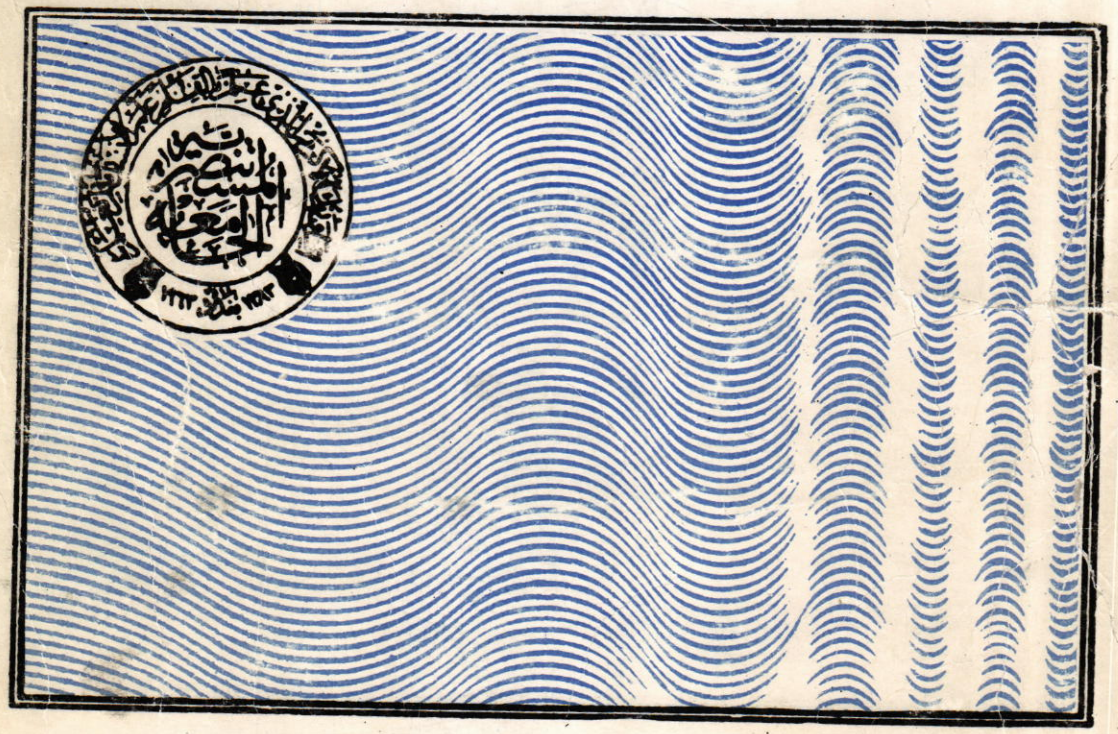

A Scientific periodical issued by College of Science, Al-Mustansiriya University.

All correspondence should be addressed to:

The Secretary Editor, Al-Mustansiriya Journal of Science

College of Science, Al-Mustansiriya University.

Al-Waziriya, Baghdad, Iraq

Telex: 2566 (MUSBAD IK)

Phone: 4168491 or 4168500-1 (Ext-276)

Volume: 6 No. 1

Year: 1996

AL-MUSTANSIRIYA JOURNAL OF SCIENCE

INSTRUCTIONS FOR AUTHORS

1. The journal accepts manuscripts in Arabic and English languages, which had not been published before.

2. Author (s) has to introduce an application requesting publication of his manuscript in the journal. Three copies (one original) of the manuscript should be submitted. They should be written with double spacings. A margin of about 2.5 cm should be left on both sides. A4 white papers of good quality should be used.

3. The title of the manuscript together with the name and address of the author (s) should be typed on a separate sheet in both Arabic and English. Only manuscript's title to be typed again with the manuscript.

4. For manuscripts written in English, full name(s) of author(s) and only first letters of the words (except prepositions and auxiliaries) forming title of the manuscript should be written in capital letters. Author(s) address(es) to be written in small letters.

5. Both Arabic and English abstracts are required for each manuscript. They should be typed on two separate sheets (not more then 250 words each).

6. Figures and illustrations should be drawn using black China ink on tracing papers. Two photocopies (plus original) of each diagram should be submitted. Captions to figures should be written on separate papers. The same information should not be repeated in tables unless it is necessary and required in the discussion.

7. References should be denoted by a number between two brackets on the same level of the line and directly at the end of the sentence. A list of references should be given on a separate sheet of paper, following the international style for names and abbreviations of journals.

8. Whenever possible, research papers should follow this pattern: INTRODUCTION, EXPERIMENTAL (MATERIALS AND METHODS), RESULTS, DISCUSSION and REFERENCES. All written in capital letters at the middle of the page, without numbers or underneath lines.

9. The following pattern should be followed upon writing the references on the reference sheet: Surname(s), initials of author(s), title of the paper, name or abbreviation of the journal, volume, number, pages and (year). For books give the author(s) name(s), the title, edition, pages, publisher, place of publication and (year).

Volume. 6 Year : 1995

المحتويات

البحوث الانكليزية

Page no.

البحوث العربية رقم الصفحة

Al-Mustansiriya J. Sci Vol. 6 , No. 1 , 1996

Sphere Bundles over Spheres

AMAAL I. AL-ATTAR AND BASSAM G. B. AWBI
Department of Mathematics, College of Science, AL-Mustansiriah University, Baghdad, IRAQ.
(Recieved 26 Dec. 1992; Accepted 18 June, 1994)

الخلاصة

اذا كان Mn منطوياً مغلقاً المس ومتوا شجاً من شدة 7 , $u\geq 17$ وكان $P_2(M^u)\neq 0$ فتوجد عائلة (M^u_{α}) معدودة عند منتهية من المنطويات الملساء والمغلقة غير المتكافئة تفاضلياً والمختلفة هوموتوبياً فيما بينها لكن كل عنصرين فيها (M^u_{α} متكافئة في صنف المنطويات الملساء. ($M^n\neq$

ABSTRACT

The objective of this work is to prove that for each smooth closed 7-connected manifold M^n, with $p_2(M^n)\neq 0$ and $n\geq 17$, there exists a countably infinite family $\beta(\alpha)$ of smooth closed manifolds which are mutually non-diffeomorphic, in fact they have different homeotopy types but the connected sum of each with M^n are diffeomorphic. [where $P_2(M^n)$ is the second pontrjagin class of the manifold M^n].

INTRODUCTION

In [19] C.T.C. Wall asked whether subtraction is possible in the monoid of smooth oriented 2n-manifolds with connected sum. The answer is negative if n is even and he gave many examples.

In 1971 Goldstein and Lininger ([5]) proved that if M^n is smooth closed manifold with $W_1(M^n)\neq 0$, then $M^n \# S^1 \times S^{n-1}$ is diffeomoephic to $M^n\#k$, [where $W^1(M^n)$ is the first whitney class of the mnanifold M^n]. where K is the non-trivial (n-1)-sphere bundle over S^1. They also proved that $M^n\#S^2 \times S^{n-2} \equiv M^n \# K$, where K is the non-trivial (n-2)- sphere bundle over S^2, for a simply connected smooth closed manifold M^n with $W_2(M^n)\neq 0$, [Where $W_2(M^n)$ is the second Whitney class of the manifold M^n]. On the other hand in 1981 (in [15]) A.G. Naoum proved that M^n is a 3-connected smooth manifold, $n\geq 8$, with $P_1(M^n)\neq 0$, then $M^n \# S^4 \times S^{n-4} \equiv M^n \# \beta(\alpha)$ [where $P^1(M^n)$ is the first pontrjagin class of the manifold M^n]. for infinitely many $\alpha\varepsilon\ \Pi_3(SO(n-3))$ where $\beta(\alpha)$ is the (n-4) sphere bundle over S^4. With characteristic class α.

In this paper we will prove a result for a 7-connected closed smooth manifold M^n with $P^2(M^n)\neq 0$ and $n\geq 16$ (i.e $M^n \# S^8 \times S^{n-8} \equiv \beta(\alpha)$ where β is the (n-8) sphere bundle over S^8 with characteristic class α.

φ. 1 Canonical and twisted framing.

Let M^n be a 7- connected smooth closed n-manifold and $n\geq 16$. A framing $(F=(f_1,f_2,\ldots,f_{n-7}))$ of the normal bundle of a differentiably embedded 7-sphere S^7 in M^n is called canonical if there exists an 8-disk D8 differentiably embedded in M^n with boundary S^7 and the framing $f_1,f_2,\ldots,f_{n-8}$ can be extended to framing of the normal bundle of D^8.

A non-canonical framing is called twisted.

An embedding of S^7 with the framing of its normal bundle will be denoted by (S^7,F).

If $\alpha\varepsilon\ \Pi_7(SO(n-7))$, we shall denote by αF the framing induced from F by any map from S^7 to SO(n-7) representing α.

Remark 1.1

One can easily prove that:

1- If $\alpha 1$ is homotopic to $\alpha 2$ then $\alpha 1F$ is cononical if $\alpha 2F$ is canonical .

2- If g represents a generator of $(\Pi_7(SO(n-7))$ and if (S^7,F) is twisted , then (S^7,gF) is canonical. (For more detaile see [5]).

Theorem 1.2 :

Let M^n be a smooth closed 7-connected manifolds $n\geq 16$. and (S^7,F) be a canonical embedding.

Let $P_2(M^n)\neq 0$, Then for each non zero α in $\Pi_7(SO(n-7))$ We have $(S^7,\alpha F)$ is a twisted embedding.

Proof :

Suppose $(S^7,\alpha F)$ is not a twisted embedding, then it is canonical, So αF can be extended to the framing of the normal bundel of $D_+^8(D_+^8CD^8)$.

Since (S^7,F) is canonical, then F can be extended to the framing of the normal bundle of $D_-^8(D_-^8CD^8)$.

So we obtain a non-trivial normal bundel over $S^8(=D_+^8 \cup D_-^8)$ which is a contradiction to

$P_2(M^n)(=P_2(\tau(M^n))=P_2(n(S^8,M^n))=0$. ♦

Theorem 1.3:

For all $\alpha\varepsilon\Pi 7(So(n-7))$, $n\geq 17$ there exists a smooth 7-connected manifold M^n with canonical embedding (S^7,F) such that $(S^7,\alpha F)$ is also a cononical embedding.

Proof :

For all $\alpha\varepsilon\Pi 7(So(n-7))$, Let M^n be a smooth closed 7-connected manifold which contains a sphere S^8 such that $\upsilon(S^8,M^n)$ is the normal bundle of S^8 in M^n) with characteristic class $\alpha\varepsilon\Pi_7(So(n-8)[\Pi_7(So(n-8))\equiv\Pi_7(So(n-7))]$.

S^8 such that αF is also canonical, we denote such a manifold by $\beta(\alpha)$.

since $n\geq 17$, α has a cross section s, and $S(S^8)\subset\beta(\alpha)$ has a normal bundel characterized by α. Notice that one can easily see that theorem 1.2 is true for n=16 ♦

φ. 2 Construction and Connected Sum of manifold.

Let M^n, L^n be 7-connected oriented manifolds, $n\geq 16$, and (S^7,F),(S^7,F) be a canonical embedding in M^n, L^n respectively

such that $F=(f_1,,f_2,...,f_{n-7}),F=(f_1,,f_2,...,f_{n-7})$ are the framinings of the normal bundles of S^7 in M^n, L^n respectively. It is well known that the tubular neighbourhood of any smooth manifold in another is diffeomorphic to its normal bundle ([6]) so we identify M^n & L^n along the tubular neighbourhood of S^7 by the linear map K such that

$K(f_1)=f_1 \quad i=1,2,.....,n-7, \ \forall f_i \varepsilon F$
$K(x)=x \quad \forall x \varepsilon S^7$

Now by removing the interior of the tubular neighbourhoods and rounding the corners we get a smooth oriented manifold $(M^n,F)o(L^n,F)$ which depends only on the framings F and F´.

Remark 2.1:

1. Observe that if $\alpha \varepsilon \Pi_7(So(n-7), n\geq 16$ then $(M^n,F)o(L^n,F)\equiv(M^n,\alpha F)o(L^n,\alpha F')$ [Where $\equiv$ stands for diffeomorphic].

2. This binary operation is associative and commutative.

Theorem 2.2 :

Let M^n ,L^n be 7-connected oriented smooth and $(S^7,F),(S^7,F')$ be framings of the normal bundle of S^7 in M^n and L^n respectively . Then:

1. If (S^7,F) and (S^7,F') are both canonical or both twisted, then $(M^n,F)o(M^n,F')\equiv M^n\#L^n\#S^8XS^{n-8}$.

2. if one of them is canonical and the other is twisted, then $(M^n,F)o(L^n,F')\equiv M^n\#L^n\#\beta$

Where β is a non-trivial (n-8) sphere bundle over S^8[Where # stands for connected sum] ♦

Proof:

1. Embed D^8 in M^n and L^n, with boundary S^7, and take the tubular neighbourhood of each embedding. Then identify M^n and L^n as in the construction of manifolds if we take the connected sum of M^n and L^n and assume that the identification is taking place in the interior of these neighbourhoods, we deduce that

$(M^n,F)o(L^n,F')\equiv M^n\#L^n\#\lambda$ .....(1)

where $\lambda = (S^n,T)o(S^n,T)$ and is a canonically framed S^7 in S^n.

To prove $(S^n,T)o(S^n,T) \equiv S^8X\,S^{n-8}$ consider S^n as the boundary of $D^8 \times D^{n-7}$ and the canonical embedding $((S^n,T)$ is in the body of $D^8 \times D^{n-7}$.

Take tow copies of $D^8 \times D^{n-7}$ and identify the normal bundles of S^7 in S^n. Since $S^8=D^8 \cup D^8$. Then we get S^8XD^{n-7} From the identification. So $(S^n,T)o(S^n,T)$ is the boundary of $S^8 \times D^{n-7} = S^8 \times S^{n-8}$ .....(2) .From (1)and (2) we get $(M^n,F)o(L^n,F')\equiv M^n\#L^n\#S^8 \times S^{n-8}$.

Now suppose that both of them are twisted. By remark 1.1$(S^7,\alpha F)$ and $(S^7,\alpha F)$ are cononical where α is a genrator of $\Pi_7(So(n-7))$ and from the above proof we obtain the result. as in figure (1):-

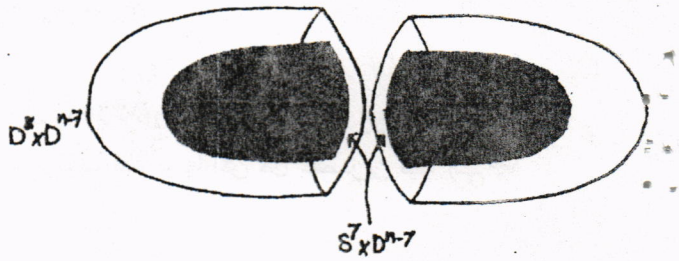

Figure 1

2. If one of them is cononical say F and F´ is twisted. then the proof is analogous to part one except that λ is $(S^n,T)o(S^n,T')$ where T is cononical and T´ is α T ($\alpha:S^7\to So(n-7)$, which a canonical framing so the identification is by a map which is not the identity. Thus we obtain a non-trivial sphere bundle over S^8.

If F is twisted and F´ is canonical then the proof follows from the commutativity of 'O)(Remark 2.1).

Theorem 2.3:

If each of M^n,L^n is a 7-connected manifold and each of F,F´ is canonical framing ($\alpha\varepsilon\prod_7(So(n-7))$. then $(M^n,\alpha F)o(L^n,F')\equiv M^n\#L^n\#\beta(\alpha)$.

proof:

Since each of M^n,L^n is a 7-connected manifold and S^8 is contained in each of them, let $\upsilon(S^8,M^n)$ and $\upsilon(S^8,L^n)$ be the normal bundles of S^8 in M^n and L^n respectively. Then α is the characteristic class of the normal bundle. And since F,F´ are canonical framing and $S^7 \subset S^8$.

Then α induces a canonical framing αF such that (S^7,F) and $(S^7,\alpha F)$ are cononical embedding and by 1.3. there exists a manifold $\beta(\alpha)$ which is the total space and by part two of 2.2 we obtain $(M^n,\alpha F)o(L^n,F')\equiv M^n\#L^n\#\beta(\alpha)$. ♦

Theorem 2.4:

Let M^n, α, $\beta(\alpha)$ be as above. Then $M^n\#\beta(\alpha)\equiv M^n\#S^8X\,S^{n-8}$.

proof:

Let(S^n,T) be canonical such that T is the canonical framing of S^7 in S^n. By part one of 2.2

$(M^n,F)o(S^n,T)\equiv M^n\#S^n\#S^8X\,S^{n-8}$
$\equiv M^n\#S^8X\,S^{n-8}$ .....(1)

(since S^n is the identity of the connected sum).

since each of F and T is canonical and $\alpha\varepsilon\prod_7(S_n(n-7))$ which is the characteristic class of the normal bundle of S_7 then αF and αT are canonical. And by 2.3

$(M^n,\alpha F)o(S^n,\alpha T)\equiv M^n\#S^n\#\beta(\alpha)$
$\equiv M^n\#\beta(\alpha)$ .....(2)

By Remark 2.1 (1)

$(M^n, \alpha F)o(S^n, \alpha T) \equiv (M^n, F)o(S^n, T)$ .....(3)

From (1),(2)&(3) we get the result . ♦

Let M^n be a 7-connected manifold, where $n \geq 16$.

Let $H_8(M^n, Z) = H_8(M^n) \cong \prod_8(M^n)$. Following Wall [19], We define a map $\gamma: H_8(M^n) \to \prod_7(So(n-8))$ as follows for each $x \varepsilon H_8(M)$, x can be represented by an embedding sphere S^8 in M^n such that α is the characteristic class of the normal bundle of S^8 in M^n ($\alpha \varepsilon \prod_7(So(n-8))$[13]).

put $\gamma(x) = \alpha$. If $n \geq 17$, then for each $x,y \varepsilon H_8(M^n)$, $\gamma(x+y) = \gamma(x) + \gamma(y)$. if n=16 Thus dim S^8=1/2 dim M^n and then $\gamma(x+y) + \gamma(x) + \gamma(y) + x.y\,\partial_{i8}$

Where x.y is the intersection number of x and y and ∂ is the boundary homorphism in the homotopy exact sequence.

Of fibration $S^8 = So(9) / So(8)$, and i8 is a generation of $\prod(S^8)$.

Proposition 2.5 :

Let M^n be a 7-connected manifold, $n \geq 17$, for each α is image γ we have :

$$M^n \# \beta(\alpha) \equiv M^n \# S^8 X\, S^{n-8}$$

The proof follows from theorem 2.4 ♦

Now the mapping $P: H_8(M^n) \to Z$ defined by $P(x) = P_2(y)$ $\forall X \varepsilon$ (M^n) (where P_2 is the second pontrjagin class of $\gamma(x)$) where P is a homomorphism (see[14]) and in fact it follows from [12] that image of P is a sub group of 6Z.

theorem 2.6 :

Let M^n be a smooth closd 7-connected manifold $n \geq 17$, and $P_2(M^n) \neq 0$.

For infinitely many α in $\prod_7(So(n-7))$, and if $P: H_8(M^n) \to Z$ is onto 6Z. then $M^n \# \beta(\alpha) \equiv M^n \# S^8 X S^{n-8}$ for all α in $\prod_7(So(n-7))$.

Proof :

Since $\alpha \varepsilon \prod_7(So(n-7))$, thus $\alpha \varepsilon \prod_7(So(n-8))$ and M^n is a smooth closed 7-connected manifold and by 1.3 there exists a mainfold $\beta(\alpha)$, for all α and $n \geq 17$. And by Th.2.4. $M^n \# \beta(\alpha) \equiv M^n \# S^8 X S^{n-8}$ for infinitely many α . If the map P is onto $6 \geq$ then $M^n \# \beta(\alpha) \equiv M^n \# S^8 X S^{n-8}$ for all α . ♦

3. Application

Let $P: S^{15} \to S^8$ be the Hopf fiber bundle (see[8]&[17]) and let $S^8 = KP^1$ (the Cayley line see [21]). The mapping cone of P is a 16-manifold which is called the Cayley projective plan (see [21]).

Proposition 3.1 :

KP^2 is 7-connected.

proof :

Since KP^2 is pathwise connected and by using the short exact sequence

$$0 \to S^8 \xrightarrow{i} KP^2 \xrightarrow{j} S^{15} \to 0 \to \ldots\ldots\ldots \to$$
$$\prod_{n+1}(S^{15}) \to \prod_n(S^8) \xrightarrow{i} \prod_n(KP^2) \xrightarrow{j} \prod_n(S^{15})$$

We can see that $\prod_n(KP^2) = 0$, i=1,...,7 and $\prod_8(KP^2) = Z$

So KP^2 is 7-connected.

Theorem 3.2:

$Kp^2 \# KP^2 \# (-KP^2) \equiv Kp^2 \# S^8 X S^8$

Proof :

Since KP^2 is a 7-connected 16-manifold, Embedd D^{16} differentiablly in KP^2 and $(-KP^2)$ and remove the interior of D^{16} we get $KP^2{}_0 = KP^2$-int D16. Where $KP^2{}_0$ is the mapping cylinder of P which is a disk bundle over S^8(see[17]).

By taking the connected sum of KP^2 and $(-KP^2)$ we get a sphere bundle over S^8 with characteristic class (say α) and we denote the new manifold by $\beta(\alpha)$.

(By 1.3)

Since KP^2 is connected thus by (Th.2.4) we get

$KP^2 \# \beta(\alpha) \equiv KP^2 \# S^8 X\, S^8$

ie.

$KP^2 \# KP^2 \# (-KP^2) \equiv KP^2 \# S^8 X\, S^8$ ♦

REFERENCES

[1] AL-Attar;A.I. , semi-free amooth actions of S1 on homotopy spheres, A Thesis of Doctor of Philosophy, September (1981).

[2] Borel; A., Topology of Lie groups and characteristic classes. Bull, Amer. Math. Soc., vol 61,pp.397-432, (1955).

[3] Conner; P.E. and Floyd; E.E., Differentiable periodic maps. Springer-Verlag, (1974).

[4] Dubrovin; B.A. and fomenko; A.T. and Norikov; S.P. modern geometry methods and applications. Springer-Verlag, New York Heidelberg Berlin, (1985).

[5] Goldstein; R.Z. and Lininger; L., A classification of 6-manifolds with free S´ actions, proceedings of the second conference on transformation groups, Lecture Notes in Mathematics, Vol 298, Springer-Verlag, PP.316-323.

[6] Guillemin; V. and Pollack; A. , Differential Topology, prentice-nall, Inc. Englewood Cliffs, New Jersey, (1974).

[7] Hirzebruch; F., Topologica methods in Algebraic geometry, 131, (1962).

[8] Husemoller; P. Fibre Bundles, Springer-Verlag, New York Heidelberg Berlin, (1966).

[9] James; I.M and Whitehead; J.H.C., On the homotopy theory of sphere- bundles over spheres, proc. london Math. Soc., vol. 4, (1954).

[10] Kervaire; M.A., A note on obstructions and characteristic classes, Amer. J. Math., vol 81, p 773-784, (1959).

[11] Kervaire; M.A., On the pontryagin classes of certain So(n)bundles over manifods, Amer. J. of Math., vol 80, P 632-683, (1958).

[12] Kervaire; M.A. and Milnor; J.W., Groups of homotopy spheres I, annals of math.; vol 71, No.3, P.504-537, (1963)

[13] Milnor; J.W. and Stasheff; J.D., Characterisitic classes, Princeton. University, Annals of Math. studies 76 Princeton Univ., press, (1974).

[14] Milnor ; J.W., Differentiable structures; on spheres, Amer. J. Math., vol 81, P 962-972, (1959).

[15] Naoum; A.G., Connected Sums of 3-Connected manifolds with sphere bundles over spheres, Iraqi J. Soc., vol 22,No, P 100-107, (1981).

[16] Raoul; B. and Loring ; W.T., Differential forms in Algebraic topology, Springer-Verlag, New York, Heidelberg, Berlin, (1982).

[17] Spanier; E.H., Algebraic Topology, McGraw-Hill New York, (1966).

[18] Steenrod; N., The Topology of Fibre Bundles, Press 9th Printing, Princteon Univ. (1974).

[19] Wall; C.T.C., Classification of (n-1)-connected 2n-manifolds, Annals of Math., vol. 75, No.1, P163-189, (1969).

[20] Wallace; A.H. , Differential Topology, first steps, University of Pennsylvania,(1968).

[21] Whitehead; G.W. , Elements of Homotopy Theory,Springer-Verlag, New York. Heidelberg. Berlin, (1978).

Al-Mustansiriya J. Sci Vol. 6, No. 1, 1996

On Rational Valued Characters of Z_3^n

MUHAMMED SERDAR KIRDAR and FUAD AL-HEETY
Department of Applied Science, University of Technology, Baghdad, Iraq.

(Recieved 27 Jun., 1994; Accepted 29 Mar, 1994)

الخلاصة

تم التوصل الى صيغة لحساب عناصر التجزئة الدورية للزمرة الكسرية لزمرة دوال الصفوف على زمرة المميزات العامة للزمرة Z_3^n حيث ان $n > 1$.

ABSTRACT

The cyclic decomposition of the factor group of the group of all rational valueed class function of Z_3^n (n>1) modulo the group of its generalized characters, was determined.

INTRODUCTION

Throughout this paper Z_3^n denotes the direct sum of the cyclic group Z_3 with itself n times. Each element of Z_3^n, and it's inverse generates the same cyclic subgroup, So Z_3^n can be partitioned into $(3^n+1)/2$ conjugate classes, called the Q-classes of Z_3^n, and they are:- the identity element o and $(3^n-1)/2$ classes represented by the n-tuples $\lambda_s^n=\{\lambda_s^n,-\lambda_s^n\}$.

Following [2], Let $Cf(Z_3^n,Z)$ be the group of all Z-valued class function of Z_3^n with constant values on the Q-classes, and $R(Z_3^n)$ be the group of all Z-valued vertual characters of Z_3^n, this group is generated by the characters $\phi j=Xj+\overline{Xj}$, where $Xj \in Z_3^n$, the dual of Z_3^n.

The factor group $Cf(Z_3^n,Z)/\overline{R}(Z_3^n)$ will be denoted by $K(Z_3^n)$, this is finitely generated Z-module.

We shall denote the square matrix whose rows and columns corresponding to the characters ϕj and the Q-classes of Z_3^n respectively by $\equiv(Z_3^n)$. For Q-class λ, we call f_λ the characteristic Q-function of λ if $f_\lambda(\lambda)=1$, $f_\lambda=0$ otherwise.

Our main purpose in this paper is the determination of cyclic decomposition of $K(Z_3^n)$ Which can be obtained by determining the invariant factors of $\equiv(Z_3^n)$.

RESULTS

We will first prove the following lemma.

LEMMA 1.

$k(Z_3^n)$ has only one cyclic subgroup of order 3^n.

Proof: Let f_o be the characteristic function on the identity class, and let $N:cf(Z_3^n) \to cf(Z_3^n, Z)/\langle f_o, \overline{R}(Z_3^n)\rangle$ be the natural homomorphism.

For Q-class λ, $N(f_\lambda)=f_\lambda+\langle f_o, \overline{R}(Z_3^n)\rangle$, but there exists $a \in Z^+$ such that $a.[2f_o-f_\lambda] \in \overline{R}(Z_3^n)$. This is exactly the character $(X_i+\overline{X}_i)\uparrow Z_3^n$, where X_i is non principal irreducible character of $\langle\lambda\rangle$.

Hence, $a.N(f_\lambda) \in \langle f_o, \overline{R}(Z_3^n)\rangle$ and $N(f_\lambda)$ has order a divisor of 3^{n-1}.

Hence $K((Z_3^n)/Z_3^n$ has no factor Z_3^n, but the coset $f_o+\overline{R}(Z_3^n)$ has order 3^n, hence the results.

For $i \geq 2$, the Q-classes of Z_3^i, are the i-tuples $\lambda_s^i \in Z_3^n$ with $\lambda_s^i+\lambda_t^i=0$ one way of writing and ordering them is as a uinon of finite sequences of n-tuples,

$$\{(\lambda_s^{i-1},0)\}_{s=1}^{(3^{i-1}+1)/2},$$

$$\{(\lambda_s^{i-1},1)\}_{s=1}^{(3^{i-1}+1)/2},$$

$$\{(\lambda_s^{i-1},2)\}_{s=2}^{(3^{i-1}+1)/2}$$

where λ_s^{i-1} are the (i-1) tuples corresponding to the Q-xlasses of Z_3^{i-1}.

Since $Z_3^n \cong Z_3^n$, so we can identify the row and the columns of $\equiv^*(Z_3^n)$ with the Q-classes, and suppose that they are arranged in the same order as above.

We now add 2 times column $(\lambda_1^{n-1}, 1)$ to first column, for each $2 \leq s \leq (3^{n-1}+1)/2$ add the sum of column $(\lambda_1^{n-1}, 1)$ and $(\lambda_1^{n-1}, 2)$ to column $(\lambda_1^{n-1}, 0)$. then, we perform similar operations on the rows of $\equiv(Z_3^n)$ except for the first row, we add row $(\lambda_s^{n-1}, 1)$ to it. then the matrix $\equiv^*(Z_3^n)$ will be reduced to the form

$$\begin{bmatrix} 3 \equiv (Z_3^{n-1}) & 0 \\ 0 & M_{n-1} \end{bmatrix},$$

where M_{n-1} is a $3^{n-1} \times 3^{n-1}$ matrix, and we obtain the following :

LEMMA 2. If $K(Z_3^n) = \oplus \sum_{i=0}^{n-1} Z_{3^i}^{a_i}$, then

$K(Z_3^n) = \oplus \sum_{i=1}^{n} Z_{3^i}^{a_{i-1}} \oplus H$, where H is the direct sum of cyclic Z-modules of orders the distinct invariant factors of M_{n-1}.

Another way of writing the representatives of Q-classes of Z_3^i, is

$$\{(\lambda_s^{i-1},0)\}_{s=1}^{(3^{i-1}+1)/2}.$$

$$\{(X_t,1)\}_{t=1}^{3^{i-1}}, \text{ where } X_t \text{ are the elements of } Z_3^{i-1} \text{ in anatural way of ordering.}$$

If we rearrange the rows and columns of M_{n-1} as in the second sequence, then M_{n-1} takes the block form

$$\begin{bmatrix} M_{n-2} & M_{n-2} & M_{n-2} \\ M_{n-2} & M_{n-2} & C_{n-2} \\ M_{n-2} & C_{n-2} & B_{n-2} \end{bmatrix},$$

where, for each $0 \le J \le n-2$

$$M_{j+1} = \begin{bmatrix} M_j & M_j & M_j \\ M_j & B_j & C_j \\ M_j & C_j & B_j \end{bmatrix},$$

$$B_{j+1} = \begin{bmatrix} B_j & B_j & B_j \\ B_j & C_j & M_j \\ B_j & M_j & C_j \end{bmatrix}, \text{ and}$$

$$C_{j+1} = \begin{bmatrix} C_j & C_{jj} & C_j \\ C_j & M_j & B_j \\ C_j & B_j & M_j \end{bmatrix}, \text{with } M_0=B_0=-1, C_0=2$$

Let

$$E_{j+1} = \begin{bmatrix} E_j & E_j & E_j \\ 0 & E_j & 0 \\ 0 & -E_j & E_j \end{bmatrix} \text{ and}$$

$$F_{j+1} = \begin{bmatrix} F_j & 0 & 0 \\ F_j & F_j & 2F_j \\ F_j & F_j & F_j \end{bmatrix} \text{ with } E_0=F_0=1.$$

Clearly, for $j \ge 0$

$M_j + B_j + C_j = 0$, (1)

and $\det(E_j)=1$, $\det(F_j)=(-1)^j$. (2)

$E_{j+1}\, M_{j+1}\, F_{j+1} =$

$$\begin{bmatrix} 3(E_j M_j F_j) & 0 & 0 \\ 0 & F_j(B_j+C_j)F_j & E_j(2B_j+C_j)F_j \\ 0 & 0 & E_j(C_j-B_j)F_j \end{bmatrix}$$

Since the rows of the two symmetric matrices M_j and B_j are exactly the same with some permuted order, and by (1), M_{j+1} is equivalent to the quasidiagonal matrix

$D[3(E_jM_jF_j), -(E_jM_jF_j), E_j(C_j-B_j)F_j]$ (3)

and we have $E_{j+1}(C_{j+1}-B_{j+1})F_{j+1}$ is equivalent to

$D[3E_j(C_j-B_j)F_j, -E_j(C_j-B_j)F_j, 3(E_jM_jF_j)]$ (4)

This imlies that the invariant factors of M_{n-1} are $\pm 3^j$, with $0 \le j \le n-2$. If we replace the ± 3 by the invariant x, we obtain a function F which associates with each M_j apolynomial of degree j,

$$F(M_j) = \sum_{r=0}^{j} a_r x^r,$$

Where a_r is the number of $\pm 3^r$ appearing in the rational canonical from of M_j.

Now, By (3) and (4),

$F(M_{j+1}) = (X+1)F(M_j) + F(C_j - B_j)$, (5)

and $F(C_j-B_j) = (X+1)F(C_{j-1}-B_{j-1}) + xF(M_{j-1})$. (6)

Form (5),

$F(C_{j-1}-B_{j-1}) = F(M_j) - (x+1)F(M_{j-1})$. (7)

Substituting in (6), we obtain,

$F(M_{j+1}) = 2(x+1)F(M_j) - (x+1)^2F(M_{j-1}) + xF(M_{j-1})$. (8)

and we give the following

LEMMA 3.

For $n \ge 0$, $F(M) = \sum_{i=0}^{n} i^n (x+1)^{n-1} \cdot x^{\{i\}}$,

where $\{i\} = \begin{cases} \frac{i}{2} \text{ if } & i = 0,2,4,6,\ldots \\ \frac{i+1}{2} \text{ if } & i = 1,3,5,7,\ldots \end{cases}$

Proof: $E_0M_0F_0 = -1$, so $F(M_0)=1$,
$E_1M_1F_1=D[-3,1,3]$, so $F(M_1)=2x+1=(x+1)+x$.
Assume the statement holds for $n\le k$.
Hence by (8)

$$F(M_{k+1})=2\sum_{i=0}^{k}\binom{k}{i}(x+1)^{k-i+1}x^{\{i\}} - \sum_{i=0}^{k-1}\binom{k-1}{i}(x+1)^{k-i+1}x^{\{i\}} + \sum_{i=0}^{k-1}\binom{k-1}{i}(x+1)^{k-i+1}x^{\{i\}+1}$$

The 3rd term can be rewritten as

$$\sum_{i=2}^{k+1}\binom{k-1}{i-2}(x+1)^{k-i+1}x^{\{i\}}$$

But for $2\le i\le k-1$,

$$2\binom{k}{i}-\binom{k-1}{i}+\binom{k-1}{i-2}=\binom{k+1}{i}$$

Hence

$$F(M_{k+1})=\sum_{i=0}^{k+1}\binom{k+1}{i}(x+1)^{n-1}.x^{\{i\}},$$

and we have the results stated.
Now

$$F(M_n)=\sum_{i=0}^{n}\sum_{m=0}^{n-i}\binom{n}{i}\binom{n-1}{m}x^{n-i+\{i\}-m},$$

put $n-i+\{i\}-m=r$, then the coefficient of x^r is

$$a_r=\sum_{i=0}^{n}\binom{n}{i}\binom{n-i}{(n-r)-(i-\{i\})} \quad (9)$$

Since the finite sequence,

$$\{i-\{i\}\}_{i=0}^{n}=\begin{cases}0,0,-1,-1,\ldots,\frac{n-2}{2},\frac{n-2}{2},\frac{n}{2}, & \text{if } n=0,2,4,6,\ldots\\ 0,0,-1,-1,\ldots,\frac{n-3}{2},\frac{n-1}{2},\frac{n-1}{2} & \text{if } n=1,3,5,7,\ldots\end{cases}$$

So (9) can be rewritten, as

$$a_r=\sum_{i=0}^{[n]}\left[\binom{n}{2i}\binom{n-2i}{(n-r)-i}+\binom{n}{2i+1}\binom{n-(2i+1)}{(n-r)-i}\right]$$

.....(10)

Where $[n]=\begin{cases}\frac{n}{2} & \text{if } n=0,2,4,\ldots.\\ \frac{n-1}{2} & \text{if } n=1,3,5,\ldots.\end{cases}$

Then we have

Theorem 4.

$$K(Z_3^n)=Z_3^n\oplus\sum_{r=0}^{n-1}Z_{3^r}^{r}, \text{ where}$$

$$\alpha_r=\sum_{k=(n-r-1)}^{n-1}\sum_{i=0}^{k}\left[\binom{k}{2i}\binom{k-2i}{(n-r-1)-i}+\binom{k}{2i+1}\binom{k-(2i+1)}{(n-r-r)-i}\right]$$

Proof: For $r < n$, it follows from lemma 2, that α_r is the sum of a_{r-j} in $F(M_{n-j-1})$, where $0\le j\le r$, Then by applying (10) together with lemma 1, we obtain the results stated.

REFERENCES

[1] Curtis,C. ; Reiner, I. Methods of Representation theory Vol.(1) A wiley-interscience publication, New York, (1981).

[2] Kirdar, M.S. on factor group of the Z-valued class function modulo the group of the generalized characters, thesis, University of Birmingham, (1982).

[3] Serre, J. P. Linear representations of finite groups springer-verlag (42), New York, (1977).

Al-Mustansiriya J. Sci Vol. 6 , No. 1 , 1996

Photostabilization of low density polyethylene by aromatic schiff bases

SALAH M. ALIWI*, FAUAD M. SAID AND BAN Y. AL-BANNA
Chemistry Department , College of Science, AL-Mustansiriah University, Baghdad, IRAQ.
(Recieved 20 Sep. 1993; Accepted 3 Nov, 1993)

الخلاصة

تم دراسة التثبيت والتجزئة الضوئية لخمسة انواع من رقائق البولي اثيلين واطئ الكثافة (بسمك ٢٠٠ مايكرون) تحتوي على مثبتات ضوئية مختلفة وهذه الرقائق هي :١. بولي اثيلين خالٍ من المثبتات (PE)٢. بولي اثيلين يحتوي على ٤٪ سليسليدين (٤) برومو اثلين كقاعدة شيف (I)٣. بولي اثيلين يحتوي على ٤٪ سليسليدين (٤) كلورو اثيلين كقاعدة شيف (II)٤. بولي اثيلين يحتوي على ٤٪ كيما سورب (٨١) كمادة ممتصة للضوء (III)٥. بولي اثيلين يحتوي على ٤٪ كيما سورب (٩٤٤) كمادة مانعة للاكسدة وقانصة للجذور الحرة(IV). تم متابعة سرعة التجزة الضوئية لهذه الرقائق بقياس صيف الاشعة تحت الحمراء في العدد الموجي ١٧٢٠ سم$^{-1}$ (امتصاص مجموعة الكاربونيل) وذلك خلال تشعيع الرقائق بضوء من مصباح الزئبق العالي الضغط بطول موجي من (٣١٠-٤٥٠ نانوميتر) واستخدم مرشح زجاجي لامتصاص الاطوال الموجية الاقصر من (٣١٠) نانوميتر . عينت سرعة التجزئة لقواعد شيف وكيما سورب (٨١) وذلك من خلال متابعة التغير في مطيافيه الاشعة فوق البنفسجية والمرئية بين (٢٠٠-٥٠٠ نانوميتر). اوضحت النتائج بان سرعة التجزئة لهذه الرقائق تتغير حسب الترتيب الاتي:

$$PE > II > III \geq I > IV$$

بينما تتغير سرعة التجزئة الضوئية للمثبتات الضوئية المختلفة حسب الترتبب الاتي:

$$II > I > III$$

ABSTRACT

In this paper, photostabilization and photodegradation of five types of low density polyethylene (LDPE) films (thickness 200 microns) containing different types of light stabilizer have been investigated. These files are: (1) LPDE containing no additive PE (control), (2) LPDE cotaining 0.4% of salicylidene-4-bromoaniline schiff base(I), (3) LDPE containing 0.4% cinnomylidene-4-chloroaniline Schiff base (II) , (4) LDPE containing 0.4% chimassorb 81 as Uv absorber (III) and (5) LDPE film containing 0.4% chimassorb 944LD as polyhindered amine light stabilizer(IV). The rates of photodegradation of these films are monitored by following the infrared sbsorption intensity of the carbonyl group (C=O) at 1720 cm^{-1} developed during illumination of the polymeric film samples (at 30°c) using high pressure mercury lamp with windows glass filter giving light in the spectral between 310 to 450 nm. The rates of photodecomposition of the Schiff base I, II and chimassorb 81 (sample III) were determined by following the changes in the UV-absorption spectra of the films between 200 and 500 nm. Experimental results generally show that rates of photodegradation of LDPE film follow the order: PE>II>III≥I>IV Whereas the rates of photodecomposition of the different types of light stabilizer follow the order: II>I>III Chimassorb 944LD (sample IV) show very high stability during the irradiation test period.

INTRODUCTION

The susceptibility of photo-oxidative degradation of low density polyethylene (LDPE) has been the subject of various research investigations during the last two decades (1-5). The photo-oxidation mechanism is based around the formation and distruction of hydroperoxides (ROOH) which are considered the most important species in initiation of the photodegradation process (6,7). However, the presence of some chromophoric groups (carbonyl, unsaturated groups or metalic impurities such as Ti^{+n}, V^{+n} metal ions) are also believed to take part in photodegradation process but to a small extent (8,9).

It has traditionally been accepted that there are three general stabilization mechanisms (9-11): (1) UV-absorption/ screening. (2) excited state quenching and (3) antioxidant mechanisms. Most if not all stabilizers of polyolefins are believed to be multifunctional in nature(12-14). However, it has been demonstrated that antioxidant mechanism are the most important in photostabilization (3,13,14).

The simplest and effective stabilizer for polylefines are the Uv-absorbing/screening materials. These act by interfering with the first step in photooxidation process, i.e. light absorption by polymeric matrix. UV-absorber should have high molar

extinction coefficient in the spectral range 290-400nm (the Uv-region of the solar spectrum reaches earth's surface). The most important examples of these materials that being used commercially as UV-absorber in LDPE are : 2-hydroxybenzophenones, 2-hydroxybenzotriazoles and cinnamate aromatic esters (5).

In the present work, we investigate a different type of aromatic schiff base UV-absorber in photostabilization of low density polyethylene. These are: salicylidene -4-bromoaniline (I) and 2-cinnamylidene-4-chloroaniline (II) Schiff bases. Chimassorb 81 (2-hyroxy-4-octylbenzophenone)((III) as UV-absorber/ screener and chimassorb 944LD (polyhindered piperidine) (IV) as radical scavenger antioxidiant material were also used as a well known commercial photostabilizer for LDPE.

Experimental

a- Materials

Schiff bases saclicylindene-4-bromoaniline

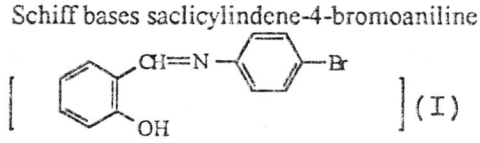

(I)

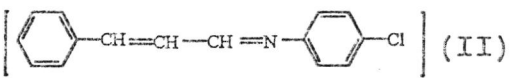

(II)

cinnamylidene-4-chloroaniline

(I) and (II) were prepared by the method suggested by cornwell and Hocksna (15). Equimolar amounts of the apropirate amine and aldehyde were refluxed in ethanol for one hour. The yellow solution was cooled and the Schiff base is precipitated, seperated by filtration, washed with ethanol to give yellow crystals. Purification was carried out by recrystallization from absolute ethanol. The shiny crystals were dried under reduced pressure at room temperature. m.p. of (I)=111° C and (II)=96° C. Both Schiff bases are soluble in most organic solvents. The molar extinction coefficient of these Schiff bases were determined in chloroform at λ=390 nm and found 9560 and 8680 mol^{-1} lcm^{-1} for Schiff bases I and II respectively.

Chimassorb 81

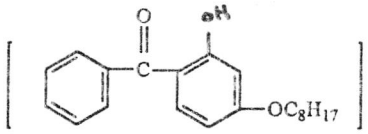

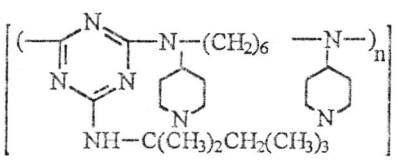

Chimassorb 944LD

Chimassorb 81 and chimassorb 944LD were supplied by Ciba-Giegy-Switzerland. Low density polyethylene (density 0.920 g/cm^3, MFI=0.3g/10 min.) was also supplied by Ciba-Giegy used for film preparation.

c b- Tecn ique

Low density polyethylene films of thickness 200±5 microns were made by mixing 0.4% by weight of different additive materials with LDPE pellets at 150° C using Brabender mixer (Germany). Then the polymer blends were thermally pressed at 130° C using compressing molding equipment)type moor (UK) to tin polymeric films of homogeneous thickness as a circle shape of 10 cm diameter. Five types of LDPE films were made for photodegradation and photostabalization studies, these are : (1) LDPE without any additive (PE), (2) LDPE film contains 0.4% schiff base (I), (3) LDPE film contains 0.4% of schiff bass (II), (4) LDPE film contain 0.4% of chimassorb 81, and (5) LDPE film contains 0.4% chimassorb 944LD. The films cut into 1X4 cm pieces and irradied behind window glass filter of 3mm thickness. Irrdiation was performed by UV-light from 250 Watt high pressure mercury lamp (type Mazda/ED). The average incident light intensity between 310-540 nm was about 105 mw/cm2. Air stream was passed over the films samples to keep the temperature below 30° C during the irradiation experiments.

The degree of photodegrsdation process was determined by measuring the precent carbonyl group (%CO) generated during the photolysis process following the equation:

$$\%CO = A/a\,\ell \times 100$$

where A= carbonyl absorbance at 1720 cm^{-1}, a= absorbitivity of low density polyethylene which is equal to 0.193 and ℓ is the thickness of sample in mile (1000 mil =1.0 inch). Carbonyl index (CI) is determined by dividing the absorbance at 1720 cm^{-1} and the absorbance of the reference peak at 1890cm^{-1}; $CI = A_{1720}/A_{1890}$

Infrared spectra were recorded by pye unicam SP3-100 spectrophotometer. UV-visible spectra were recorded by Hitachi U2000 spectrophotometer.

Results and Discussion :

The rate of photodegradation of the five types of LDPE films were followed by measuring the increase in carbonyl concentration (%CO), created during exposure to UV-light, with irradiation time. Figure 1 shows the variation of %CO with irradiation time at 30° C for all types of LDPE films used in the present work. It is clear from figure 1 that both Schiff bases I and II are effective in photostabilization of the LDPE films. Schiff base I is more efficient than Schiff base II as it is clear from figure 1. The chimassorb 81, as UV absorber has nearly the same efficiency in photostabilization with Schiff base I. However, chimassorb 944LD, as a radical scavenger antioxidant, has the highest activity among all types of additive used. The induction period (t_{in}), which is the period of retarded autoxidation of polymer, shown in Figure 1 also illustrate that the additive used as UV absorber or radical scavenger is longer than the induction period shown in LDPE film without additive (Control PE). The rate of photodegradation (i.e. the rate of C=O formation) follows the order:

PE > II > III ≥ I > IV

The effectiveness of Schiff base I over that of Schiff base II might be explained by the rapid tautomerism of the excited state resembles that of chimassorb 81 and benzotriazols UV

absorbers (2). The photo-tautomerism might be presented in the following proposed photochemical reaction:

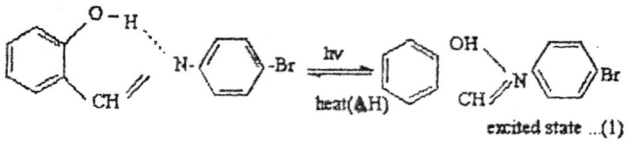

excited state ...(1)

The intramolecular proton transfer between "keto" and "enol" tautomers upon UV-absorption shown in reaction 1 is exclusively responsible about the dissipation of the absorbed UV-energy. This might explain that schiff base I is more active in UV-stabilization of polymer than Schiff base II, since the latter has a molecular structure unable to from a tautomer from like that formed by Schiff base I.

it is well known that the photodegradation of polyethylene involves the following well known chain reaction (16):

$$P^{\bullet} + O2 \xrightarrow{h\nu} POO^{\bullet} \quad \text{.....(2)}$$

$$POO^{\bullet} + PH \rightarrow POOH + P^{\bullet} \quad \text{.....(3)}$$

(where PH and $P^{\bullet}$ are the polyethylene molecules and its macro radical respectively).

Reaction (3) is the photodegradation rate determining step, which is found to be directly proportional to the square root of carbonyl index $(CI)^{1/2}$. Figure 2 illustrates the straight line relationship between $(CI)^{1/2}$and irradiation time for all types of stabilized and non-stabilized LDPE films. Results shown in figure 2 depict experimentally the square-root relationship and the steady state kinetics suggested by Chew *et al.* (16) for the oxidation of polyethlene and polypropylene.

it is found that during the photoirradiation of LDPE films, the additives I,II and III sacrify from photodecomposition phenomenon, but additive IV shows good stability against photodecomposition. figure3 illustrates the change in the UV-visible spectra of these additives in polyethylene films with irradiation time. As one can see from figure 3 that Schiff bases I and II and chimassorb 81 decompose and the strong absorption bands between 200 and 400nm decreases in intensity with irradiation time. The decrease in the absorption wavelength 300 nm was followed and the polt of In (A_t-A_∞) versus irradiation time in a straight line. A_∞ is the absorbance at 300 nm after 350 hours of irradiation and A_t is the absorbance in the scame wavelenght at irradiation time t. This straight line relationship indicates that the photodecomposition of additives I,II and III is first order reaction. The values of the first order rate constant (K_d) of the photo-decomposition process were deduced and the results are presented in table 1.

It is also observed that chimassorb 944LD (additive IV) is stable against irradiation under the condition employed (~350 hr irradiation), and the absorption spectrum is not appreciably changed. This is of course due to fact that this additive does not absorb above 300 nm and the irradiation light is the range between 310 to 450 nm.

It is now generally accepted (1) that chimassorb 81 UV-absorber, beside photochemically tautomerize, its excited state react with the polymeric radicals ($PO^{\bullet}$ or $POO^{\bullet}$) by hydrogen abstraction reaction to chimassorb 81 radicals and these ultimatly terminated to pinicol derivative which does not absorb UV light above 300 nm, so becoming inactive UV-absorber.

The photodecomposition of Schiff base I and II might follow similar mechanism of the photodecomposition of chimassorb 81 (1) either by hydrogen abstraction by the generated polymeric radicals ($RO^{\bullet}$ or $ROO^{\bullet}$) or addition of these radicals with double bond present in these Schiff bases. It seems to us that the photolytic products are not active since they are not appreciably absorb light above 300nm. The detail mechanism and the identification of the photolytic products are under investigation.

However, Allen and coworkers (17) demonstrate the possibility of protection of chimassorb 81 and benzotriazoles UV-absorbers from photodecomposition by the presence of hindered pipyridine or hindered pyridinum oxide derivatines in polymamatrix.

These workers found that the presence of chimassorb 944LD greatly reduce the rate of photodecomposition of UV-absorber in polyethylene and polypropylene (17). It seems to us that a mixture of schiff base I or II with chimassorb 944LD or any radical Scavenger light stabilizer will also reduce the rate of photodecomposition of these Schiff bases used and ultimately improve their effectiveness in light stabilization of LDPE.

Conclusions

A new aromatic Schiff base are successfully applied as a novel Uv absorber photostabilizer for LDPE film. The disadvantag of these additives is mainly their photosensitivity to UV-irradiation between 310 to 450 nm. This problem could be solved by the addition of hindered pipyridines which act both in radical scavenging antioxidant and to protect the Schiff bases from photodecomposition. Further work on other types of Schiff bases of variable structure including polymeric Schiff bases and their mixtures with polyhindered piperidine or hydroperoxide decomposer (e.g. transition metal chelates) as light stabilizer for LDPe film is a possible extension of the present work.

References

[1] Gugumus, F. "3rd Inter. Conf. on Advances in the Stabilization and Controlled Degradation of Polymers" Lucern, Switzerland, 1-3 June (1981).

[2] Ranby B. and Rabek J.F. (eds.) "Photodegradation, Photooxidation and Photostabilization of Polymers", John Wiley. N.Y. (1973).

[3] Allen N.S. in "New Trends in Photochemistry of Polymers" Allen N.S. and Rabek J.F. (eds.)", Science Publishers, London, Chapters 9 and 13 (1985).

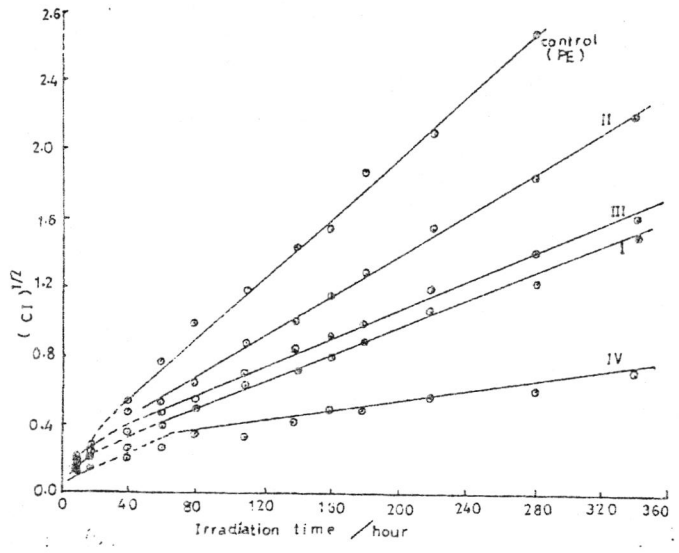

Figure 1. Variation of carbonyl concentration(%), created during photodegradation of LDPE films, wiith irradiation time at 30°C.

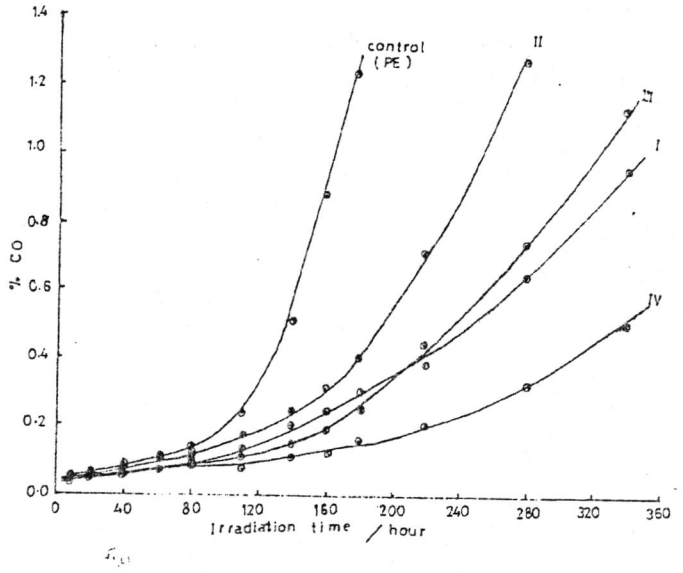

Figure 2 Variation of square root of carbonyl index $(CI)^{1/2}$ with irradiation time for LDPE filems without and with UV-stabilizer I,II,III and IV.

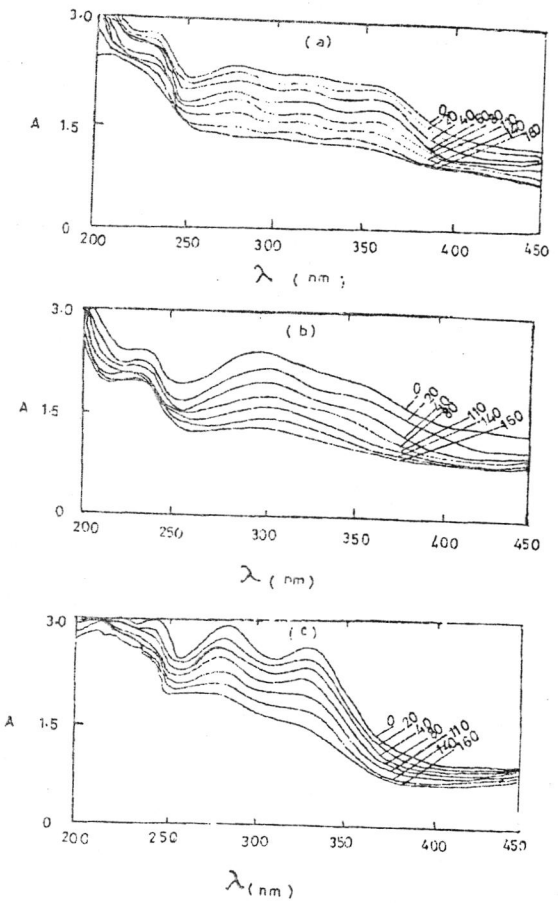

Figure 3. Change in UV-visible absorption spectra with irradiation time of (a) Schiff base (I), (b) Schiff base (II) and (c) chimassorb 81 (III), concentration is 0.4% in LDPE films of thickness 200 microns. Numbers shown on spectra represent the time of irradiation in hours.

[5] Chirinos A.J. Pardon, Photochem J. and Photobiology, A-Chemistry, 49, 1(1989).
[6] Scott, G. Polymer Deg. Stab., 10, 97 (1985).
[7] Scott, G. Photochem, J. 25, 83 (1984).
[8] Allen, N.S. Chem. Soc. Rev., 15,373 (1986).
[9] Chakraborty K.B. and Scott, G. Eur. polymer J., 13, 731 (1977).
[10] Al-Malaika S. and Scott G. in "Degradation and Stabilization of Polyolefines" Allen N.S. (ed.). Applied Sci. Publishers, London (1983), page 283.
[11] Allen, N.S., Chirinos A.J. Pardon and Herman, T.S., Polym. Deg. Stab., 13,31 (1985).
[12] Carlesson D.J. and Wiles, D.M. Macromol J. Sci. Rev., Macromol. Chem., 14,155 (1976).
[13] Scott, G. Br. Polym. J., 16.271 (1984).
[14] Carlesson D.J. and Wiles D.M. Polym. Deg. and Stab., 3, 61 (1980).
[15] Cornwell N.H. and Hocksan, H. J. Am. Chem. Soc., 67, 1658 (1945).
[16] Chew C.H. Ganard L.M. and Scott. G. Eur. polymer J., 13, 364, (1977).
[17] Allen, N.S. Gardette J.L. and Lemaire, J. Appl. polym. Sci., 27, 276 (1982).

Table (1): Values of the rate constant (K_d) for the photodecomposition of Schiff baseI,II and chimassorb 81(III)

Additive	Schiff base(I)	Schiff base (II)	Chimassorb 81(III)
$K_{d(S^{-1})}$	$9.44x10^{-6}$	$2.52x10^{-5}$	$7.34x10^{-6}$

Al-Mustansiriya J. Sci Vol. 6 , No. 1 , 1996

Some Physical Properties of Binary Mixtures of N-Methylpyrrolidone-Chlorobenzene at 288.15, 298.15, 308.15 and 318.15k

MUSTAFA K. AL-NORRI
Department of Chemistry, College of Science, University of Baghdad, IRAQ.
(Recieved 15 Oct. 1993; Accepted 4 Nov., 1993)

الخلاصة

تم قياس كثافة (ρ) ولزوجة (μ) وثابت العزل (ε) ومعامل الانكسار (n_D) لمخاليط N- مثيل بايرولدون مع الكلوروبنزين في درجات حرارة مختلفة وشملت المدى الكلي لكسورها المولية، ومن القياسات السابقة تم ايجاد الحجوم المولارية الاضافية V^E والطاقة الحرة لجبس الاضافية ΔG^{*E} وثابت العزل الاضافي $\Delta\varepsilon^E$ والاستقطاب P° والاستقطاب الاضافي للدرجات الحرارية المختلفة . وجد ان هذه المحاليل تعطي حيوداً سالباً في حجومها المولارية الاضافية VE عن المحلول المثالي حيث يزداد هذا الحيود بازدياد درجات الحرارة، كما لوحظ ان الطاقة الحرة لجبس الاضافة ΔG^{*E} قد اعطت حيوداً موجباً، قل بزيادة درجات الحرارة، والذي اعزي الى وجود تأثيرات الجزيئات الغير متشابهة بين ال N- مثيل بايرولدون والكلوروبنزين التي تزداد بارتفاع درجات الحرارة، والذي قد يكون بسبب انتقال الشحنات، وكانت هذه التأثيرات اقل من القيم الموجودة بين N- مثيل بايرولدون والبنزين او التولوين للدرجات الحرارية ذاتها، والذي يعزي الى وجود مجموعة ساحبة للالكترونات (Cl) مما يقلل من تأثيرات الجزيئات الغير متشابه بين المذيب وحلقة البنزين. كما لوحظ ايضاً ان ثابت العزل الاضافي $\Delta\varepsilon^E$ واستقطاب الاضافي ΔP^E قد اعطت حيوداً سالباً عن المحلول المثالي الا ان هذا الحيود يقل بارتفاع درجات الحرارة، مما يشير الى وجود التأثيرات البين جزيئية للجزيئات الغير متشابهة.

ABSTRACT

Excess molar volume V^E, viscosities η, dielectric constant ε, excess dielectric constant $\Delta\varepsilon^E$, refractive index n_D. polarization, excess polarization ΔP^E and excess molar Gibbs free energy of activation ΔG^{*E} of viscous flow for N-methylpyrrolidone (NMP) + chlorobenzene mixture have measured at 288.15, 298.15, 308.15 and 318.15 K for the whole mole fraction range. The mixture exhibit negative V^E, $\Delta\varepsilon^E$ and ΔP^E which suggest that the molecular interaction between the NMP and chlorobenzene might be formed a sort of charge transfer complexes. Such behaviour were discussed on bases of molecular interactions.

INTRODUCTION

Excess molar quantities have extensive application in studying the intermolecular interaction in binary mixtures including those leading to molecular association, dissociation or complex formation [1]. Our earlier studies on the binary mixtures of 2 - pyrrolidone + water [2], γ - butyrolacton + water [3] and N - formylmorphyline (NFM) with chlorobenzene [4,5], revaled that the molecular interaction present in such mixtures in form of hydrogen bonding or charge transfer complex formation, and are sensitive to both concentration and temperature variations, as a continuation to these studies, the present paper reports, densities, viscosities, dielectric constant, refractive index, polarization, excess molar volume V^E, excess dielectric constant Δε, excess polarization ΔP^E and excess molar Gibbs free energy of activation ΔG^{*E} for viscous flow of binary mixtures of NMP + chlorobenzene over the whole mole fraction range at 288.15, 298.15, 308.15 and 318.15K.

Experimental

Chlorobenzene (Puriss. p.a.) and NMP (Puriss.p.a.) obtained from fluka, the NMP was distilled under vacuum at 340 K, the chlorobenzene was fractinated distilled, then they were dried with reactivated molecular sieve type 4A°until used. The mixtures of both where prepared in 100 gm batches by weigh out the two liquids to the nearest 0.1 mg, all solutions were store in dark bottles away from light.

All measurements were carried out at 288.15, 298.15, 308.15 and 318.15 K using a thermostated bathes with ±0.01°C.

The densities were determined with an Anton Paar digital densimeter (DMA 601). the overall stated precision of density measurement is estimated to be better than 5×10^{-6} gm cm^{-3}.

Automatic Schott - Gerate viscometer model AVS

300 supplied with ± 0.01 sec. timer was used for viscosity measurements. The glass ubbholde viscometer was standardized with water and benzene they have the following time in sec. with deionized water 260.31 sec at 288.15 K ; 203.76 sec at 298.15 K ; 165.69 sec at 308.15 K and 138.34 sec at 318.15 K.

Dielectric constant ε of the pure and binary mixtures of NMP and chlorobenzene over the whole mole fraction range at several temperatures were measured at 0.9 MHz with measuring cell type (OH - 911), using of Radelkis precision dielectrometer type (OH - 302) with maximum error on the dielectric constant scale of ± 0.02%.

Refractive index n_D was measured by using Sodium light and an Abbe refractometer with a precision of the reading of ± 0.0002.

Results and Discussions

The experimental results of the density ρ, viscosity η, dielectric constant ε, refractive index n_D and polarization P', at 288.15, 298.15, 308.15 and 318.15 K are presented in Table1.

The experimental values of excess molar volume V^E results obtained from precise density measurements for the system NMP + chlorobenzene at 288.15,298.15, 308.15 and 318.15 K are given in Table 2 and plotted in figure 1 by using the equation of the form

$$V^E(cm^3mole^{-1}) = \frac{M1X1 + M2X2}{\rho 12} - (X1V°1 + X2V°2)$$

where M_1 , M_2 the molecular weight of NMP and chlorobenzene respectively.

X_1, X_2, the mole fraction of NMP and chlorobenzene.

V'_1, V'_2 the molar volume of NMP and chlorobenzene.

ρ_{12} the density of the binary mixture.

Excess molar Gibbs free energy of viscous flow for the binary mixture, ΔG^{*E} were calculated from the following equation [6,7],

$$\Delta G^{*E} (J\ mole^{-1}) = R\ T\ [\ln \eta V - (x_1 \ln \eta_1 V_1' + x_2 \ln \eta_2 V_2')]$$

where , V in the molar volume

η, η_1', and η_2' represent respectively the viscosity of the binary mixture, viscosity of component one (1= NMP) and component two (2 = Chlorobenzene). The obtained results are given in Table 2 and illustrated in figure 2.

Excess dielectric constant $\Delta\varepsilon^E$ at 288.15, 298.15, 308.15 and 318.15 K are calculated from the experimental values of ε from the following equation,

$$\Delta\varepsilon^E = \varepsilon_m - x_1\varepsilon_1 - x_2\varepsilon_2$$

where, ε_1, ε_2 and εm represents respectively the dielectric constants of component one (1=NMP), component two (2= chlorobenzene) and the binary mixture. The obtained $\Delta\varepsilon^E$ values from the ε calculation are listed in Table 2 and plotted versus the mole fraction of NMP in figure 3.

Polarizabilities are calculated using the following equation,

$$P° = \left[\frac{(\varepsilon-1)(\varepsilon+2)}{9\varepsilon} - \frac{(n_D^2-1)(n_D^2+2)}{9n_D^2}\right]V$$

where, V is the molar volume, ε and n_D are the dielectric constant and refractive index of the binary mixtures respectively, the calculated data listed in Table 1. The excess polarization ΔP^E were calculated from the following equation,

$$\Delta P^E = P'_m - x_1 P'_1 - x_2 P'_2$$

where, P'_m , P'_1 and P'_2 represent the molar polarization of the binary mixture NMP and chlorobenzene respectively. The ΔP^E values listed in Table 2 and plotted in figure 4.

It is well known that, in mixing of two liquids, the interaction between like and unlike molecules determine the extent to which the structure of pure components are modified. Figure 1 shows the excess molar volume V^E of NMP + chlorobenzene mixtures as a function of mole fraction of NMP at 288.15, 298.15, 308.15 and 318.15 K, the curves at all temperature examined are negative over the entire composition range, the change in free volume arises from two components namely, geometrical effect and interaction between the component molecules [8,9]. The magnitude of the interaction is determined by the dipole - induced dipole interaction between the benzene of the chlorobenzene and the carbonyl group of NMP, which is greater than the dispersive and dipole - dipole interaction. Comparing our results of VE for NMP + chlorobenzene with that previously studied [4,5] for NFM + chlorobenzene, the presence of the methyl group in NMP produced negative deviation of the VE values that of NFM. This is due to the inductive effect of the methyl group, which leads to greater dipole - induced dipole interaction than dipole - dipole interaction. Hence, the negative V^E values of NMP + chlorobenzene system indicate probably the presence of charge - transfer complex interaction, the formation of the charge - transfer complex might be due to the electron doner ability of the aromatic hydrocarbon and the weak acceptor ability of NMP, moreover, the presence of Cl atom on the benzene decrease the inductive effect of donating electrons to the benzene ring, thus, decreasing the dipoleinduced dipole interaction between NMP and chlorobenzene, at the same time this explains the lower negative excess molar volume V^E for NMP + chlorobenzene system than NMP - benzene and NMP - Toluene system[10].

The excess dielectric constant are negative over the whole mole fraction range, figure 3, which suggest the charge - transfer formation in NMP + chlorobenzene mixtures. This data support the volumetric behaviour discussed above. The point of interest, is that the extent of the negative region of V^E increase as the temperature increases. In contrast the negative region of $\Delta\varepsilon^E$ decrease as the temperature increases. Such trend can be explained by the tendency to promot topologically more contract structure as temperature increasing, for the V^E values. While, this may be due to contribution from

steady state direct current conductivity which increase $\Delta\varepsilon^E$ the temperature increases. The induced dipole - dipole interaction between NMP and chlorobenzene enhance the polarization to more positive as illustrated in figure 4[11].

The order of excess molar Gibbs free energies of viscous of flow ΔG^{*E}, figure 2, does not follow the same sequences as V^E and $\Delta\varepsilon^E$, this is probably due to the geometrical and steric factors of NMP and chlorobenzene molecules which have direct effect on the viscous flow of these mixtures.

Acknowledgment

The author wish to express his gratitude to Dr. A.H. Al-Dujaili of college of education and Dr. F. Kanbor of college of science for very helpful discussion and comment.

Table 1 - Experimental densities ρ, viscosities η, dielectric constant ε, refractive index n_D and polarization P" of N - methylpyrrolidone + chlorobenzene at 288.15, 298.15, 308.15 and 318.15 K.

X_{NMP}	ρ (gm cm-3)	η (centipoise)	ε	n_D	P°
			T=288.15 K		
0.0000	1.11014	0.8707	5.83	1.5259	46.9
0.0565	1.10739	0.9581	7.17	1.5237	60.7
0.1673	1.10153	1.1217	9.74	1.5191	89.0
0.2745	1.09527	1.2699	12.33	1.5143	117.4
0.3796	1.08857	1.4057	14.95	1.5093	146.2
0.4817	1.08154	1.5285	17.61	1.5040	175.2
0.5818	1.07413	1.6403	20.33	1.4986	204.9
0.6783	1.06652	1.7399	23.08	1.4930	234.5
0.7733	1.05857	1.8302	25.97	1.4873	264.7
0.8655	1.05042	1.9104	28.70	1.4814	295.1
0.9557	1.04204	1.9819	32.20	1.4754	325.7
1.0000	1.03777	2.0114	33.51	1.4724	341.1
			T=298.15K		
0.0000	1.09945	0.7458	5.69	1.5206	44.3
0.0565	1.09683	0.8153	6.87	1.5183	58.2
0.1673	1.09121	0.9457	9.30	1.5141	86.1
0.2745	1.08518	1.0643	11.77	1.5095	113.7
0.3796	1.07870	1.1734	14.33	1.5045	141.4
0.4817	1.07188	1.2726	16.93	1.4994	169.9
0.5818	1.06467	1.3633	19.59	1.4940	198.4
0.6783	1.05724	1.4446	22.26	1.4885	226.8
0.7733	1.04947	1.5188	24.99	1.4828	255.5
0.8655	1.04148	1.5853	27.74	1.4770	284.3
0.9557	1.03325	1.6451	30.52	1.4710	313.3
1.0000	1.02906	1.6725	31.92	1.4680	327.9
			T=208.15K		
0.0000	1.08850	0.6558	5.47	1.5152	43.0
0.0565	1.08614	0.7128	6.66	1.5132	56.5
0.1673	1.08100	0.8214	8.98	1.5091	83.4
0.2745	1.07535	0.9219	11.25	1.5046	110.2
0.3796	1.06917	1.0164	13.79	1.4999	137.2
0.4817	1.06256	1.1042	16.28	1.4949	164.4
0.5818	1.05556	1.1865	18.82	1.4897	191.8
0.6783	1.04815	1.2624	21.38	1.4843	219.2
0.7733	1.04039	1.3340	23.99	1.4788	247.0
0.8655	1.03237	1.3995	26.62	1.4730	274.8
0.9557	1.02404	1.4609	29.27	1.4672	302.7
1.0000	1.01978	1.4900	30.61	1.4642	316.8
			T=318.15 K		
0.0000	1.07726	0.6075	5.42	1.5098	42.4
0.0565	1.07527	0.6526	6.50	1.5079	55.4
0.1673	1.07077	0.7386	8.71	1.5038	81.3
0.2745	1.06562	0.8187	10.96	1.4995	106.9
0.3796	1.05983	0.8944	13.27	1.4948	132.7
0.4817	1.05350	0.9650	15.62	1.4899	158.6
0.5818	1.04661	1.0315	18.02	1.4848	184.7
0.6783	1.03933	1.0932	20.37	1.4795	210.7

0.7733	1.03156	1.1514	22.79	1.4741	236.9
0.8655	1.02344	1.2057	25.33	1.4685	263.2
0.9557	1.01495	1.2566	27.82	1.4627	289.8
1.0000	1.01057	1.2808	29.07	1.4597	303.1

Table 2 Excess molar volum VE, excess molar actination energies AG*E, excce dielectric constant Δε and excess polarization ΔPE of N-methylpyrrolidon + chlorobenzene at 288.15, 298.15, 308.15 and 318.15K

X_{NMP}	VE (ml)	ΔG* (J. mole^{-1})	ΔεE	ΔPE
		T=288.15 k		
0.0000	0.00	0.00	0.00	0.0
0.0565	-0.102	113.73	-0.35	-2.8
0.1673	-0.263	265.66	-0.91	-7.1
0.2745	-0.381	345.26	-1.30	-10.3
0.3796	-0.449	376.27	-1.54	-12.4
0.4817	-0.469	371.62	-1.63	-13.4
0.5818	-0.457	340.13	-1.59	-13.2
0.6783	-0.411	288.73	-1.43	-11.9
0.7733	-0.334	221.06	-1.15	-9.6
0.8655	-0.219	141.42	-0.76	-6.4
0.9557	-0.077	51.70	-0.28	-2.3
1.0000	0.000	0.00	0.00	0.0
		T=298.15 k		
0.0000	0.000	0.00	0.00	0.0
0.0565	-0.102	105.38	-0.30	-2.1
0.1673	-0.274	247.59	-0.78	-5.6
0.2745	-0.393	323.08	-1.11	-8.4
0.3796	-0.461	353.13	-1.32	-10.2
0.4817	-0.491	349.07	-1.39	-10.9
0.5818	-0.479	319.70	-1.36	-10.8
0.6783	-0.423	217.23	-1.22	-9.8
0.7733	-0.346	206.93	-0.98	-8.0
0.8655	-0.230	131.21	-0.65	-5.4
0.9557	-0.088	45.81	-0.24	-2.0
1.0000	0.000	0.00	0.00	0.0
		T=308.15 k		
0.0000	0.00	0.00	0.00	0.0
0.0565	-0.118	92.19	-0.28	-2.0
0.1673	-0.324	217.66	-0.74	-5.4
0.2745	-0.457	285.01	-1.06	-8.0
0.3796	-0.548	311.64	-1.26	-9.8
0.4817	-0.578	308.57	-1.33	-10.5
0.5818	-0.561	282.70	-1.30	-10.5
0.6783	-0.500	239.94	-1.17	-9.5
0.7733	-0.406	183.09	-0.94	-7.8
0.8655	-0.273	115.74	-0.62	-5.2
0.9557	-0.094	40.46	-0.23	-2.0
1.0000	0.000	0.00	0.00	0.0
		T=318.15 k		
0.0000	0.000	0.00	0.00	0.0
0.0565	-0.152	74.29	-0.25	-1.7
0.1673	-0.399	177.67	-0.66	-4.7
0.2745	-0.561	234.24	-0.95	-7.0
0.3796	-0.657	258.04	-1.12	-8.6
0.4817	-0.702	256.45	-1.19	-9.4
0.5818	-0.684	235.56	-1.16	-9.3
0.6783	-0.616	200.65	-1.04	-8.6
0.7733	-0.498	153.34	-0.84	-7.1
0.8655	-0.330	97.29	-0.55	-4.8
0.9557	-0.116	33.84	-0.20	-1.8
1.0000	0.000	0.00	0.00	0.0

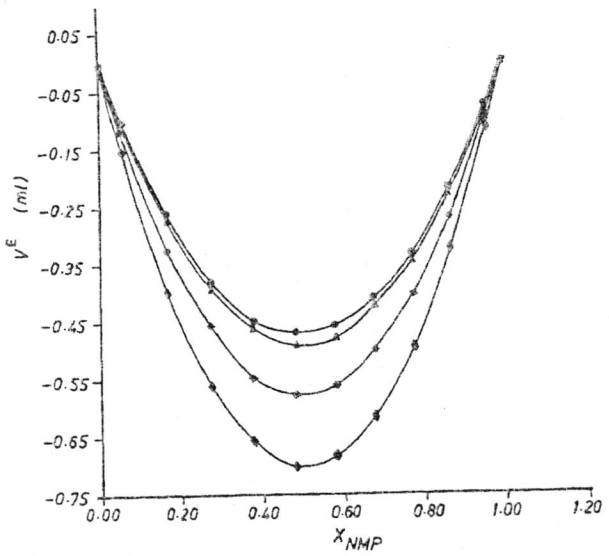

Figure(1) Excess molar volumes for x(NMP)+(1-x)chlorobenzene at 288.15 (0), 298.15 (Δ), 308.15(*) and at 318.15k (♦).

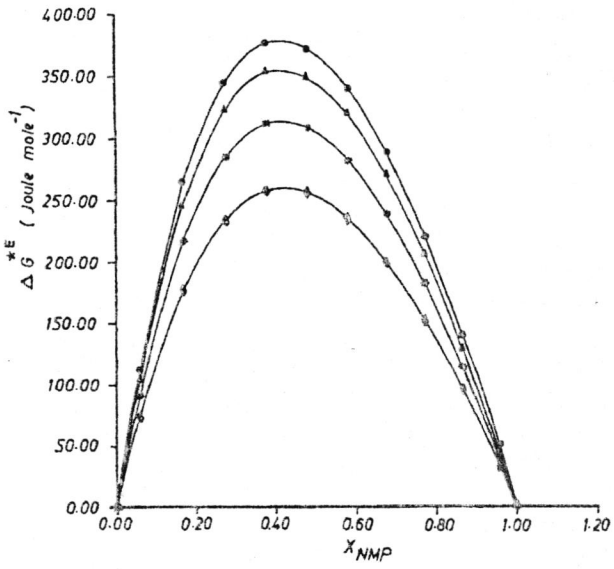

Figure(2) Excess molar Gibbs free energy of Activation of viscous flow for x(NMP)+(1-x)chlorobenzene at 288.15(0), 298.15(Δ), 308.15(*) and at 318.15k(♦).

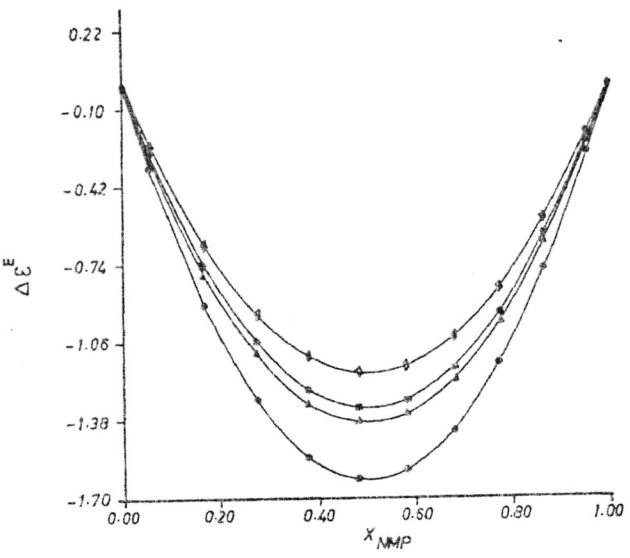

Figure(3) Excess dielectric constant $\Delta\varepsilon^E$ for x(NMP)+(1-x)chlorobenzene at 288.15(0), 298.15(Δ), 308.15(*) and at 318.15k (♦).

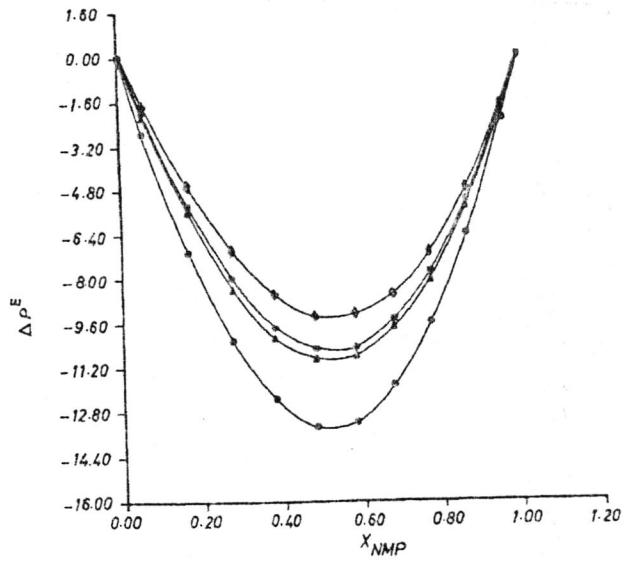

Figure(4) Excess Excess polarization ΔP^E for x(NMP)+(1-x)chlorobenzene at 288.15(0), 298.15(Δ), 308.15(*) and at 318.15k (♦).

REFERENCES

[1] Valers J., Lopez M., Gracia M. and Gutierrezolosa, "Excess Enthal-pies of Some (bromoalkane+n-alkane) Mixtures".J. chem. Thermodyn. 12,627(1980).

[2] AL-Azzawi S., Awaad A.M., AL-Dujaili A.H., and AL-norri M.K., "Dielectric Constant and Excess Volumes of 2-pyrrolidone+water at Several Temperatures. "J.Chem. Eng. Date, 35,463,(1990).

[3] AL-Dujaili A.H., AL-Norri M.K. and Awaad A.M., "Dielectric Constant of Aqueous Mixtures of r-Butyrolactone at 25°C. " to be published in J. Pet. research (1993).

[4] AL-DujailiyA.H., AL-Norri M.k., Mohammed A.A. and Awaad A.M., "Some Properties of Binary Mixture of N-Formy lmorpholine and Chlorobenzene at 298.15K. " to be Published in J. of College of Education for Women, no. 4 (1993).

[5] AL-DujailiyA.H., AL-Norri M.K, and Mohammad A.A., "Dielectric Constants of N-Formylmorpholine+ Chlorobenzene Mixture at 25, 35, and 45°C. "to be published in J. of College of Education of EL-Mustinsayria University, no. 3, (1993).

[6] Heric E.L. and Coursey B.M., "Some Properties of Binary System of Hexane and Normal chloroalkanes. " J. Chem. Eng. Date, 17,41,35(1972).

[7] Delamas G., Purves P. and Romain P.D., "Viscosities of Mixtures of Branched and Normal Alkanes With Tetrabutylin-Effect of the Orientational Order of Long-Chain Alkanes on the Entropy of Mixing." J. Phys. Chem., 79, 142, 1970, (1974).

[8] Munozembid J., Santos I.V. Otin and Gutierrezlosa C., " Excess Enthalpies of 1-Iodoalkane + n-Alkane Mixtures Mesurement and Analysis in Terms of Group Contributions (DISQUAC). " Fluid Phase Equilibria, 38,1 (1987).

[9] Monk P. and Wadso I. , " A Flow Micro Reaction Calorimeter," Acta, Chem. Scand., 222, 1842, (1968).

[10] AL-Madfai S.F, AL-Assadi Z.A., Alchi W.T., Kanbour F.I., "Excess Volumes of N-methylpyrrolidone and aromatichydrocarbon. " J. of Pet. Research, 1,77,(1982).

[11] Awaad A.M., AL-Dujaili A.H. and AL-Khyat B.H., "Dielectric Constant and viscosity of pure 2-pyrrolidone, N-Methylpyrrolidone and r-butyrolactone at Several Temperatures. " Proc. 5th.Sci.Conf. SRC-IRAQ-Baghdad Vol.2 Part 2, 176,(1989).

Al-Mustansiriya J. Sci Vol. 6, No. 1, 1996

Hydro-Chemical Evaluation of Groundwater in Babylon University Complex

QASSEM H. JALUT, FIKKRAT M. HASSAN* AND DIKHAL N. TAHA**
Department of Civil Engineernig, *Department of Biology,**Department of Chemistry, University of Babylon.Iraq.
(Recieved 26 Dec. 1992; Accepted 25 Oct., 1993)

الخلاصة

الدراسة شملت جمع وتحليل للمعلومات الهيدواوجية والكيمياوئية للمياهالجوفية في منطقة جامعة بابل من اجل تقيم اداء نظام البزل الموجود ونوعية المياه الجوفية فيها. تم استخدام ثلاثة ابار ومبزليين حقليين في القياسات الحقلية لمناسيب المياه الجوفية والفحوصات الكيميائية. أجريت عدد من الفحوصات الكيميائية شملت قياس تراكيز الحامضية. التوصيل الكهربائي، العسرة الكلية، الكالسيوم، المغنيسيوم، الكلوريد، الصوديوم والمواد الصلبة المذابة، المعلومات الهيدرولوجية اثبتت ان نظام البزل الحالي لا يعمل ونتائج الفحوصات الكيميائية اعطت دليلا على تلوث المياه الجوفية من ابار المياه الثقيلة المنتشرة في المنطقة.

ABSTRACT

Hydro - chemical data of groundwater was collect and synthesized to evaluate the quality of groundwater and the performance of the existed drainage system in Babylon University Comples. Three wells constructed at different locations and two field drains were considered in the hydrological and chemical analysis. Tests such as (PH, EC, Total Hardness, Ca, Mg, Cl, and Na) were conducted on each samples. Hydrological data shows that the existed drainage system is not functioning with high indication of sewage water contamination to the underground groundwater.

INTRODUCTION

Groundwater is considered as a vital source for both domestic and agricultural purposes. As the number of people is increasing rapidly, the importance of groundwater quantity and quality becomes eminent. The quantity and quality of groundwater problems have been the focus of many researchers. In many parts of the world, with the increased withdrawal of groundwater, the quality of groundwater has been continously deteriorating, causing much concern to both suppliers and users (6,5).

Groundwater contamination is one of the biggest problem that control an increasing share of the national attention in the comming century. It is necessary to perform a hydro-chemical study at a given site to determine if localized ground water contamination had occured as a result of potential leakage from different sources such as sewage storage tanks, buried chemicals, and agricultural activities (5,12).

Recently researchers classify problems concerning studies of groundwater contamination into four categories: (1) Chemical problems such as evaluation and prediction of certain chemicals in groundwater due to excessive fertilizer applications, hazardous waste, and chemical waste injection. (2) Bacterial problems associated with artifical recharge, sanitary l and fills, ...etc (3) Thermal problems such as injection of hot water into groundwater aquifers, and problems associated with the development of geothermal energy; and (4) Multiphase problems such as problems concerning air-water interfaces, oil - air-water interfaces which covers steam water systems and oil recovery system respectively (15).

Many researchers had studied the groundwater quality in different parts of Iraq. Al-Rawi et al (3) study the quality of groundwater in some parts of Mousul city. Their results show highly saline water which is also obsereved by Layla et al (1). The second second study obsereced locally some level of contamination caused by sewage effluents or agricultural effluents. Habib et al (9) and Mhamoud. Zangana (14) study groundwater quality in Arbil city. Their results indicated the presence of some elements with high concentration higher than the maximum allowable concentration for the drinking water. They believe that the source of contamination comes from human and surface activites.

Jamil et al (11) evaluate the quality of some water sources in the governorate of Al-Tamiem for the purpose of civil, industrial, and irrigation uses. They observed very high concentration of total hardness, S04, and EC which exceed the acceptable level for civil, industrial purposes.

Materials and Methods

A detial map for the study area (Babylon University Complex) is presented in fig. (1). The map shows the master plan for the complex with the sewage system (Dot line) and the location of wells (well 1,2, and 3). It also shows the location of the treatment plant and the two field drain considered in the study. Hydrological study of the area includes a detial montiering of groundwater fluctuation throughout the year starting from May 1991 until May 1992 using the three wells. The chemical analysis is acheived using the standard methods (4). One liter sample bottles were taken from each well Sub-samples were taken directly to the laboratory for PH, EC measurements and the analysis of Ca, Mg, Total Hardness, Cl, Na, and T.D.S.

PH was measured by PH meter Philips. EC measured by conductivity meter model 4010 Jenway. Total Hardness, Ca, and Mg by using the method of titration with EDTA (4). Cl was analysed by using the titration with Silver Nitrate (13). Flame Photometer was used to measured Na concent. Finally the Total Dissolved Solid was analysed using the standard method.

Results and Discussion

Soil investigation indicates that the upper layer is light brown silty sand with organic materials down to 40 cm below natural ground surface. It is followed by dark brown sandy silty clay about 100 cm thick. The final layer is gray dense fine sand to the ends of borings.

Fig. (2,3 and 4) show the groundwater fluctuation at well 1,2, and 3 respectively. All figures indicate that the average drain water level is higher than the surrounding groundwater levels during most of the year. This observation suggest that the drain system act as a recharging body of water to the underlying aguifer. Field observations indicate that the underlying aquifer is single unconfied since the behavior of water level fluctuation is the same (see fig 5), (10). Results in fig (2,3, and 4) show a build up in groundwater level of 50 cm in the three locations during one year. This proves that the existed drainage system is not functionning.

Table (1) represent the chemical data for the study area. PH values are ranging from (7.2 - 7.9) and this considered acceptable according to W.H.O standarad. Values of conductivity show a wide range.

The maximum value was 31.1 obtained at well 1 while the minmum value was 2.9 obtained at well 3. According to these values the groundwater at well 1 and 2 can not be used neither for drinking nor for agricultural and cooling purposes. EC values in drain N and drain S looks reasonable.

According to all standard level presented in table (2), values of T.D.S were considered extermely high. These values usually come from dissolved inorganic compound. Degree of hardness in the three locations ranges from 1029 to 11564 mg Caco3/1 which considered very hard water according to (13). These values can be attributed to the present of high concentration of calicum and magnesuim in the study area (2). These high values of groundwater hardness may be caused by the contamination from sewage system to the nearby wells (well 1 and 2), (16,8). Value of hardness in drain N and S support our conclusion since it is very low compare to the value of hardness in well 1 and 2.

The results show that calcium and magnesuim concentration in wells 1 and 2 were very high (730-1414 mg/1 for Ca, 1048-2142 mg/1 for Mg) while in well 3 faraway from sewage tanks these values were reasonable (78-235 mg/1 for Ca, 125-476 mg/1 for Mg). We believe this variation is caused by sewage tanks near by well 1 and 2.

According to Middle Asia Classification, all wells agree with the recommended concentration of sodium. On the other hand only well 3 is considered acceptable according to E.P.A standards (Table 2) (7,17). The maximum and minimum concentration of chlorides estimated at well 1 and 2 ranged from 2529 to 8279 mg/1 and for well 3 ranged from 169 to 1149 mg/1. Only well 3 met the Middle Asia Classification. Here again, well 1 and 2 were regarded unsuitable (Table 2).

Conclusion

1. The existed drainage system act in an opposite way (most of the year) which leads to a continous recharging of water from drain to the underground water.
2. The trend of chemical analysis suggest high effect of sewage system in well 1 and 2 which are located nearby the underground sewage tanks.

Recommendation

1. Redesigning of the existed drainage system for the study area. with the complete linking with the surrounding collector drains.
2. Continuous monitoring and maintenance to the unversity sewage system.

REFERENCES

[1] Al-Layla, M.A., Akrawi, S.M., and Kharrufa, S.N. Groundwater in Mosul (left bank) and suitability for human consumption, 2nd Iraqi Conf. on Eng. ICE. Engineering and Technology, Special issue (1988).

[2] Al-Layla, M.A, Al-Rawi, S.M, and Al-Kawaz, H.A Physico-chemical evaluation of groundwater around Saddam Lake used for drinking and domestic purposes. 2nd Sci.Conf. of Saddam Dam Ressearch Centre, Mosul University. Mosul, Iraq (pp 173) (1990).

[3] Al-Rawi, S.M, Al-Azzo, S.I, and Abbawi, S.A Hydrogeochemical evaluation of groundwater in some parts of Mosul City and suitability for irrigation. 2nd Sci.Conf. of Saddam Dam Ressearch Centre, Mosul University, Mosul, Iraq (pp 173), (1990).

[4] APHA, AWWA, WPCF Standard method for examination of water and waste water. 16th ED. APHA, Washington. D.C, U.S.A (1985).

[5] Bear, J., and Verruijt, A. Modeling groundwater flow and pollution Reidel Pub. Company, Dordrecht, Holland (1987).

[6] Bouer, H. Present and future challenges in hydrology. Proceedings of the fifth annual AGU Front Range Branch, Hydrology Days Pub., Fort Collins, Colorado, U.S.A (pp 145) (1985).

[7] E.P.A Interim primary drinking water requlations, U.S.A (1983).

[8] Gordon, M.F, John, C.G, and Daniel A.O Water and Waste Water Engineering, Vol 1 (water supply and waste water removal). Pub. by John Wiley and sons, Inc. (1966).

[9] Habib, H.R, Al-Saigh, N.H, and Hassan, Z.M Geochemistry of underground water in Erabil City, Iraq. 2nd Sci. Conf. of Saddam Dam Research Centre. Mosul University. Mosul, Iraq (pp 207) (1990).

[10] Jalut, Q.H Conjunctive use model of groundwater and surface water in irrigation command area. Ph.D thesis. Colorado State University Fort Collins. Colorado. U S.A (1989).

[11] Jamel, A.S.A, Fadel, L.M, and Taleea, A.A.Y Study of qulitative properties of some water sources in the governorate of Al-Tamiem for civil, industrial and irrigational uses. 2nd Sci. Conf. of Saddam Dam Research Centre, Mosul University, Mosul, Iraq (pp 84) (1990).

[12] Kadwell, R.J Hazardous waste and cleanup - a case of history. Proceedings of the fifth annual AGU Front Range Branch, Hydrology Days Pub., Fort Collins, Colorado, U.S.A (pp 235) (1985).

[13] Lind Handbook of common methods in limnology. C.V. Mosby (1979).

[14] Mhamoud, F.H, and Zangana, J.M Quality of underground water in Erabil City, Iraq. 2nd Sci. Conf. of Saddam Dam Research Centre Mosul Unversity, Mosul, Iraq (pp 74) (in Arabic) (1990).

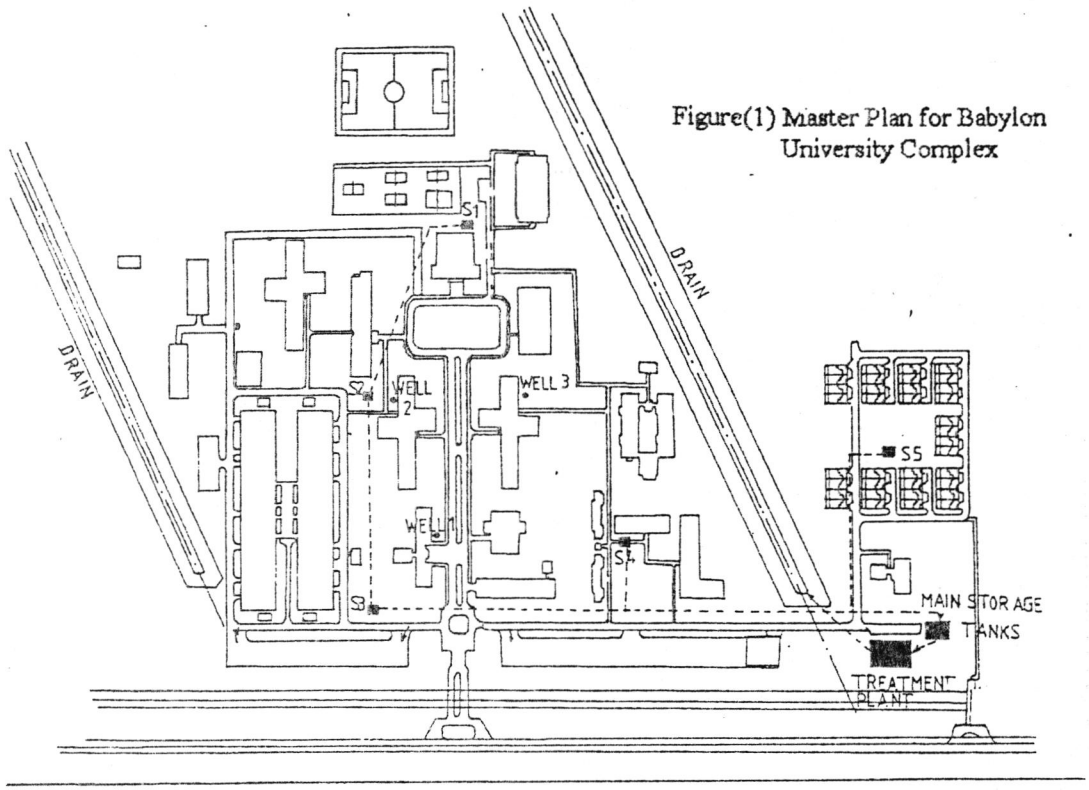

Figure(1) Master Plan for Babylon University Complex

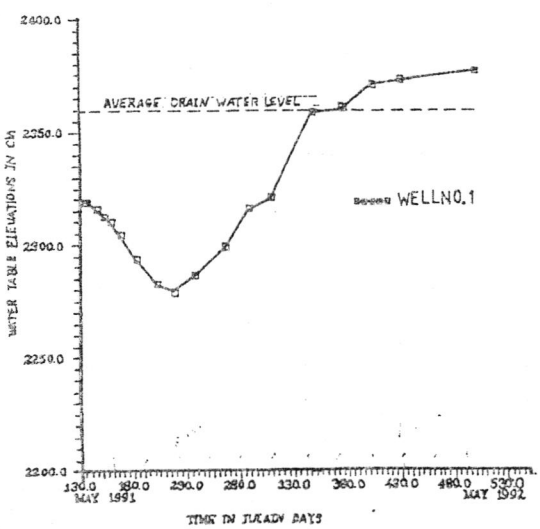

Figure(2)Water table varaus time at well no. 1.

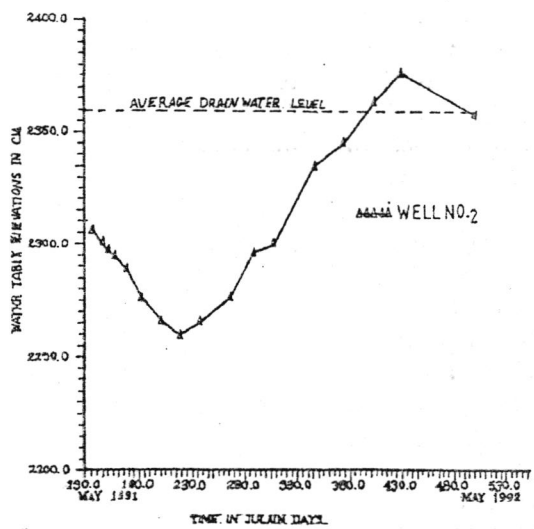

Figure(3)Water table varause time at well no. 2.

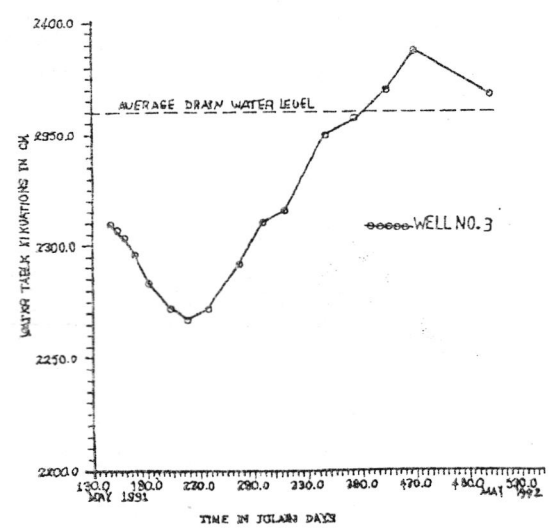

Figure(4)Water table varause time at well no. 3.

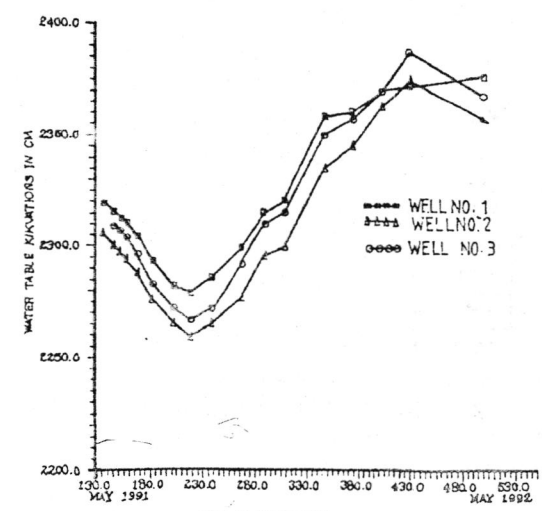

Figure(5)Hydrographs of walls no. 1,2 and B.

Table (1) Chemical data for groundwater in babylon university complex

Data of sampling: Dec 5, 1991

FACTORS	WELL 1	WELL 2	WELL 3
PH	7.88	7.85	7.61
EC (ms.cm-1)	24.40	20.40	3.00
TDS (mg/l)	26000.00	21000.00	2900.00
Total Hardness (mg/l)	7128.00	6138.00	1029.00
Calcium (mg/l)	793.50	730.09	206.33
Magnesium (mg/l)	1250.29	1048.19	125.00
Chloride (mg/l)	2529.21	2869.11	259.91
Sodium (mg/l)	290.00	225.00	90.00

Data of sampling: Jan 5, 1992

FACTORS	WELL 1	WELL 2	WELL 3
PH	7.80	7.60	7.90
EC (ms.cm-1)	24.40	20.40	3.00
TDS (mg/l)	26800.00	21500.00	3100.00
Total Hardness (mg/l)	9212.00	8820.00	2156.00
Calcium (mg/l)	1021.32	1178.35	78.55
Magnesium (mg/l)	1618.49	1427.94	476.18
Chloride (mg/l)	3698.85	4208.69	169.94
Sodium (mg/l)	285.00	240.00	60.00

Data of sampling: Jan 30, 1992

FACTORS	WELL 1	WELL 2	WELL 3
PH	7.34	7.52	7.54
EC (ms.cm-1)	31.10	30.40	2.90
TDS (mg/l)	33500.00	32790.00	2800.00
Total Hardness (mg/l)	11564.00	10976.00	1764.00
Calcium (mg/l)	1099.79	1414.02	235.67
Magnesium (mg/l)	2142.22	1808.80	285.63
Chloride (mg/l)	4178.70	4998.45	237.92
Sodium (mg/l)	285.00	295.00	30.00

Data of sampling: Feb 13, 1992

FACTORS	WELL 1	WELL 2	WELL 3	DRAIN N	DRAIN S
PH	7.20	7.62	7.60	8.10	8.50
EC (ms.cm-1)	30.00	29.60	5.00	11.40	17.20
TDS (mg/l)	32300.00	31900.00	4800.00	4500.00	5000.00
Total Hardness (mg/l)	9702.00	10584.00	2940.00	3920.00	4566.80
Calcium (mg/l)	1099.79	942.68	549.98	628.54	785.56
Magnesium (mg/l)	1689.87	1999.46	380.72	571.15	632.92
Chloride (mg/l)	5298.35	8297.42	1149.60	2399.25	3398.94
Sodium (mg/l)	300.00	295.00	105.00	165.00	240.00

Table (2) Selected international drinking water regulations

FACTORS	W.H.O		E.P.A		M.A.C		IRAQI STANDARI	
(MG/L)	REC.	MAX.	REC.	MAX.	REC.	MAX.	REC.	MAX.
PH	----	----	6.5	8.5	----	----	6.5	8.5
TDS	500	1500	500	----	1500	3000	----	----
Total Hardness	100	500	----	----	30	80	----	500
Calcium	----	----	----	----	150	350	----	200
Magnesium	----	150	----	----	75	150	50	150
Chloride	200	600	250	----	600	900	200	600
Sodium	----	----	20	200	400	800	----	200

W.H.O = World Health Organization
E.P.A = Environmental Protaction Agency
M.A.C = Middle Asia Classification

[15] Prickett, T.A, Haymik, T.G, and Lonnquist, G.G A "Random walk" solute transport model for selected groundwater quality evaluation. Illinos State Water Survey, Illinos, U.S.A. Co., St. Louis, U.S.A (1981).

[16] Steel, E.W. Water Supply and Sewerage. 4th ed. McGraw Hill (1960).

[17] W.H.O Guide linefor drinking water quality recommendations Vol 1, Geneva. (1984).

Al-Mustansiriya J. Sci Vol. 6 , No. 1 , 1996

Synthesis and Identification of a Series of 4-Phenylginoline Derivatves by palladium Coupling Reaction

NAJY M. ALI, MUSA A. KADAM AND ABDULLA M. ALI
College of Education, Department of Chemictry , University of Koufa, IRAQ.
(Recieved 15 Oct. 1993; Accepted 31 May, 1994)

الخلاصة

تم في هذا البحث تحضير سلسلة من مشتقات 4 - فينايل كوينولين بواسطة مركبات 4 - (1H) - كوينولون باستخدام POCL3 ومن ثم ادخال مجموعة الفينايل في الوضع الرابع بواسطة تفاعل الازدواج الحاصل بين فينايل حامض البورونيك مع مشتقات 4 - كلورو - كوينولين بوجود معقد البلاتين كمحفز.

ABSTRACT

A series of 4-phemylquinoline derivatives were prepared by chlorination of 4-(1H)- quinolone compounds using phosphoryl chloride as chlorinating agent. The introduction of a phenyl group at position four was made by palladium catalysed cross-coupling reaction between phenylboronic acid and 4- chloroquinoline compounds.

INTRODUCTION

Few works have been published for the synthesis of 4-phenylquinoline compounds. Dienys and co-workers (1) were able to isolate the picrate derivative of the compound in very low yield (20-35%) and they found that the electron-withdrawing groups like NO 2 make the cyclization processes more difficult.

In this paper we were able to synthesis a series os 4-phenylquinoline derivatives by chlorination of 4-(1H)-quinolone followed by a cross-coupling reaction with phenylbronic acid to give the required 4-phenylquinoline derivatives in good yield (7).

Experimental

Melting points were determined on an Electro-thermal melting point apparatus, Infrared spectra were recorded on Perkin-Elmer Infrared spectrophotometer. Proton NMR spectra were recorded on EM-90 MHZ with (TMS as internal standard.

Preparation of 4-(1H)-quinolone derivatives

A solution of 2,2-dimethyl-1, 3-dioxane-4, 6-dione (2) and trimethylortho formate was heated under reflux for two hours then a solution of arylamine derivative in trimethylorthe formate was dadded and heating under reflux as continued for a further five hours. Evaporation of the solvent under reduced pressure gave a yellow solid of crude arylamino - methylene derivatives. Recrystallization from methanol gave the corresponding arylaminomethylene derivatives (Table 1).

Cyclization of these derivatives was carried out in boiling diphenylether and the cyclized products were isolated as solids and recrystalized from petroleum ether and the results are shown in Table 2.

Preparation of 7-methoxy-4-chloroquinoline (8).

A solution of 7- methoxy-4-quinolone (3 g, 12mmol) in phosphoryl chloride (20)ml was heated under reflux with stirring for 3 hours. The reaction mixture was then poured into ice and neutralised with 10% NaOh. The solid which seperated was collected by filtration and dried to give 2g (95%) of crude 7-methoxy-4-chloroquinoline.

Recrystallization from cyclohexane gave 1.8g (89%) of pure product as colorless meedles. The results of all chlorinated derivatives are shown in Table 3.

Preparation of 4-phenyl-7-methoxyquinoline dreivatives

A solution of phenyl boronic acid (1.5g, 12mmol) in ethanol (3 ml) was added to a stirred mixture of tetrakis (triphenyl phosphine) palladium (0.5g, 4 mmol), benzene (20 ml), 4-chloro-7-methoxyquinoline (2g, 10 mmol), and aqueous sodium bicarbonate (10 ml, 2M). The reaction mixture was heated under reflux with stirring for 30 hours. The reaction mixture as extracted by stirring with ethylacetate (2x100 ml) and the combined organic extracts were wased with water. dried (MgSO4), filtered and evaporated under reduced pressure to give a thick brown syrup which solidified on scratching. Recrystallization from toluene gave the pure products. The physical data of all 4-phenylquinoline compounds are given in Table 4.

Results and Discussion

The aim of this work is to study the effect of electron withdrawing or electron-donating groups on the cyclization of an arylaminomethylene Meldrum's acid derivatives since Dinny's and co-workers (3) found that the cyclization processes of B-(O-nitroanilino) propiophenone using HCL/ ethanol as cyclizing ageht more difficult. It is clear that from the results of cyclization in (Table 4) that the electronic effect do not have a marked influence on the cyclization step to form the pyridone ring.

Our method involves the chlorination of 4-(1H)-quinolone which gave the 4-chloroquinoline in good yield. The successful palladium catalysed cross-coupling of phenyloboronic acid with haloarynes developed by Miyaura et al (4) promped us to investigate this procedure for the synthesis of phenylated quinoline compounds, especially because Miller and Dugar (5) were able to prepare mononitrobiphenyls by this method. Thus the coupling reaction of phenylboronic acid with a number of 4-chloroquinoline gave a good to moderate yield as showen in Table 3.

Finally 4- phenylquinoline compounds were considered as precursors for the synthesis of novel tetracyclic aromatic alkaloids with antineoplastic activity and powerful Ca-releasing activity in Sarcoplasmic Reticulum (6).

Table 1: The Physical date of arylaminomethylene derivatives

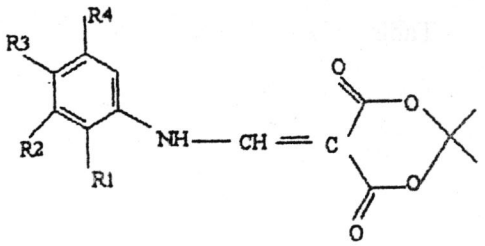

Comp.	R1	R2	R3	R4	Yield %	M.Pc	HNMR(CDCL3)	IR $_2$Cm^{-1}
1	H	OCH3	H	H	85	160-162	8.5(1H,D,J=14Hz,CH), 7.6(4H,M,Ar H)1.5(6H, S,CH3),4.1(3H,S,OCH3)	NH 3120 CO 1720 and 1675
2	OCH3	H	H	NO2	70	185-188	8.5(1H,d,J=14Hz,CH), 7.5(3H,m,ArH),1.6 (6H,S,CH3),4.1(3H,S,OCH3)	NO2 1580 and 1375 NH 3300 CO 1725 and 1675
3	NO2	H	H	H	65	202-205	8.6(1H,d,J=(14HZ,CH),7.7 (4H,m,ArH)1.7(6H,S,cH3)	No2 1580 and 1375 1725 and 1675
4	HO	H	H	H	78	155-158	1.7(6H,S,CH3),8,7(1H,d,J= 14HZ,CH),7.5(4H,m,ArH)	
5	H	OCH3	OCH3	H	75	140-144	1.6(6H,S,CH3),4.1(6H,S,0CH3) 8.7(1H,d,J=14H_2,CH),7.5 (3H,m,ArH)	NH 3120 CO 1720 AND 1675
6	CH3	CH3	H	H	65	135-138	1.6(6H,S,CH3),1,1.8(6H,S, CH3), 8.7(1H,d,J=14H_2,CH 7.6(3H,m,ArH)	NH 3130 CO 1720 CO 1720 and 1675

Table 2 Preparation of 4-(1H)- Quinolone derivatives

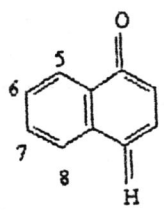

Comp.	Yield%	M.PC°	^{1}HNMR(CDCL3)	IR Cm^{-1}
7-methoxy	85	242-44	4.0(3H,S,0CH3),7.1(3H,m.ArH), 7.0.7.2(1H,d,J=6H_2,NH-CH=C), 8-8.4 (1H,d,j=6H,NH--C=CH)	CO 1620
8-hydroxy	75	220-223	7.1(3H,m,ArH) 7-0-7-2(1H,d,J=6H_2, NH-CH=C),8-8.4(1H,d,J=6H_2,NH-C=CH)	OH 3300 =C-H 3030-3050
8-nitro	62	310-315 dec	7.2(3H,m,ArH),7-7.5(1H,d,J=6H_2, NH-C=CH),8-8.4(1H,d,J=6H_2,NH-CH)	CO 1625
8-methoxy	70	238-241	7.1(2H,m,ArH), 7.2-7.5(1H,d,J=6H_2, NH-CH=C),8.83(1H,d,J=6H_2,NH-C=CH, 4.0(3H,S,0CH3)	CO 1600 =C-H 3020-3040
6,7-dimethoxy82	82	265-268	7.0(2H,m,ArH),4.0)6H,S,0CH3), 7-2-7.5(1H,d,J=6H_2,NH-C=CH), 8-8.3(1H,d,J=6H_2,NH-C=CH)	NO2 1550 AND 1675 CO 1600 =C-H 3020-3040
7,8-dimethy172	172	255-258	7.0(2H,m,ArH,3.5(6H,S,CH3), 7-2-7-5(1H,d,J=6H_2,NH-C=CH) 8-8.3(1H,D,J=6H_2,NH-C=CH)	CO 1600

Table 3: Preparation of 4-chloro -quinoline compounds

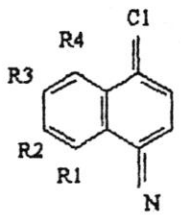

Comp	R1	R2	R3	R4	Yield %	M.P.C.	^{1}HNMR(CDCL3)	IRCM^{-1}
1	H	OCH3	H	H	80	85-87	4.0(3H,S,OCH3),8-8.6(1H,d, J=3H_2,N=CH),7-7.8(3H,M,ArH) 7-67.64(1H,d,J=3H_2,CH=C-C1)	C=C 1600 C=C aro. 500
2	OCH3	H	H	NO2	85	12-121	4.0(3H,S,OCH3)8.6-8(1H,d,J= 3H_2,N=CH)7.5-7.6(1H,d,J=4H_2,CH =C-C1),6.9-7.8(2H,d,ArH)	NO_2 1580 and 1310
3	NO2	H	H	H	50	90-93	8.08.6(1H,d,J=3H2,N=CH),7.4-7.6 (1H,d,J=3H_2,CH=C-C1),7.0-7.3 (3H,m,ArH)	NO2 1580 and 1310
4	CH3	CH3	H	H	82	125-127	7.0-7.4(2H,m,ArH)3-3.4(6H,S, CH3),8-8.4(1H,d,J=3H2,N=CH), 7.5-7.7(1H,d,J=3H_2,CH=C-C1)	C=C 1600
5	H	OCH3	OCH3	H	90	115-118	4-4.3(6H,S,OCH3),8.6-8.7(1H. d,J=3H_2,N=CH),7.5-7.7 (1H, d,J=4H_2,CH=C-C)7-7.2(2H,d,ArH)	C=C 1600
6	HO	H	H	H	75	112-115	8.6-8.7(1H,d,J=3H_2,N=CH),7.6-7.8 (1H,d,J=4H_2,CH=C-CL),7.0-7.4 (3H,M,ArH)	OH 3300-3500

Table 4: Preparation of 4-Phenylquinoline derivatives

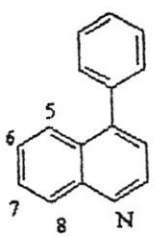

Comp.	Yield	M.P.C.	^{1}HNMR(CDCL3)	IRCM^{-1}
7-methoxy	80	108-110	4.0(3HS,OCH3),7-0-7.4 (9H,m,ArH),8.6-8(1H,d, J=3H_2,N=CH)	C=C 1600
5-nitro-8-methoxy	81	136-140	4.0(3H,S,OCH3),8.0-80 (1H,D,J=4H_2,N=CH)6.8-7.6 (8H,m,ArH)	NO2 1550 and 1350
8-nitro	65	125-127	7.6-8.0(9H,m,ArH)8.8(1H,d N=CH)	NO2 1355 and 1555
7,8-dimethyl	83	102-104	3-3.4(6H,S,OCH3),7-6-8(7H,m,ArH), 8.8 (1H,d,N=CH)	C=C 1600
6,7-dimethoxy	85	114-117	4.0(6H,S,OCH3),7-7.4(7H,m,ArH), 8.8(1H,d,N=CH)	C=C 1600
8-hydroxy	73	106-109	7.7-8.3(9H,m,ArH),9.0 (1H,d,J=3H_2,N=CH)	OH 3200-3400

REFERENCES

[1] Dienys, G., Gureniciene, J., and Steponavicius, J. Cyclization of B-arylamino Propiophenone into 4-Substituted quinolines. Chem-Abs.87(53052w). (1977).

[2] Davidson, D., Bernhard, S.A. Preperation of 2,2-dimethyl-1,3-dioxane-4,6-dione (Meldrum's acid). J. Am- Chem-soc.70(3424-3426). (1948).

[3] Dienys, G. and Co-worker. Cyclization of B-arylamino propiophenone into 4-substituted quinolines. Liet. TSR Mokslu Darb. 1(33-38). (1977).

[4] Miyaura, N., Yanagi, T., and Suzuki, A. Palladium catalysed cross-coupling of phenyl boronic acid with haloarenes. Synth. commun. (510-513). (1981).

[5] Miller, R.B. and Dugar, S. Stoichi-ometric synthesis of unsymmetrical mononitro-biphenyls via the palladium-catalysed cross-coupling of arylboronic acids with aryl bromides Organometallics. 3(1261-1263). (1984).

[6] Kobayashi, J., and Co-Worker. Cystodytins A, B, and C, Novel tetracyclic aromatic alkaloids with potent antineo plastic activity from the Okinawan tunicate cystodytes dellechiajei. J-Org-Chem-53 (1800-1804). (1988).

[7] Stavenuiter, J., Hamzinz, M., Zomer, G. Palladium-catalysed cross-coupling of phenyl boronine acid with heterocyclic aromatic halides. Heterocycles. 26 (2711-2715). (1987).

[8] Kubo, A., and Shinsuke, N. Synthesis of Amphimedine , A new fused aromatic alkaloid from a pacific sponge, Amphimedon sp. Heterocycles. 27 (7095-2098). (1988)

Photoacoustic Detection of Laser Induced Damage in Optical Materials

LATFY A. MAHMOOD, RAFA M. SAIED AND MOHAMED N. ALWAHHAB
Department of Physics, College of Education, University of Tikrit, Tikrit, IRAQ.
(Recieved 11 Oct. 1993; Accepted 12 Feb., 1994)

الخلاصة

تم في هذا البحث دراسة طريقة جديدة لاكتشاف المراحل الاولى من دمار الليزر المستحث في المواد البصرية بلاعتماد على الظاهرة الصوت ضوئية Photoacoustic effect . لقد وجد بان حد العتبة للدمار المستحث باعتماد هذة الطريقة يكون دائما اقل من حد العتبة المقاس بطريقة اخرى.

ABSTRACT

In this work a real-time monitoring technique of the early stages of laser induced damage in optical materials has been investigated. Damage is monitored using the phtoacoustic signal generated in the optical component and detected by a pizoelectric transducer attached to the sample. It was found that the damage threshold measured using this technique was always less than the reported in the literature.

INTRODUCTION

photoacoustic effect is the production of an acoustic signal when a sample of matter is exposed to a beam of intensity modulated radiation or a transient heating. The concept on which the photoacoustic is based is quite old and the analogous effect commonly referred to us the optoacoustic effect has been used for many years in the study of optical absorption in gases. The change of name from optoacustic to photo acustic has been instituted to reduce the confusion with the acousto-optic effect in which light interact with acoustic or elastic waves in solids.

The phoyoacoustic effect was discovered in the nineteenth century by Alexander Graham Bell [1]. After the initial flurry of interest by Bell's original work, experimentation with the photoacoustic effect apparently ceased. The effect was obviously considered as being no more than an intresting courusity of no great scientific or practical value, furthermore, the experiment were difficult to perform since they required the investigater's ear to be the signal detector. The photoacoustic effect was forggoten for nearly fifty years until the advent of microphones, since then a progressive improvement and development has occured.

The advent of lasers provided a major impetus to the photoacoustic effect with application especially in spectroscopy.

Experimental

This is shown in figure (1), the laser was a CO_2-TEA laser described fully in ref (2), this laser generates a pulse which is 80 ns (FWHM) and contain 70 mj of energy. This pulse was fecussed on the sample to a spot-zise of 0.25 mm by short focus germanium lens. The energy density of the sample surfase was varied using thin polythene sheets which experimentally found to attenute the laser energy independedlly as shown in figure (2).

The samples were circular discs 50 mm in diameter and 5 mm thickness, the samples were always placed at the focus of the laser beam. One of the transducers descirbed elsewere[3] was attached acostically to the rear surfase of the sample with a viscuos fluid as silicon grease. The sample-transducer assembly was mounted on a holder which permitted the rotation of the sample about its axis with the transducer being on the axis so that the distance from each illuminated site is the same. Part of the laser energy was diverted by sodium chloride flat acting as a beam splitter for the porpose of energy measurement.

Results and Discussion

A range of samples were damage tested, these included mettalic samples, dielectrics and thin films. The mettalic samples were :

1- high purity copper
2- Aluminum, type BS 325 S21
3- Stainless steel type BS1477/HF30TF
4- Molybdum.

The first three samples uderwent roughing on a grinding mechain before being wet polished on a circular lap with 0.25 m particles abrasive to an optical finish. The dielectric samples were sodium chloride and pottasium chloride while the thin film samples included high reflection films on germanium, copper-nikel mirror with hard gold coating and gold film on aluminum substrrate.

Laser induced damage was detected by gradually increasing the energy density on the sample surfase until a big increase in the magnitude of the photoacoustic signal was recorded by the transducer. Each data point is obtained at different site on the sample, table 1 list the measured damage thresholds of the samples tested, also shown are the published damage thresholds for the same samples. les.

A typical form of the photoacoustic signal recorded by the transducer is shown in figure 3, this signal was recorded in sodium chloride.

The scope was triggered by the CO_2 laser pulse, the delay to the first peak is associated with the time for the photoacoustic signal to reach the transducer from the illuminated site, while the hight of the first peak correspond to the longitudinal wave which travel directly to the transducer, this also taken as a measure

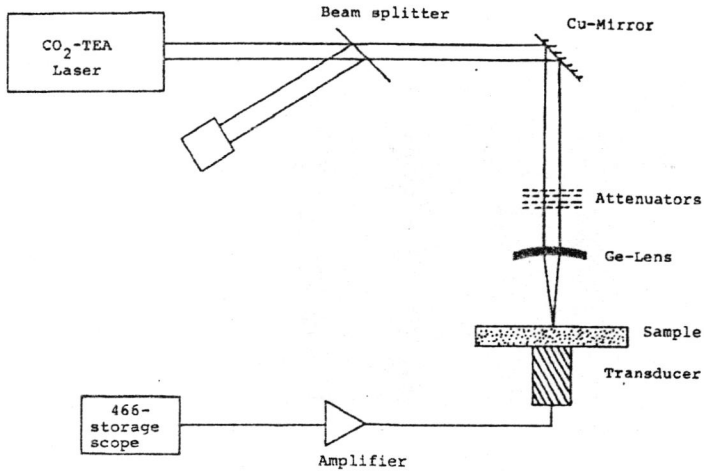

Figure(1): The experimental set-up

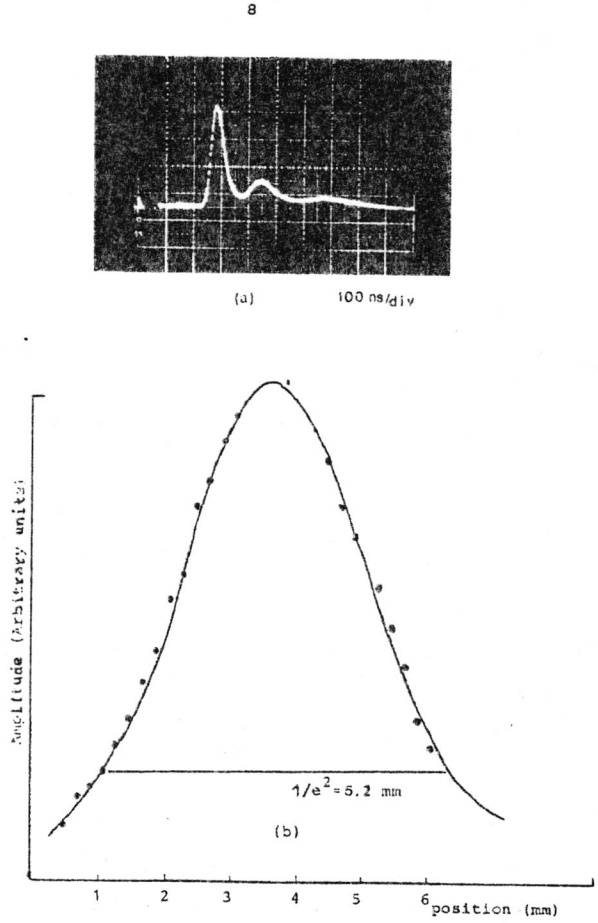

Figure(2): a)the temporal profile of the CO2 laser pulse.
b)The spatial profile of the CO2 laser pulse.

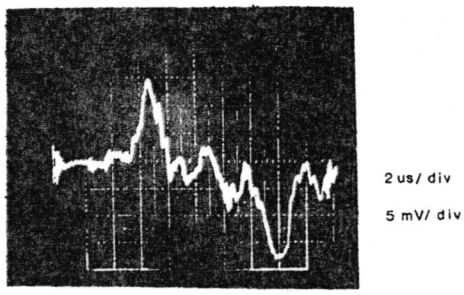

Figure(3): Typical from of the photoacoustic signal in sodium chloride, incident energy is 10.52 mj

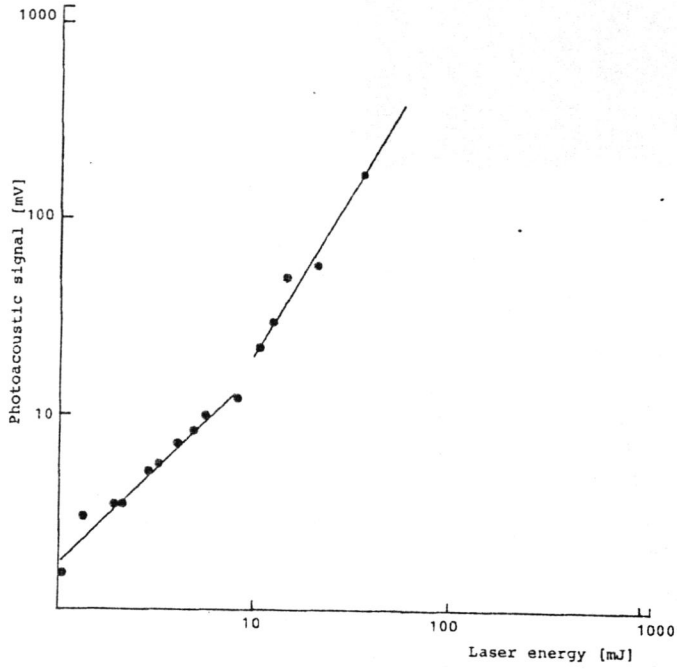

Figure(4): Photooacoustic signal as a function of laser energy in Sodium Chloride

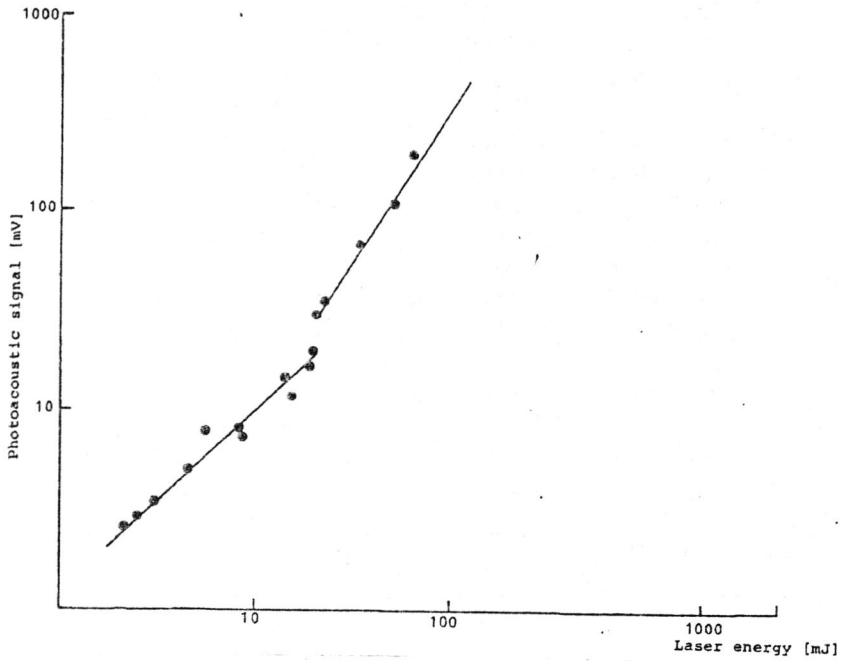

Figure(5): photooacoustic signal as a function of laser energy in Molybednum

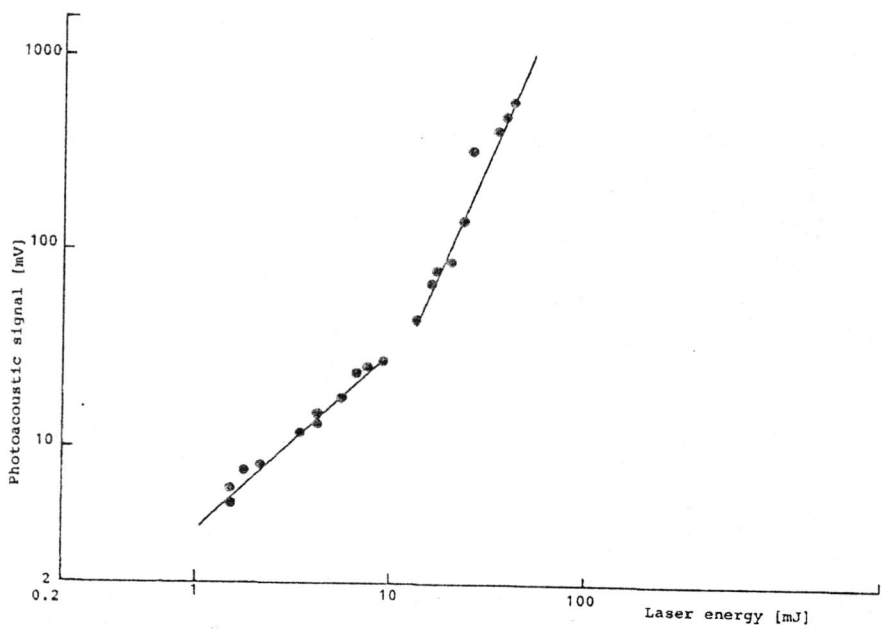

Figure(6): Photooacoustic signal as a function of laser energy in HR-germanium

of the absorbed energy to avoid any reflection or mode conversion arriving at the transducer later on. Care was taken to prevent any scattered light from reaching the transducer, figure 4,5 and 6 show the photoacoustic signal as a function of the laser energy for sodium chloride, molybdium and Hr film on germanium substrate respectively. The slpoes of these figures were measured and found to be 1±0.05, 1.17±0.24 and 1.02-+0.003, therefore the photoacoustic signal shows an essentially linear dependence on the incident laser energy before damage, when damage start to occur the signal increases noticeably and for energy densites greater than the damage threshold of the sample the photoacoustic signal appear to follow a simple power law behaviour with the energy i,e;

$$S = A E^n$$

Where S is the photoacoustic signal, n is the power dependence of the signal and A is a constant.

The magnitude of n depends on the nature of the sample and its value is generally less than 3 for metals while for dielectrics materials n is greater than 3. The measurement of the energy at the point where the graph between the incident energy and the measured photoacoustic signal change its gradient marks the damage threshold of the sample unde r damage test.

A photoacoustic signal is always present whenever any of the laser pulse is absorbed by the sample. This signal is always detected by the transducer since the wavelength of the photoacoustic signal generated is considerably larger than the focussed spot-size of the laser pulse on the sample surfase.

Figure 4,5 and 6 show the photoacoustic signal suffers a major change when damage occurs. One might think that the increase in the signal is due to the acoustic emission assciated with the mechanical change, this, however is not the case, it must be kept in mind that below damage most of the absorbed energy will be converted to heat at the sample surfase and a photoacoustic signal will be produced immediatly. When damage start some of the absorbed energy will be used in breaking bonds and some will be used for melting. Therefore, a decrease in the signal shoud be expected rather than an increase. The increase in the signal is therefore is not due to the increased acoustic emission, it is due increased absorption process. It is well known, for example, that the reflectivity of most metals is reduced when they they are subjected to a high intensity laser pulses (4,5,6,7) or metals may undergose anamolous absorption.

Beyond damage threshold the increase in the photoacoustic signal continue at the same rate.

Table 1

sample	damage thre J/cm2	published thre	ref
stainless steel	4.07	4.60	8
Al	11.90	14.00	9
Cu	63.69	67.00	8
Gehr	16.70	--	--
Mo	24.06	25.00	8
Kcl	51.00	52.20	10
Nacl	68.00	92.00	10
N1/cu	20.90	--	--
Au/Glass	21.20	--	--

REFERENCES

[1] Bell, A.G., generation of sound by modulated light, Phil. Mag., 11,510(1881).

[2] Stark, D.S et al, a compact sealed pulsed CO2 TEA laser, IEEE. J. Quantum. Electronic . , QE-11,1381(1975).

[3] Mahmood, L.A.,ph.D theses, Loughborough University of Technology, Loughborough. U.K(1985).

[4] Zavecz, T.E, Saifi. F, transient reflectivity of aluminm subjected to a high power laser radiation, Apll. Phys. Lett., 26.165(1975).

[5] Chun, M. K. and Rose.K, effect of laser radiation on the reflectivity of metallic surfases. J. Appl. Phys., 41,614(1971).

[6] Duley.W.W, "CO2 lasers., effects and application" Academic press (1970).

[7] Ready, J.F. "effect of high power laser radiation " Academic press (1971).

[8] Figueire ,J.F and Thomas, S.J, damage thresholds at metal surfaces for short pulse IR laser., IEEE. J.quantum. Electronics. QE-18.774(1982).

[9] Spark, M and Loh, E,Jr, laser induced damage in optical materials, part I melting., J.Opt.Soc.Am.,69,874(1979).

[10] Porteus, J.O, Soilcau, M.J and Fountain, C.W., laser induced damage in optical materials.. NBS spec pub.,462.165(1976).

Al-Mustansiriya J. Sci Vol. 6, No. 1, 1996

Measurement of Removal Cross Sections of 14.5 MeV Neutrons for A1, Fe and H_2O

ABBAS JEWAD AL-SAADI
Physics Department, College of Eduecation, AL-Anbar University, Anbar, IRAQ.
(Recieved 1 Dec. 1992; Accepted 10 Nov, 1993)

الخلاصة

وجدنا في هذا العمل توهينا للنيوترونات ذات الطاقة (14.5) مليون الكترون فولت في كل من المواد(الالمنيوم والحديد والماء) وقد عين بأستخدام الكاشف الوميضي العضوي السائل نوع (NE213) . ان توهين فيض النيوترونات الاولية في مواد مختلفة يمكن وصفه بصورة جيدة بأستخدام المقطع العرضي للازالة الذي عين في هذا البحث. ان القيم الحاصلة للمقاطع العرضية للازالة مطابقة للقيم النظرية ضمن حدود الخطأ. اما الانحراف الحاصل بين هذه النتائج والبيانات الحاصلة من قبل عدة باحثين فيمكن ايجازه بواسطة الاختلاف في منظومات القياس.

ABSTRACT

In the present work the attenuation of 14.5 MeV neutrons in different types of shietlging materials (A1,Fe and H_2O) are determined, using the NE-213 detector for detection of the primary neutrons. The attenuation of primary flux in different materials is well defined by simple exponential relation based on the removal cross section which were determined. The predicted values of removal cross sections are in agreement with the theoretical determinations. The devation between the present resurlts and the earlier data obtained by the other authors can be explained by the geometry difference of the measurements.

INTRODUCTION

The concept of removal cross section can be used for a rapid estination of the neccessary shielding for neutron sources. The macroscopic removal cross section $\sum_R (cm)^{-1}$ is defined as the effective probability for the removal of neutrons from incident energy range. The microscopic removal cross section per atom δ_R (barn) equal the sum of microscopic inelastic and absorption cross sections plus a fraction of the microscopic elastic cross section. Tle relation between The macroscopic and microscopic removal cross sections for any element is given by {1,2,3]:

$$\sum_R = \frac{0.602 * \delta_R * \rho}{A} (cm)^{-1} \qquad (1)$$

Where ρ is the density of the element in gm/cm^3 and A is the atomic weight.

The flux of primary neutrons at a distance r from the point source of the strenght s is represented by [2,4]:

$$\phi(r) = \frac{S}{4\pi r^2} * e^{-\sum_R (r-r)} \qquad (2)$$

where $\sum_R$ is the macroscopic removal cross section and (r-r)=x is the total thickness of shield traversed. When the distance r is fixed, the flux of primary neutrons can be defined by the relation [1,5]:

$$\phi(x) = \phi(0) e^{-\sum_R \cdot x} \qquad (3)$$

Where $\phi(x)$ & $\phi(0)$ are the flux of primary neutrons for a shielding of thickness x and with out shielding respectively.

Removal cross sections has been measured [3,4,5,6] for various elements and construction materials by activation threshold detectros.

The NE213 detector seems to be a suitable technique to determine the removal cross section in a more rapid way and additionally gives the possibility of studying the induced secondary radiadions [7,8]. Using fixed source detector geometry, the logarithms of relative intesities (I/I.) plotted against x results is a straight line with a slop of $\sum_R$ from which the δ_R for different materials can be determined.

Experimental arrangement

The geometrical arrangement used in this work is shown in Fig.1. The neutron generator (High Voltage Engineering type T400) produces deutrons with an energy of 110 KeV at current of 100 μA, the deutrons impinge on a target which consist of tritum absorbed in titanum layer on copper. Neutrons were produces in the $^3_1[H(d,n)]^4_2$ He reaction. The anergy and yield of neutrons emitted from the target depend on the angle between the incident deutron beam and the emerging neutrons [1,2].

The energy of neutrons emitted in the zero direction to the incident deutron beam (in the forward direction) was 14.5 ±0.15 MeV and the maximum neutrons output per second is about $5*10^8$.

The samples of A1 and Fe shaped in rectangular plates with dimensions of 60 cm x 60 cm and aluminium containers used for water samples.

Two liquid organic scintillator detector type NE-213 used in this research, one of them was used to detect the primary neutrons that of threshold energy 14 MeV in the forward direction of the deutron beam, and the second was used as a source strenght

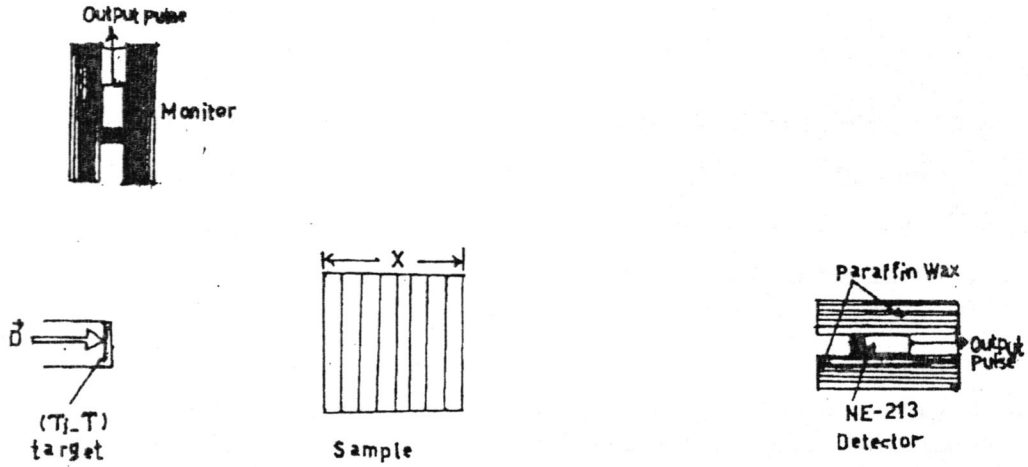

Figure(1): Geometrical arrangent of the measurement

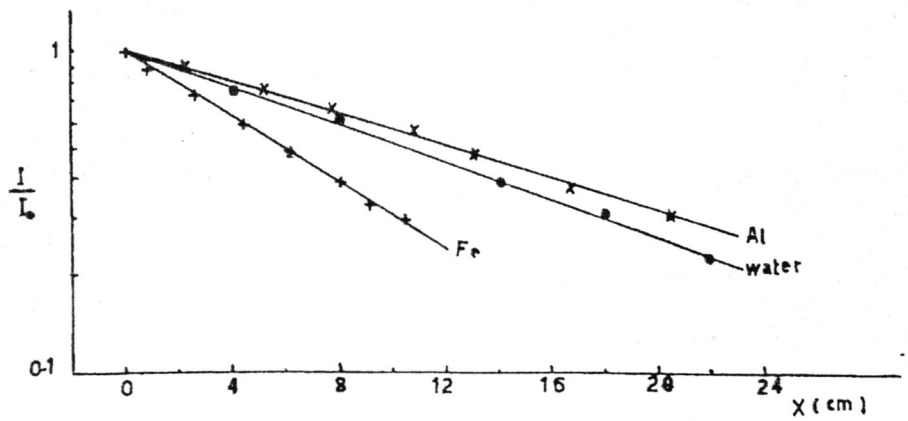

Figure(2):Semilogarithic plots of the relative intensities as a function of shield thickness.

mointor positioned at an angle of 90° to the forward direction of the deutron beam. The detectors were shieldedwith a 40 cm deep paraffin wax sylindrical collimator with a diameter 7 cm.

The distances of source -sample and source- detector are 130 cm and 450 cm respectively.

Results and Discussion

After performing the neutrons intensity measurements with different shield thickness (x), the values of Ln(I/I) as a function of x can be well approximatedby straight line (see Fig.2). The macroscopic removal cross sections obtained in this experiment for various materials are given in Table 1. The error are determined from the least-squares fitting. The macroscopic removal cross sections were also deduced using formula (1).

Experimental values of δR for A1 and Fe obtained show good agrrement with the calculated [1] and with the measured by activation threshold detectors [4,6], the previous valus of $\sum_R$ =0.07190 ± 4% for water [3] is good agreement with our result, therefore, the deviation between the present results and the earlier data obtained by activation threshold dectors is about (7%) this difference is due to the variation of neutron energy, dimensions of sample and the purity of the elements inthe sample

Table(1): Experimental results

Shielding Material	Present work $\sum_R$ $(cm)^{-1}$	δ_R(barn)	Previous work $\sum_R$ $(cm)^{-1}$	δ_R(barn)	Reference Number
A1	0.0570+0.0021	0.9450+0.034	-----	1.04	(1)
			0.0622+0.003	1.04± 0.04	(4)
Fe	0.1122+0.0035	1.325+0.041	-----	1.52	(1)
			0.1200+0.01	1.41± 0.04	(4)
H_2O	0.0672+0.0027	-----	0.0719+0.003	-----	(3)

REFERENCES

[1] Nargolwalla, S.S. and Przybylowicz E.P. " activation Analysis with Neutron Generators; J. Wiley and Sons, New York, London, (1973).

[2] Csikai,J."Hand book of Fast Neutron Generators," Vol.1,pp.(313-316), CRC Press, Florida, (1987).

[3] Varadia, Mr. and Bunkzo, Cs. "Determination of Macroscopic Removal Cross Section of 14 MeV Neutrons for phantom Solution, "Radiation Protection Dosimetry, Vol. 22 No.2.pp.(123-126),(1988).

[4] Bcufragect, A., Peto,G. and Csikai, J., "Removal Cross Section for 14.8 MeV Neutrons", Acta Physica Hungarica, 55(1-4), PP.(303-3100, (1984).

[5] Pozvap, o. and Day, L.R., Attenuation of 14 Mev Neutrons in Shields of Concrete and Paraffin Wax, Health Physics, Pergamon Press, Vol. 28,PP. (101-109),(1975).

[6] Cooper P.n. and Kabar, S.M.,"The Removal Cross Section of Iron at 14 Mev, Journal of Nuclear Energy, Vol. 26, PP. (569-571), (1972).

[7] Knoll, G."Radiation Detection and Measurement". J.Wiley and Sons New York, (1979).

[8] Al-saadi, Abbas J., Thesis, Study of Neutrons flux Distribution in Some Materials and Structures of Shielding Materials, University of Baghdad. (1990).

Al-Mustansiriya J. Sci Vol. 6. No 1, 1996

The Behavior of the Vertical Distribution of Atmospheric Ozone

KAMAL R. AL-RAWI
Department of Physics, College of Science, The University of Anbar, Anbar, IRAQ.
(Recieved 21 Nov. 1992; Accepted 24 June, 1993)

الخلاصة

حسب توزيع الاوزون مع الارتفاع باستخدام طريقة (امكر). حُسبت مراكز الثقل لكميات مختلفة من الاوزون الجوي. ان (ارتفاع مركز الثقل) يتناسب عكسياً بصيغة أسية مع كمية الاوزون الجوي. ان الجزء العلوي (والجزء السفلي) لطبقة الستراتوسفير، اكثر (واقل) حساسية لتغيرات كمية الاوزون. انهما يتاثران اكثر من المدى(المتوقع) واقل من المدى(المتوقع) على التوالي. الجزء الوسطي للستراتوسفير يميل لكسب الاوزون، بينما الجزء العلوي للستراتوسفير يميل لفقدان الاوزون.

ABSTRACT

The vertical distributien of ozone is estimated by Umkehr methed. The center of gravity for different atmespheric ozone has been computed. It is inversely prepertienal form with total atmospheric ozone. The upper and lower stratospheric layer are the most and least sensitive to total atmospheric ozone variations. They show undersheeting and overshooting. respectively. The midstratosphere has a gaining tendency for ozone, while the upper stratosphere has a loosing tendency.

INTRODUCTION

Eventhough, the thickness of the atmospheric ozone column is around (0.25±0.1)cm, at standard temperature and press are (OC°, 101. 325KPa), the ozone layer is crucial to both the general circulation of the atmosphere and to the existence of life on earth, due to the absorbtion of ultraviolet radiation (1).

Only in recent years, ozone became one of the most majer issue of public concerns. However, scientists studied atmospheric ozone and its vertical distributions long time age (2,3,4,5,6).

The variation of the ozone column density "can have significant effects on the relaxation rates of both ozone and temprature perturbations in the stratosphere" (7). In addition to the determination of vertical distribution of ozone, this paper has been conducted to analyze the response of the vertical distribution of ozone, to atmospheric ozone variations.

Methodology

The intersity of sunlight in the ultravielet region, at the earth surface, depends on both, the vertical distribution of ozone, and the sun zenith angle.

To determine the vertical distribution of ozone, the atmosphere has been divided into five layers, (0-10)km, (10-25)km, (25-35)km, (35-50)km, and over 50km. The ozone content for the above layers is designated as x4, x3, x2, x1, and x0, respectively.

The intensity of the primary scattered light, at the surface is (4);

$$I = k\beta \sum_{0}^{4} Ar 10^{-\alpha x_r} \quad \text{.....(1)}$$

Where K is a constant, β is the scattering coefficient, α is the absorbtion coefficient per centimeter of ozone. X is the path length in centimeters of ozone. For better accuracy in X, each layer has been divided into sublayers of one kilometer thick. A_r is the scattering integral;

$$Ar = \int_{0}^{p_0} 10^{-\beta F} \, dp \quad \text{.....(2)}$$

Where F is the air path from the top of the atmosphere to the scattering height, and from there vertically downward to the observer.

o eliminate the constant K, intensity ratie of two wavelengths, (3112A° and 3323A°), which have different absorbtion (1.23 and 0.08) and scattering (0.464 and 0.350) coefficients has been taken;

$$\frac{I(\lambda 1)}{I(\lambda 2)} = \frac{\beta 1}{\beta 2} \frac{\sum_{r=0}^{4} \int_{0}^{p0} Ar_{,}10 - \alpha 1 \, xr}{\sum_{r=0}^{4} \int_{0}^{p0} Ar_{,}10 - \alpha 2 \, xr} \quad \text{.....(3)}$$

The above equation is a function of x, x1, x2, x4, and the sun zenith angle. The value of x3 can be determined (x3=x-x1-x2-x4). For simplicity, ozone is treated as uniformly distributed through all the layers, except that for the upper stratosphere, where ozone is treated as exponentialy distributed. This is actually true in the troposphere (8). The total atmespheric ozone, x, is obtained from direct sun observations. xo is assumed equal zero (no ozone over 50 km altitude). Ozone concentration in the troposphere is affected by weather conditions; (9,10). However,

it is assumed to represent 7% of total atmospheric ozone (4). Two unknowns, x1 and x2 are left to determine. There are infinite different values of x1 and x2 to satisfy equ.(3). Therefore, observations for two different zenith angles (80° and 86.5°), are needed. The intersection of the two (x1, x2) curves, represents the numerical solution for x1 and x2. Observation for a third zenith angle (84°) has been employed for checking. The values of the $I(\lambda 1)/I(\lambda 2)$ were observed at Arosa (47°N), Switzerland, for three different values of x (0.40cm, 0.35cm, and 0.30cm) (11).

The center of gravity (CG) of the vertical distribution of ozone is computed as follow;

$$CG(\text{km}) = \frac{\sum_{r=1}^{n} h_r x_r}{\sum_{r=1}^{n} x_r}$$

Where h is the mean height of the rth layer in km.

Results and Discussion

The Vertical Distributions of Ozone:

Most of the atmospheric ozone is concentrated in the lower-stratosphere (10-25)km, see fig (1). The vertical distributions of atmospheric ozone (from bottom to top layer)are 0.028cm, 0.2865cm, 0.024cm, 0.0615cm for 0.40cm ozone. And 0.0245cm, 0.2435cm, 0.020cm, 0.062cm for 0.35cm ozone. And 0.021cm, 0.3005cm, 0.018cm, 0.605cm for 0.30cm ozone.

The centre of gravity for the above distributions is 21.596km, 22.123km, and 22.767km, for 0.40cm, 0.35cm, and 0.30cm ozone, respectively. Other centres of gravity have been derived from published vertical distributions of different amount of atmospheric ozone (3,6,12).

The centre of gravity is plotted against the total atmospheric ozone x. It shows that, the centre of gravity is inversely propertional in exponential form, with total atmospheric ozone, see fig (2). The main production region for ozone lie in midstratosphere, (13), and upperstratosphere (14), where the amount of air molecules and ultraviolet radiation is optimum for ozone production. Therefore we can conclude that, the center of gravity of vertical distribution of ozone, moving downward, toward the lowerstratosphere as atmospheric ozone increases. So we can say with out any doubt that, there is a downward vertical diffusion of ozone. This movement and long photochemical life time of ozone in lowerstratosphere explores the high ozone density at lowerstratosphere. Downward movement of ozone at midlatitude has been observed (15). This phenomena is very clear at low atmospheric ozone ($x < 0.200$cm). The phenomena becomes weaker as x increases. It becomes undetectable for atmospheric ozone of greater than 0.300cm.

The Ozone Distribution Index (ODI):

The auther defined the (ODI) for the rth layer, as the ratio of the actual gain (less) to the weighted gaim (less) of ozone content for that layer, where x changed by Δx (± 0.05cm)

CDI=(actual gain (loss)/weightrd gain (loss)

$$= \frac{\Delta x_r / \Delta x}{x_r / x}$$

$$\text{ODI} = \frac{\Delta x_r / \Delta x}{x_r / x} = \begin{cases} > 1 & \text{over-shooting} \\ = 1 & \text{normal} \\ < 1 & \text{under-shooting} \\ < 0 & \text{reverse-shootin} \end{cases}$$

Fig (3) shows that, the lower-stratosphere and the upperstratosphere, are the most and least sensitive regions to the atmospheric ozone variations. They are out of phase by π While the lower-stratosphere shows over-shooting tendency (ODI = 1.24 at 17.5km altitude), the upper-stratosphere shows under-shooting tendency. In addition to that, there is a weak reverse-shooting (ODI= -0.06 at 42.5km altitude). In other words, ozone decreases at this altitude, eventhough, atmospheric ozone increases.

The Ozone Distribution Index Gradient (ODIG):

The auther defined the ODIG for rth layer as the rate of change of ODI to atmospheric ozone variation x;

$$\text{ODIG} = \Delta(\text{ODIG})/\Delta x = \begin{cases} >0 & \text{gaining tendency} \\ =0 & \text{neutral} \\ <0 & \text{loosing tendency} \end{cases}$$

Each atmospheric layer, has different ODIG. The mid stratosphere shows gaining tendency (ODIG= 0.07mm^{-1} at 30km altitude). In other words, the ODI increase 7% for every one mm increase in atmespheric ozone. The upperstratosphere shows loosing tendency (ODIG= -0.023mm^{-1} at 42.5km altitude). See fig (4).

Summary and Conclustions

The center of gravity for vertical distribution of atmespheric ozone is inversely proportional in exponential form with total atmospheric ozone. The center of gravity moves from 26.6km altitude at x=0.160cm, to just about 20.8km altitude at x=4.0cm. The upper and mid stratosphere are the ozone production regions. Therefore there is a downword diffusion of atmospheric ozone. Increasing ozone concentration will increase the temperature at that layer, due to absorption of sun light. Temprature rise will alter the dynamic structure of the atmesphere, and will produce an injection process carrying ozone to the lower-stratosphere.

The value of ODI is diviated from unity in both lower and upper stratosphere. The lowerstratosphere shows over-shooting tendency (ODI > 1), While the upperstratosphere shows under shooting tendency (ODI<1).

As ODIG concern, the midstratosphere shows gaining tendency for ozone (ODIG > 0), while the upperstratosphere shows loosing tendency (ODIG < 0).

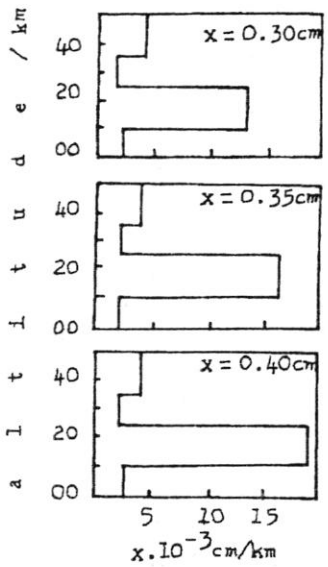

figure(1)

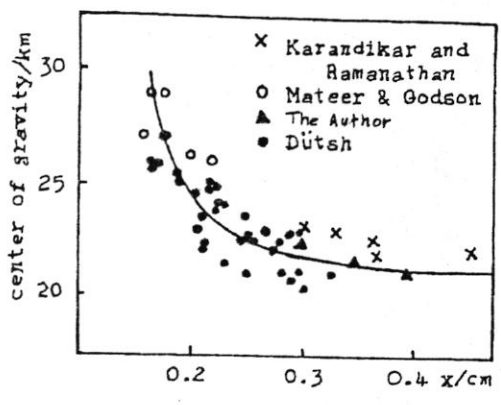

figure(2)

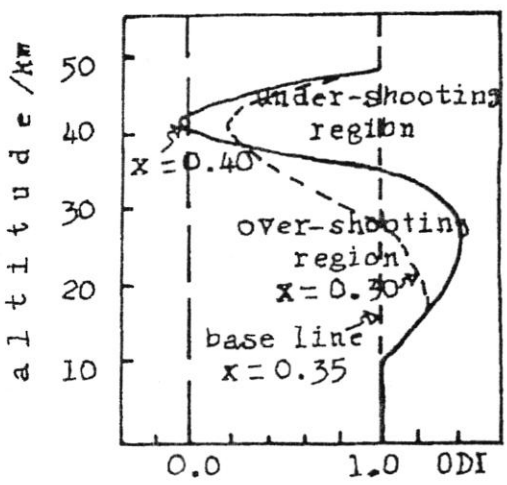

figure(3)

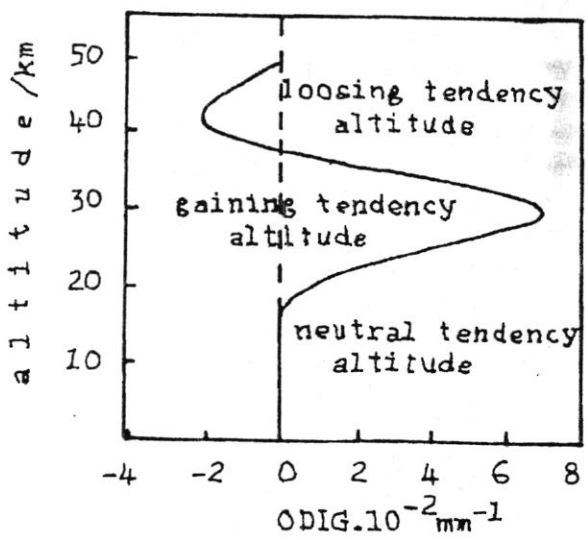

figure(4)

REFERENCES

[1] Holton J R,"An Introduction to Dynamic Meteorology", 2nd ad. Academic press, (1979)

[2] Gotz F W, Meetham A R, Dobson G M B, "The Vertical Distribution of Ozone in the Atmosphere", Royal soc. proc. series A 145-416, 417-447, (1934)

[3] Karandikar R V, and Ramanathan K R, "Vertical Distribution of Atmospheric Ozone in Low Latitudes", proc. Ind. Acad. Sci., 29, 330-348, (1949).

[4] Walton G F, "The Calculation of The Vertical Distribution of Ozone by Gotz Umkehr-Effect", Ann. I. G. Y., 5,9-22, (1957).

[5] Dutsh H U, "Vertical Distribution for Umkehr Observations", Meteor. Geoph. Bloki. All, 240-251, (1959).

[6] Mateer C L, and Godson W L, "The Vertical Distribution of Atmospheric Ozone over canadian stations from umkehr observations", Royal Meteor. Soci. Lond. 86,512-518, (1960).

[7] Hartmann D L, " A Note Concerning the Effect of Varying Extinction of Radiative-Photochemical Relaxation", J. Atmos. sci., 35,1125-1130, (1978).

[8] Wolff G T, Lioy P J, Meyers R E, Gederwall R T, Wight G D, Pascerl R E, and Taylor R S, "Anatomy of Two Ozone Transport Episodes in The Washington, d.c., to Boston, Mass., Carridor" Envir. Sci., Tech., 11,5,506-510, (1977).

[9] Guicherit R, and Van Dop H, "photo-Chemical Production of Ozone in Western Europe (1971-1975) And its Relation to Meteorology". Atmos. Environ., 11,145-155,(1977).

[10] Appling A J, Sullivan E J, Williams M L, Ball D J, Bernard R E, Derwent R G, Eggleton A E J, Hampton L, and Waller R E, "Ozone Concentrations in South-East England During The Summer of (1976)" Nature. Lond.269, 569-573,(1977).

[11] Mateer C L, "On The Information Content of Umkehr Observations", J. Atmos. Sci., 36, 350-364, (1979).

[12] Dutsh H U, "Evaluation of The Umkehr Effect by Means of a Digital Electronic Computer", Sci., Rep. No.1,USA, Contract No. AF(514)-905,(1957).

[13] Brewer A W, and Wilson A W, "The Regions of Formation of Atmospheric Ozone", Quart. J. Roy. Meteor. Soc., 94, 249-265, (1968).

[14] Hartmann D L, and Garcia R R, "A Mechanistic Model of Ozone Transport by Planetary Waves in The Stratosphere", J., Atmos., Sci., 36, 350-364.

[15] Dutsh H U, "Photochemistry of Atmospheric Ozone", Advan. Geophysics, 15, 219-322, (1971).

The Topographical Vertical Wind in Iraq

RASHEED H. S. AL-NAIMI AND BIDOOR H. YASEEN
Department of Physics, College of Science, AL-Mustansiriya University, Baghdad, IRAQ.
(Recieved 19 Dec. ,1992; Accepted 25 Oct., 1993)

الخلاصة

ان هدف البحث هو تحديد التوزيع العام لحركة الرياح الراسية في العراق الناتجة من عدم استواء سطح الارض معرفة تأثيرها في ظاهرة الغبار. ونظرا للتعقيدات الرياضية في الموضوع ولعدم كفاية المعلومات فقد وجد ان من المناسب استخدام طريقة مبسطة تفي بتحقيق اهداف البحث. لقد أضهرت النتائج ان الرياح الافقية الشمالية والشمالية-غربية والشمالية-شرقية والشرقية تنتج رياحاً رأ سية صاعدة في المنطقة الوسطى وأغلب اجزاء المنطقة الجنوبية من العراق والعكس بالعكس كذلك وجد ان الرياح الرأسية تلعب دوراً في تغذية وتلاشي الغبار في القطر.

ABSTRACT

This work is an attempt to give a broad-brush sketch of the vertical wind component, created by sloping terrain in Iraq, and to determine its influence on dust phenomenon. Due to mathematical complexities of the subject and to the lack of data therefor it is found convenient to use simplified methods to achieve the above purpose. Calculations showed that horizontal wind with northerly, northwesterly, northeasterly and easterly directions results in upward topographical wind motion in the middle and most parts of the southern regions of Iraq and vice versa. It has been found that the topographical wind plays an important role in feeding and suppressing dust in the country.

INTRODUCTION

Although the option of the atomospheric scientists who are interested in dust phenomenon in Iraq, covered a wide area in this field but it may be divided, generally, into three major categories. These categories are, the study of the effects of climatological and meteorological parameters [1,2,3,4], the estimations of the concentration, The size distribution of the particulates [5,6,7,8], and the understanding of the annual frequencies and its prediction [9,10]. However, researchers attention has not been directly oriented to the role of the vertical wind component, which is the most important element in dust and cloud development.

Vertical motion may be caused by one or more of the following:

a)Direct heating of the air layer close to the ground.
b)Large scale convergence and divergence of the horizontal wind near the earth surface.
c)Cold fornt.
d)Sloping terrain.

This work deals with the vertical motion, created by the latter effect with relation to dust phenomenon.

PRINCIPLES AND METHODOLOGY

In case of synoptic scal motion, the vertical winf component is typically of the order of less than 0.1 m/sec. However, the accuracy of general meteorological wind instrument is about 1 m/sec, thus, in general the vertical component is not measured in routine observation, hence, must be inferred from other measured parameters. However, there are practical difficulties involoved in this method. The calculation of orographical vertical wind component is rtunately, exceegingly being simplified. The simplification can be made in a manner similar to that suggested by patterson [11], which is based on the kinematical boundary conditions:

If the earth surface has has the equation [12]

$$\psi(x,y,z)=0 \qquad (1)$$

and is rigid and at rest, then normal component of motion is zero. In other words, the motion is tangential to the earth surface, so

$$V \cdot \nabla\psi=0 \qquad (2)$$

where $\nabla\psi$ is normal to the earth surface.

Suppose that the height above the mean sea level is given by:

$$z=z(x,y) \qquad (3)$$

Then

$$z-z(x,y)=\psi(x,y,z)=0 \qquad (4)$$

Hence

$$\overline{W_0} = \overline{U}.\frac{\partial z}{\partial x} + V.\frac{\partial z}{\partial y} \qquad (5)$$

where W_0 is the vertical velocity created by the sloping terrain and u and v are the horizonal wind components in east and north directions respectively.

Equation (5) is used to calculated W_0, where the horizontal wind is analyzed into u and v components. The values of these components are interpolated in a network of grid points with intervals of 110 km. The gradient components $\frac{\partial z}{\partial x}$ and $\frac{\partial z}{\partial y}$ are estimated for each of the grid point using the 1:5 x 10^5 scale topographical map of Iraq.

In spite of the fact that equation (5) gives W0 mathematically, nevertheless, practically it has to have some extrapolating and smoothing approximations. For instance, the observing stations are irregularly arranged, thus it is obvious that the horizontal wind component has to be extra grid points. Also the height of the terrain has to be smoothed for the minor irregularities.

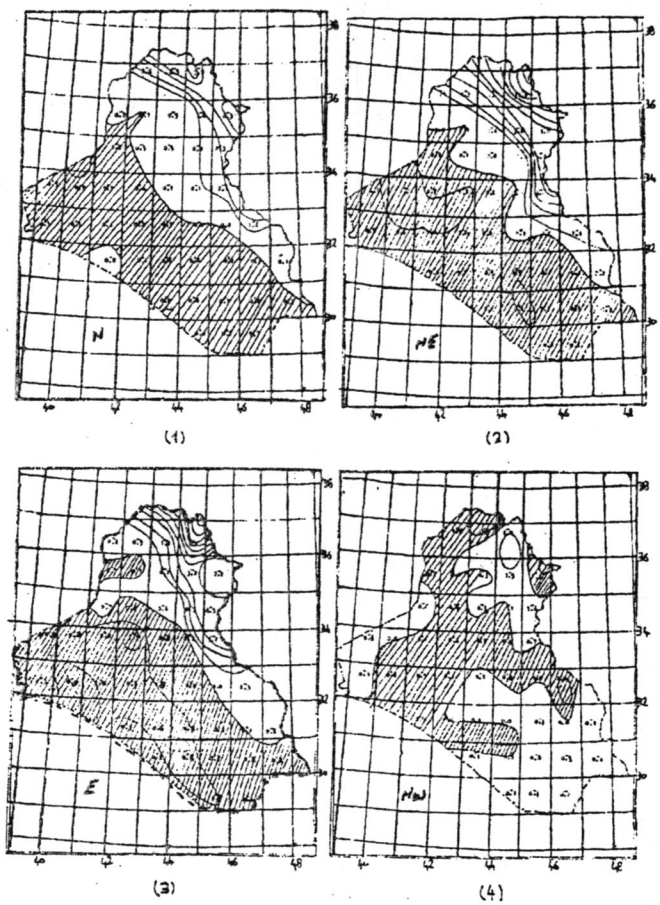

Figures (1-4) The general patterns of vertical wind componenet by assuming a horizontal wind of (1.N), (2-NE), (3-E), (4-NW) direction respectively. (+) upward (-) downward

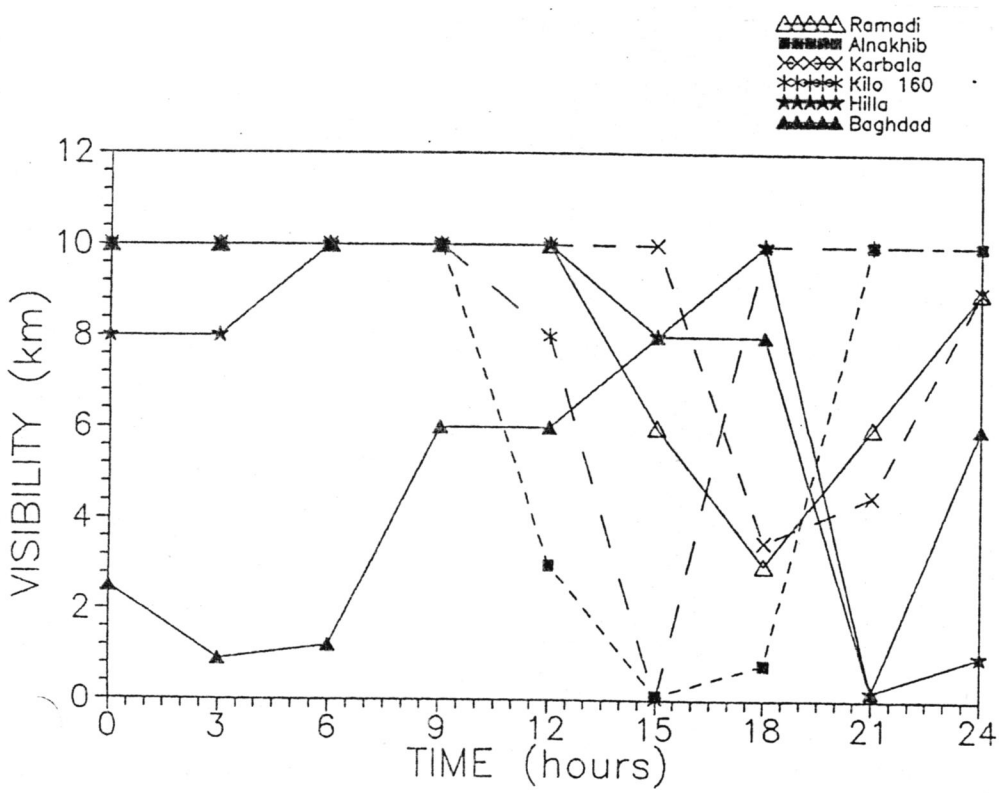

Figure (5) The time variation of the visibility on 1st April 1990

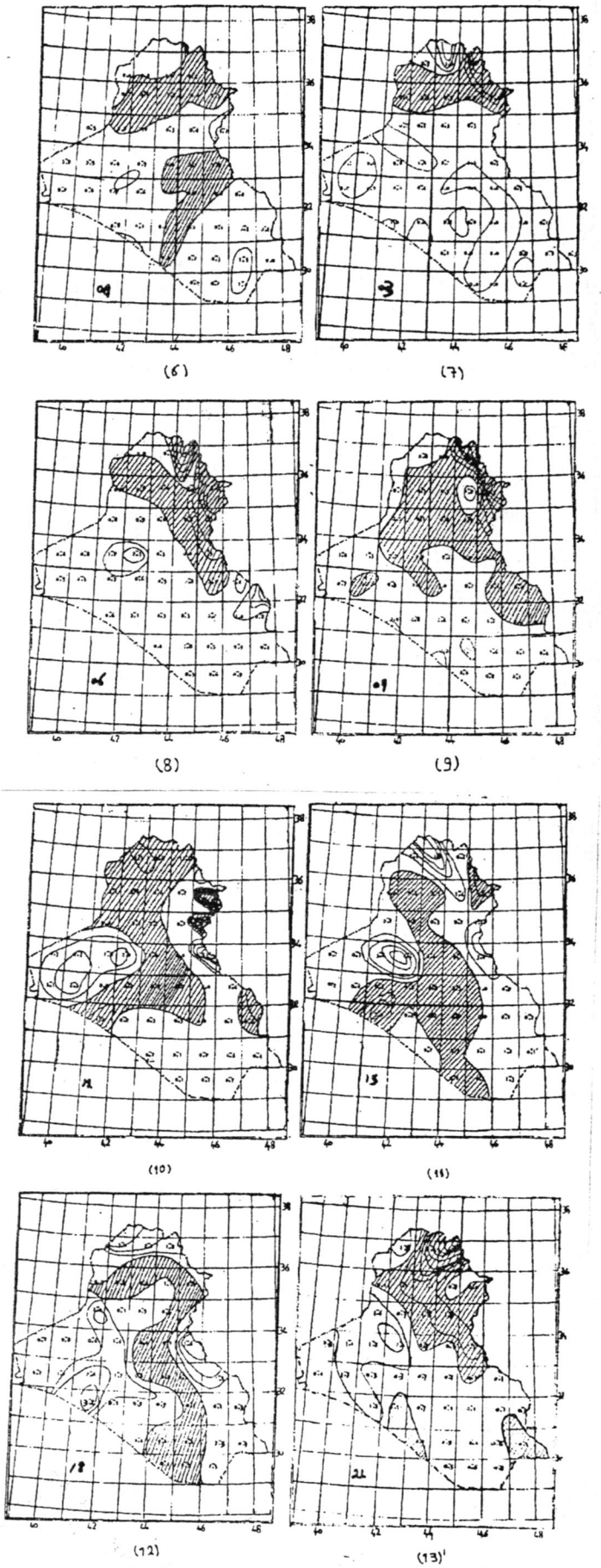

Figures (6-13) The patterns of topographical vertical winds for a stormy day on 1st of April 1990 at times (6-0300), (12-2100), (13-2400 GMT) respectively.

RESULTS AND DISCUSSION

The general pattern of the vertical wind component created by sloping terrain in Iraq are shown in figs. 1,2,3 and 4. These figures obtained by assuming a typical horizontal wind velocity of 5 m/sec and varies analogous to the eight wind rose directions.

Briefly, figures 1,2,3 and 4 show that with horizontal wind of northerly, northeasterly, and easterly directions. ascending wind is domiated in southern region and the west parts of the middle reginos of Iraq, while the northern region and the eastern parts of the middle region experienced descending motion and vise versa. The northwesterly wind causes an updraft in many places, however in the extreme west of the middle and the southern regions of Iraq a downdraft is prevailing.

In determining the significance of the topographical vertical winds calculated by equation (5) in the dust phenomenon, the dust storm of 1st of April, 1990 is examined in detail as a case study where data are available. As observed by the Iraqi meteorological organization, the time visibility in the meteorological, which are influenced by the storm are shown in fig.5, accorgingly the exact advancement of the storm is that, it is started in AL-Nakhaib and shortly after kilo 160 followed by Ramadi, Karblala, Baghdad, and finally Hilla and then vanished.

The patterns of the topographical vertical winds calculated by equation (5) for that stormy day are shown in figs 6 to 13. Ignoring the mountain regions which is assumed to be not a proper area for dust initiation, a simple comparison between figs 6 to 13 and fig 5 draws the following conclusions:

1) The stormy day started with either subsident or stable wind prevailed all over the country. The visibility was generally good. This condition persisted till 0900 GMT.
2) At 1200 GMT an updraft wind is established in many parts of the middle region with the core at the southwest of AL-Nakhaib. The storm start being more severe at the AL-Nakhaib where the visibility started to deteriorate seriously.
3) At 1500 GMT, The updraft wind increased in both AL-Nakhaib and Kilo 160, meanwhile the storm became more sever and visibility was nil. The general meteorological pattern at the surface is showing in fig (14).
4) At 1800 GMT, the vertical wind is reversed in both AL-Nakhaib and Kilo 160 to a downdraft whereas the updraft motion maintained in Ramadi, Baghdad, and south of them. The visibility improved in AL-Nakhaib and kilo 160 and deceased in Ramadi, Kerbala, Baghdad, and Hilla successively.
5) At 2100 GMT, the situation is settled down in most part of the country except Baghdad and Hilla where the storm, -as reported - vanished an hour after midnight.

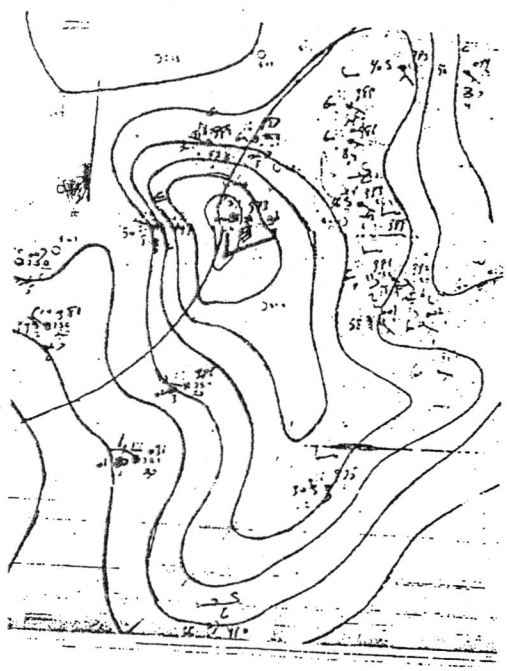

Figure (14) General meteorological pattern at the surface at 1500 GMT of 1st April 1990

Conclusions and Suggestions

There is a very high outstanding relation between the topographical wind patterns and the advancement of the dust storm. It can be concluded that the topographical vertical wind is an encouraging criterion for interpreting dust storm initiation and vanishement in Iraq. However, one can not judge other factors which may enhance the process such as surface susceptibility, human activities and other factors producing vertical motion. As the topographical vertical motion seems to be a poweful factor in dust phenomenon, it is suggested that researchers are required to extend this work to comprise other factor taking part in the vertical motion. However, this suggestion is limited at the present time due to the inadequacy of the wind observations available.

REFERENCES

[1] Akrawi, A., M. Al-Riahi, A. A. AL-Baali, and I. Hameed: Analysis of severs dust storms and its effects on solar radiation and weather parameters in Baghdad. (1989).

[2] Al-Najim, F. A. : Dust storm in Iraq. Bull. Coll. Sci., Vol. 16, No. 2., pp. 437-451. (1975).

[3] Awad, A. Dust Phenomena at Baghdad airport. Meteorological Memirs, Baghdad, Vol. 1, PP. 1-6, (1962).

[4] لجنة متخصصة: ظاهرة الغبار في العراق الهيئة العامة للانواء العراقية (١٩٨٧)

[5] Abdulla, S. A., H.M. Al-Rizzo, and M.M. Cyril: Particle size distribution of Iraqi sand and dust storms and their influence on microwave communication system. IEEE.Tarns. A.P., Vol. 36,No.1, PP. (599-620), (1989).

[6] Al-Juboory, S., A.A. Al-Baali, N.I. Al-Hamdani, M. Al-Riahi, and J.I. Haba: Characterization of dust particles in Baghdad. (1988).

[7] Al-Sayigh, A.H. : Geological and statistical study of the dust falling over Mosul town. Bull. Coll. Sci, Vol 17,No. 1,PP. 159-177, (1976).

[8] Salman, H.H., and A.s. Saadallah: Dust fallouts in central and southern part of Iraq. J. of Water Resources, Vol. 5, No. 1, PP. 599-619, (1986).

[9] النعيمي. رشيد حمود، التنبو طويل الامد بحالات الغبار في بغداد (مجلة علوم المستنصرية)المجلد الثاني (١٩٩٠)

[10] حديد. احمد سعيد والحسني. فاضل والعاني. حازم، المناخ المحلي-جامعة بغداد-وزارة التعليم العالي والبحث العلمي. مديرية دار الكتب للطباعة والنشر-جامعة الموصل.(١٩٨١)

[11] Petterson, Weather Analysis and Forecasting. 2nd Edition. Vol 1, Mcgrow-Hill book company, New York. (1964).

[12] WMO, Compendium of Meteorology Vol. 1, No. 364, (1973).

Al-Mustansiriya J. Sci Vol. 6 , No. 1 , 1996

Creep Test of Laser - Welded Lead

RAID A. ISMAIL* and GHAZI Y. NASSER**
*Applied Science Department, University of Technology, Baghdad, Iraq. **Department of Physics, College of Science. AL-Mustansiriya University, Baghdad, Iraq.

(Recieved 13 Feb. ,1993; Accepted 24 June., 1993)

الخلاصة

تم في هذا البحث انجاز لحام الدرز التقابلي-نوع التوصيل المحدود لعينات من الرصاص تحت ظروف الضغط الجوي الاعتيادي باستخدام ليزر النيديميوم-ياك. لقد أجري اختبار الزحف على كل من العينات الملحومة والاصلية-الغير ملحومة-وتم حساب أس الاجهاد وثوابت الزحف الاخرى.

ABSTRACT

In this work, Seam welding" Conduction limted type" butt joint, at atmospheric environment was achived using pulsed Nd:Yag laser to weld lead speciments. Creep test was carried out for welded and parent lead. In addition to that the stress exponent and constants related to the creep were calculated.

1. INTRODUCTION

Creep test is performed by applying a constant load on the specimen and observing the increment in the strain (or extension) with time.[1] A typical extension-time curve is shown in Fig.(1), which identifies three regions[2]:-

1 To 2
------: Primary creep- creep proceeds at diminishing rate due to work hardening of the metal.

2 To 3
------: Secondary creep- creep proceeds at a constant rate because a balance is achieved between the work hardening and annealing (thermal softening) processes.

3 To 4
------: Tertiary creep- the creep rate increases due to necking in local stress and failure is at pt(4). Secondary creep rate for a particular metal depends on many variables the most important of which are stress and temperature. The most commonly used expression for relating secondary creep rate (ε) to stress σ (when $\sigma \leq 5$ N/mm^2) and absolute temperature (T) has the form (2)

$$\varepsilon^{\circ} = A\,\sigma^{n}\, e^{-\sigma E/RT} \qquad (1)$$

where:

(A): constant, (n): stress exponent, (E): The activation energy for creep, and (R): is the universal gas constant (8.31 J/mol.k).

This equation shows that the creep rate increases by increasing either the stress or the temperature. By taking the natural logarithms we get

$$\ln \varepsilon^{\circ} = \ln A + n \ln -E\sigma/RT \qquad (2)$$

For the creep rate when $\sigma > 5$ N/mm^2 there is another exponential expression which has the form(2).

$$\varepsilon = B e^{\alpha}\, \sigma\, e^{-E/RT} \qquad (3)$$

where:

(B) and (α) are constants. Laser welding has many advantages over conventional methods. These may be summarized as follows:-

1-small heat affected zone (HAZ) of a value that depends on the metal[3].
2-Vacuum-free process(4).
3-Contactless handing of workpeice (abolishes any possible contamination).
4-possibility of different joining schemes "Lap, corner, and T-joints"[5].
5-Possibility of welding dissimilar metals.[6,7]

2. EXPERIMENTAL WORK

A-Laser system description:

An nd: Yag laser of (10) msec. pulses operates at (1.06)μ m with fundamental transverse mode (TEM_{00}) was used. A (20)cm focal length lens was employed in conduction with the laser system to focus the laser beam onto the workpeice.

The system, supplied with (X-Y) table, facilitates the provision of variable energies(1-24) joule. Fig.(2) shows the specimen used for the creep test.

B-Seam welding mechanism:

This was achieved by over lapping laser pulses on the lead specimen. To materialize this properly, the specimen was allowed to move (0.25)mm after each pulse. The whole work was arranged to operate the system at a fixed laser pulse energy (1.15)joule and repletion rate of 30 ppm.

3. RESULTS AND DISCUSSION

Figs. (3) and (4) show the strain-time curves (creep curves) for parent and welded lead specimens. At various stress levels, the creep constants (α,A,B) and stress exponent (n) were calculated for parent and welded lead as shown in table (1). The fracture location was always in base metal in all welded specimens giving an indication that the welded zone gained more strenght than that of the base metal a "phenomenon that is sometimes called creep grain boundary". This is due to the fact that laser welding makes grain refining. It means that the base metal has equiaxed grains zone of creep resistance less

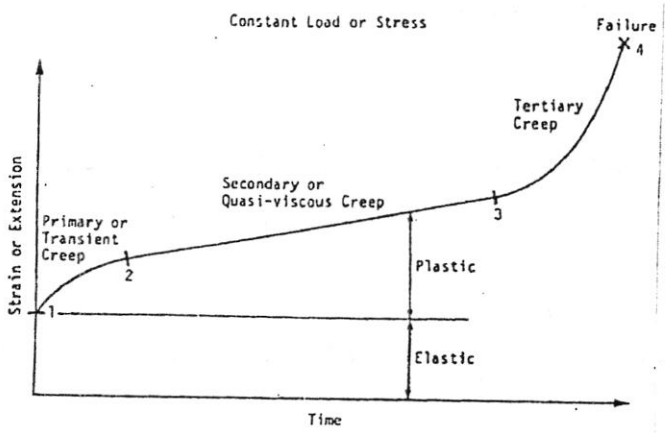

Figure(1) Typical extension - time curve

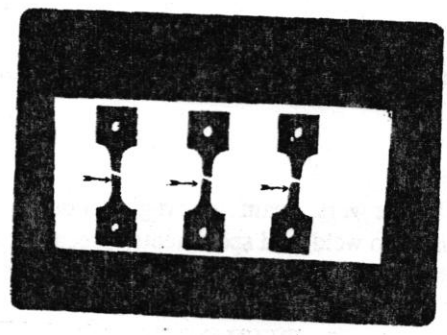

Figure(2) Creep test lead specimen

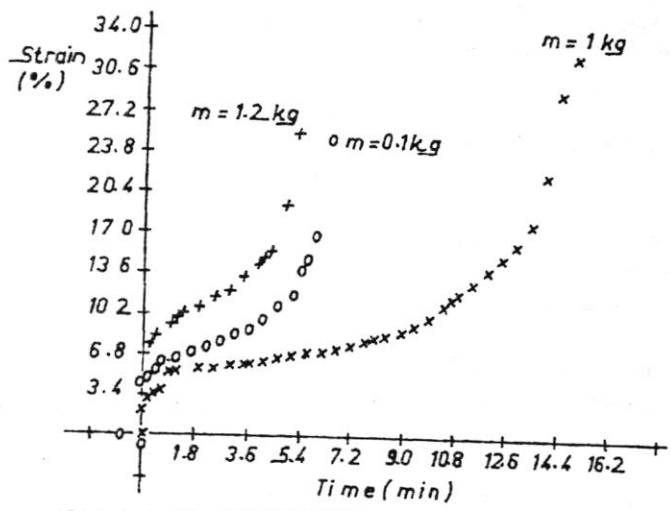

Figure(3) Strain - time curvr for weleded

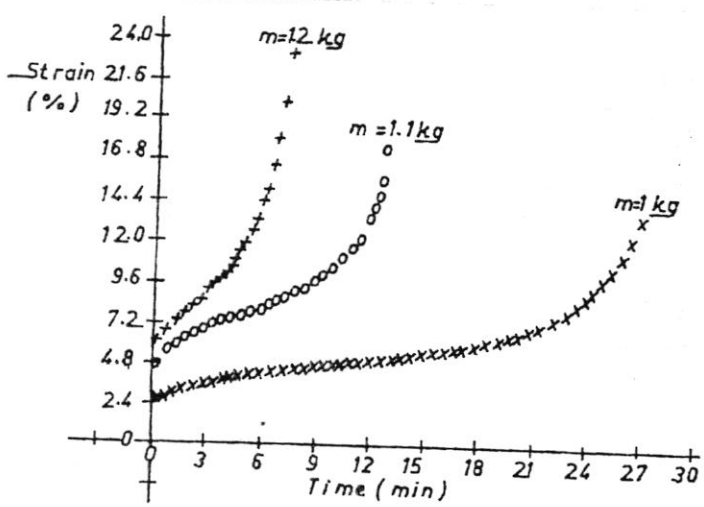

Figure(4) Strain - time curve for parent lead

than that of weld zone. This looks as an attractive point of the laser welding. Throughout the welding process careful overlapping was assured at a ratio of (70%). When poorly overlapping the laser pulses a tiny defect "BLOW HOLES" which weakens the welding may be generated. This defect will disapper with proper overlapping since remelting the regions will accord this defects. There was no stress concentration in the weld zone because of the full penetration welding.

The resulted creep rate for welded lead was larger than that of the parent, this can be explained as follows:-

The long laser oulse used offer slow heating therfore allowing some kind of annealing to take place. This increases the elasticity and giving longer time to reach the fracture point for the scame lead as compared with the parent.

4. CONCLUSTION

1-Creep resistance for parent metal was less than that of the welded metal. This explains the fracture location as being always in the base.

2-There was no stress concentration in the welded metal sincethe fully- penetrating welding was always the case.

3-Creep rate for welded metal was larger than that of the parent. This comes about by the associated annealing.

4-No micro - cracking nor porosities were noticed.

Table (1) Shows the creep constants and stress exponent values

Lead Speciment	A	B	n	α
Welded	3.32	1.68	12.75	1.2
Parent	3.66	2.71	8	0.9

REFERENCES

[1] باقر، حسين مبدى هندسة المعادن والمواد-(ترجمة) ، تأليف ف بيلي ص-٢٩٤ الجامعة التكنولوجية-بغداد- عام ١٩٨٥

[2] Creep mesurement apparatus (SM 106 MK2) manual (P.2-5) Equipment Company, England.

[3] حمودي، وليد خلف و اسماعيل، رائد عبد الوهاب دراسة لحام الدرز بواسطة ليزر Nd:Yag لبعض سبائك الحديد والنحاس الاصفر- مجلة الهندسة والتكنولوجيا، المجلد الحادي عشر، العدد الاول، ص-١٢٨- (١٩٩٢).

[4] Sayegh, G. , Cazes, R., Sciaky, A.M. " The laser position in the industrial market place " Welding and metal fabrication, Vol. (47), No.(8). , p. (567),(1979).

[5] Charschan, S.S. "Laser in industry" Van Nostrand Reinhold Co., P.(169), (1972).

[6] Dr. Walid K. Hamudi, Raid A.Ismail (M.Sc) "Nd:Yag laser welding of thermocouples" (sent for publication), Engineering and technology journal (Baghdad).

[7] Dr. Walid K. Hamudi, Raid A. Ismail (M.Sc.)" Nd:Yag laser welding of dissimilar steel sheets " (Accepted for publication) Engineering and technology journal, Baghdad,(1993),

Characteristics of Unbalanced Optical Phase Dtector(OPD)

GUIDAA A. SUHEAL, RAAD S. FYATH AND KALID H. SAYHOOD
Department of Electrical Engineering, College of Engineering, University of Basrah, Basrah, IRAQ.
(Recieved 27 Dec. 1992; Accepted 24 June, 1995)

الخلاصة

يستخدم التثائي الضوئي المزدوج عادة ككاشف طور ضوئي في نظم الاتصالات الضوئية. هنا تم تقصي أداء الكاشف غير المتزن باستخدام الطريقة التقليدية لعملية المزج الضوئي. تعبيرات عامة تتعلق بخواص كسب الكاشف ومعامل تخفيت الاشـاراة قد استحصلت لمجالات معينة من الليزر المستقطب. النتائج تبين ان منظومـة قفل الطـور الضوئيـة(OPLL) مـن نـوع (DC-coupled) تتطلب كاشف طور متزن بشكل كامل تقريباً مقارنة مع منظومات قفل طور من نوع (AC-coupled) أو كوستاس(Costas).

ABSTRACT

A dual-photodlode is usually used as an optical phase detector (OPD) in homodyne optical communications. Here the performance of unbal anced OPD has been investigated using a classical model for the optical mixing process. A generalized expressions related to the detector gain characteristic and signal suppression factor are developed for arbitrary polarized laser fields. The results indicate that a DC-coupled optical phase locked loop (OPLL) requires almost a completely balanced OPD compared with Ac-coupled or Costas Oplls.

INTRODUCTION

Recently, different techniques have been reported to increase receiver sensitivity in optical communication systems. Among these are: employing advanced avalanche photodiodes [1,2], optically preamplied receivers [3,4], and coherent transmission [5,6]. However, coherent lightwave techniques offer nearly ideal detection sensitivity as well as selectivity similar to that obtained at radio frequencies. These features enable us to use the vast bandwidth of the optical fiber more efficiently. Coherent detection is achieved by employing nonlinear mixing between the information-bearing optical wave and a locally generated optical wave; the mixing is done using a photodetector. When the signal and local oscillator (LO) frequencies are identical, the process is called homodyne detection and the information appears directly at baseband frequencies. Homodyne detection of a phase shift keying modulation gives the best theoretical receiver sensitivity of any binary modulation schemes [5]. Unfortunately, homodyne scheme requires an optical phase locked loop (OPLL) to synchronize the signal and the LO lasers and this has proven difficuilt to achieve unless a very narrow linewidth optical sources are used [7].

However, on going progress in the development of semiconductor lasers let us hope that problems associated with practical OPLLs might be overcome. In demonstrated systems OPLL is usually realized using a dual- detector optical mixer as phase detector (PD) to cancel the LO excess noise and to use efficiently the LO power. Unfortunately, unbalanced optical mixer does not behave as an ideal PD and this will degrade the performance of the OPLL incorporating it. The purpose of this paper is to address this problem in details.

THEORETICAL MODEL

Figure 1 shows a simple model of a homodyne optical receiver. The weak received signal of average power P_S is spatially combined with a strong L_O signal of average power P_L using fiber direction -al coupler with coupling ratio ($0<\alpha<1$). For n= 0.5 and identical photodetectors a balanced optical mixing will be achieved when the two optical paths are equal.

The central theme of the analysis is that light is described by a stochastic vector field and that photoelectron events are represented by a doubly stochastic poission point process [8,9]. To derive the probability distribution of the photo-counts for arbitrary polarized laser fields, the total integrated intensity may be regarded as the sum of two statistically independent integrated components, one for each of the polarization component of the wave after passage through a polorization instrument that diagonalizes the coherency matrix [8]. The optical intensity incident upon each detector can be expressed as follows [10]

$$S(t) = S_1(t) + S_2(t) + S_X(t) \qquad (1)$$

where $S_i(t)$, i=1,2 are the direct detection intensity components (one for each incident field) and $S_X(t)$ is the homodyne mixing cross-term. The detector photocurrent $S^D(t)$ obtained by low-pass filtering the optical intensity down to the detector bandwidth (which is much lower than the optical frequency).

$$S^D(t) = S^D_1(t) + S^D_2(t) + S^D_x(t) \qquad (2)$$

where the superscript denotes low-pass filtering.

Taking both detectors into account and after resolving the two arbitrary polarized input fields into orthogonal components with respect to the same X and Y axis it can be shown that the total photocurrent $I_T = S^D$ can be related to the system parameters through the relation

$$I_T = [A_1 b^2 + A_2 b \sin(e_e + e_e) + A_g] P_L \quad (3)$$

where

$$A_1 = (1-\alpha)R_1 - \alpha R_2 \quad (4a)$$

$$A_2 = 2[R_1 + R_2]\sqrt{\alpha(1-\alpha)K_p} \quad (4b)$$

$$A_g = \alpha R_1 - (1-\alpha)R_2 \quad (4c)$$

Here $b^2 = P_s / P_L$ is the power ratio (i.e. b is the field ratio), θ_e is the phase offset between the two input fields and R_1 (R_2) is the responsitivity of the first (second) photodiode. Both K_p and θ_e are related to the polorization of both laser fields [11],

$$K_p = K_{sx}K_{Lx} + K_{SY}K_{LY} + 2\sqrt{K_{sx}K_{Lx}K_{sy}K_{Ly}}\cos(\delta_L - \delta_S) \quad (5a)$$

$$\theta_e = \tan^{-1}\left[\frac{\sqrt{K_{SY}K_{LY}}\sin(\delta_L - \delta_S)}{\sqrt{K_{SX}K_{LX}} + \sqrt{K_{SY}K_{LY}}\cos(\delta_L - \delta_S)}\right] \quad (5b)$$

where K_{SX}, K_{SY}, K_{Lx}, and K_{LY} represent the fraction of P_S and P_L in the X, Y planes respectively. Further δ_S and δ_L are the phase shift between signal components and LO components respectively. Perfect matching between the signal and LO fields (i.e $K_P=1$, $\theta_P=0$) results in photocurrent I_T proportional to $\sin\theta_e$ rather than $\sin(\theta_e + \theta_P)$. Thus polorization misalignment introduces error in the P_D performance.

For balanced receiver ($R_1=R_2=R$, $\alpha=0.5$) the terms A_1 and A_2 in eqn. 3 vanish leaving

$$I_T = 2 B R P_L \sqrt{K_p}\sin(\theta_e + \theta_P) \quad (6a)$$

for the general case of polarizaition misalignment and

$$I_T = 2 b R P_L \sin\theta e \quad (6b)$$

When the states of polarization of both optical waves are identical. Equations 6 reveal that perfect matching in polarization is very essential to make the performance of a balanced dual-photodiode mixer approaches that of a pure sinusoidal P_D.

Different schemes have been reported in the literature to reduce the effect of the polarization mismatching in coherent optical communication [12]. Advances in polarization preserving fiber continue to be reported and automatic polarization compensation schemes based on mechanical or electooptic devices have been demonstrated. In addition to that a polarization diversity reception offers a more general solution. In the rest of the paper we will assume a negligible polaraization misalignment at the receiver input and focus our attention on the performance degradation of unbalanced optical mixer.

CHARACTERIZATION OF UNBALANCES OPD

Different parameters are used to characterize the performance of PD in PLL circuits [13,14]. Among these are the normalized detector characteristic g(0e), the detector sensitivity k_d and signal suppresion factor η. In the following we present a brief summary of the calculation for these parameters in the case of dual-photodiode optical mixer along with illustrative results.

A completely general computation very quickly becomes unwidely and as this would detract from the aims of this study the following simplifications are used: (I) the optical mixer is realized with perfectly matched photodiodes (i.e $R_1=R_2$ and taken to be 1 to demonstrate the results). (II) Both laser signals are aligned in polarization at the receiver input. Thus the deviation of α from 0.5 gives a measure of the degree of unbalance. The unbalance factor δ is taken to be $[(\alpha-0.5) / 0.5]=2\alpha-1$ in this paper.

NORMALIZED DETECTOR CHARACTERISTIC

The normalized detector characteristic can be evaluated by normalizing $I_T(\theta e)$ with respect to $I_T(\pi/2)$. With the aid of egn. 3 we get

$$g(\theta e) = I_T(\theta e) / I_T(\pi/2) = B_1 + B_2 \sin\theta e \quad (7)$$

where

$$B_1 = (A_1 b^2 + A_g) / A_1 b^2 + A_2 b + A_g) \quad (8a)$$

$$B_2 = A_2 b / (A_1 b^2 + A_2 b + A_g) \quad (8b)$$

Equation 7 indicates clearly that the normalized output of the unbalanced OPD can be split into two parts: one is independent of the phase difference (i.e B_1) and the other shows a pure sinusoidal characteristic with peak gain B_2. Note that both B_1 and B_2 are functions of $b \equiv [p_S/p_L]^{1/2}$ and they reduce to zero and 1, respectively for the ideal case of balanced mixer.

Figuers 2a and 2b exhibit the b-dependence of the OPD gain for $\alpha=0.45$ and $\alpha=0.55$, respectively. The dashed line corresponds to the balanced case of $\alpha=0.5$ which is independent of the signal to LO power ratio b^2 and included in these figures for comparsion purpose. From the examination of these curves, we conclude the following:

(I) Even unbalance factor $|\delta| = |2\alpha-1|$ as low as 10% makes the gain characteristic of the OPD degrades from the ideal sinusoidal performance and this effect is more pronounced at lower values of power ratio.

(II) The behaviour of an unbalanced OPD depends on the sign of δ in addition to its magnitude.

(iii) As expected from the analysis the detector has a biased sinusoidal characteristic. The high level of the dc component at the detector output under certain conditions will affect the acquisition behaviour of the OPLL. Thus toreduce the effect of unbalanced OPD the dc component at the detector output should be subtracted using advanced OPLL structures such

as AC-coupled or Costas loops. It is worth to emphasise that Scholtz et al. [15] has realized a 10μm homodyne optical receiver using a DC-coupled OPLL with dc-offset compensation and they have suggested to use an AC-coupled loop (without compensation scheme) for advanced receivers Detector sensitivity

This can be evaluated by partiaily differentiating IT with respect to θe

$$K_d \equiv \frac{\partial I_T}{\partial \theta_e}\Bigg] = 2(R1 - R2)\sqrt{\alpha(1-\alpha)}bP_L \qquad (9)$$

The maximum value of K_d occurs when a = 0.5

$$(K_d)_{max} = (R_1 + R_2)\, bp_L$$

$$= (R_1 + R_2)\sqrt{P_s P_L}$$

For balanced mixer $R_1=R_2=R$ then $(K_d)_{max} = 2R\sqrt{P_s P_L}$

Figure 3 shows the variation of detector sensitivity (normalized to $R\sqrt{P_s P_L}$) versus the coupling ratio α as obtained from eq. 9 for identical photodiodes. Note that a small deviation of α from 0.5 has a negligible effect on k_d. In fact for $0.4 < \alpha < 0.6$ the sensitivity is within 2% less than that for the ideal case α= 0.5.

It is important to note that according to eq.9 the detector sensitivity kd is always positive. This parameter can be related to the slope of
g(θe) evaluated at θe=0 by the following expression.

$$K_d = I_T(\pi/2)\left.\frac{\partial g(\theta e)}{\partial \theta e}\right|\theta e = 0 \qquad (11)$$

Thus when the slope of g(θe) is negative at the origin we expect $I_T(\pi/2)$ to be negative for that case.

SIGNAL SUPPRESSION FACTOR

In general, the phase of the output signal of optical laser source will fluctuate around mean value. This will intorduce a phase noise in OPLL which is related to the linewidth of both lasers (signal and LO). The spectral linewidth of semiconductor optical sources is one of the most important parameters in coherent optical communication. Significant progress has been made recently in the achievement of narrow linewidth (<10MHZ) semiconductor lasers [16]. In addition to that a nonnegligible contributions to phase error come from receiver shot noise and data phaselock crosstalk [17]. If the phase fluctuation is defined as φ with probability density function P(φ) then the average output of the unbalanced receiver can be expressed as

$$g(\theta e) = \int_{-\pi}^{\pi} g(\theta e - \phi)\, p(\phi)\, d\phi \qquad (12)$$

Because of the periodic PD characteristic which extends over a period of 2π, the angle φ is taken to be modul o-2 π

The influnce of phase noise does not only involve the degradation of the output signal at the PD, but also the slope at the null may be degraded by a phenomeanon which is called signalsuppression factor η [14].

$$\eta \equiv \left.\frac{\partial g(\theta e)}{\partial \theta e}\right|\theta e = 0 \qquad (13)$$

Making use of eqns. 7, and 8 yields

$$\eta = B_2 \int_{-\pi}^{\pi} \cos\phi\, p(\phi)\, d\phi \qquad (14)$$

n = B2-n ****

assuming K_p=1. Note that $\eta=B_2$ when the phase noise is neglected.

Figuers 4a and 4b show the variation of signal suppression factor η as a function of the standard deviation of the phase noise σφ for
α=o.45 and 0.55, respectively. The solid lines correspond to the unbalanced case with different values of b while the dashed line refers to α =0.5 which is independent of b. the results are calculated assuming truncated Gaussian phase noise. These figures highlight the following facts:

(I) Even for the ideal case of negligible phase noise (σφ=o) the signal suppression factor for the unbalanced receiver differes from that for the balanced mixer.

(II) When σφ increases the magnitude of the suppression factor η decreases for all receivers (balanced or unbalanced).

(III) At given value of σφ the parameter η will be proportional to B_2 according to eq. 14. Thus ηwill be positive of negative according to the sign of B_2. To be more precise the sign of the denomiator of eqn. 8b [i.e $D=A_1B^2+ A_2b+A_g$] will play the key role in determining if η greater or less than zero. The assumptions used in the calculations give $A_1=-A_g= 1-2\alpha$. Thus $D=(1-2\alpha)(b^2-1) +A_2b$ with $A_2>0$. For practical receivers b<1 then the term D will be always positive for
α>0.5 leading to η>0 as shown in Fig 4a. For
α<0.5 the value of D will be positive (negative) if the magnitude of $(1-2\alpha)(b^2-1)$ is less (greater) than A_2b. The critical value of b can be estimated by approximating D by $(2\alpha-1)+A_2b$ assuming $b^2<<1$. Thus $b=b_c=(1-2\alpha)A_2$ will make $\eta\to\infty$. Operating at power ratio $>b^2_c$ leads to positive values of η which is decreasing function of b (since D is linearly related to b within the approximation $b^2<<1$). For $b<b^2_c$ η is negative and its value increases with b.

(IV) It has been shown [11] that for a homodyne optical PSK receiver an rms phase error of 10° results in 1dB penalty at 10^{-9} bit error rate. If the maximum allowable rms phase noise is limited to 10° in practical receivers then the variation of η with σφ can be neglected in this regime.

CONCLUSION

The performance of optical mixer incorporating a dualphotodiode has been investigated as a phase detector; emphasize being placed on the operation in the unbalanced regime. The optical mixing process is classically analyzed for arbitrary polarized optical fields which results in general expressions related to the characteristics of both balanced and unbalanced mixers. The analysis indicates that optical mixer behaves as an optical phase

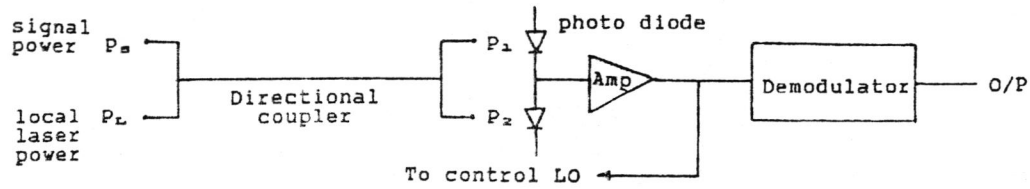

Figure(1) A simple model of a homodyne optical receiver

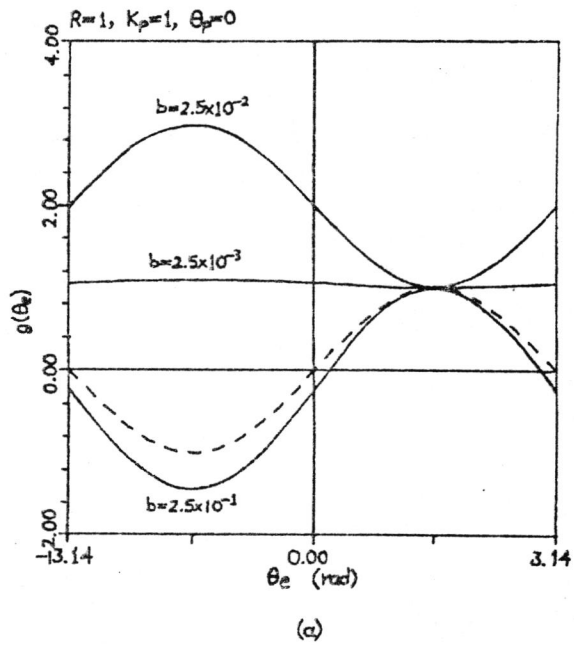

(a)

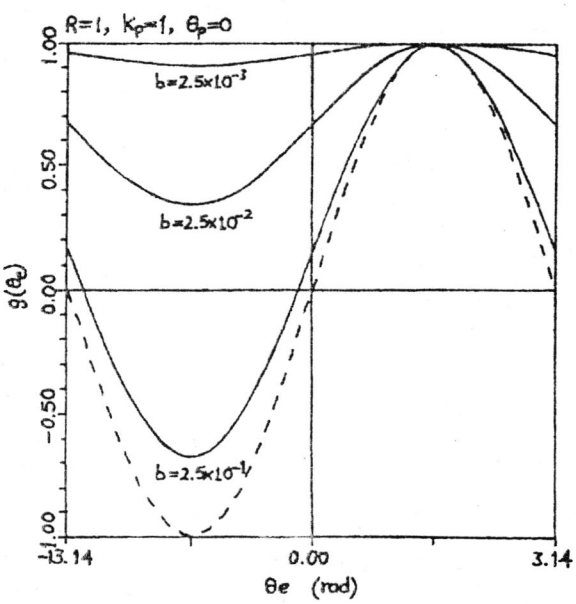

(b)

Figure(2) Normalized gain characterist of optical phase detector. The dashed lines correspond to balanced mixer (α=0.5) which are independen of b.
(a) α=0.45 (b) α=0.55

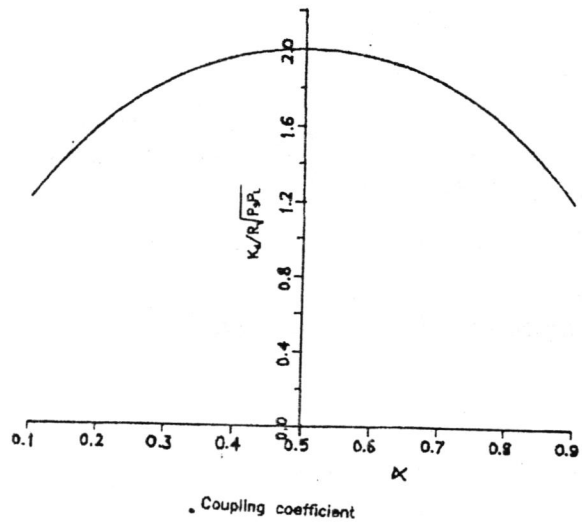

Figure(3) Sensitivity of optical ohase detector versus coupling coefficient

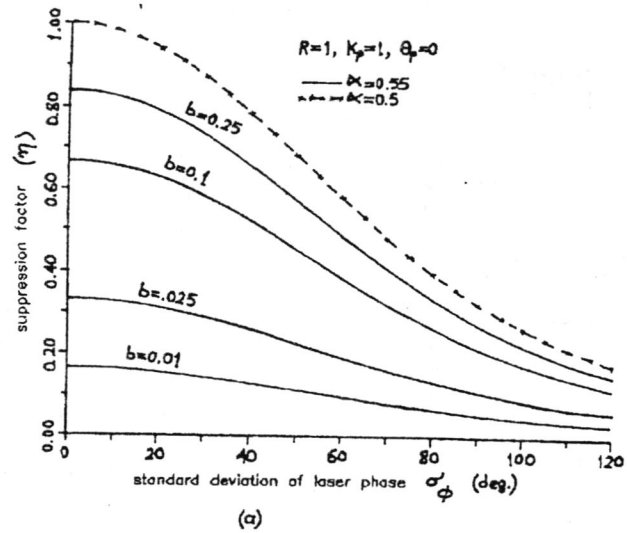

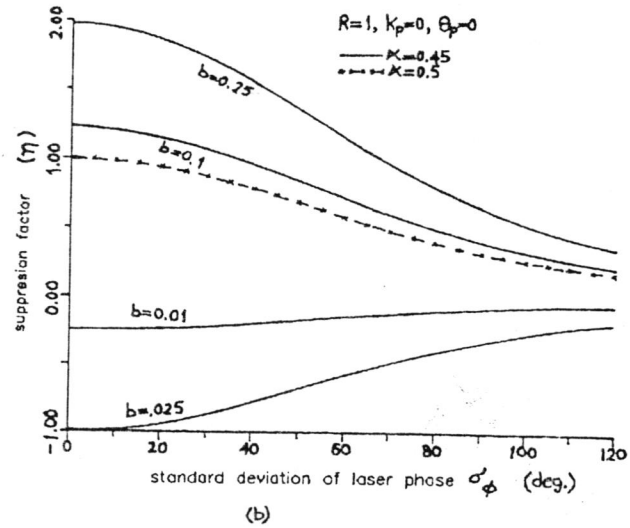

figure(4) Signal suppression factor as a function of rms phase noise. (a) α=0.45 (b) α=0.55

detector with a blased sinusoidal gain characteristic. The dc offset at the detector output is more pronounced at lower values of $b^2=p_S/P_L$ and can not be ignored even for an unbalanced factor as low as 10%. Thus DC-coupled OPLL required almost perfectly balanced OPD. This restriction is more relaxed for Ac-coupled or Costas OPLL where the dc offset is automatically concelled. It is also found that the signal suppression factor is significiantly affected by the unbalanced factor even at low values of rms phase noise. Again the power ratio b^2 governs the variation of this parameter. In the other hand the effect of unbalanced factor on detector sensitivity can be neglected for practical receivers.

The analysis and results here can be used as a guideline to asses the performance of homodyne optical receivers. The work in this direction is still in progress with attention to multichannel transmission.

References

[1] Fyath, R.S. and O' Reilly, J.J. " Effect on the Performance of Staircase APDs of Electron Impact Ionization within the Graded-Gap Region IEEE Electron. Devices, 135: 101-108, (1988).

[2] Fyath, R.S. and O' Reilly, J.J. " Comparison of Novel Supperlattice Structures and Convenioal APDs with Implications for Performance of of Optical Fiber Systems" 2nd IEE National Conf. on Telecommunications : 106-110, April (1989).

[3] Hagimoto, K., Nishi, S. and Nakagawa, K. "An Optical Bit-Rate Flexible Transmission System with 5-Tb/s. Km Capacity Employing Multiple In-Line Eribum-Doped Fiber Amplifiers" IEEE J. Lightwave Technol., 8: 1387-1395, (1990).

[4] Medeiros, C.R., Fyath, R.S. and O' Reilly, J.J. " Multigigabit Optically Preamplified Receiver Designs with Improved Timing Tolerance" IEE Proc., pt.J, 139: 143-147, (1992).

[5] Linke, R.A. and Gnauck, A.H. "High Capacity Coherent Lightwave Systems " IEEE J. Lightwave Technol., 6:1750-1769, (1988).

[6] Hooi jmans, P.W. et al. " Coherent Optical Transmission " Philips Telecomm. Review, 50: 39-45, (1992).

[7] Kazovsky, L. G. and Atlas, D.A. " A 1220-nm Experimental Optical Phase-Locked Loop : Performance Investigation and PSK homodyne Experiment at 140 MB/s and 2Gb/s" IEEE J. Lightwave Technol., 8: 1414-1425, (1990).

[8] Goodman, J.W. "Statistical Optics", John Wiley and Sons, New Yprk, (1985).

[9] Fyath, R.S and O' Reilly, J.J. " Comprehensive Moment Generating Function Characterization of Optically Preamplified Receivers" IEE Proc., Pt.J, 137: 391-396, (1990).

[10] Nazarathy, M., Sorin, W.V., Baney, D.M. and Newtor, S.A. " Spectral Analysis of Optical Mixing Measurements" IEEE J. Lightwave Technol., 7:1083-1096, (1989).

[11] Hodgkinson, T.G. " Receiver Analysis for Syschronous Coherent Optical Fiber Transmission Systems" IEEE J. Lightwave Technol., 5:573-586, (1987).

[12] Okoshi, T. and Kikuchi, K. " Coherent Optical Fiber Communications" KTK Scientic Publisher, Tokyo (1988).

[13] Blanchard, A. "Phase Locked Loops", Wiley, New York (1976).

[14] Garder, F. M. "Phaselock Techniques', 2nd edition. Wiley. New York (1979).

[15] Scholtz, A.L., Leeb, W.R., Flatscher, R. and Philip, H.K. "Realization of 10-μm Homodyne Receiver" IEEE J. Lightwave Technol., 5: 625-632, (1987).

[16] Koch, T. L. and Koren, U "Semiconductor Lasersfor Coherent Fiber Communications" IEEE J. Lightwave Technol., 8 : 274-293, (1990).

[17] Kazovesky, L. G. "Balanced Phase-Locked Loop For optical Homodyne Receiver: Performance Analysis Design Considerations, and Laser Linewidth Requirements" IEEE J. Lightwave Technol., 4 : 415-425, (1986).

The Optimum Tilt Angles For Solar Collectors in the Southeast and Southwest Directions of Mosul City

RAAD A. RASOUL
Department of Physics, College of Education, University of Mosul, Mosul, IRAQ.
(Recieved 5 Dec. 1992; Accepted 18 June, 1994)

الخلاصة

من الامور المهمة والواجب اتباعها في تنفيذ مشاريع الطاقة الشمسية تعيين الزوايا المثلى في الاتجاهات الجنوبي الشرقي والجنوب الغربي والتي يتركز عندها سقوط الاشعة الشمسية خلال اوقات النهار. ولذلك فقد تم تقدير الزوايا المثلى لجميع أشهر وفصول السنة اعتماداً على القياسات العملية الاشعاع الشمسي الكلي والمنتشر الساقط على السطح الافقي في مدينة الموصل. وقد تمت مقارنة الطاقة المستحصلة عند الزوايا المثلى في الاتجاه الجنوب الجغرافي نسبة الى الطاقة المستحصلة عند السطح الافقي، كذلك فقد تم استبيان الطاقات المستحصلة عند الزوايا المثلى ٣٠°، ٦٠°، ٩٠°، في كل من الاتجاهين الجنوب الشرقي والجنوب الغربي. ونظراً لاهمية الزوايا المثلى في تحديد مساحة المجمعات الشمسية المطلوبة للعمل، فقد تم تحديد كفاءة المجمعات تبعاً لميلها عن سطح الارض وكذلك كفاءتها تبعاً لمواجهتها في الاتجاهات الجنوب الشرقي والجنوب الغربي. وقد تم ايضاً استنباط علاقة تجريبية لتحديد قيم الزوايا المثلى في الاتجاهات الجنوب الشرقي والجنوب الغربي لمدينة الموصل.

ABSTRACT

The estimation of the optimum tilt angles is one of the most important procedures in implementing the solar energy system. These angles lie usually between east and west south-facing directions. This paper includes an estimate of these angles for Mosul City. The estimate is based on experimental measurements of the global and diffused solar radiation on horizontal surface for every month and season. The comparis on is made for the energy gained at the optimum tilt angles relative to horizontal surface for south-facing direction. Also the energy gained for the optimum tilt angles at angles 30°, 60°, 90° between southeast and southwest directions are shown. The resuits are used to evaluate the areas which can be determined by the required effeciency of the collectors according to firstiy; the inclination from the earth surface and secondly; according to their south-facing directions South to East (S/E) and between South to West (S/W). Finally an empirical relation for the determination of the optimum tilt angles is formulated.

INTRODUCTION

The increasing activities in the field of solar energy and its application in Iraq (1,2) require the knowledge of the optimum tilt angles. Since Mosul city lies in the morthern half of the hemisphere, the surface of the solar collectors must be psitioned towards the southeast and southwest directions (3.4).

The tilt angle depends on three components of solar radiation. These components are:

a- direct solar radiation
b- sky diffused solar radiation.
c- ground reflected diffuse solar radiation.

Fig. (1,2) illustrates that the optimum tilt angle β is the angle between the collector and earth surface at which the intensity of the incident radiation is maximum (5,6).

Studies concerning the estimation of tilt angles have not yet been made for Mosul city, except one which includes the estimation of these optimum tilt angles at south direction only (7).

In this paper an attempt is made to estimate the optimum tilt angles in the angular direction range through east-south-west, i.e in the south-facing directions between east to west in the southern half.

METHODOLOGY:

2.1 Optimum Tilt Angles Distribution:

According to (8), the global solar radiation $H_{\beta\gamma}$ incident on a surface with inclination angle β is calculated

$$H_{\beta\gamma} = \underbrace{(H - Hd)Rb}_{\text{direct rad.}} + \underbrace{Hr + Hs}_{\text{diffuse rad.}} \qquad (1)$$

whee H, Hd are the global and diffuse solar radiations incident on horizontal surface.

Rb is the radiation between extraterrestrial soiar radiation incident on an inclined surface to the extraterrestrial solar radiation incident on horizontal surface, and can be calculated theoretically (9).

Hr is the ground reflected diffuse radiation and can be calculated by using the following equation.

$$Hr = 1/2\ H\rho\ (1-\cos\beta) \qquad (2)$$

where ρ is the ground albedo which equals 0.25. Since the surface of the study area is acombination of grass, sand, and concrete its ground albedo is chosen to be 0.25. This value represents the average of these materials albedoes (10).

Hs is the sky diffuse radiation which can be calculated by the following equation:

$$Hs=Hd[Rb(H-Hd)/Ho+1/2(1+\cos\beta)(1-(H-Hd)/Ho)] \quad (3)$$

Hr, Hs both can be calculated without the need of experimental measurements, only H and Hd need to be obtained experimentally.

In this paper the values of H and Hd are obtained from the Meterological Station at the Education College of the University of Mosul for the period from 1988 to 1991.

This station is Located at 36° 19′ N Latitude and 46° 09′ E Longitude and at an altitude of 223 m above the see level. The values of H and Hd were obtained by using two kipp and Zonen pyranometers. The expected accuracy of these values is ± 10%.

The values of $H\beta\gamma$ for each month are measured at every 5° in the angular directions between south to east and south to west and for all the inclination angles between 0°-90° by using computer facilities.

At south facing angles of every 5° in the 180° range between east-south-west there will be (91) values of HBY, each corresponds to one inclination angle. The optimumn tilt angle is then considered to be the one at which $H\beta\gamma$ is maximum.

The results are then presented graphically by projecting the values of angular directions on the x-axis and the optimum tilt angles on the y-axis.

Fig. (3) demonstrates curves representing Dec., Jan., Nov., Feb., Oct., and Mar.

Fig. (4) demonstrates curves representing Sept., Apr., Aug., and May.

Months June and July are execluded due to the fact that their corresponding optimum tilt angles for the whole angular direction angles between east and west towards south face were found to be zero degrees. Figs. (5,6) are similar to figs (3,4) except that they show seasonal and annual average optimum tilt angles.

2.2 Maximum Solar Radiation of Optimum Tilt Angles:

The relations between the energies gained at the optimym tilt angles and the energies gained at horizontal surfaces for the south-facing directions from South to East and South to West (S/E and S/W). The relations are presented in Figs (7,8).

These figures show that solar radiation at optimum tilt angle for $\gamma=0°$ (i.e southern direction) is greater than the solar radiation at any angle in southeast and southwest ranges.

The observed annual energy gain at optimum tilt angles with respect to the horizontal surfaces is about 25% for the southerly direction (i.e $\gamma=0°$). The annual energy gain at any other of the optimum tilt angle with respect to its horizontal surface is not known, since the energy at this surface is unknown. However, the energy gain at any optimum tilt angle can be found if the solar radiation at its corresponding horizontal surface is measured experimentaly.

2.3 The Evaluation of The Collector's Effeciency:

The area which is effectively used (i.e. which recieves solar radiation) by the solar conversion system is always smaller than its total area. This is due to the inclination of the solar collectors and the directions that the collector is facing, note that this directions lies between E-S and S-W (11).

To evaluate the effective area of any solar collector or solar cell Figs (9,10) are prepared.

Fig (9) shows the efficiency percentages of a collector versus its optimum tilt angles. For simplicity the values of the optimum tilt angles are used with reference to the latitude angle of Mosul city (L = 36°). In this figure the efficiency percentage at the optimum tilt angle (L + 2) for the southerly direction (γ = O°) is considered as 100% according to Figs (5,6). The efficiency percentage at any optimum tilt angles for any directions between South to East and between South to West (S/E and S/W) is then determined with respect to the efficiency of the collector inclined at L+2. For instance, if the optimum tilt angle equals 22* (L-12) the effeciency of the collector will be 63%.

Fig. (10) shows the efficiency of the collector versus south-facing directions (directions between E.S.W). Again in this figure the efficiency at the southerly is considered as 100%. The efficiency at any other direction is then determined with reference to the efficiency at the southerly direction. For instance, if the collector is directed towards
30° at southeast then the efficiency at the collector will be 85%.

2.4 The Empirical Relation for Determining The Optimum Tilt Angles:

The measurements of this study (optimum tilt angle θ_{opt}, global solar radiation incident on horizontal surface H and south-facing directions in southeast and southwest γ) are used to design a model which can be used directly to find the optimum tilt angle from the solar radiation incident on horizontal surface at any south-facing direction between southeast and southwest.

The model is derived using a STATGRAF program. This program is usually used to modulate an equation according to some empirical data given as an input.
The resultant model is found to be as follows:

$$\theta_{opt} = A + BH + C\gamma^2 \quad (4)$$

where A, B and C are constants whose values are given in table (1). According to this table, the correlation coefficient (r) between the optimum tilt angle calculated from eq (4) and those calculated previously from eq (1) is one, i.e they are 100% correlated. This indicates that the estimated model is fairly accurate (12).

Discussions and Conclustions:

Figs (3,4) are useful for the changeable solar conversion systems such as heating, cooling and water pumping systems, since they provide the inclination angles of solar collectors or solar panels cells.

The optimum tilt angles for June and July are considered as Zero degree because the solar altitude angles for them are 88° and 84° respectively. This means that the sun makes an altitude angle of 90°, i.e the sun will normal to the earth surface.

Figs (5,6) show that the optimum tilt angles for Winter and Autum are geater than those for Summer and Spring. This result assures firstly, the inverse relationship between the optimum tilt angles and solar altitude angles and secondly, the solar declination angles. These two figures (i.e figs 5,6) are useful for fixed solar conversion systems such as panel cells above buildings and electrical generator stations.

Figs (7,8) are useful for estimating the energy gained at the optimum tilt angles. The maximum energy gain is found to be at the south geography direction.

Figs (9.10) can be used as references to estimate the area (A) which is effectively used by the solar system thereby determining the effeciency percentages of the inclined collector and the effeciency percentage at different tilt angles using the following equation:

The effective area (A) = Total area (B) * Effeciency percentage due to inclination* Effeciency percentage due to the deviation of the collector from south direction.

Note that the total area (B) is always greater than the effective area (A).

The model for calculating the optimum tilt angle which has been formulated in section (2.4) can be used directly without the need of applying eq. (1).

Table(1) Show the values of constants A,B and C and the Corelation coefficients r with respect to the period in southeast and southwest from eq. (4).

South East				
The Period	A	B	C	r
Winter&Autum	90.6311	0.0055	-0.0087	0.983
Summer&Spring	-6.8254	0.0026	-0.0014	0.996
Annual	64.2894	-0.0041	-0.0053	0.993
South West				
The Period	A	B	C	r
Winter&Autum	-10.3178	0.01357	-0.004	0.974
Summer&Spring	-94.2442	0.0141	-0.0003	0.999
Annual	-54.4118	0.0143	-0.0021	0.982

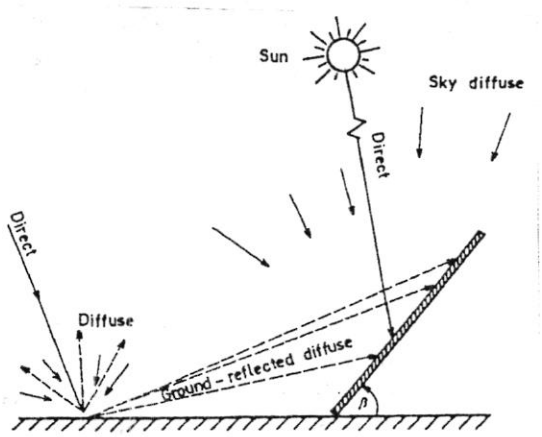

Figure(1) Incidence of direct, sky diffuse, and ground reflected radiation on an inclined surface

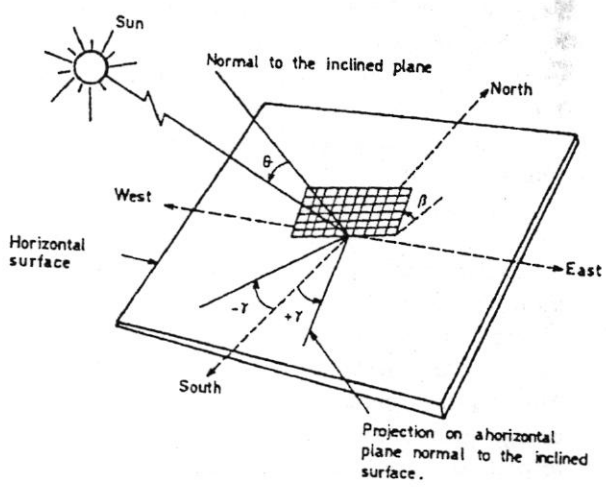

Figure(2) Position of sun relative to an incline plane

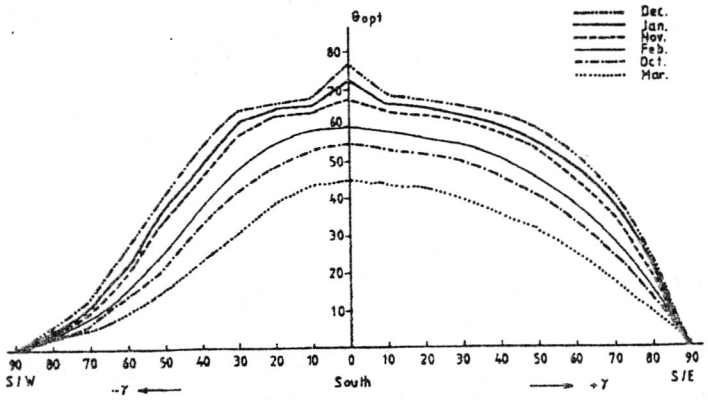

Figure(3) Shows the optimum tilt angle versus south-facing directions between (East-South-West), the value of optimum tilt angles are those at which Hβγ is maximum

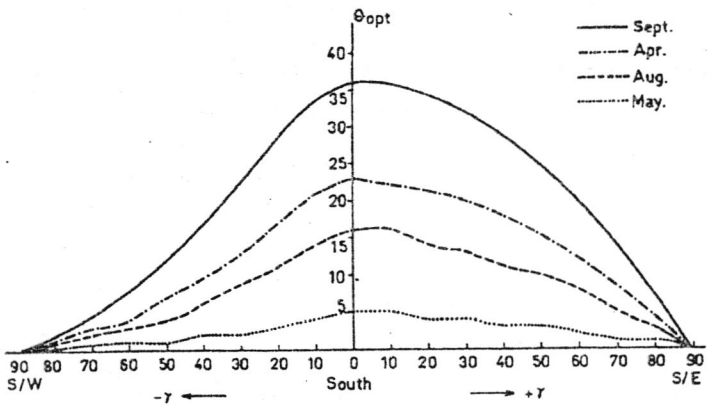

Figure(4) Same as Fig.(3) for months Sept., Apr., Aug., and May

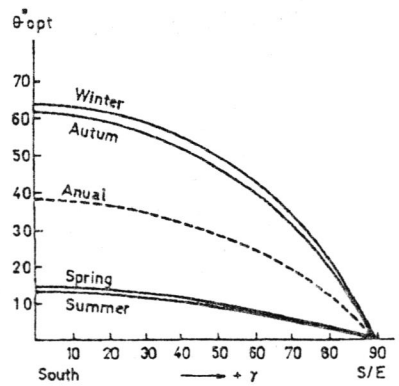

Figure(5) Shows seasonal average of tilt angle versus south-facing directions between E/S

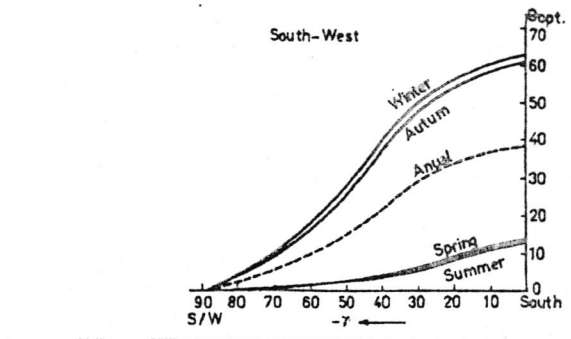

Figure(6) Same as Fig.(5) for the south-facing directions between S/W

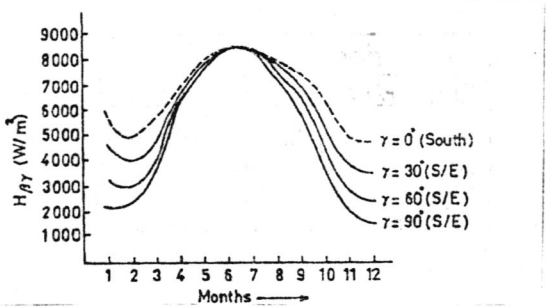

Figure(7) Shows the ratio between the energy gained at optimum tilt angle to the energy gained at horizontal surface for the south-facing directions between (East to South)

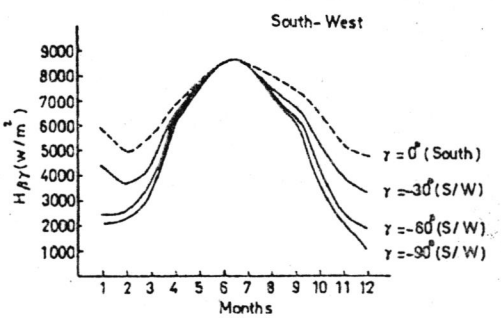

Figure(8) Same as Fig.(7) for the S/W directions

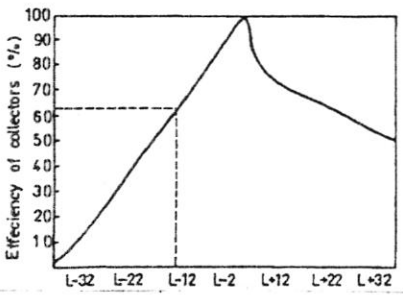

Figure(9) Efficiency percentage versus optimum tilt angle

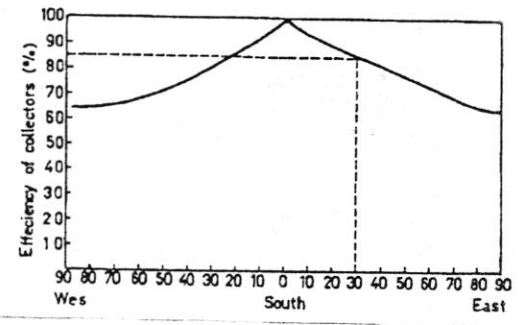

Figure(10) . Efficiency percentage versus south-facing directions between (E-S-W)

REFERENCES

[1] Akrawi, A., "Absoltte radiometric seaks and sclar constant measurements", journal of spaces and astronomy research. 2(1) ; 85(1985).

[2] ASHRAE, "Hand book of fundamentals", New Yourk (1985).

[3] Manes, A. and Antez, "on the optimum exposure of flat-plate fixed solar collectors", solar energy, 31(1): 21(1983).

[4] Mel-kassaby, M., "The optimum seasonally and yearly tilt angle for south facing solar collectors" 3rd arab international solar energy conference-Baghdad Iraq, 76-81 (1988).

[5] Iqbal, M., "An introduction to solar radiation", Academic press canada (1983).

[6] Villarubia, M. and coronas, A., "Solar radiation incident on tilted flat surfaces in Barcelona, SPAIN", solar energy, 25(1): 359 (1980).

[7] Abdullah, A., "The optimum tilt angles for south facing solar collectors in IRAQ". Journal of education and scince, 8(2): 165(1989).

[8] Rasool, R.A., "Study of solar radiation in IRAQ". M Sc. Thesis, Technology University (1986).

[9] Klein, S.A., "Calculation of monthly avarage insolation on tilted surfaces; solar energy, 19(4): 325(1977).

[10] Klucher, T.M. "Evaluation of models to predict insolation on tilted surfaces", solar energy, 23(2): 111(1974).

[11] Amar, H.A. "World of solar energy", University of Calro, Eygpt (1986).

[12] Mosallam Shaltont, M.A. "Solar energy input and photovoltaic water pumping in western doesert oases of Egypt", 2nd international conference of desert development, Jan., 25 (1987).

Al-Mustansiriya J. Sci

Vol. 6. No 1, 1995

Photooxidation of RNase N from Aspergillus niger

MUKARAM SHIKARA and SAMI F. AL-WAN
Department of Biology, College of Education, University of Kufa, Najaf, IRAQ.

(Recieved 14 Jun.,1992; Accepted 30 Nov., 1993)

الخلاصة

تم استعمال الاكسدة الضوئية لصبغة المثيلين الزرقاء لغرض ايقاف نشاط الانزيم الهاضم للرنا ن مما ادى الى حدوث تغيير في عدد ثلاثة احماض أمينية (هستدين، سيرين، تايروسين) من مجموع الاحماض الامينية المكونة لجزيئة الانزيم، ولم تتأثر سرعة الاكسدة الضوئية بوجود الاوكسجين او درجة الحرارة او تركيز الانزيم، وانما تأثرت بتركيز الصبغة ونوع الآس الهيدوجيني. أدت الاكسدة الضوئية لمولين من الحامض الاميني هستدين ولثلاثة مولات للحامض الاميني تايروسين الى أيقاف النشاط الانزيمي تقريباً، بينما تأثر مولان فقط من مجموعة ثمانية مولات للحامض الاميني سيرين، ولهذا تقترح النتائج ضرورة وجود مول او مولين من هستدين وتايروسين (وربما سيرين) في مركز نشاط الانزيم.

ABSTRACT

RNase N was inactivated by methylene blue-catalyzed photo-oxidation at pH 7.0 with changes in the number of histidine, erine and tyrosine residues in the molecule. The rate of inactivation was not affected by oxygen, temperature or enzyme concentration, but effected by the concentration of the dye and the pH photo-oxidation of about two moles of histidine and three moles of tyrosine residues resulted in a complete inactivation of the enzyme, at which point only two serine residues were effected. The results suggest the participation of histidine, tyrosine and may be serine in the catalytic function of RNase N. They may be part of its active site.

INTRODUCTION

Various ribonucleases (RNases), such as RNase A(1), RNase T1 (2) and RNase M (3) are known to be inactivated by photo-oxidation in the presence of a photosenitizer dyes such as methylene blue, riboflavin, rose bengal, neutral red and fluorescein.

RNase N from Aspergillus niger was purified (4), crystallized (5), and some of its physical and chemical properties were studied.

In this paper, the amino acid composition of the enzyme is reported with some results obtained by photo-oxidation of RNase N in the presence of methylene blue, riboflavin and rose bengal.

MATERIALS & METHODS

Enzymes

Aspergillus niger purified RNase N was prepared according to the procedure described in the previous paper (4,5), RNase TI was a commericial preparation (Worthington Biochemical Coporation) and RNase M was a gift from professor Masachika Irie, Faculty of Pharmaceutial studies, University of kyoto, Japan.

Determination of an RNase activity

A.niger RNase N activity was determined by measuring acid-soluble digestion products from yeast RNA at 260 nm in spectrophotometer as described in the previous paper (4). RNase TI and RNase M activities were determined as described by Takahashi (2) and Irie (3) respectively.

Buffers

Acetate, Phosphate and Tris-HCI buffers were used between pH 4-5. 5, 5.8-7.6 and 7.0-10.0, respectively.

Amino acid analysis

Native RNase N were hydrolyzed with 6N HCI at 110°C for 24h in evacuated sealed tubes and analyzed using a Beckman-Spinco model MS automatic amino acid analyzer according to the procedure of Spackman *et al* (6).

The recoveries of cystine and tyrosine residues in RNase N are often low owing to decompostion on acid analysis. Isoleucine and valine are known to be liberated imcompletely in 24h of hydrolysis.

The tryptophan contents of the enzyme were determined by dimethylaminobenzaldehyde method of Spies and Chambers (7,8).

RNase N was photo-oxidized at pH 7.0 until about 2-3% of the initial activity was remaining. Methylene blue was removed from the reaction mixture by means of a small IRC-50 colum (10x1 cm., then the amino acid composition of photo-oxidized RNase N (abbreviated as Pox RNase N) was analyzed as described above and compared with that of native RNase N.

Protein determination

Protein contents were usually determined by the method of Lowry et al (9) using lysozyme as a standard.

Photo-oxidation

Photosenitizer dye catalyzed photo-oxidation was carried out according to Fuji *et al* (10) as modified by Shikara.

RNase N (2mg) (or RNase TI or RNase M) was dissolved in 1 ml of phosphate buffer, pH 7.0 and was kept in a Pyrex tube (18mm diamete) and kept in

a circulating water bath with a constant stirring at 37°C for 15 min. 0.1mg of the dye was added and the reaction mixture was irradiated vertically from a distance of 30cm with a 200W spot light, A water layer of 2cm thickness was inserted between the reaction vessel and the lamp to eliminate the effect of ultraviolet light. Aliquots (0.1ml) were withdrawn out, after appropriate intervals, and assayed using RNA, as described before, for enzymatic activity. The changes in activity were corrected for those of the control enzymes.

Control experiments were carried out without dye, light or atomospheric oxygen.

RESULTS AND DISCUSSION

Inactivation of RNase N by photo-oxidation

The irradiation of RNase N in the presence of methylene blue caused a rapid inactivation of the enzyme. About 30%, 50% and 70% of RNase N activity was lost during the first 20, 30 and 60min. of irradiation, respectively. After 120 min. of irradiation, only 5% of the enzymatic activity remained, and the activity disappeared completely at 240 min of irradiation (Fig.1a).

RNase TI and Nase M activities were reduced to about 50% after 20 and 50min of irradiation, respectively. All the activities were lost after 180 and 240 min. of irradiation, respectively.

Only a slight decrease in RNase N activity was observed with any of the control samples incubated without methylene blue. Similar results were obtained with RNase TI and RNase M(Fig. 1a).

The rates of inactivation of the enzymes were dependent on the dye concentrations.

The irradiation of RNase N, RNase TI and RNas M in the presence of another photosensitizer such as riboflavin or rose bengal showed that the RNases were photo-inactivated, but the rates of inactivation were far slower than those in the presence of methylene blue. The inactivation was incomplete.

Riboflavin and rose bengal seem to be far less potent than methylene blue under the present photo-oxidation conditions (Fig. 1b), and for this reason methylene blue was used through all the experiments.

Effect of various pHs and dye concentrations on the photochemical action of RNase N

The RNase activity was found around pH 7.0, using phosphate buffer in the presence of 0.1-0.2mg. ml^{-1} methylene blue (Fig. 2). The RNase activity was found around 0.1-0.2mg.ml^{-1} of various dyes and it was with sodium phosphate buffer (Fig.2) in the presence of 0.1-0.2mg. ml methylene blue. The rate of inactivation declines below and above these concentrations (Fig. 3) It is assumed that a slower reaction at low dye concentration may originate from the smaller number of excited molecules per unit of time, whereas the dye at high concentration will absorb some of the light which led to a decreased transmission of light.

Photochemical action of methylene blue on RNase N in air or oxygen

The rate of inactivation of RNase N was slightly affected when pure oxygen affected replaced the air in several experiments (Fig. 1a) and for this reason, all the successive experiments were carried out in air.

Photochemical action of methylene blue on RNase N at various temperatures

The enzyme has an optimum temperature (34 -38°) and the activity disappears completely at 54°(4). The rate of inactivation of RNase activity, when photo-oxidation as carried out between 20-55°C, for 10, 20 and 30 min, was identical. This suggests that the rate controlling step in the photo-oxidation of the enzyme is photochemical in nature.

Decrease in histidine, serine and tyrosine contents

The complete inactivation of RNase N suggests the destruction of specific amino acid residues in the active center of the enzyme. Amino acid analysis of photo-oxidized samples (Table 1) showed a significant decrease in histidine, serine and tyrosine residues only, and that other amino acid residues remained almost intact.

The destruction of one of the four tyrosine residues and one of the five histidine residence during photo-oxidation led to a marked decrease in 60% and 70% in RNase activity, respectively. However, at the point of 90% inactivation, when one mole of histidine and two moles of tyrosine were photo-oxidized, about seven moles out of the eight serine residues remained unchanged (Fig. 4). At a complete inactivation, about six moles of serine remained intact as analyzed by the method of Spies et. al (7,8). It is reasonable to assume that the loss of one or two of histidine residues and two or three tyrosine residues-were responsible for the inactivation of the enzyme. These results indicate that one or two of these residues are of essential importance in the catalytic function of the enzyme, although the participation of one or two serine residues in catalytic function cannot be excluded.

It is tempting to postulate that there is at least one or two histidine residues in the actiave center of RRNase N. Histidine residues were discovered in the active catalytic center of several RNases such as RNase A(11). RNase I(12), RNase TI(13) and ERNase M(14).

In these RNases, histidine acts as a general acid in concert with glutamic acid which acts as a general base.

In these RNases, histidine acts as a general acid in concert with glutamic acid which acts as a general base.

Fjurther studies on the nature of the active center of RNase N are in process.

Acknowledgments

The authors wixh to express their thanks to Dr F.Z. Al-Rhman, Department of Agriculture for the use of Amino acid analyzer.

Table (1) Amino acid composition of RNase Nphoto-oxidized in the presence of methylence blue

	No. of residues	(moles per moles protein)	(a)
Amino acid	Control	Theoritical residual no. of RNase N	Pox RNase N(with 25% remaining activity)
Aspartic acid	9.3	9	9.1
Threonine	3.1	3	2.7
Serine(b)	7.8	8	5.9
Glutamic acid	4.0	4	4.0
proline	8.1	8	8.3
Glycine	12.2	12	12.1
Alanine	7.2	7	6.8
Half cystine	3.3	3	3.0
Valine	2.1	2	2.7
Isoleucine	5.6	6	4.9
Leucine	6.9	7	6.0
Tyrosine (b)	4.0	4.1	1.1
Phenylalanine	3.0	3	3.0
Lysine	2.3	2	2.0
Histidine (b)	5.1	5	2.2
Arginine	12.3	12	11.7
Tryptophan	3.1	3	3.7
Methonine	1.7	2	1.3
Ammonia	10.2	10	9.8

a) The number of residues are calculated by assuming the number of glycine residue per molecule to be 12 and no corrections has been made for losses resulting from decomposition during acid hydrolysis.

b) The values of amino acid residues which sufferd a significant change.

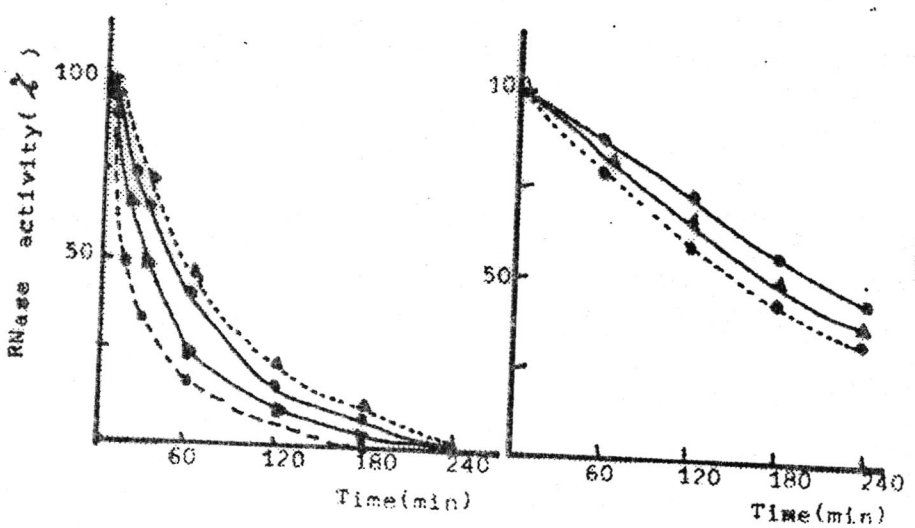

Figure(1)Rates of inactivation of RNase N , RNase M and RNase T1 in the presence of air. Enzyme crystals (smg) were dissolved in 0.02M phosphate buffer, pH 7.0 and the photosenitizer dyes (methylene blue in Fig.1a and riboflavin in Fig.1b) were added as in Methods. Fig.1a shows the rate of inactivation of RNase N in pure oxygen ( ) instead of air.

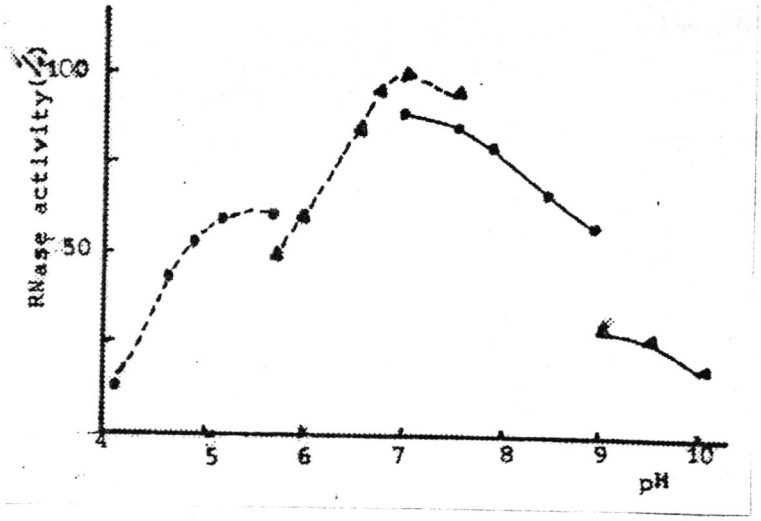

Figure(2) Influence of pH on the photochemical action of methylene blue on RNase N. The enzyme crystals (5 mg) was dissolved in 1ml of 0.02M suitable buffer(acetate , phosphate , Tris-HCl and glycine).

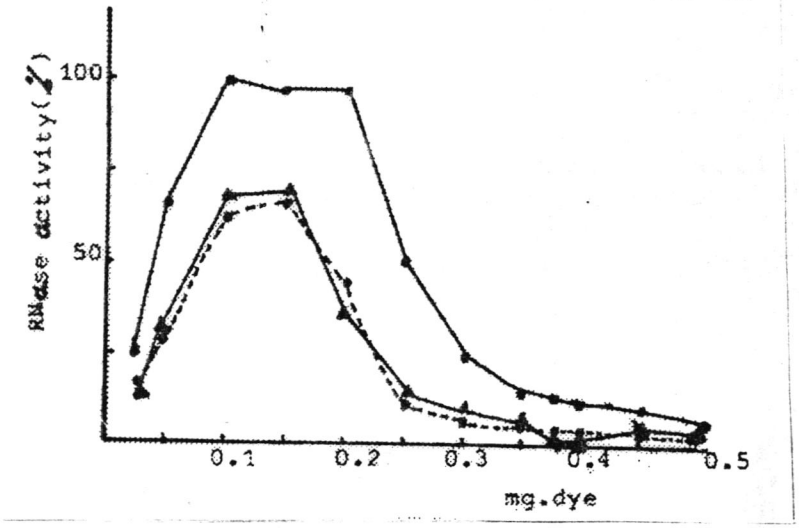

Figure(3) Effect of various concentrations of days on the photochemical action of RNase N. The enzyre crystals (5mg) was disolved in 0.02M phosphate buffer, pH 7.0 and days (methylene blue , riboflavin and rose bengal) were added as in Methods.

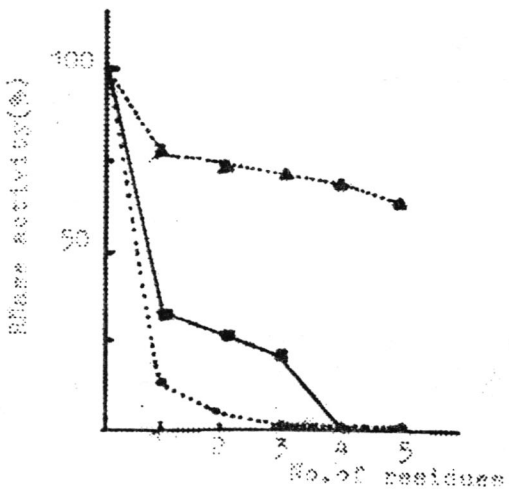

Figure(4) The relationship between histidine (•), serine (Δ), and tyrosine (◊) residues photo-oxidized per molecule of protein to the extent of inactivation.

REFERENCES

[1] Scheraga, H.A. and Rupley, J.A., Photo-oxidation of RNase A, Advances in Enzymol., 161-169, 24 (1963).

[2] Takahashi, K., The structure and function of RNase TI (X11), J. Biochem., 331-338, 69 (1971).

[3] Irie, M., Isolation and properties of an RNase from Aspergillus saitoi, J. Biochem., 509-518, 69 (1967)

[4] Shikara, M., Purification and properties of an RNase from Aspergillus niger, Iraqi J. Biol. Sci. (in print).

[5] Shikara, M., Purification & properties of an RNase inhibitor from Aspergillus niger, Al-Mustansiriyah J., 3(1) (1991).

[6] Spackman, D.H., Stein, W.H. and Moore, S., Automatic recording apparatus for use in the chromatography of amino acids, Anal. Chem, 1190-1205, 30 (1958).

[7] Spies, J.R. and Chambers, .D.C., Chemical determination of tryptophan p-dimethylaminobenzaldhyde and sodium nitrite in sulfuric acid solution, Anal Chem., 30-39, 20 (1948).

[8] Spies, J.R. and Chambers, D.C., Determination of tryptophan with p-dimethylaminobenzaldhyde with photochemical development of colour, Anal. Chem. 1209-1220. 22 (1950).

[9] Lowry, O.H., Rosevrough, N.J. Farr, A.L. and Randall, R.J., Protein measurement with the Folin phenol reagent, J. Biol. Chem., 265-275, 193 (1951).

[10] Fuji, Y., Kobashi, K. and Nakai, N., photo-oxidation of histidine residues in rat M1 and L-Type pyruvate kinase, J. Biochem., 1289-1296, 95 (1984).

[11] Rupley, J. A., Further studies on RNase A, Biol. Phys. Acta, 11-14, 1190 (1989).

[12] Naka, M.I. and Lee, R. Riboflavin-sensitizes photo-oxidation of RNase I, Amer. J. Biol. Sci., 1-10, 240 (1988).

[13] Scott, L.S. and McDonald, K., Photo-oxidation of histidine & tryptophan residues in RNase T1. Amer. J. Biol. Sci., 130-36, 241 (1988).

[14] Irie, M. and Yutaka, Y., photo-oxidation of RNase M, Biol. Chem. Acta, 338-344, 140 (1988).

Al-Mustansiriya J. Sci Vol. 6 , No. 1 , 1996

Consumption and Utilization of Date Fruits by two Ephestia spp. Larvae

HUSSAIN F. ALRUBEAI, ZAHERA A. AL-GAHRBAWI* and FAWZI S.AL-ZUBIDE* *
*Department of Agricultural Research Nuclear Research center, Baghdad, Iraq.
**Department of Biology , College of Science, University of Babylon , Hella, Iraq.
(Recieved 4 Mar., 1992; Accepted 30 Nov., 1992)

الخلاصة

تمت دراسة الاستهلاك الغذائي وكفاءة التحويل في يرقات حشرتي Ephestia calidella و E.cautella على ثمار التمر تحت ظروف الخزن الطبيعية ولكل جيل من اجيال هاتين الافتين فضلا عن دراستهما تحت ظروف مختبرية مثلى ثابتة مقدارها٢٧ ± ١م و ٦٥ ± ٥٪ رطوبة نسبية و ١٦ ساعة ضوء. اشارت النتائج ان يرقات النوع calidella تستهلك غذاء اكثر مما تستهلك يرقات النوع الثاني cautella وخلال الاجيال المختلفة. وظهر بان اعلى وزن جسم مكتسب قد حصل خلال جيل التشتية ولكلا النوعين مع ذلك فقد اظهرت نتائج قياس معدلات الاستهلاك ان افضل معدل كان خلال الجيل الاول للنوع calidella والجيلين الثاني والثالث للنوع الاخر. اما معدلات النمو فقد كانت على اعلاها في الجيلين الاول والثاني للنوع calidella وفي الثالث للنوع cautella. وبالرغم من وجود فروق معنوية بين قيم الهضم التقريبي لاجيال النوع الواحد فقد كانت النسب الناتجة عالية وبمدى يتراوح مابين ٨٠-٩٠٪ للنوع calidella و ٩١-٩٧٪ للنوع cautella . اما كفائتي تحويل كل من الغذاء الماكول والغذاء المهضوم الى مادة حية فقد كانتا منخفضة جداً في كافة اجيال النوعين علما ان اعلى قيم حدثت اثناء جيل التشتية. تمت كذلك مناقشة العلاقة ما بين النتائج المستحصلة والاهمية الاقتصادية لكلا النوعين.

ABSTRACT

Food consumption and utilization efficincies of larvae of Ephestia calidella (Guenee) and E>cautella (Walker) fed on date fruits were determined under natural storage conditions for each generation and optimum laboratory condititions of 27±°C, 65+5% R.H. and 16 hr photoptase. The results indicated that E.calidella larvae consumed more food than E. cautella larvae during their different generations. The highest body weight gain occured during overwintring generation for both species. However, the consumption indices were found to be the best during 1st generation of E.calidella and 2nd and 3rd generations of E. cautella. In term of growth rate the 1st and 2nd generational larvae of E.calidella had the highest rate, while in E. cautella was the 3rd generational larvae. Although, there were significant differences between values of approximate digestibility of different generation in each species the percentages were high and ranged between 80-92% for E.calidella and from 91-97% for E. cautella. Efficiencies of ingested and digested food were too low for both species in all generations, though the highest valeus were during over wintering generation. The rerationship between these findings and the economic status of both specices was also discussed.

INTRODUCTION

Ephestia spp. are important pests of date fruit in Iraq. Economically, dates are one of the important crops in the central and southern parts of Iraq. Due to the level of damage caused by these insects, several researches were conducted in order to plan a pest management programe for date in Iraq (1-5). The present study is a part contribution to this programe.

It has been clearly indicated that food type, greatly affected the biological performance of insects (6,7). No previous studies were conducted on food consumption and utilization by Ephestia spp. (8). This is an unfortunate gap in our knowledge about these pests, since such information is of obvious importance to physiology, nutrition, ecology and economic entomology. Therefore, the present study was conducted to evaluate the qualitative effects of ripe date fruits on food consumption and utilization of two species of Ephestia.

MATERIALS AND METHODS

Nutritional indices were calculated on a wet weight basis using the formulae in Table (1) (9). Growth rate and consumption indices are measurements of the fresh weight gain or weight of food eaten by the larvae. The weight of the faeces is the amount of frass produced by the larvae during larval feeding period. Approximate digestibility (AD) measures the precentages of food ingested which is retained or utilized by the larvae. While the efficiency of conversion of ingested food (ECI) is an overall measurement of the larval ability to utilize the ingested food for growth, and the (ECD) measures the efficiency of conversion of digested (assimilated) food. Corrections for water evaporation from date fruite; were obtained from standered calculated evaporation factor, by holding uninfested control date fruites under natural conditions of sucssesive generations. The initial fresh weight of newely hatched first instar larva was calculated by using

the average weight group of 100-200 individules. While, the final wet weight of ceased feeding last instar larbvae was determined individully. Six segregation of the larvae were done depending on the reddish tests of the male.The experimental insects, E. calidella and E.cautella were obtained from cultures reared for at least one year out-door under natural storage conditions. The control cultures were reared in a rearing room, under conditions of 27±°C 65% RH and 16 hr photophase. At least 50 newly hatched larvae of each species were placed in an individual vials containing two preweighed date fruits and kept under natural conitions till the end of last instar. All experiments and measurements were repeated for all generations of each speacies used at the natural onset generational time. Data were subjected to analysis of variance and means were separated by Duncans new multiple range test.

Table 1. Nutritional Index Formula: fresh weight eaten (FWE), Fresh weight gain (FWG), ; Fresh weight of Faces (FWF), Fresh weight of larvae during the feeding period (FWL); Duration of feeding period (t).

$$\text{Relative Growth Rate (GR)} = \frac{FWG(mg)}{t(days)\,X\,\bar{x}FWL}$$

$$\text{Consumptive Index (CR)} = \frac{FWE(mg)}{t(day)\,X\,\bar{x}FWL}$$

$$\text{Approximate Digestibity (AD)} = \frac{FWE(mg)-FWF(mg)}{FWE(mg)} x100$$

$$\text{Efficiency of Conversion of Digested Food (ECD)} = \frac{FWG(mg)}{FWE(mg)-FWF(mg)} X100$$

$$\text{Efficiency of Conversion of Ingested Food (ECI)} = \frac{FWG(mg)}{FWE(mg)} X100$$

RESULTS

Study results are illustrated in Fig (1) which represents the amounts of food consumed and body weight gain of E. calidella, males and females. The amount of food eaten was at its highest level during the 3rd generation (overwintring). While, the lowest amount was that of larvae reared under constant conditions of the rearing room. It is obvious that females larvae consumed more food than males under all circumstances. The fresh weight gain was diractly correlated with the amount of food eaten. Considering the differences in generational period, the growth rates were the highest in 1st and 2nd generations compared with the 3rd generation and indeed it was at its highest rate under constant environmental conditions. The same trend was found with consumption (Table 2I).

food consumption and utilization efficiencies reselts are shown in Table 2. The data indicated a significant differences between 1st and 2nd generations and with the 3rd generation of all three parameteres. It is clear

At the control trial, the lowest AD values encountered by the highest level of conversion efficiency.

In regard to E. cautella larvae, the data obtained are represented in Fig (2). It is evident that larvae of E. cautella consumed significantly more food (597 mg in average) during 3rd generation. This is even more clear in terms of measuring the consumption rate which was the highest (2,59 in averge). The body weight gain was at its highest level during 4th generation (overwintring), however, the growth rate was not (Table 3).

Food assimilations (AD) were significantly different among generations (Table 3), with its highest level in the 3rd generation, and with larvae reared under controlled conditions. In regared to food utilization efficiencies, the data indicated that larvae of the 4th generation had the best conversion efficiencies.

DISCUSSION

The pyralide species, including E. calidella and E. cautella, are a prolific, highly polyphagous insects that infests fruits and cereals in stores and / or fields. As a results of their cosmopolitin distribution, they can survive and thrive under a wide variety of climatic and nutritional conitions, not all of which are optimal in terms of food consumption and utilization effeciency. Although, several research papers have been published on the utilization of food by many insect species (8), non of these cover the subject during generational periods of the insect pest in concerne and under natural conditions. It is clear that the total amount of food consumed by E. calidella larvae during its three generations was higher than that of E. cautella larvae. This means that E. cautella consumes less amount but they do have a higher rate of consumption, relative to its shorter larval period of each generation, which resulted in a relatively higher growth rate. This basic informations should have some value in the assisment of the level of damage caused by each species tested to date fruits.

The efficiency of absorption of food from the gut (AD) was relatively constant for all generations, though with slight significancy, for both species. Reynolds et.al. (10) mentiond that when constant and optimised AD encountered in an insect, this could be in order to maximise its grouth rate. Meanwhile, the values of ECI and ECD showed the same trend of consistancy, though with greater signifcaut differences between E. cautella generations. This implies that a specific proportion of absorbed nutrients are diverted into metabolic activities that do not led to growth (11). In general, the utilization profile of both species indicated that although the date fruites were highly digestable but the digested food was not efficiently utilized for better growth. In this respect, it was suggested that the feeding behaviour of the tabacco hornworm larvae, which is specialised for raped growth achieved primarly by a high rate of food acquisition, is adapted to maximizing the rate at which nutrient is absorbed, thus permitting the maximal rate of growth, even though this leads to lower efficiency of food utilization than could otherwise achieved (10).

Taking into consideration that interrelationships between evironmental nutritional conditions and food utilization are often assumed but seldom quantified, the results of the present study showed that when temperatures turns to fall, during the onset of 3rd and 4th generations, larvae of both species consumed food with relatively high level of conversion values in comparsion with other generations. This could be an artifact of slower development and slower food movement through the gut there by allowing more time for digestion and absortion to occur (12), though less of this food was utilized for growth and development.

The results also suggested that rearing of both species on dates under controlled (optimum) conditions will be more advantagous for **E. cautella**, which has faster growth rate.

Finally, and from the view point of economic entomology and damage assissment, larvae of **E. calidella** caused more damage to dates compaired with that of **E. cautella.**

Table(2) Food consumption and utilization of E. calidella generations under natural storage condition.

Indices	GI		GII		GIII		Control	
	♀	♂	♀	♂	♀	♂	♀	♂
G.R.(gd-1)	0.047	0.047	0.048	0.048	0.017	0.015	0.011	0.108
C.I(d^{-1})	1.189	1.040	0.998	1.204	0.281	0.271	1.185	0.919
A.D.(%)	89.10±0.75a	90.59±0.58a	91.56± 0.39a	92.30± 0.67a	80.44±39b	79.23± 1.93ba	62.91±2.99c	50.23±5.63c
E.C.I.(%)	3.99±0.160a	4.125±0.30a	4.843± 0.21a	4.139± 0.29a	6.320± 0.76b	5.458±0.32b	11.311± 1.41c	19.67±4.4c
E.C.D.(%)	4.54±0.18b	4.56±0.36b	5.27±0.23b	4.48±0.34b	7.819±33a	6.991±0.34a	21.94±4.80c	43.39± 13.15c

Mean in the same line followed by the same later are not significantly different (Duncans multipe range test;p 0.05)

Table (3) Food consumption and utilization of E. cautelia generations under natural storage condition.

Indices	GI		GII		GIII		GIV	
	♀	♂	♀	♂	♀	♂	♀	♂
G.R.(gd-1)	0.051	0.055	0.055	0.051	0.062	0.067	0.013	0.015
C.I(d^{-1})	1.311	1.371	2.751	2.487	2.348	2.842	0.241	0.315
A.D.(%)	94.49±0.54b	95.35±0.54b	96.93±0.35a	97.59±0.34a	97.21±0.18a	97.59±152a	91.40±1.01c	93.33±0.43c
E.C.I.(%)	4.13±0.39b	4.17±0.39b	2.78±0.24c	2.41±0.21c	2.70±0.12c	2.45±0.15c	5.69±0.49a	5.33±0.45a
E.C.D.(%)	4.37±0.42b	4.38±0.43b	2.88±0.25c	2.48±0.22c	2.70±0.13c	2.51±0.12c	6.27±0.57a	5.73±0.51a

Indices	Control	
	♀	♂
G.R.(gd-1)	0.072	0.075
C.I(d^{-1})	2.936	3.393
A.D.(%)	97.38±0.3a	97.83±0.4a
E.C.I.(%)	2.57±0.24c	2.33±0.15c
E.C.D.(%)	2.58±26c	2.39±016c

Mean in the same line followed by the same later are not significantly different (Duncans multipe range test;p >0.05)

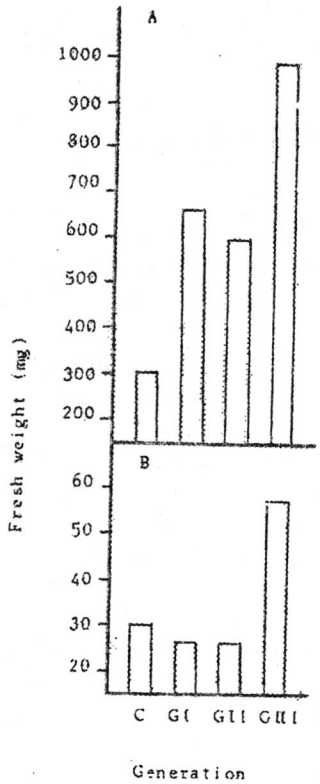

Figure(1) Nutritional performance of E. calidella larvae at different generations. (A) Fresh weight consumed, (B) Fresh weight body gain.

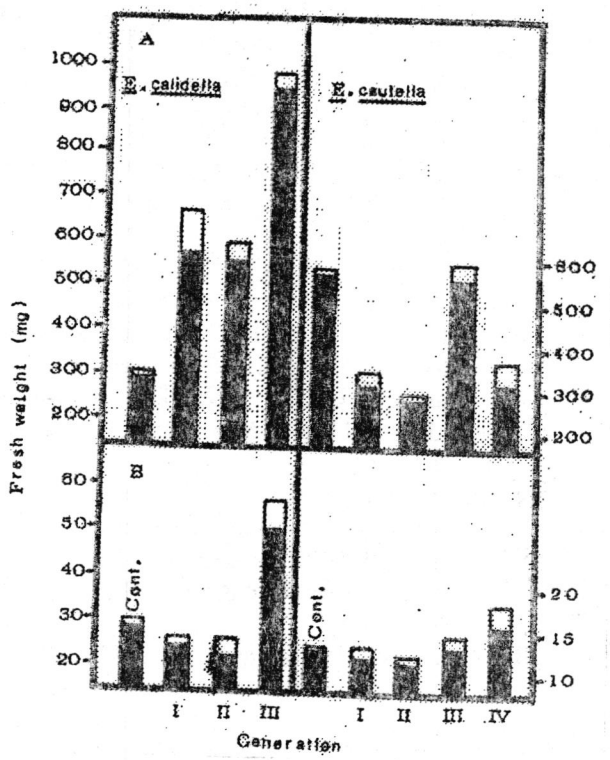

Figure(1) Nutritional performance of Ephestia spp larvae at different generations. (A) Fresh weight consumed, (B) Fresh weight body gain. □ Female, ■ Male.

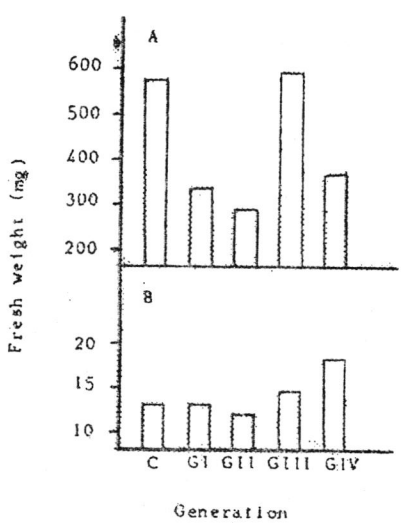

Figure(2) Nutritional performance of E. calidella larvae at different generations. (A) Fresh weight consumed, (B) Fresh weight body gain.

REFERENCES

[1] Ahmed, M.S.H. ; Al-Taweel, A.A. ; Hameed, A.A.; Auda, H.Combination treatment of gamma radiation and elevated temperature as a quarntine treatment against two principal stored date insect species. Modern Insect Control: Nuclear Techniques and Biotechnology, Proc. of Symp., Vienna, 1987.PP. 357-367. (1988).

[2] Al-azawi, A.F.;El-haidari, H.S.;Aziz, F.M.;Murad, A.K. Effect of high temperatures on figmoth Ephestia cautella walker (Lepidoptera, Pyralidea). Date palm J.2: 79-85. (1983).

[3] Al-maadhidi, J.F.; Alrabeai, H.F.;Khalaf, S.H.;Abbas. A.K. Protection of date fruits from Ephestia calidella infestation by Bacillus thuringiensis vars. Proceeding of 3rd Nat.Conf. of Pest and Dis, of Veg. & Fruits, Egypt. II: 618-628. (1989).

[4] Alrubeai, H.F.;Al-gahrbawi, Z.A.Induction of sexual sterility in Ephestia calidella males by sublethal heat treatments. Proceeding of 3rd Nat.Conf. of Pest & Dis. of Veg. & Fruits, Egypt. I; 207-220. (1989).

[5] Al-Taweel, A.A.; Ahmad, M.S.H.; Kadhum, S.S.; Hameed,A.A. Effects of gamma radiation on the progeny of irradiated Ephestia cautella (Walk) (Lepidoptera: Pyralidae) males.J.Stored Prod Res. 26: 233-236 (1990).

[6] Beckwith, R.C. Influence of host on larval survival and adultfecundity of choristoneura conflitana (Lepidoptera: Tortricidae). Can. Entomol. 102: 1474-1480 (1970).

[7] Kehat, M.; Wyndham,M. The effect of food and water on development, longevity and fecundity in the Rutherglen Bug, Nysius vinitor (Hemiptera: Lygaeioae). Aust.J.Zool. 20:67-78. (1972).

[8] Bhattacharya, G.B.;Pant, N.C.Studies on the host plant relationships: Consumption and utilization profile in insects. Proc. Nat.Acad, Sci.India. 46:274-301. (1976).

[9] Waldbauer, G.P. The consumption and utilization of food by insects. Adv.Insect Physiol. 5:229-288. (1968).

[10] Reynolds, S.E.;Nottingham, S.F.; Stephens,A.E.Food and water economy and its relation to growth in fifth-instar larvae of the tobcco hornworm, Manduca sexta. J.Insect Physiol. 31: 119-127. (1985).

[11] Reynolds, S.E.; Nottingham. S.F. Effects of temperature on growth and efficiency of food utilization in fifth-instar caterpillars of the tobacco hornowrm, Manduca sexta. J.Insect Physiol. 31: 129-134. (1985).

[12] Schmidt, D.J.; Reese, J.C. The effects of physiological stress on black cutworm (Agrotis ipsilon) larval growth and food utilization. J.Insect Physiol. 34: 5-10. (1987).

The Synchronized Effect of Iron Shift-up on The Physiology of Cyanobacterium (Blue-Green Alga) Calothrix parietina M 102 Thuret

IHSAN A. MAHASNEH* AND ABDULLAH H.A. AL-MOUSAWI**
* Department of Biological sciences, Mu'tah University, P.O. Box 7, Mu' tah, JORDAN.
** Department of Biology, College of Science, University of Basrah, IRAQ.
(Recieved 15 July, 1992; Accepted 19 June, 1993)

الخلاصة

جرى تقدير بعض الاستجابات الفسلجية لاضافة الحديد الى مزرعة الطحلب Calothrix parietina MI02 تعاني من نقص الحديد. ادت اضافة الحديد بتركيز ٤ ملغم/لتر في اليوم العاشر من النمو في مزرعة محدودة الحجم تعاني نم نقص في عنصر الحديد الى زيادات متوازية ومتزامنة في محتوى الخلايا من الحديد (٩٠٠٪)، نشاط انزيم النتروجينيز(١٢٠٠٪)، البناء الضوئي (٥٥٠٪)، التنفس(٣٠٠٪) محتوى كلوروفيل-أ-(٦٠٪) والوزن الجاف(١٣٠٪). وكانت هذه الاستجابات محسوسة خلال ساعة من الاضافة واستمرت حتى استعادت المزوعة الى نموها الطبيعي. وادت اضافة بعض مثبطات النمو بعد اضافة الحديد الى اختزال ملحوظ في نشاط انزيم النتروجينيز، البناء الضوئي والتنفس تمت مناقشة اهمية هذه الظواهر على فسلجة السلالة المدروسة.

ABSTRACT

An account is given to the particular physiological responses of an iron deficient culture of Calothrix parietina M 102 to the shift - up of iron, during growth in batch culture, the shift - up (0.4 mg. l^{-1} at day 10) of the iron deficient culture has led to parallel and synchronized increase in cellular iron (900%), nitrogenase activity (1200%), photosynthesis (550%), respiration (300%), chlorophyll - a content (60%), dry weight (130%). These responses were detectable within one hour and continued well until normal growth of alga had resumed. The addition of inhibitors, subsequent to the shift - up of iron, led to a marked reduction in nitrogenase activity, photosynthesis and respiration. The importance of these observations on physiology of the strain is discussed .

INTRODUCTION

Iron appears to be one of the most important nuterient factors influencing the physiology of cyanobacteria (blue - green algae), particularly the nitrogen fixers [1]. Iron is a component of nitrogenase as well as cytochromes, non - heme protein and ferredoxin, which are required for electron transport to supply reductant for nitrogen - fixation [2]. Previous works on the importance of Iron in microalgae indicate that iron (among phosphorus and molybdenum) is a dey element that can enhance nitrogen limitation [3,4,5,6, and 7] and contribute to death of algae [8,9,10,11,12, and 13]. In contrast with the studies on mixed planktonic forms, there are, apparently, some shortage of information in the literature about the effect of iron on physiology of specific species or genera of cyanobacteria [see 1]. Calothrix is one of the larger genera of the Rivulariaceae group, being widespread in aquatic environments and often a nitrogen fixer ; a feature which may cause a further iron - stress on the alga to match its demand for the element. The aim of the present study therefore is to characterize, for one strain, the physiological changes taking place in response to the deficiency and shift - up of iron.

MATERIALS AND METHODS

Organism and Growth Conditions

The organism used for this study was an axenic strain of Calothrix parietina Thur. (M 102) from the Mu'tah Culture Collection. The culture was a gift from Dr. B.A. Whitton and originally isolated from an upland freshwater stream from Sand Sike, Upper Teesdale,U.K. [14].

The organism was grown in batch culture at 32°C under continuous illumination of 5000 lux supplied by cool white fluorescent tubes. The Chu - 10 D (-N) medium (Table 1), was modified from the No. 10 formula of [15].

The concentrations of iron were changed according to each experiment. The inocula were prepared in a version of medium similar to that used for the experiment.

Measurements of Photosynthetic and Respiratory Oxygen

The rates of photosynthesis (under saturation light) and respiration (in the dark) were measured by a polarographic Clark electrode.

Chlorophyll - a determination

The chlorophyll - a content was determined according to the method of [16].

Nitrogenase activity

Algae were harvested at various times during growth in batch culture in order to monitor the changes in nitrogenase activity. Estimates of nitrogenase activity using the acetylene reduction assay technique (ARA) was made according to [17]. All experiments were carried out in flasks with 25 ml medium covered with a gas - tight subaseal bungs while continuously shaking in a thermostatically controlled tank. The results of nitrogenase were expressed as μmol. ethylene.mg dry wt^{-1}. min^{-1}.

RESULTS

The physiological changes of Calothesis parietina M 102 during growth in batch culture in control medium are given in Figure 1. The chlorophyll - a showed a rapid increase during the first week of growth before it reached the plateau of 3 mg l^{-1}. In contrast, the dry weight of the alga showed a gradual increase, which continued well over the rest of the period. Gellular iron showed an initial increase reaching 1.8% dry weight, followed by a subsequent decrease to attain the lowest level (0.2% dry weight). The peak of nitrogenase activity come at about the end of the first week of growth reaching a maximum of 6 µmole. ethylene.mg dry $wt^{-1}.min^{-1}$, followed by a subsequent decrease.

The physiological changes (cellular iron, nitrogenase activity, photosynthetic and respiration rates, chl-a content, dry weight) before and after the shift-up of iron deficient Calothrix M 102 are given in Figures 2 and 3. During growth in iron deficient medium (using ultra pure water), the cellular iron decreased sharply to attain the lowest level at about day 10. The initail increase in nitrogenase activity (about day four), appeared to be caused after the iron carried over in the inoculum was used in growth, presumably at the time when most of the trichomes became symetrical with the basal heterocyct.

The shift-up of iron, addition of 0.4 mg 1-1 iron at day 10 (Fig.2), led to a parallel and synchronized increase in both cellular iron (900%), and nitrogenase activity (1200%), both were detectable within one hour and reached a maximum within 24h. The addition of chloramphenicol (chlo.; after 28h of iron addition) to the shifted-up culture had led to a marked reduction in nitrogenase activity (Fig.2). The shift-up of iron had also led to a rapid re-greening of cultures and hormogonia production (microscopic observation) within 24h followed by subsequent resumption of normal growth. This was judged when 90% of trichomes showed hormogonia production, followed by an increase in both chlorophyll - a and dry weight, until they approached the level obtained during growth under controlled conditions. These data is in accordance with the rapid increase in both photosynthesis (550%) and respiration (300%), under a range of iron 0.1 - 1.0 mg 1-1 (Fig.3). Moreover, the separate additon of 3- (3, 4-dichlorophenyl)-1-1 dimethl urea (DGMU) and carbonyl cyanide -m- chlorophenyl hydrazone (CCCP) after the point of shift-up had led to progressive reduction in photosynthesis and respiration respectively (Fig. 3).

DISCUSSION

The increase in chl-a (60%) and dry weight (130%) of Calothrix parietina M 102, in response to the shift-up of iron, were above that found for growth under iron deficiency (Fig. 2). This is comparable with changes reported for chl-a (25%) and for the dry weight (150%) of the Trichodesmium [13]. The stimulation rate of nitrogenase activity in response to the shift-up of iron (Fig.2) was comparable with that (500%) reported for blooms of blue-green algae [18]. The striking increase in nitrogenase activity was about four times of the activity found before the shift-up of iron and even higher (60%) than that found during exponential growth under control condition (Fig. 1). This is a marked contrast to other circumestances where such a rate of activity needs several days to be achieved; suggesting that the shift-up of iron cause a rapid synthesis of some iron - containing protein, presumably nitrogenase. This was confirmed by showing the suppressible effect of the chloramphenicol at the transcriptional level of the N_2-Fixation process (Fig. 2).

The stimulation range of photosynthesis (80-360 mol.0_2.mg chl-$a^{-1}h^{-1}$) (Fig. 3) was comparable with that (100-200 mol. 02.mol.chl-$a^{-1}h^{-1}$) reported for the Trichodesmium [13], though comparable with that (28 mol.02.mol.chl-$a^{-1}h^{-1}$) reported for the nitrogen fixing phytoplankton [19]. The suppressible and respective effect of the DCMU and CCCP (Fig. 3) on photosynthesis and respiration after the shift-up of iron confirms that stimulation of photosynthesis and respiration was in fact due to the shift-up of iron.

CONCLUSION

Addition of iron to the culture of the cyanobarium Calothrix parietina M 102 Thuret at the time of iron deficiency resulted in a sharp increase in some of its physiological processes presumably through the production of some enrymes. This was documented by the addition of bio-inhibitors.

ACKNOWLEDGMENTS

The authors would like to thank Dr.B.A. Whitton (Department of Biological Sciences, University of Durham, U.K.) for providing culture.

Table (1) Chemical composition of Chu 10-D(-n) medium (mg 1-1 of salts)

KH_2PO_4	7.36
$MgSO_4.H_2O$	25
$FeCL3.6H_2O$	2.42
$NaEDTA.2H_2O$	3.18
$NnCL_2.4H_2O$	0.045
$NaMoO_4.4H_2O$	0.007
$ZnSO_4.7H_2O$	0.055
$CuSO_4.5H_2O$	0.01
$COSO_4.7H_2O$	0.011
H_3BO_4	0.715
$NISO_4.7H_2O$	0.012
HEPES	600

* N-2-hydroxpiperazine-N-ethane sulponic acid. p^H adjusted to 7.6

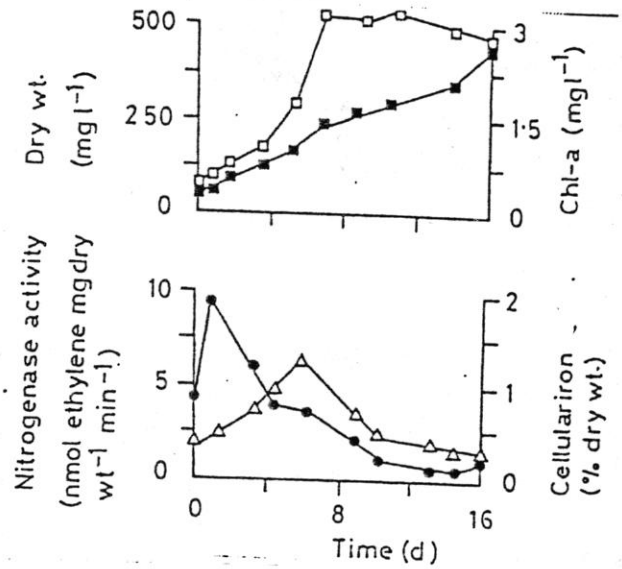

Figure(1) Changes in Chlorophyll-a (□), dry weight (▬), cellular iron (•) and nitrogenase activity(Δ) of Calothrix parietna M102 during growth in batch culture under control condition. Iron concentration was 0.4 mg|-1

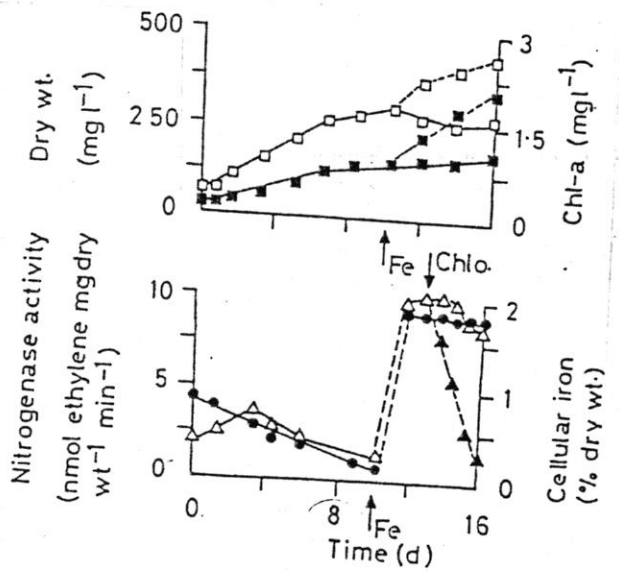

Figure(2) Changes in Chlorophyll-a (□), dry weight (▬), cellular iron (•) and nitrogenase activity(Δ) of Calothrix parietna M102 during growth in batch culture before(——) and after (-----) the shift-up of iron (0.4 mg|-1). The nitrogenase activity is also shown after addition of chloramphenicol (chlo.) at concentration of 25 mg|-1

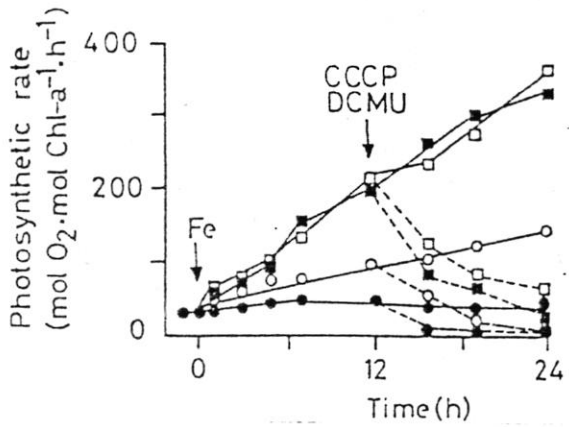

Figure (3) Changes in Photosynthesis of Calothrix Parietina M102 in response to the up-shift of iron (mg|$^{-1}$;0.0, (•);0.1, O; 0.4, ■; and 1.0, □) before (——) and after (-----) additions of DCMU at concentration of 25 mg|$^{-1}$. The respiration rate (Δ) is shown at iron shift-up 0.4 mg|$^{-1}$ before (——) and after (-----) addition of CCCP at concentration of 25 mg|$^{-1}$.

REFERENCES

[1] Boyer, G.L., Gillam, A.H. and Trick, C.G. Iron Chelation and Uptake. In: Van Baalen, C.(ed). The Cyanobacteria. pp. 415-436. Elsevier Science, New York, (1987).

[2] Syrrett, P.J. Nitrogen Metabolism of Microalgae in: Platt, T. (ed.). Physiological Basis of Phytoplankton Ecology. pp. 182-210, (1981).

[3] Doremus, C.Geochemical Control of Dinitrogen Fixation in The Open Ocean. Biol. Ocean. 1, 429-436, (1982).

[4] Paerl, H.W., Crocker, K.M. and Prufert, L.E. Limitation of N2-Fixation in Costal Marine Water: Relative Importance of Molybdenum, Iron, Phosphorus and Organic Matter Availability. Limnol. Ocean. 32,525-536, (1987).

[5] Rueter, J.G. and Patersen, R.R. Micronutrient Effects on Cyanobacterial Growth and Physiology, New Zeal.J. Marine and Freshwater Res. 21,435-445, (1987).

[6] Howarth, R.W., Marino, R. and Cole, J.J.Nitrogen Fixation in Freshwater, Estuarine and Marine Ecosystems.l. Rates and Importance. Limmol. Ocean.33, 669-689, (1988).

[7] Howarth, R.W. Marino, R. and Cole, J.J.Nitrogen Fixation in Freshwater, Estuarine and Marine Ecosystems. 2. Biogeochemical Controls.Limnol. Ocean. 33,688-701, (1988).

[8] Ohki, K. and Fujito, Y.Aerobic Nitroginase Activity Measured as Acetylene Reduction in The Marine Non-Heterocystous Cyanobacterium Trichodesmium Spp. Grown Under Artificial Conditions. Mar. Biol. 98, 111-114, (1988).

[9] Guikema, J.A. and Sherman,L.A. Organization and Function of Chlorophyll in Membranes of Cyanobacteria During Iron Starvation. Plant Physiol. 73, 250-256, (1983).

[10] Ructe, J.G. and Ades, D.R. The Role of Iron Nutrition in Photosynthesis and Nitrogen Assimilation in Scenedesmus quadricauda (chlorophycease) J.Physol. 23,452-457, (1987).

[11] Foster, F.W., Barton, L.L. and Johnson, G.V. Differential cellular Response of Anabaena variabilis to Iron. J.Plant Nut. 11, 1191-1203, (1988).

[12] Rueter, J.G.Iron Stimulation of Photosynthesis and Nitrogen Fixation in Anabaena 7120 and Trichodesmium (Cyanophycease), J.Phycol. 24,249-254, (1988).

[13] Rueter, J.G., Ohki, K. and Fujito, Y. The Effect of Iron Nutrition on Photosynthesis and Nitrogen Fixation in Culture of Trichodesmium (Cyanophycease). J.Phycol. 26, 30-35, (1990).

[14] Livingstone, D., Khoja, T.M. and Whitton, B.A. Influence of Phosphorus on Physiology of Hair-Forming blue-gfreen alga (Calothrix parietina) From an Upland Stream. Phycol. 22,345-350, (1983).

[15] Chu.S.P. The Influence of The Mineral Composition of The Medium of The Growth of Planktonic Algae. l. Methods and Culture Media. J.Ecol.30, 284-325, (1942).

[16] Marker, A.F.H., Nusch, E.A. and Riemann, B.The measurements of Photosynthetic Pigments in Freshwater and Standardization of Methods: Conclusion and Recommendations. Arch. Hydrobiol. 14,91-106, (1980).

[17] hardy, R.W.F., Burns, R.C. and Holsten, R.D. Application of The Acetylene-Ethylene Assay For Measurement of Nitrogen Fixation. Soil Biol. Biochem. 5;47-51, (1973).

[18] Elder,J.F. and Horne, A.J.Biostimulatory Capacity of Dissolved Iron For Cyanophycean Bloom in a Nitrogen-Rich Reservoir. Chemosph. 9, 525-530, (1977).

[19] mague, T.H., Mague, F.C. and Holm-Hansen, O. Physilogy and Chemical Composition of Nitrogen-Fixing Phytoplankton in The Central North Pacific Ocean. Mar.Biol. 41,75-82, (1977).

Life History and Production of the Castropod Theoduxus Jordani in the Shatt AL-Arab River

YAHYA T. DAOUD*, BALSAM A. MARINA** AND ADIL F. SHIHAB**
*Department of Biology, College of Science, Babylon University, Babylon, Iraq.
**Department of Biology, College of Science, Basrah University, Basrah , Iraq.
(Recieved 10 Oct. 1992; Accepted 19 Jan., 1993)

الخلاصة

دراسة دورة الحياة والانتاجية للنوع Theodoxus jordani (بطنية القدم) في شط العرب. يتضمن البحث أخذ عينات شهرية للجماعة السكانية التي تعود للحيوان الرخوي Theodoxus jordani لمدة سنة منذ شهر كانون الاول١٩٨٥ ولغاية تشرين الثاني ١٩٨٦ من منطقة الصالحية في شط العرب، وذلك لدراسة الكثافة السكانية، ومعدل النمو وبنية الجماعة السكانية وعدد الاجيال المكونة للجماعة السكانية. تراوحت الكثافة من ٢٥٧/م٢ في شهر ايلول الى ١٣٤١/م٢ بعد انتاج الصغار في شهر تموز. ولقد تبين بأن الجماعة السكانية تتكون من جيلين. ومعدل الانتاجية السنوي هو ٤٥٣,٣٩ غم/م٢ ومعدل الكتلة الحيوية ١٨٩٩ غم/م٢ والنسبة بين الانتاجية والكتلة الحيوية هي ٠,٢١.

ABSTRACT

A popluation of Theoduxs jordani (sowerby 1836) was sampled monthly in shatt al-Arab for one year (Dec. 1985- Nov. 1986) to measure density, growth rate, population size structure, cohort composition and production. Population density showed a well defined pattern of fluctuation and varied between 297 m^{-2} in September and 1314 m^{-2} in July after recruitment. The population was basically made up of two cohorts, Annual production (p) was 453.39 $gm^{-2}$and the mean biomass ($\bar{B}$) was 1899 gm^{-2}. The P/B catio was 0.21.

INTRODUCTION

The gastropod Theoduxus jordani (Sowerby) is common and widely dispersed throughout Satt Al-Arab gegion (1,2). It inhabits the intertidal zone of the river and its tributaries.

The life history of Theoduxus jordani and other gastropods has been studied by the previous authers but they did not give any detailed informations on the analysis of population structure except that by (3). Furthermore there was no study concerning the estimation of production rates for natural population of this species.

The present work deals with seasonal variation in population density, population size structure. Life cycle pattern and production.

Study area

The sampling site is on area of about 40m long of the river bank. It is located near the Basrah city cerntre where the intertidal zone is muddy and covered with plants froming a green mat for most part of the year.

Shatt Al-Arab in this region, is an oligohaline brackish water of a comparatively high temperature during summer and moderately low temperature during winter. It is also influenced by the semidiurnal tide of the Arabian Gulf. Among the other molluscs found in the same habitat are Melanopsis preaemorsa Ferussac, Melanoides tuberculata (Muller), Gyrulus convexisculus (Hutlon), Corbicula fluminalis (Muller) and Corbicula fluminea (Muller).

MATERIAL AND METHODS

This study is based on samples collected monthly from the intertidel zone in the period between December 1985 and November 1986. Ouadrates (20x20cm) were taken on each occassion. Three quadrates were taken along every transect (3 samples at each transect). The first transcet situated at the minimum water level while the second and third ones were at 15 and 30 meters from the minimum water level respectively.

Each sample was then placed in a separate plastic bag, and brought to the laboratory where sorting through 0.425mm mesh-sized sieve was done. This mesh size was fine enough to retain all size groups of the gastropod. Identification of snails based on (4).

The gastropod were then grouped into 0.5mm total length size classes and different cohorts separated by probability paper ploting (6,7).

Density and growth were determined by following the change in number and mean lengths of each generation over successive sampling periods. To estimate monthly mean biomass and mean weight, the mean lengths of the Theoduxus jordani were converated to mean weight using an empirical lenght-weight regression equation. For this purpose live individuals of Theoduxus jordani of different sizes were collected and each individual was measured for length and the dry weight determined over heating at 60 °C for 24hrs. Weight of individuals were measured to the nearst 0.01 mg by a sartorius-type balance.

Annual mean biomass was calculated from the monthly means of biomass and used for computing the production-biomass ratio (P/B). The production of each generation and the total annual production were estimated by measuring the survivorships and mean weight increments of each generation separately using the expression of (8).

$$P = \sum_{t=0}^{t-1} \frac{\overline{Nt} + \overline{Nt+1}}{2} \bullet \overline{W}$$

where $\overline{N}$ = mean population density at time and t + 1, $\overline{W}$ = The mean weight increment between successive samples.

Measurments of some environmental factors were made at the time of sampling. A mercury thermometer was used for temperature records. The Winkler method was used to determine dissolved oxygen. Samples were fixed in the field and titrated later in the laboratory, Calcium ion concentration was determined by titration with permanganate. Samples for the above analysis were taken at 5 cm beneath the surface water over the sampling area and usually between 10.00 and 12.00 hours.

RESULTS

Physico - chemical factors

A maximum water temperature of 35°C occurred in July 1985 and a minimum of 14°C in January 1985 and February 1986. Dissolved oxygen concentration showed marked seasonal differences. This appeared to correlate with water temperature (Fig 1). Calcium ion concentration was relatively high (105-230)mgl^{-1} and reached its peak concentration in March 1986. The concentration was particularly high during the period when calcium was most required for shell growth and was always much higher than minimum concentration required for gastropod survival (9,10).

Population density

Fig (2) shows that the densities of T.jordani were high during the summer and low during winter and Autumn. These densities ranged between 105.5 m^{-2} in November to 1171 m^{-2} in April.

The snails seemed to be aggregated in their spatial distribution. When the value of slope (b) of the relationship between the variance and the mean (5) was utilized as an index of aggregation, it was apparent that the population was highly aggregated (b=1.6). Aggregation could have been a response to exposure, because sampling was carried out at low tide, when most of the snails were exposed to air (11).

Analysis of variance on the population counts from different transect indicated that densities of T.jordani did not differ significantly ($P > 0.05$). This revealed that the gastropod can exist in the exposed sites during the whole period of the low tide.

Population structure

The size class distribution (Fig 3) shows that the growth occured mainly during April 1986 to September 1986. Growth slowed considerably during October to March and most mortality occured this time.

The result of probability analysis of data on size frequency distribution showed that the population consisted of two cohorts from April 1980 to July 1986. The 1985 cohort disappeared on July 1986. As the adults of 1985 cohort died after breeding, the 1986 cohort dominated the population from April 1986 to November 1986. The latter cohort grew fast, attaining adult breeding size by November 1986.

Breeding season

Theoduxus jordani commence breeding in December, when egg capsules were first observed. Capsules laying continued through january, February and March and deposited on hard objects. Eggs were laid in semi rounded protective capsules, attached to soild objects, these objects included the shells of other moullusces and the hard surfaces of aquatic macrophytes. From April to July, the capsules opened and the youg snails were librated. Development is direct without living planktonic larva, as is common to most prosobranchs. The hatchings had 1mm long semitransparent soft shells with weak coloration.

Cohort density

Fig (2) shows that the generation 1985 gradually declined in numbers during Spring and early summer except in June 1986 (This could be attributed to sampling error). Virtually all the individuals of this generation had died by the end of June 1986.

Generation 1986 was present in a relatively high numbers through out the summer and gradually decreased in abundance during the Autumn time (August - November 1980).

Growth rates

Growth rates were based on length increment which converted to dry weight using a regression of dry weight in length log (dry weight) mg = 3.0045 log (length) mm- 0.7194 $r = 0.986$ ($P > 0.001$).

The mean dry weights of each generation during successive months are shown in Fig 4. Members of generation 1985 showed no growth during winter and early summer. This could be due to the low temperature and death of aged individuals after reproduction.

Generation 1986 showed a gradual growth from April until November. This could be attributed to the favourable temperature which ranged during this period from 22 to 16°c.

Biomass and Production

The estimation of biomass for each generation obtained from the mean monthly weight and the monthly density of each generation (Fig. 5). The monthly total biomass of the population showed a peak

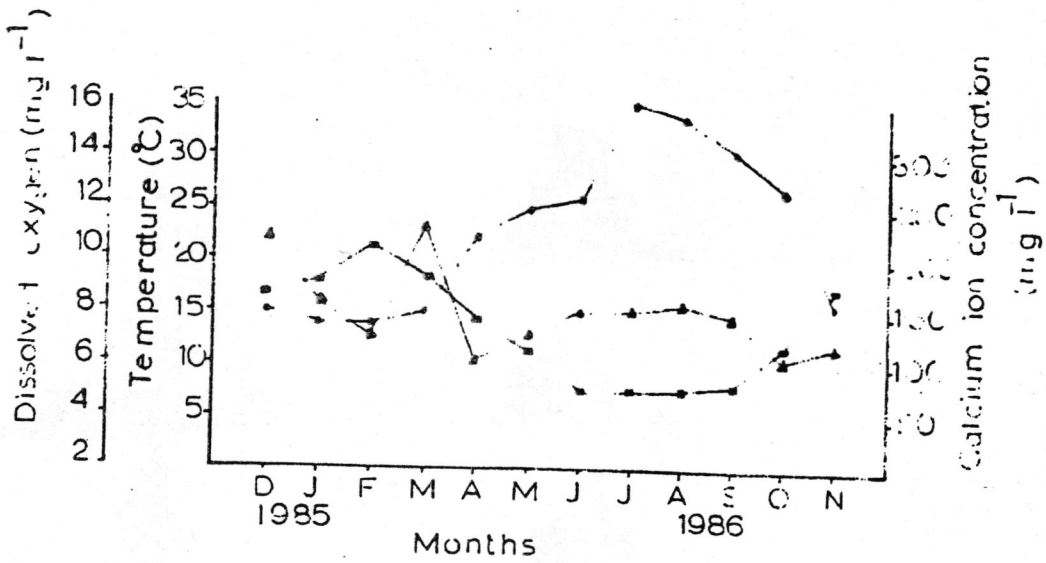

Figure(1) Temperature dissolved oxygen and calcium ion concentration of the water of Shatt AL-Arab at the study site • Temperature, ♦ dissolved oxgen, ▲ calcium ion cocetration

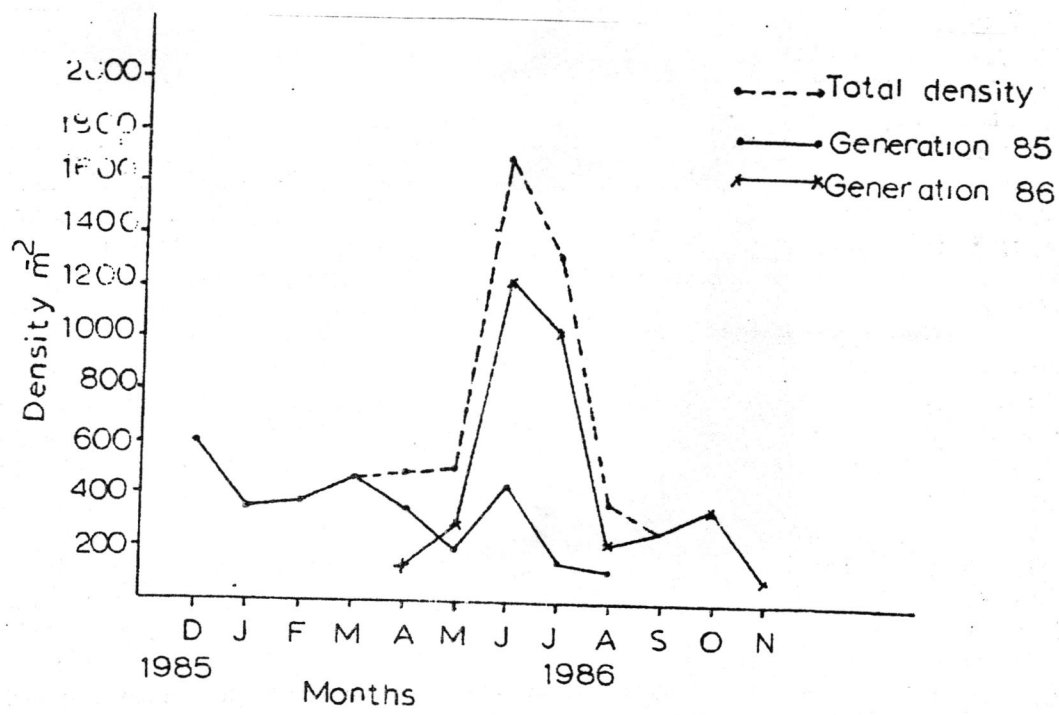

Figure(2) Total population density and population density of each generation of Theodoxus jordani in Shatt AL-Arab region from December 1985 to November 1986

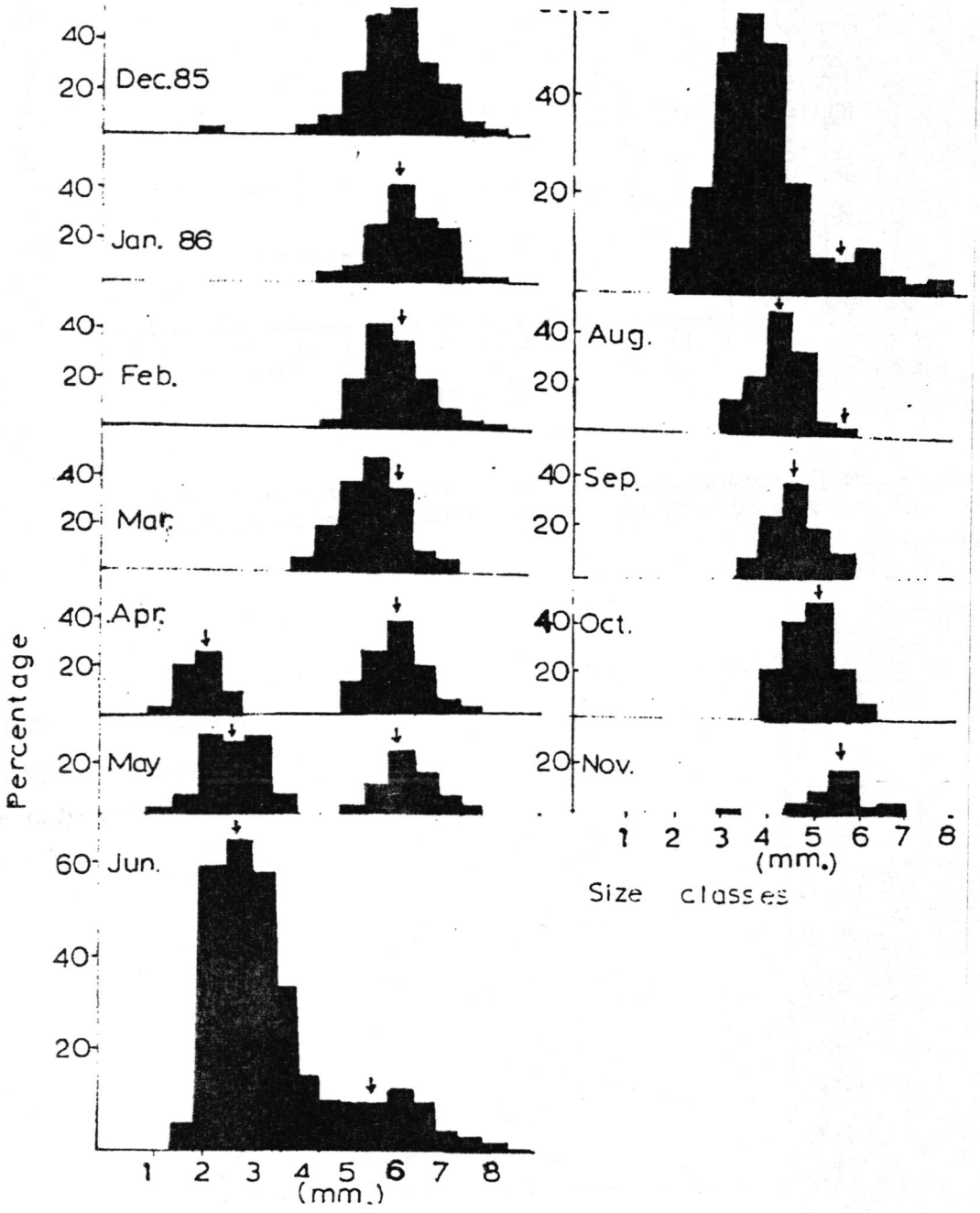

Figure(3) The size frequency distribution in percentage of I. jordani population , Arrows indicate the position of mean cohort size

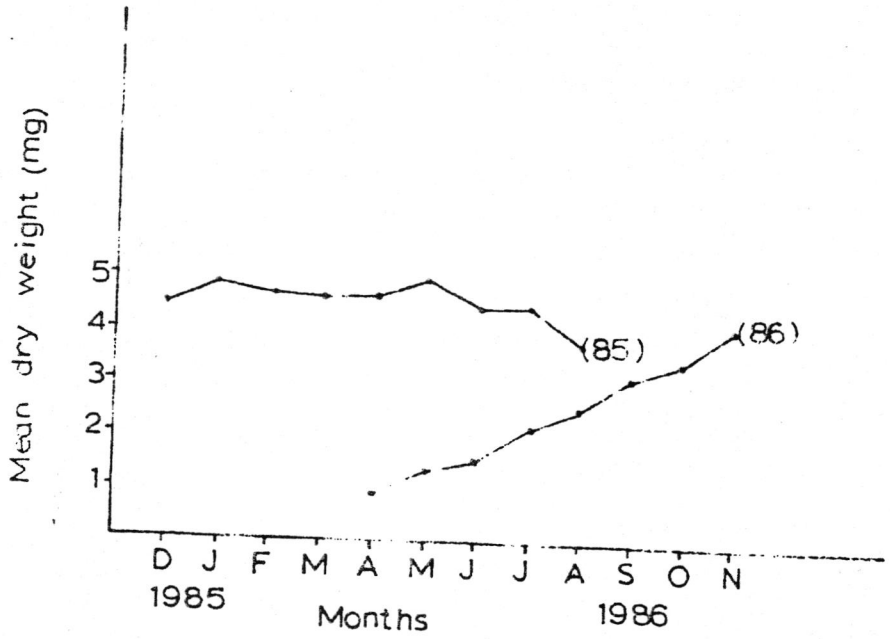

Figure(4) **Theodoxus jordani**, Mean dry weight of Generation 85 and 86 in the Shatt AL-Arab region

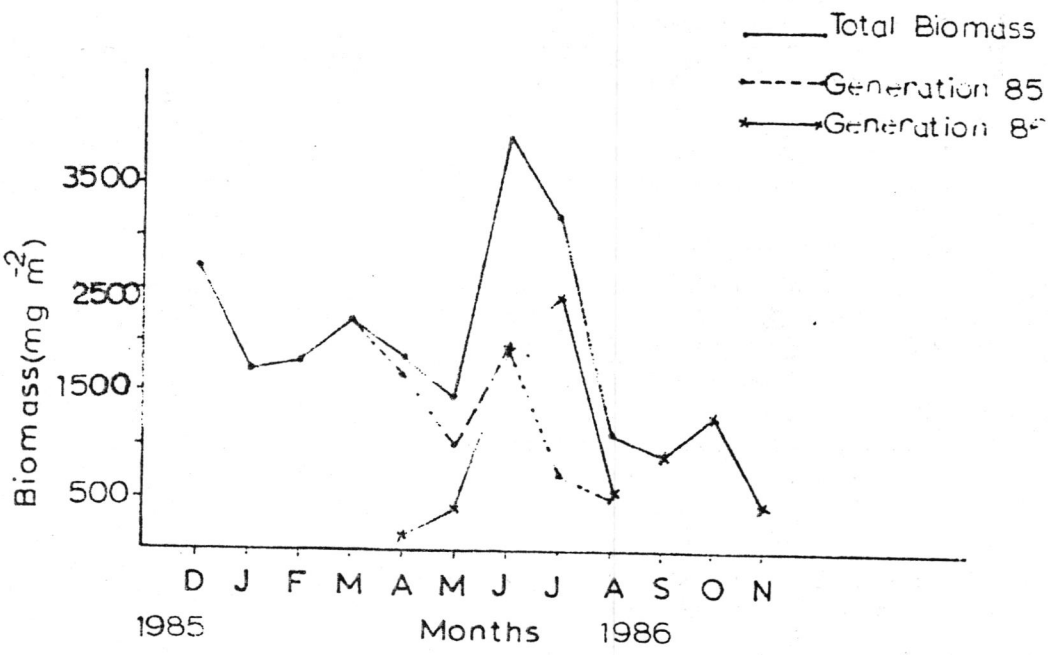

Figure(5) **Theodoxus jordani**, Mean monthly biomass for total population and for both generation in Shatt AL-Arab for the period from December 1985 to November 1986

during June 1986 (3970 mg dry weight/day).

Both generations showed high values of biomass during June and July 1986. This could be due to high density of individuals as result of reproduction (Fig 2).

The mean biomass $\overline{B}$ (calculated from the total biomass of each census divided by total number of census time) was 189.9 gm^{-2}.

The production for generation 1985 was 107.39 gm^{-2} while for generation 1986 was 346.43 gm^{-2}. The overall annual production was 453.82 gm^{-2} and the overall annual turnover ratio was 0.21.

DISCUSSION

The population densities of the present study were greater than those given by Al-Dabbagh and Daoud (1). Their estimation of a density was ranged between 29-208m-2 while the maximal and minimal densities of the present study ranged between 297-1341m-2. The differerence might be as result of change in the environment. The salanity increased four times as before (1%0 - 4%0) while (12) explained considerable increase in water pollution. (13) reported that T. jordani is an exclusive which feeds on ephiphytic algae and its population are largest where the aquatic vegetation is lmost luxuriant. This explaines the large population of T. jordani from may to August 1986 when epiphytic algae was abundant during this period.

The appearance of youg T. jordani measuring 1.5 mm long during April 1986 indicates that T.jordani reproduces once a year. (2) reported that the population of two cohorts, the old once disappeared as the adult died after breeding and the young ones appeared in April. They added that T. jordani is an annual species with life span not more than 15 months. (13) recorded that T. jordani reproduces twice a year in lake Tiberias but the number of eggs recovered during August was much lower than those in April.

Thus, it could be concluded that the population of T. jordani composed of two cohorts, 1985 and 1986. The former cohort dominated the population from December to March and disappeared by August while the latter cohort appeared in April and dominated the population from April to October.

The general picture of the growth for old cohort (1985) was irregular without a clear pattern. This is might be attributed firstly, to low temperature during winter months (December-April). Secondly to the death of old individuals after reproduction. On contrast 1986 cohort showed a gradual increase of growth rate which coincide with raising temperature during summer months. Thus, the contribution of 1985 cohort for production was little.

In spite of the high production value (453.82 gm^{-2}), the turnover ratio was very low (0.21). This could be due to, as indicated from density data (Fig 2), the high density of T.jordani and low rate of growth particulary 1985 cohort. Most population studies of aquatic gastropods have either ignored production estimation or based on a single standing crop value rather than expressing it as a rate. However, the estimated annual production rate for Lymnaea auricularia and Melanopsis praemorsa were 55gm^{-2} and 202.98 gm^{-2} respectively (3,14).

REFERENCES

[1] Al-Dabbagh, K.Y. & Daoud, Y.T. The ecology of three gastropod molluscs from Shatt Al-Arab River JBSR (1985).

[2] Al-Dabbagh, K.Y. & Luka. J.Y. Population dynamic of the gastropod Theoduxus jordani (Sowerby) in the Shatt Al-Arab River Freshwater Biology, 6, 443-448 (1986).

[3] Marina, B.A., Daoud, Y.T. & Shihab, A.F. (in press) population Biology and production of Melanopsis praemorsa L. (Gastropoda) in the Shatt Al-Arab River.

[4] Ahmed, M.M. Systematic study on mollusca from Arabian Gulf and Shatt Al-Arab. Iraq. Basrah. University press, Basrah, (1975).

[5] Taylor, L.R. Aggregation, Variance and Mean. Nat 189, 732-735 (1961).

[6] Harding, J.P. The use of probability paper for the graphical analysis of polymodal frequency distribution. J. Mar. Biol. Ass. U.K. 28, 141-153, (1949).

[7] Cassie, R.M. Some uses of probability paper in the analysis of sixe frequency distribution. Aust. J. Mar. & Freshwat. Res. 5, 513-522 (1954).

[8] Crips, D.T. Energy flow measurment. In: Holme, N.A., McIntyre, A.D. (eds.). Methods for the study of marine benthos, IBP handbook No. 16-Blackwell, Oxford. P. 284-372 (1984).

[9] Harman, W.N. Snails, Mollusca, Gastropoda In: pollution Ecology of Fresh water Invertebrates, Eds C.W. Hart, jr and S.L.H. Fuller). Academic press, New York 91974).

[10] Russell-Hinter, W. Physiological aspects of ecology in nonmarine molluscs. In: physiology of Mollusca (Eds. K.M. Wilbur and C.M. Young). Academic press, New York (1964).

[11] Moulton, J.M. Intertidal clustering of Australian gastropod, Biol. Bull. Mar. Biol. lab., 123, 170-178 (1962).

[12] Douabul, A.Z., Abaychi, J.K., Al-Asadi, M.K. & Al-Wadi, H. Restoration of heavily polluted branches of Shatt Al-Arab River. Wat. Res. 21(8): 955-960 (1989).

[13] Tchernove, E. The mollusca of the sea of Galilee Malacologia 15: 147-184 (1975).

[14] Rabie, A.A.S. The ecology of two species of pulmonate snails Lymnaea auricularia (L.) and physa acuta in Shatt Al-Arab River. M.Sc. Thesis, University of Basrah, (1986).

Isolation and Characterization of hydrocarbon Degrading Flavobacterium aquatile

SUBHI J. HAMZA, ALIA F. HUCHIM, ZAINAB M. AL-KARKHI and THAIR I. AL-BAJJARI
Biological Research Center and Center of Analytical Chemistry P.O. Box 765, Baghdad, Iraq.
(Recieved 26 Dec. 1992; Accepted 8 May, 1993)

الخلاصة

تم اقلمة البكتريا المتوطنة في تربة معرضة لفترة طويلة لبعض المواد الهيدروكربونية على تفكيك مخلفات الدورة النفطية وعزلت البكتريا المسؤولة عن عملية تفكيك المركبات الهيدروكربونية وشخصتا على انها Flavobacterium aquatile . لقد وجد بان اغلب المركبات الهيدروكربونية المتواجدة في المخلفات النفطية قد تم تفكيكها بواسطة مزرعة نشطة من البكتريا بفترة ٤٨ ساعة وحسب ما مقدر بجهاز كروماتوغرافيا الغاز. كما وجد بان عملية تفكيك المركبات الهيدروكربونية بواسطة البكتريا يتم عن طريق عمل مستحلب للمركبات الهيدروكربونية مع الماء بواسطة افراز عامل مستحلب بكتيري خارج الخلايا تستطيع بواسطته مزج المركبات الهيدروكربونية مع الماء.

ABSTRACT

The microbial degradation of petroleum refinery waste has been studied using adapted bacterial culture. A bacterial strain which is able to utilize hydrocarbons was isolated and tentatively identified as Flavobacterium aquatile. An active culture was found able to degrade most of the hydrocarbons present in the petroleum waste within 48 h when applied at a concentration of 5% as determined by gas-liquid chromatography. The growth of Flavobacterium on hydrocarbons was accompanied by the emulsification of the insoluble carbon source in the culture medium which may attributed to the production of emulsifying agents during hydrocarbons degradation.

INTRODUCTION

A considerable quantities of petroleum refinery waste containing emulsified and free branched paraffins as well as high molecular weight aromatic and alicyclic hydrocarbons, was disposed in soil. It represent a major pollutional problem since they contain oxygen demanding material and priority pollutants known for their toxicity, persistence and bioaccumulation in the environment, and hence their biodegradation is of importance (1). Bacterial metabolism of hydrocarbons has been studied intensively (2,3,4) and it has been shown that bacteria generally degrade hydrocarbon through emulsification of the insoluble carbon in the culture medium (5). Many species of oil utilizing bacteria has been isolated. The most frequently isolated genera include Pseudomonas,. Acinctobacter, Flavobacterium, Brevibacterium, Corynebacterium and Arthrobacter (2).

In this report, a study was undertaken to isolate and identify bacteria able to degrade petroleum waste, and adapt this isolate for metabolizing most of the compounds found in petroleum waste.

MATERIALS AND METHODS

Samples

Petroleum refinery waste samples were obtained from three storage areas in Dora petroleum refinery, Baghdad. Samples were dried at 121°C for 24h prior to homogenization and dilution by ether.

Media and Culturing

The basal mineral salts solution used was as follows (g/l): K_2HPO_4, 4.5; KH_2PO_4, 3.0; NH_4NO_3, 1.5; $MgSO_4$. 0.2; $FeSO_4$, 0.002; and $CaSO_4$, 0.005. 10ml of petroleum refinery waste was added to the sterile medium. 100 ml medium were inoculated with 1 ml of 24 hr growing culture of Flavobacterium. For growth of

Enrichment Culture

The first attempts to isolate bacterial strain capable of growth on petroleum waste were made using a basal mineral salts solution with 1 ml petroleum waste as the sole source of carbon. All these attempts failed, however. For this reason, a series of new enrichment was carried out using various amounts of the test substrate, petroleum waste, oily swamp, cultivated soil, motor oil and cutting oil contaminated soil and sewage sludge were used as source of inoculation. The samples were checked daily under microscope. If evidence of biodegradation was noticed, the culture broth was then used for isolation and adaptation of the degrading microorganism to higher concentration of tested substrate. Adaptation to elevated concentration of petroleum waste was carried out using 1 to 10 ml with increase of 1 ml step wise.

Isolation and Identification of Petroleum Waste Degrading Bacteria:

Loopfules of medium from each flask were streaked onto plates containing nutrient agar. Developed colonies were recultured in basal mineral salts containing 1 ml petroleum waste. Cultures that appeared were checked for purity. Colonies were transferred three to five times between plates and flasks containing petroleum waste so that the ability to degrade petroleum waste and apparent culture purity were consistent. The isolate were characterized by using Bergey's Manual of Systematic. Bacteriology (6) and tests for characterization were done accordingly to the methods described by Weeks (7).

Liquid Chromatography

Petroleum waste or metabolized petroleum waste samples were deasphalted using column packed with 4gm Celite (60-80 mesh). The dimension of the column was 27 cm in length and 0.8 i.d. The column was sequentially developed with 40ml of n-pentane and 20ml of benzene to elute the deasphaltened oil and benzene-soluble asphaltenes. The fraction of deasphalted petroleum waste was performed on mixed Alumina/Silica gel column. Eluents used were 40 ml of n-hexane (for saturated hydrocarbons), 100 ml dichloromethane (for aromatic hydrocarbons) and 100 ml dichloromethane-methanol 2:1 (for N-, S-, and O-containing compounds).

Gas Chromatography

The chromatographic analyses of each fraction were performed using packed column type 5% SE30 installed in a Shimadzu gas chromatograph GC-7A. The dimension of the column was 3.2m in length, 3.1 cm i.d. The differential pressure of the nitrogen carrier gas through the column was 0.6 kg/cm^2 and the flow rate was 40 ml/min. The injector and detector temperatures were set at 300°C. The column was operated at 80°C and programmed at a rate of 4°C min to 260°C with a final hold time of 30 min. The gas chromatograph was connected to a computer type Shimadzu CR-3A Chrompack.

RESULTS AND DISCUSSION

Isolation of Bacteria Capable of Degrading Petroleum Waste:

A pure culture of bacteria capable of degrading petroleum waste was isolated from soil previously contaminated with motor oils and cutting oils. We believed that bacteria from such areas could have already been selected for degrading various saturate as well as aromatic hydrocarbons. To improve the capability of such isolate for degrading petroleum waste, selective continuous enrichment technique was used. This technique allows the development of bacteria capable of degrading high molecular weight hydrocarbons as well as branched paraffins and intermediates of poly cyclic aromatic hydrocarbon metabolism. It is important to remove such metabolities to achieve complete waste disposal. The degradation of petroleum waste is shown by the increase in number of viable cells as a function of time. The most striking effect of bacterial action on the petroleum waste was extensive emulsification of oil then a change in it's consistency followed by an increase in bacterial cells (Fig. 2). The emulsification of hydrocarbons in liquid media has been attributed to the production of extra cellular emulsifying agents during the hydrocarbon fermentation. A wide variety of extra cellular emulsifiers produced by bacteria has been described. The most thoroughly characterized were rhaminolipeds, lipopeptides, phospholipids and neutral lipids (8).However, little information has been published concerning the potential use of biological emulsifiers.

The isolate was identified as being of the genus Flavobacterium on the basis of a wide variety of biochemical and biophysical tests, of particular importance was the test for motility which distinctly separates this isolate from the genera Pseudomonas and Cytophaga. The cells were non motile in soft agar (swarming motility) and in hanging drop preparations. No flagella were observed when cells were flagellum-stained and compared to a Pseudomonas sp. The cells were gram negative, exhibiting a non diffusible yellow pigment. They were 1.5 μm long and 0.4 μm wide, oxidase, catalase, and phosphatase-positive. The isolate was tentatively identified as Flavobacterium aquatile by the criteria listed by many investigators (6,7).

Microbial Utilization of Petroleum Waste:

Growth of Flavobacterium aquatile on petroleum waste was investigated using mineral salts agar plates technique (9). After 1 to 2 days of incubation, bacterial colonies surrounded with transparent area (clear zone) appeared. Flavobacteria grew at the expense of solid waste since no other carbon source present in culture medium and solid waste had disappeared from cleared area (Fig.2).

To fallow the course of in Vitro biodegradation of petroleum waste, gas chromatographic analyses of the culture medium was performed. The results of these experiments show extensive degradation of saturate fraction of hydrocarbons (Fig. 3) short chain n-alkanes could be attacked first, then long chain n-alkanes. Latter, aromatic hydrocarbons will be removed (Fig. 4). No detectable residues were found after 4 days of incubation. An active culture of flavobacteria found unable to utilize aromatic hydrocarbons. The apparent utilization of aromatics in the presence of n-alkanes as opposed to the lack of growth when aromatics were the only carbon source suggested that cometabolism is involved. Similar observation on crude oil incubated with active cultures of Pseudomonas species, a Flavobacterium species and an Achromobacter species confirm this observation (10,11,12). It is demonstrated that the depletion of saturated hydrocarbons started very rapidly and that most the saturated hydrocarbons are removed within one day (Fig. 3). Moreover, depletion of aromatic hydrocarbons initiated after 2 days and level up after 5 days of incubation.

Gas chromatographic analyses of insoluble NSO fraction and asphalten indicated that no NSO components and asphalten were detected in crude and metabolized petroleum waste (Fig. 5).

Generally, the relative proportions of fractions; saturated, aromatic and NSO in the petroleum waste has a marked effect on the capabilities of the microbial populations to degrade them. The results of this study suggested the possibility of using active culture of Flavobacterium aquatile to deal with petroleum waste disposal. The chance of success of such treatment depends, in part on the modification of the chemical composition of petroleum waste, rendering it more

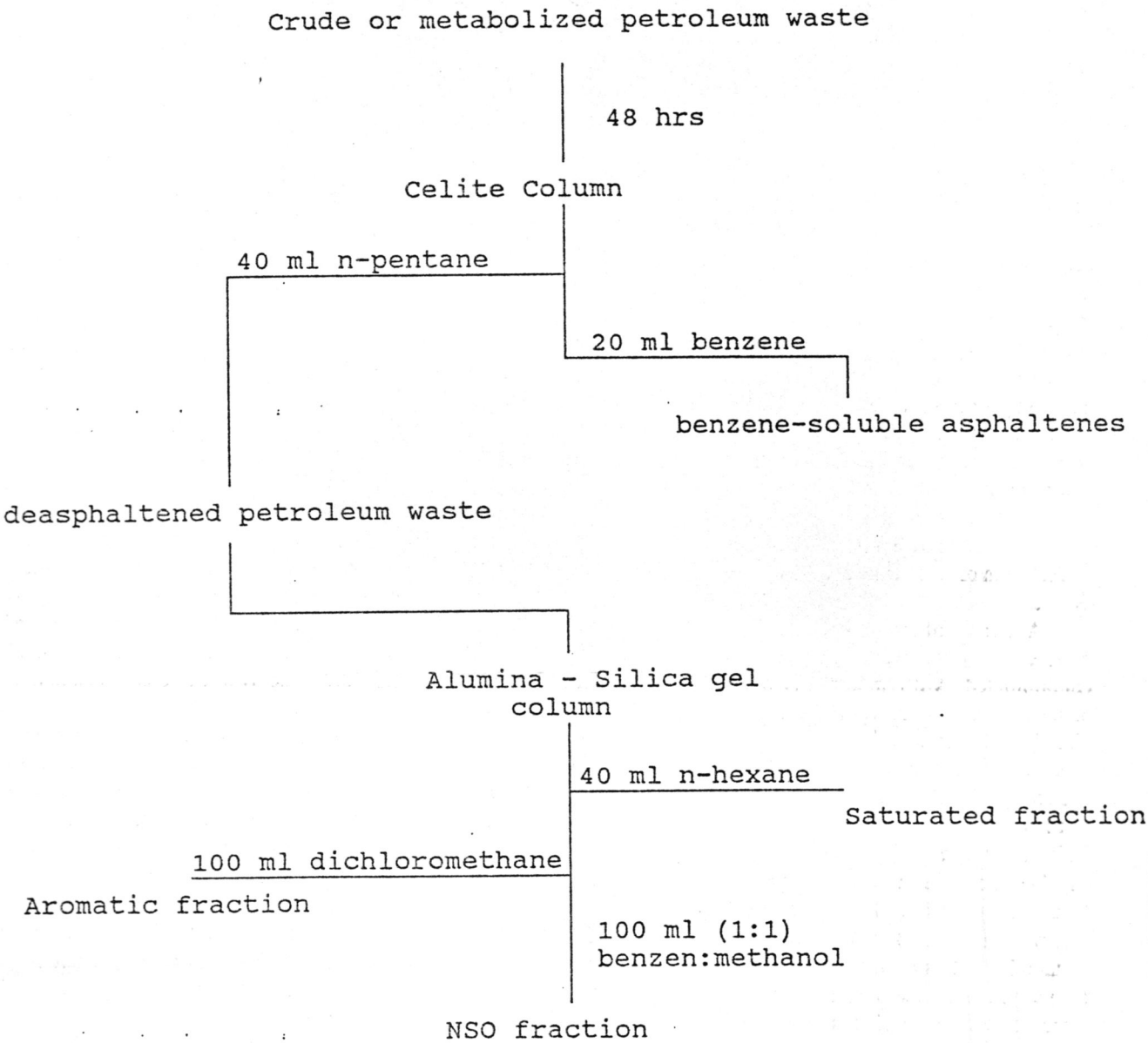

Fig. 1 Flow chart for liquid chromatographic separation of petroleum fractions.

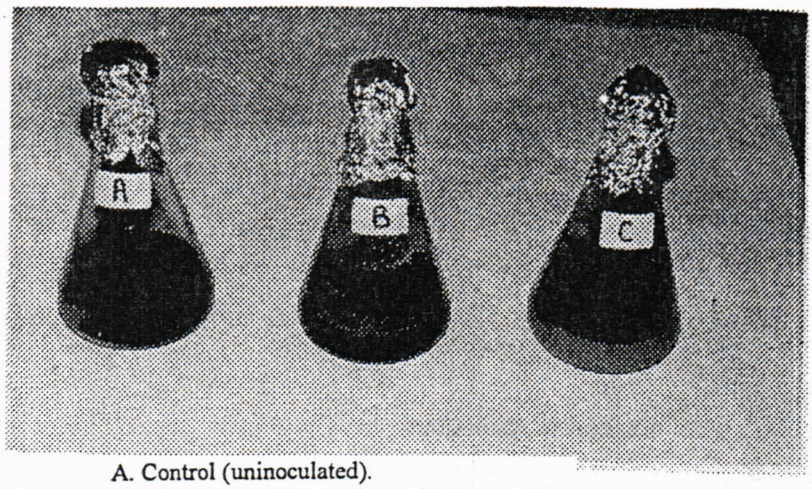

A. Control (uninoculated).
B. After 1 day of incubation with F. aquatile.
C. After 3 days of incubation with F. aquatile.

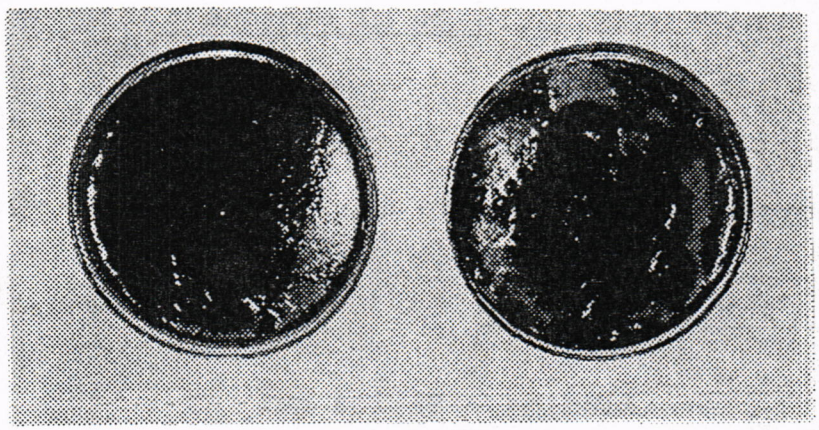

Figure(2) Microbiol emulsification and utilization of petroleum waste

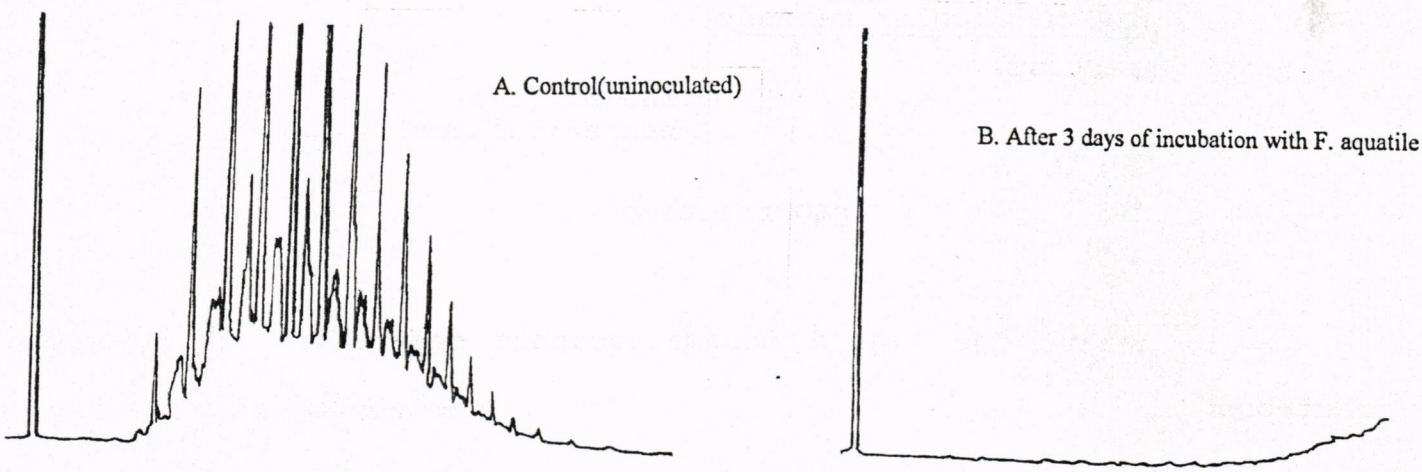

Figure(3) Gas-Liguid chromatographic analyses of saturate fraction from petroleum waste.

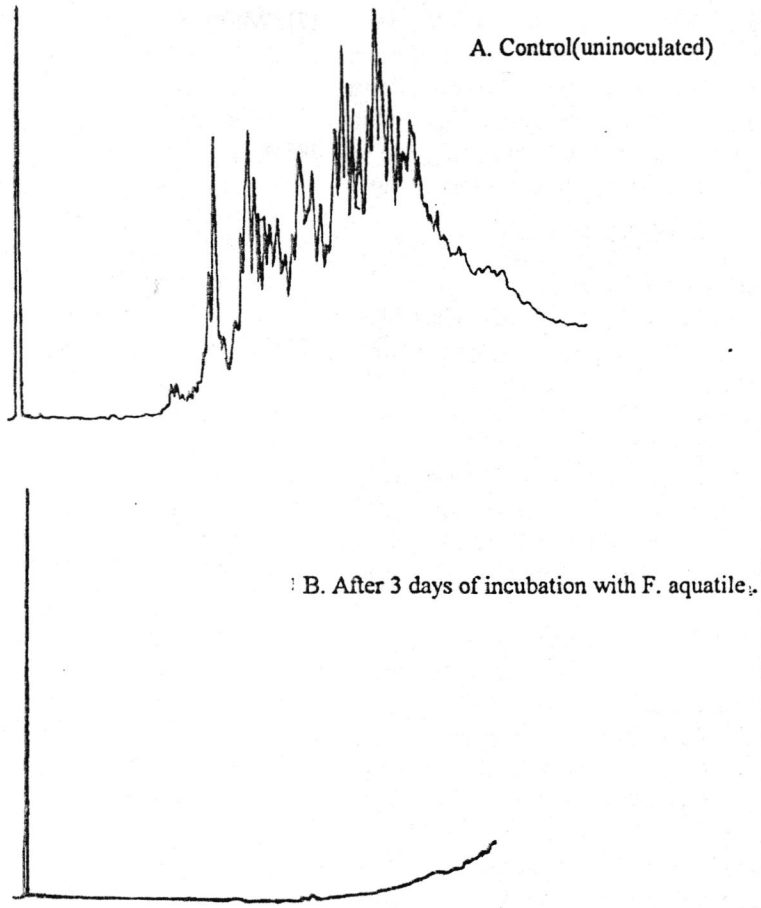

Figure(4) Gas-Liquid chromatographic analyses of aromatic fractions from petroleum waste

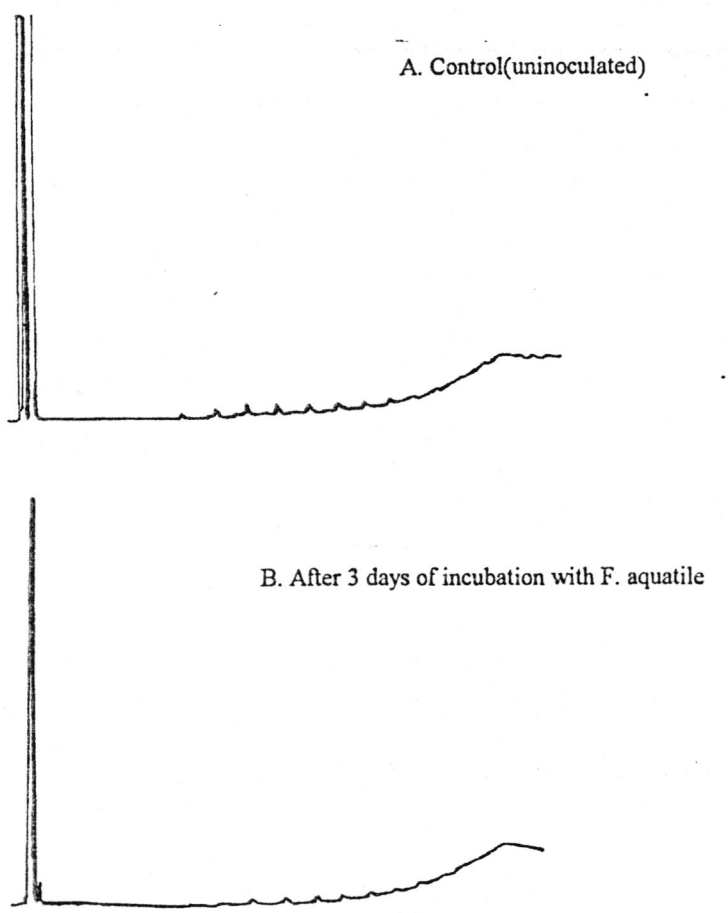

Figure(5) Gas-liquid chromatographic analyses of asphaltens

susceptible to biodegradation. This could be accomplished by the removal of toxic components, such as additives, heavy metals and changing the relative proportions of fractions; saturated, aromatic and NSO in the waste. So far it has been possible to degrade a petroleum waste completely under laboratory conditions.

REFERENCES

[1] Haines J.R. and M. Alexander, Microbial degradation of high molecular weight alkanes, Appl. Microbiol., 28, 1085, (1974).

[2] Atlas R.M., stimulated petroleum biodegradation, Crit. Rev. Microbiol., 371-385, (1977).

[3] Anderson M.S., R.A. Hall and M. Griffin, Microbial metabloism of alicyclic hydrocarbons & cyclohexane catabolism by a pure strain of Pseudomonas sp. J. Gen. Microbiol., 120, 89-94, (1980).

[4] Dibble J.T and R. Bartha, Effect of iron on the biodegradation of petroleum in sea water, Appl. Environ. Microbiol., 31, 544-550, (1976).

[5] Rosenberg E, A. Zuckerberg, C. Rubinovitz and D.L. Guthick, Emulsifier of Arthrobacter RAG-1, Isolation and emulsifying properties, Appl. Environ. Microbiol., 37, 402-408, (1979).

[6] Holmes B., R.J. Owen and T.A. McMeekin, Genus Flavobacterium, Bergey, Harrison, Breed, Hammer and Hunloon, 1923, P.353-361, In; N.R. Krieg and J.G. Holt (eds.) Bergy's Manual of Systematic Bacteriology, Vol. 1, The Williams and Wilkins Co. Baltimore, (1984).

[7] Weeks O.B., The Genus Flavobacterium, P. 1365-1370, In; P.S. Mortimer (ed.) The Prokaryotes, A handbook on habitats, isolation of bacteria, Berlin, New york, Spring Verlag, (1981).

[8] Cooper D.G., J.E. Zajic and D.F. Gerson, Interfaces and the aquatil environment, P.227-247, In; Bourquin A.W. and P.H. Pritchard (eds.) Proceedings of the Workshop, Microbial Degradation of Pollutants in Marine Environments, EPA, (1979).

[9] Kiyohara H., K. Nagao and K. Yaha, Rapid screen for bacteria degrading water-insoluble solid hydrocarbons on agar plates. Appl. Environ. Microbiol., 43, 454-457, (1982).

[10] jobson A., F.D. Cook and D.W. Westlake, Microbiol utilization of crude oil, Appl. Microbiol., 23, 1082-1089, (1972).

[11] Teschner M. and H. Wehner, Chromatographic investigations on biodegraded crude oil, J. Chromatog., 20, 407-416, (1985).

[12] Manresa M.A., M.E. Mercade, M. Robert, C. deAndres, M.J. Espuny and J. Guinea, Kinetic studies on surfactant production by Pseudomonas aeruginosa 44 TI, J. Indust. Microbiol., 8, 133-136, (1991).

Al-Mustansiriya J. Sci Vol. 6 , No. 1 , 1996

The External Morphology of the Date Palm Leaf Borer Phonapate frontalis (Fahr.)(Coleoptera: Bostrychidae) in Iraq.

NIDHAL M. Al-SANDOUK
Department of Biology, College of Education , University of Baghdad, Baghdad, Iraq.
(Recieved 24 Jun., 1993; Accepted 8 May, 1993)

الخلاصة

تمت دراسة المظهر الخارجي لحفار سعف النخيل Phonapate frontalis(Fah.) في العراق لاول مرة بالتفصيل في هذا البحث. فحصت كافة التراكيب ورسمت تحت مجهر ثنائي العدسات العينية واعطيت عناية واهتمام خاصين لتراكيب السوة الذكرية والانثوية لاهميتها في تشخيص انواع الحشرات القريبة من بعضها.

ABSTRACT

The external morphology of the leaf petiole borer infecting Date Palm trees Phonapate frontalis (Fahr.) is investigated for the first time in details in the present work. All structures were examined and illustrated under the binocular microscope. Special attention was given to the male and female genitalia since the structure are very much important in determining the closely related species of insects.

INTRODUCTION

The genus **Phonapate** compises few species distributed through the tropical and subtropical regions known as wood borer(1) .In Iraq **Phonapate frontalis** (Fahr.) found as a wood borer infesting the leaf petiole of Date Palm causing a severe damage in some places. The external morphology of the head capsule of some beetles was made by(2). The morphology of the thorax of some coleoptera was firstly studied comparatively by (3) and (4),who made the first morphological investigation on an Iraqi beetle **Scrites eurytes** (F.). Information on the wood borers infesting palm trees in Iraq are very poor .

The present study may help the workers to carry out further investigations on various aspects such as the biology and ecology of this economically important insect .

MATERIALS AND METHODS

Males and females specimens of **Phonapate frontalis**(Fahr.) were collected from Rashdia and Zaphrnia fields in Baghdad district. For this morphological study dried specimens were relaxed by placing them , pinned on cork , inside beaker containing some water . The beaker was covered by a petri dish and left overnight . The specimens were then dissected into head thorax , and abdomen . These parts were further softened and cleared of non chitinous materials for 50 minutes in a 10% solution of warm KOH .

The genitalia of male and female speccimens were dissected out . The aedeagus was pulled out throuh the opening between the last abdominal plates . When this was found difficult , either the whole termination were removed and genitalia dissected out or the abdomen was pressed forword . The geitalia were then softened in 10% solution of KOH.

To evert the internal sac of the aedeagus pressure was applied on the basal plate of the median lobe while pulling the internal sac through the median orifice. All diagrams were made with the aid of an ocular grid and squared paper. Measurements were done with an ocular micrometer.

RESULTS AND DISCUSSION

The Head: Figure(1), is dorsally hidden by the pronotum. The head capsule is small having the rounded eyes, the antennae and the mouthparts projecting downward..

Antennae: Figure(2), the present study revealed a very useful diagnostic character to differentiate between male and female. Antennae on both sexes are capitate. Male has (9) antennal segments with apical two enlarged while female antenna is composed of 10 segments having the apical three enlarged.

Mouth parts: Figure(3), mouth parts of mandibulate type. The dissection shows that they are densely hairy and very highly sclerotized having brush-like structures in appearance except the mandibles which are bare.

Thorax: Figure(4), globular in shape and strongly sclerotized, pronotum is completely covering head from above. Anteriore margin dentate while the basal margin entire. Disc of pronotum is heavily granulate.

Mesonotum and metanotum: Figure(5), these together are called Pterothorax, they are almost alike, each is subdivided into smaller sclerites, the acrotergite, prescutum, scutum and scutellatum with ahigh narrow strip representing the postnotum. Laterally the pterothorax has the anterior and posterior wing process connecting the fore and hind wings to the thorax. laterally the mesothorax and metathorax each composed of the usual pleural sclerites the epimeron and the episternum separated by obliquepleural suture figure(7).

Mesosternum & Metasternum: Figure(6), are ventrally composed of the usual meso and metasternal sclerites.

Legs: Figure(8), the fore, mid, and hind legs are slender of normal shape each comprises of the usual parts the trochanter, femur, tibia, tarsus, and the pretarsus. Claws smooth and pointed with a small rounded pad in between.

Wings: Figure(9), elytron elongate, strongly sclerotized with stria and intervals on the disc. The epipleura cover the pterothorax and the abdomen

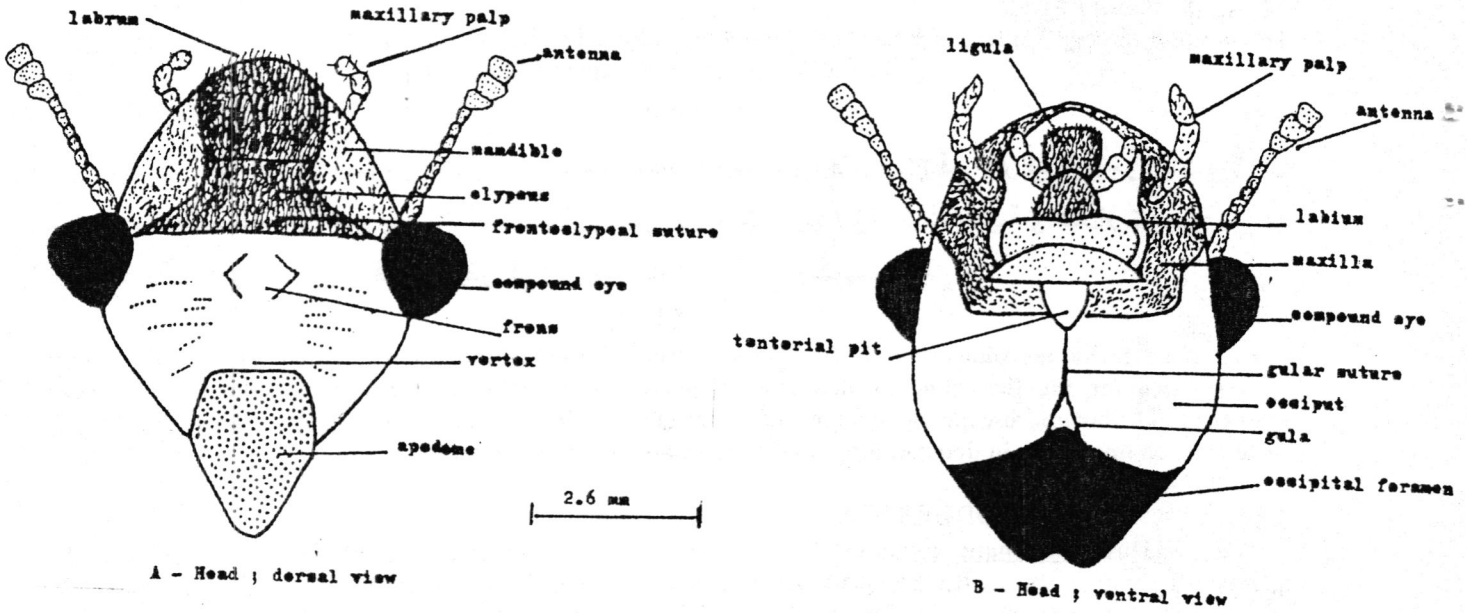

Figure (1): Head of the female

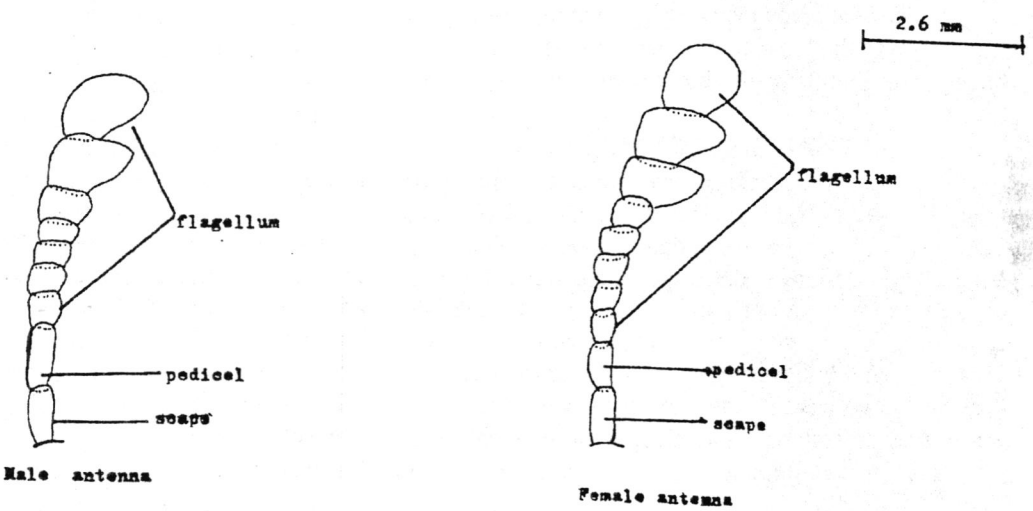

Figure (2): Antenna

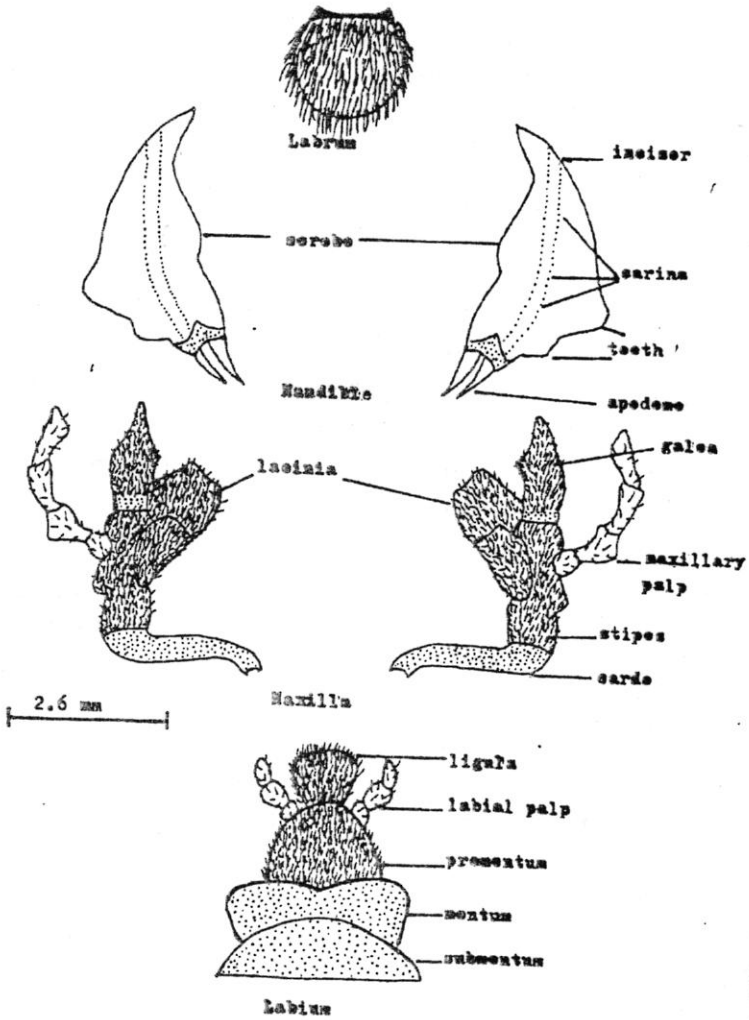

Figure (3): Meuthparts

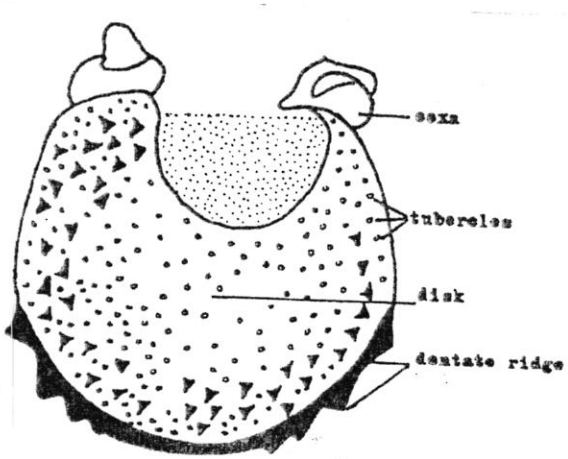

Figure (4): Prenetum

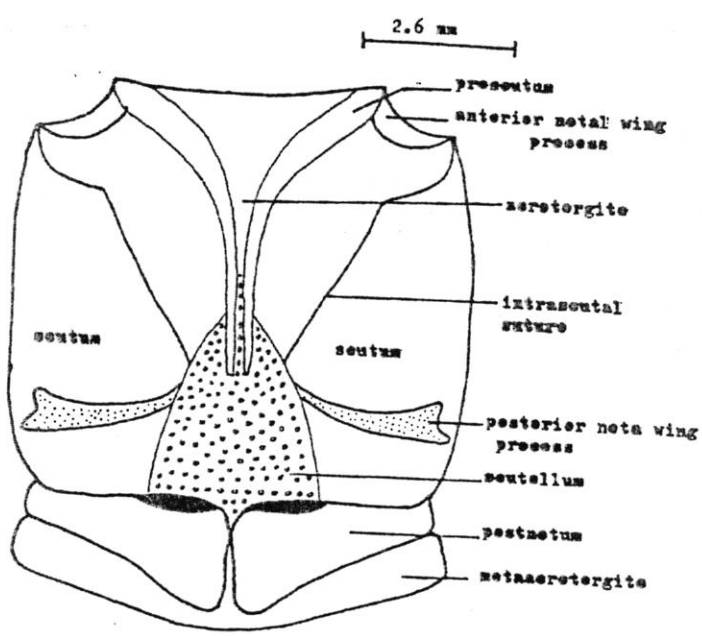

Figure (5): Mese and Metanetum

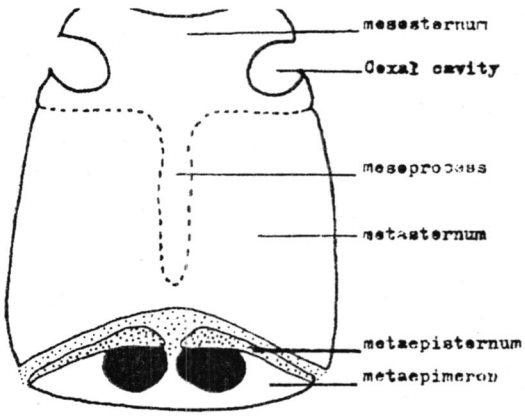

Figure (6): Mesosternum and Metasternum

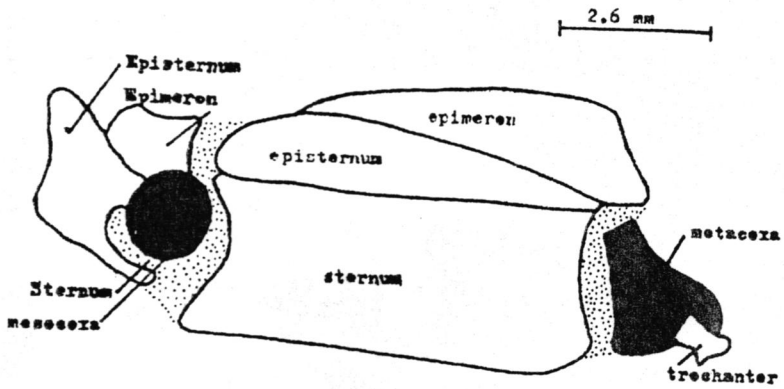

Figure (7): Thorax ; Lateral view

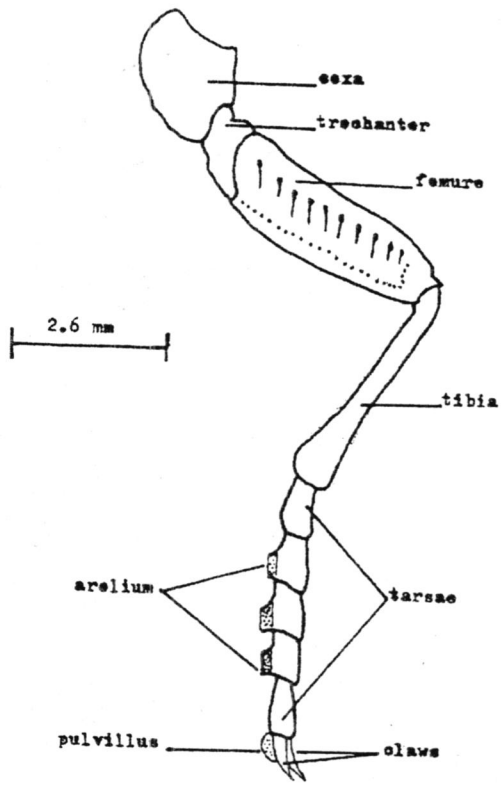

Figure (8): Fore leg

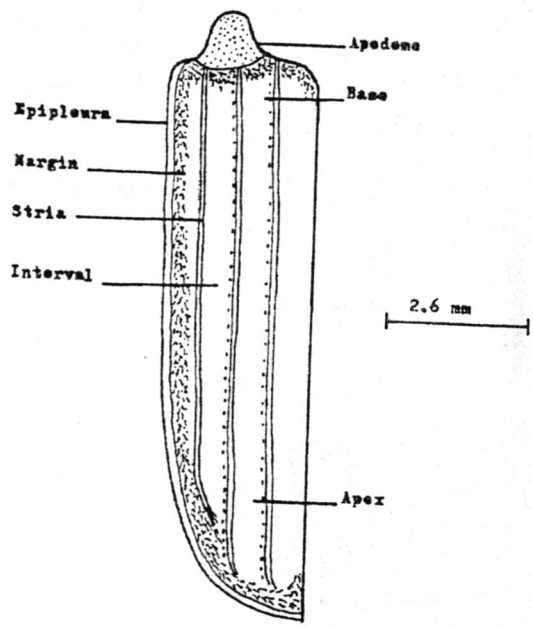

Figure (9): Fore wing (elytren)

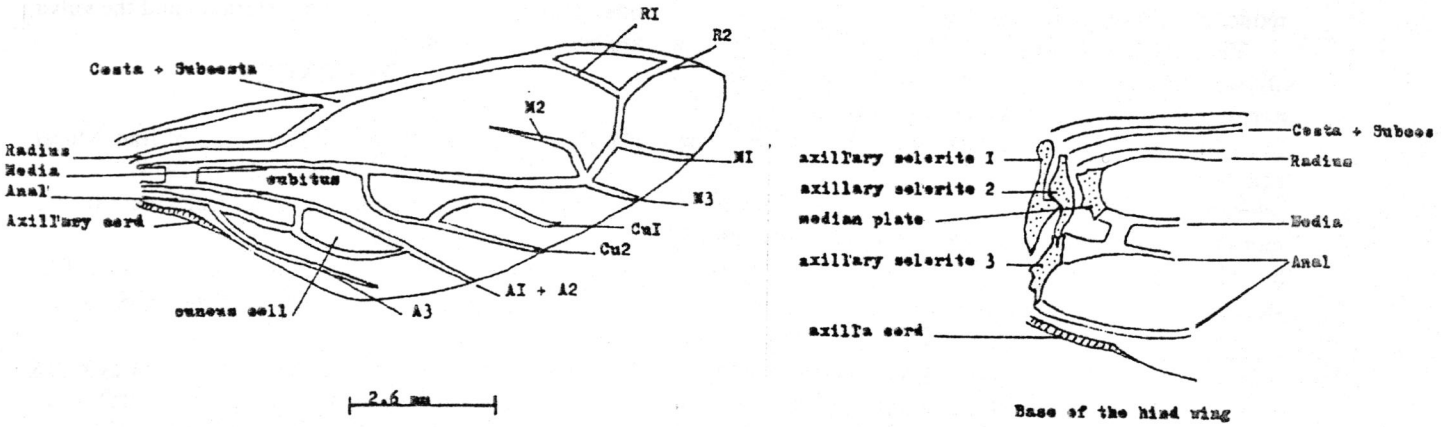

Figure (10): Hind Wing

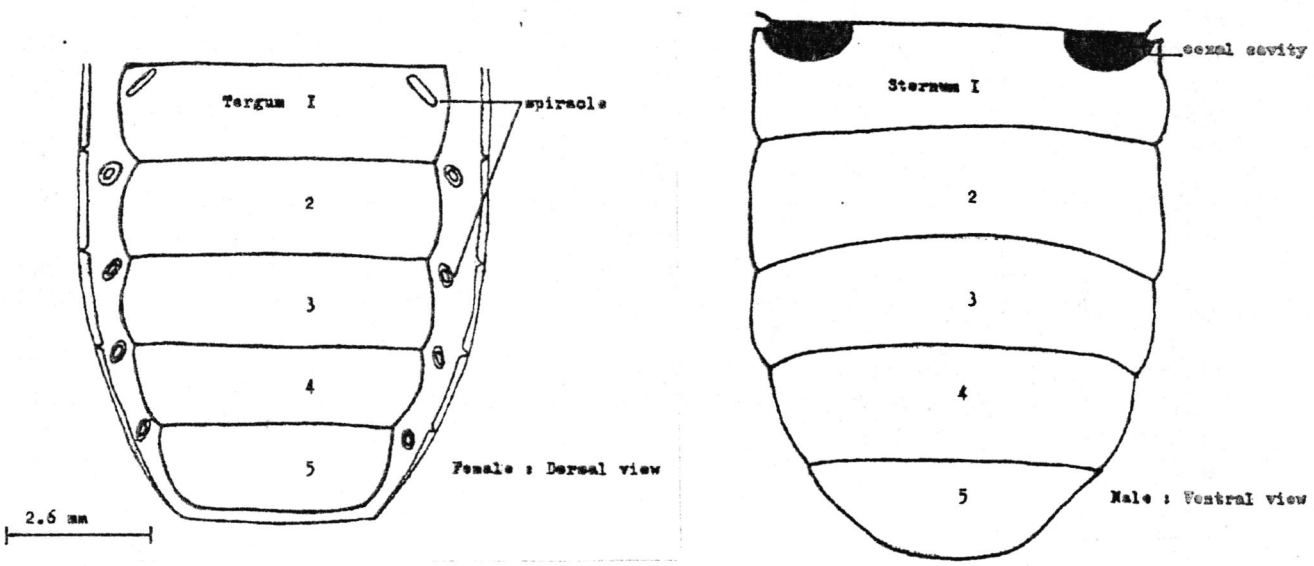

Figure (11): Male and Female Abdomen

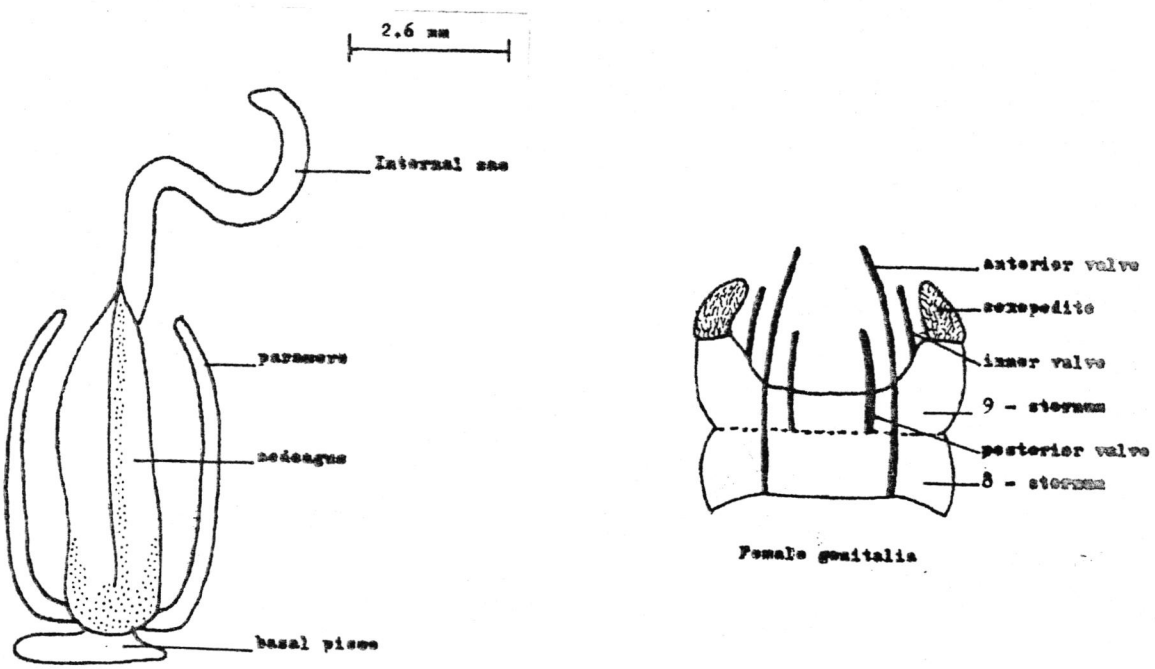

Figure (12): Genitalia

laterally. Elytral humeral angle rounded and elytra completely cover the abdomen upto the tip. Hind wings well developed membranous having the wing venation reduced as shown in figure(10).

The abdomen: Figure(11), there are five visible terga all well sclerotized and black in colour. There is a narrow membranous area on each side on which the 1st five abdominal pairs of spiracles are located. The ventral surface of the abdomen is formed of 5 sternal sclerotized and ouoescent. The 1st visible sternum is morphologically the 2nd, and is not divided completely by the metacoxae(5). The last visible abdominal sternum has distal margin rounded.

Genitalia: Figure(12), (Male genitalia). The innumerable variations male genitalia of coleoptera firstly described by (6). In **phonapate frontalis** (Fahr.) the male genitalia derived from 9th abdomial segment as appendages. They are formed of a pair of parameres(7). They are flat tapering toward their distal ends and exceeding the tip of the aedeagus. The basal piece or the phallobase according to (8) is asmall sclerite connecting the parameres basally. The aedeagus(the median lobe or the penis) is a long curved and well sclerotized tubular structure. It is attached to the parameres on its proximal end by a connective membrance. On this end the basal orifice is situated through which the ejaculatory duct enters the aedeagus. The ostium or the median orifice through which the internal sac is everted is located on the distal tip of the aedeagus and does not extend on the ventral side.

Female genitalia: The femal genitalia of the Coleoptera have been firstly investigated by(9). The female genitalia of **Phonapate frontalis** (Fahr.) consists of the 8th and 9th abdominal segments and their appendages, the later include the coxites, styles, and the valvifers which are all attached to the distal end of the 9th sternum. The coxite which are called hemisternite by (10) on each side consists of a single aclerite bearing one segmented styles. The ninth sternum and the vulva are both membranous.

REFERENCES

[1] Hussain, A., A. Date and palm pests of Iraq. Musal University Press 550 (In Arabic), (1974).

[2] Stickey, F. S. The head capsule of Coleoptera Illinos biol., 8:1-104, (1923).

[3] Snodgrass, R. E. The thorax of insects & the articulation of the wings. Proc. U.S. Nus., 36:511-596, (1909).

[4] Ali, H. A. The external morphology of **Scarites eurytes** (Fisch.) (Carabidae: Coleoptera). Bull. Biol. Res. Centre, Baghdad, 3:17-41, (1967).

[5] Jeannel, R. and Paulin, R. Morphologie abdominale des Coleopteres at systematique d' I' order. Rev. France, Ent., 11(2): 66-110, (1944).

[6] Sharp, M. A. and Muir, F. The comparative anatomy of the male genital tube in Coleoptera. Trans. ent. Soc. Lond., 477-631, (1912).

[7} Crampton, G. C. The structures called parameres in mal insects. Bull. Brooklyn ent. Soc.. 33:16-24,(1938).

[8] Snodgrass, R. E. Principles of insect morphology. McGraw-Hill Co., New York:667, (1935).

[9] Tanner, V.M. A preliminary study of the genitalia of female coleoptere. Ttans. Amer. ent. Soc., 53:5-5-,(1927).

[10] Lindroth, C.H. The principle terms used for male and femele genitalia in coleoptera. Opuscula Ent., 22:241-256, (1957).

Iraqi Spring Wheat Cultivars. II. Gel Electrophoresis and Isoelectric Focusing of Soluble Proteins

FAISAL A. SAKRI*, ZETA J. ROBERT** AND MAYSOON B. RASSAM**
*Department of Biology,College of Science, University of Baghdad, Baghdad, Iraq.
**Department of Chemistry, College of Science, University of Baghdad, Baghdad, Iraq.
***Department of Chemistry and Biochemistry,Saddam College of Medicine, Baghdad, Iraq.

(Recieved 27 Jun., 1993; Accepted 8 May, 1993)

الخلاصة

تم تحضير مستخلص البروتينات الذائبة لستة ضروب من الحنطة العراقية في ثلاث من محاليل الدارئة (Sample buffers) ذات أس هيدروجيني ٧، ٨,٩، ٩,٦ ثم درست هذه المستخلصات البروتينية وقورنت مع بعضها البعض بطريقة الهجرة الكهربائية Conventional gel electrophoresis وبطريقة تساوي الشحنة Isoelectric focusing . ان تركيز البروتينات في مستخلصات الضروب الستة من الحنطة، وباستخدام المحلول الدارئ ذو أس هيدروجيني ٨,٩، كان اعلى من المحاليل الدارئة ذو أس هيدوجيني ٧ و ٩,٦. وقد ظهر هذا واضحا في زيادة عدد الحزم البروتينية التي تم فصلها بطريقة الهجرة الكهربائية- (اراز ١١، ابو غريب ٣ وصابربك ١٣، مكسباك ١٤، ٩٦س- ١٦ وسن الجمل ٢٠ حزمة بروتينية)- والتي ظهرت فيها ايضا حزم بروتينية تنتقل الى القطب السالب بالاضافة الى الحزم البروتينية الاعتيادية التي تنتقل الى القطب الموجب في محاليل دارئة بأس هيدوجيني ٨,٩. كما تمت مقارنة البروتينات المستخلصة ايضا للضروب الستة من الحنطة بطريقة تساوي الشحنة بعد ان تم تركيزها بطريقة الميز الغشائي Dialysis وبطريقة التجفيد Lyophilization والتي اظهرت عددا اكبر من الحزم البروتينية الموزعة في مدى من الاس الهيدوجيني تتراوح ما بين ٣,٥ الى اكثر من ٩,٥. اظهرت النماذج المركزة بطريقة الميز الغشائي عدد اقل من الحزم البروتينية مقارنة بعدد الحزم البروتينية للنماذج المركزة بطريقة التجفيد.

ABSTRACT

The soluble protein extracts of six wheat cultivars in three different sample buffers with PH values of 7, 8.9 and 9.6 were studied and compared by gel electrophoresise and isoelectric focusing methods. The extracts in sample buffer PH 8.9 showed high protein content and this was exemplified by the appearance of numereous protein bands for each cultivar: (Araz, 11; Abu-Ghreb-3 and Sabir-Big 13; Mexipak, 14; Jori-C-69, 19 and Sin-A1-Gamal, 20 prctein bands) in conventional gel electrophoresis. The Protein bands exceeded the number of protein bands appearing in the extracts of both sample buffers PH 7 and 9.6. The conventional gel electrophoresis also showed proteins which were of cathodic migration in addition to the normal anodic migrating ones at PH 8.9. The isoelectric focusing of the protein extracts-both dialyzed and lyophilized- of the six cultivars in sample buffer Ph 8.9. were studied and showed also numereous protein bands distributed in PH ranging from 3.5 to more than 9.6. The dialyzed samples showed at least 33 protein bands as in Araz and up to 47 protein bands as in Jori-c-69, While the lyophilized samples gave at least 36 protein bands as in Sabir-Big and up to 49 protein bands as in Jori-C-69.

INTRODUCTION

The seed storage and/ or soluble proteins of higher plants have been considered the products of genes that are expressed at a single stage of ontogeny (1 and 2). Thus their analysis for types and numbers may be used as a tool for studying the morphological and growth differences betwwen plant species and cultivars (3-6). This study however, is an attempt to describe properties of the soluble proteins of dried kernels of the six wheat cultivars isolated and purified pareially, chatacterized chemically by one dimensional gel electrophoresis and isoelectric focusing techniques which are well accepted in protein quality control(1,3-8).

MATERIAL AND METHODS

Seed Materials: Five spring wheat cultivars (**Triticum eastivum L.**), Abu Ghreb-3, Araz, Saber-Big, Mexipak and sin-Al-Gamal, and one winter wheat cultivar (**Triticum durum**). Jori-c-69 were used.

Total Protein Extraction: For total protein extraction, 4 to 5 gm defatted kernel powder (40 mesh) were used, adopting the pro tein extraction orocedure outlined by Robert(9). Cold acetone was used for defatting and showed to be superior to diethylether, diethylether: ethanol (1:1 v/v) and pehexan(9). Three sample buffers were used separately, and in a subsequent steps as follows:

a: 0.01 M sodium phosphate buffer PH 7(10).
b: 0.01 M sodium hydroxide-glycine buffer PH 9.6.
c: 0.01 M Tris-glycine buffer PH 8.9 containing 0.38 mM sodium azide (10).

Separation by Slab Gel Electrophoresis and Isoelectric Focusing (IEF): Horizental slab gel electrophoresis was performed using the LKB-Multiphore system, following the application notes 306(11). Homogeneous 7.5% polyacrylamide gels in dimension of 125x260 mm

with C*=2.6%, T**=7.7% were prepared with sample application slots of 10 µl capacity. The gel and electrode buffers were compatible with the sample buffer used in each experiment as follows:

a) For protein extracts with sample buffer PH 7:0.2 M and 0.1 M sodium phosphate buffer PH 7 were used for gel and electrode buffers respectively.

b) for protein extracts with sample buffer PH 9.6: 0.2 M and 0.1 M sodium hydroxide-glycine buffer PH 9.6 were used for gel and electrode buffers respectively.

c) For protein extracts with sample buffer PH 8.9: The gel and electrode buffers were 0.2 M and 0.1 M tris-glycine buffer PH 8.9 containing 7.7 mM and 3.8 mM sodium azide respectively (11).

The conventional electrophoretic procedures were carried out at 4C. Ten u of 0.25% bromophenol blue was applied to one or two sample slots for the detection of the solvent front. Ten u protein extracts, 0.05-01 mg protein, of the six wheat cultivars, dialyzed or lyophilized and radissolved in distilled water, were applied to the remaining sample slots. Electrophoresis was performed for 3 hrs with a field strength of 15 v/cm and 40 ma (11). The separated protein bands were fixed 30 minutes with a solution of 11.5% trichloroacetic acid (TCA) and 3.5% sulphosaliculic acid (SSA) in 30% methanol. Stained for one hour with 0.25% coomassie Brilliant Bule R-250 in methanol distilled water:

glacial acetic acid (5:5:1 v/v/v). Destaining by diffusion was accomblished by frequent changes of the destaining solution of ethanol: acetic acid: distilled water (3:1:6 v/v/v) (11).

Isoelectric Focusing (IEF): The IEF was performed only for extracts with sample buffer PH 8.9. The experiments were performed using the LKB-Multiphore system following the instruction manual. The ready-made LKB-Ampholine PAG-Plates (260x125 mm) were used with a final acrylamide concentration of 5% and with a wide PH range of (3.5-9.5) samples extracts were loaded on sample application pieces of (10x5 mm) which absorbs approximately 50u (0.25 mg protein) and these were placed on the ampholine gel, 5 mm apparat, near the anodic strip. The IEF was carried out for 90 mins. (50mA, 1500v, 30w) (12). The sample application pieces were removed after 30 mins to forbid tailing. The focused protein bands were fixed with a solution of 11.5% (TCA) and 3.5% (SSA) in water for 60 minutes. Stained with 0.115% Coomassie Brilliant Blue R-250 in destaining solution and destained by successive immersion of the gel in a solution of ethanol: acetic acid: distilled water (3:1:8 v/v/v) (12).

The pH across the ampholine gel was determined as follows: After isoelectric focusing and before removing the ampholine gel from the cooling plate, a strip (10x125mm) of the ampholine along one line between the anode and the cathode was cut into 1 cm2 pieces and placed in 1 ml distilled water overnight at 4°c. The pH of each ampholine solution was determined by a pH-meter which gave the exact pH sequence across the Ampholine PAG-plate used in the IEF experiment.

RESULTS AND DISCUSSION

The extracts of the six wheat cultivars in the three mentioned sample buffers showed positively and negatively charged protein bands that migrated towards the cathode and the anode respectively.

The horizental slab gel electrophoresis of the extracts in sample buffer PH 7, showed one to there protein bands moving towards the anode and one or two protein bands moving towards the cathode subsequently, extracts in sample buffer PH 7 were neglected as they did not show any comparativily.

Extracts of the six cultivars with sample buffer PH 9.6 gave a total of six to ten protein bands of which only one or two were of cathodic migration (Fig. 1). The anodic protein band with R1 of 0.58, the nearest band to the sample slots, was the only repeated protein band in all the cultivars. However it was found that there are protein bands shared between two, three or four cultivars. In addition, distinct and unrepeated protein bands that are specific for each cultivar were found. This phenomenon of unsimilarity between the cultivars in respect to their protein band profile was also observed with the cathodic migrating protein bands (Fig. 1).

At pH 8.9, the one dimensional horizental slab gel electrophoretic protein pattern improved as the number of the total protein bands increased (Fig. 2). The total protein bands were ranged from eleven as in Araz and up to twenty as in Sin-Al-Gamal. The anodic protein bands were between six to ten, while the remainings bands were of cathodic migrating proteins. The anodic protein band of R_f value of 0.58, the nearest protein band to the sample slots, was found also to be the only repeated protein band in all the cultivars. In addition , a few protain bands were also found to be repeated in tow or three cultivars (Fig.2). It is evident that the extracts at pH 8.9 showed more distinct and unrepeated anodic protein bands that are specific for each cultivar compared to the extracts in sample buffer PH 9.6. Also, the cathodic protein bands of the extracts at PH 8.9 showed elevation in the number of unrepeated protein bands that are specific for each cultivar in addition to a few protein bands shared by two or three cultivars. In coclustion, the protein bands that are observed in the extracts of sample buffer pH 8.9 were higher in number and sharper than those observed in other sample buffers, and this correlates with the high protein content(9). It is also apparent from (Fig.2) that all of the six cultivars showed low molecular weight proteins that are fast in their movement towards the anode and are undistinguishable in sample buffers PH 7 and 9.6.

As it is apparent from Fig.1 and none of the cultivars are sharing completely or semi-completely in their protein profiles with each other. Thus, it is safe to say

*C=Percent linkage between methylene bis-acrylamide and acrylamide.

**T=percent cross linking concentration relative to the total concentration.

that these progenies are of different genotypes and/ or of different ancestry selections. It is also apparent that sample buffer pH 8.9 is more efficient in protein extraction both for total and relatively low molecular weight proteins as can be seen in Fig.2. These findings indicate that there is a wide range of proteins present in each cultivar reflected by its protein bands profile. However, to obtain more accurate results for such protein profiles, isoelectric focusing was implicated in this study since this technique is proved to be very sensitive tool for proteins separation (3-5). There is a noticeble number of protein bands that have migrated at pH values higher than 9.5 to position adjacent to the cathodic strip while at ph 3.5 no such protein bands were observed except for lyoohilized sample of Abu-Ghreb-3 which gave one band nly (Fig.3 A and B). Dialyzed samples showed at least thirty three protein bands as in Araz and up to fourty seven protein bands as in Jori-c69. The lyophilized asmples showed at least thitty six bands as in Sabir- Big and up to fourty nine as in Jori-c69 (Table 1, Fig. 2A and B). Hence, there was an overall increase in the total number of protein bands in the lyophilized samples in comparison with the dialyzed. It is also apparent that the proteins with acidic isoelectric points(PI) were more sensitive to the concentrating techniques. This was most prominent in the lyophilized samples of the Sabir-Big, Sin -Al-Gamal and Jori-c69 which showed a decrease of five to six of the total number of protein bands with acidic PI (PH 3.5-6.2), while there was an increase of one acidic band in Abu-Ghreb-3, Araz and Maxipak . The differences in protein pattern between the lyophilized and the dialyzed sample may be due to the digestion of proteins during the time elapsed in the process of dialysis by endogenous proteinases or may be attributed to the diffusion of low molecular weight proteins through the dialysis bags (13-17).

In contrast to what have been mentioned by Stegemann and Pietsch (18), the lyophilized samples in this study showed more stability and integrity compared to dialyzed samples. Subsequently, it is evident from the protein band profiles in Fig. 3 that the retained proteino of the lyophilized samples have been localized and distributed in the PH regions of 6.9 and up to PH 9.5 as well as in the region close to the cathodic end at PH 10. It is believed that the increased number of protein bands in the lyophilized samples might be attributed to the presence of high basic amino acids such as arginine, lysine and histidine in addition to glutamic acid and proline which are the most abundant amino acids in wheat flour(14).

The differences in distribution pattern as well as the number of protein bands within the dialyzed (Fig. 3A) or the lyophilized (Fig. 3B) samples are the true picture for the differences and similarities between the cultivars. Also , this method should prove valuable for analyzing different genotypes and selecting varieties with a particular storage protein make-up as well as for following compositional changes tha occur during seed germination and development (7).

For future work, it is recommended to study two dimensional electrophoretic patterns under denaturing conditions - the mapping of the proteins and polypeptides of each genotype (7,8)- and amino acid analysis and sequence determination. These procedures are necessary to document the genetic resources of each cultivar (8, 17, 18). This may produce new constituents unique in functional and nutritive values which may be as additive in wheat based products and other kinds of foods.

REFERENCES

[1] Wrigley, C.W. In "Biological and Biochemical applications of isoelectric focusing" N. Catsimpoolas and J. Drysdal (ens), Plenum Press, New York and London, 211-264, (1977).

[2] Dure, L. and C.Chlan> Developmental biochemistry of cotton seeds embroyogenesis and germination, Xii. Purification and properties of principal storage proteins. Plant physiol. 68: 180-186, (1981).

[3] Konarev, V. G., Gavrilyuk, I. P., Gubareva, N.K. and Peneva, T.I. Seed proteins in genome analysis, cultivar indentification, and documentation of cereal genetic resources . A review. Cereal Chem. 56: 272-278, (1979).

[4] Bushuk, W. and Zillman, R.R. Wheat cultivar identification by gliadin electrophoregrams. I. apparatus, method and nomenclature. Can. J. Plants Sci. 58: 505-515, (1978).

[5] Du Cros, D.L. and wrigley . Improved electrophoretic methods for identifying cereal varieties. J. Sci Fd. Agri. 30 : 785-794, (1979).

[6] Shewry, P. R., Faulk, A. J., Pratt, H.M. and Miflin. B.J. The varietal identification of single seed of wheat by sodium dodecyl-sulphate polyacrylamide gel electrophoresis of gliadin. J. Sci. Fd. Agri. 29: 847-849, (1978).

[7] Basha, S.M.M. Identification of cultivar differences in seed polypeptide composition of peanuts (Arachis hypogaes L.) by two dimensional polyacrylamide gel electrophoresis . Plant Physiol. 63: 301-306, (1979).

[8] Zivy, M. Thiellement, H., devienne , D. and Hoffmann, J.P. Study on nuclear and cytoplasmic genome expression in wheat by two dimensional gel electrophoresis. Theor. Appl. Genet. 63:335-345, (1984).

[9] Robert, Z.J. Iraqi spring wheat cultivars. I. Comparative study of soluble proteins Iraqi J.Sci. Vol 34 , No. 4 , (1993).

[10] O' Kennedy, B.T., Beilly, C.C., Titus, J.S. and Splittstoesser, W.W. (1979). A comparison of

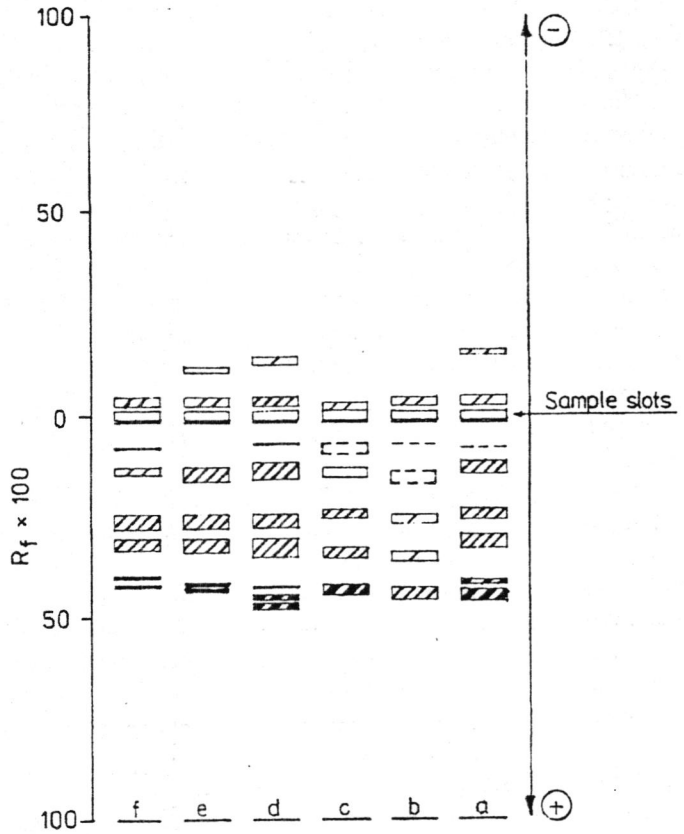

figure(1) Diagrammatic representation of conventiobal slab gel electrophoresis of the six wheat cultivars. a=Abu-Gnreb-3,b=Araz, c=Sabir-Big, d=Mcxipak, e=Sin-Al-Gamal and Jori-C-69. The samples were defatted with acetone and extracted with sample buffer PH 9.6.

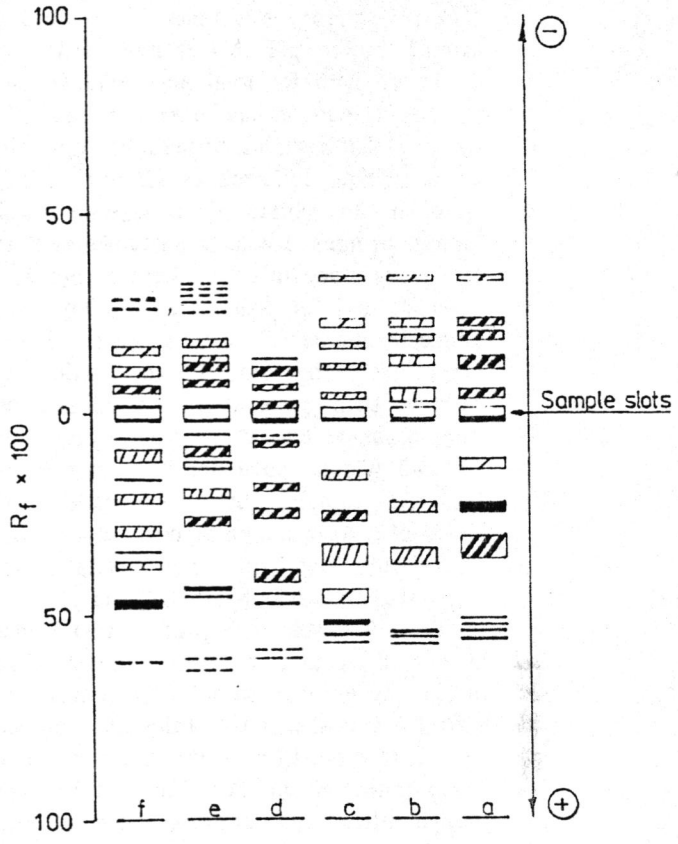

figure(2) Diagrammatic representation of conventiobal slab gel electrophoresis of the six wheat cultivars. a=Abu-Gnreb-3,b=Araz, c=Sabir-Big, d=Mcxipak, e=Sin-Al-Gamal and Jori-C-69. The samples were defatted with acetone and extracted with sample buffer PH 8.9.

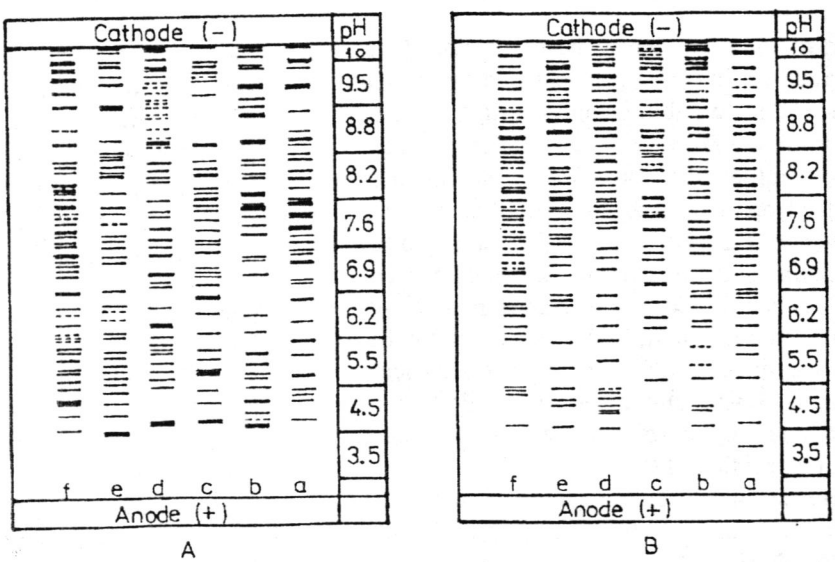

figure(3) Diagrammatic representation of IEF gels. A, dialyzed; B, lyophilized sample extracts of the six wheat cultivars. a=Abu-Ghreb-3, b=Araz, c=Sabir-Big, d=Maxipak, e=Sin-Al-Gamal and jori c-69. The samples were defatted with acetone and extracted with sample buffer PH 8.9.

Table (1) The number of protein bands at each PH vale as was observed in IEF gels for both the dialyzed (d) and the lyophilized (L) extracts of the six wheat cultivars in sample buffer PH 8.9.

pH	Number of protein bands											
	Abu-Ghreb-3		Araz		Sabir-Big		Maxipack		Sin.Al.Gamal		Jori C.69	
	d	L	d	L	d	L	d	L	d	L	d	L
3.5	–	1	–	–	–	–	–	–	–	–	–	–
4.5	4	1	5	3	3	–	1	7	4	5	3	4
5.5	3	3	4	3	4	1	7	2	6	2	7	1
6.2	2	5	2	5	3	3	3	3	5	3	7	6
6.9	5	5	3	4	5	5	4	3	3	4	6	6
7.6	6	6	4	5	6	5	5	7	6	7	8	9
8.2	6	6	5	6	6	6	5	7	4	6	7	8
8.8	4	4	2	4	1	6	6	7	3	5	2	7
9.5	3	4	5	7	6	6	9	6	4	7	4	6
10	2	3	3	3	1	4	2	4	4	2	3	3
Total number of protein bands	35	38	33	40	35	36	42	46	39	41	47	41

the storage protein (glublin) of eight species of Cucurbitaceae. Can. J. Bot. 57: 2044-2049, (1979).

[11] Fehrastrom, H. and Moberg, U. IKB-produkter AB, Bromma, Sweden. SDS and conventional polyacrylamide gel electrophoresis with LKB 2117 Multiphore, (1977).

[12] Winter, A., Ek, K. and Andersson, U-B. LKB, Produkter AB, Bromma, Sweeden. Analytical electrofocusing in thin layers of polyacrylamide gels. Application Note 250, (1977).

[13] Kaminsk, E. and Bushuk, W. Wheat proteases. I-separation and detection by starch gel electrophoresis. Cereal Chem. 46:317, (1969).

[14] Grant, D.R. and Wang, C.C. Dialyzable components resulting from proteolytic activity in extracts of wheat flour. Cereal Chem. 49: 201-207, (1972).

[15] Preston, K.R., and Kruger, J.E. Purification and properties of two proteolytic enzymes with carboxypeptidase activity in germinating wheat. Plant Physiol. 58:516-520, (1976).

[16] Waters, S.P., Noble, E.R. and Dalling, M.J. Interacelular Jocalization of peptide hydrolazes in wheate (Triticum aestiveum L.) leaves. Plant Physiol. 69: 575-579, (1982).

[17] Des Frances, C.C., Thiellement, H. and de Vienne, D. Analysis of leaf proteins by two dimenstional gel electrophoresis. Protease action as exemplified by ribulose bisphosphate carboxylase oxygenase dehydration and procedure to avoid proteolysis during extraction. Plant Physiol. 78: 178-182, (1985).

[18] Stegmann, H. and Pietsch, G. In Methods for characterization of seed proteins in cereal and legumes". In Seed Proteins". Biochemistry genetics, Nutritive value Ed. by Gottsch and Muller, H.P. Publishers, M. Nijoff/DR W. Junk, (1983).

[7] Amri. M.A., Ponaly, R. Duteutre, B. and Moll, M. Yeast flocculation: Influence of nutritional factor on cell wall Composition. J. General Microbiol, 128: 2001-2009 (1982).
[8] Stewart, G.G. and Goring, T.E. Effect of some mono valent and bivalent metal ions on the flocculation of brewer's yeast strains. J. Inst. Brew. 82, 341-342 (1976).
[9] Kamada, K. and Murata, M. On the mechanism of Browers yeast flocculation. Agric. Biol. Chem., 48 (10), 2423-2433, (1984).
[10] Kamada, K. and Murata, M. Effect of enviromental conditions of flocculation dispersion of brewers yeat. Nipponnoge Kaishi, 58 (10): 983-990 (1984).
[11] Russell, E. Stewart, G.G. Reader. H.P Jonston. J.R. and Martin, P.A. Revised nomenclature of genes that central yeast flocculation J. Inst. Brew., 86, 120-121 (1980).
[12] Walt, J.P. Vander., Criteria and Methods used in Classification In "The yeast, A taxonomic study" Amesterdam Company - London (1970).
[13] Stewart, G.G. and Russell, I. Yeast flocculation, Brew, Sci, 2: 61-92 (1981).
[14] Calleja, G.B. and Johnson, B.F. A comparison of quantitative methods for measuring yeast flocculation. Can. J. Microbiol. 23: 68-74 (1977).
[15] Mill, P.J. The nature of interactions between flocculent cell in the flocculation of Saccharomyces cerevisiae Journal of General Microbiol, 35: 61-68 (1964b).
[16] Bennett, J., Smithers, L.L. and Ward, C.T. Inhibition of DNA Synthesis mammalian cells by actidione, Biochem et. Biophys. Acta., 87: 60-69 (1964).
[17] Stewart, G.G. Russell, I. and Garrison, I.F. Some considerations of the flocculation characteristics of ale and lager yeast strains. J. Inst. Brew. 81, 248-257 (1975).
[18] Baker, D.A. and Kiroscp, B.H.Flocculation in Saccharomyces cerevisiae as influenced by wort composition and by actidione. J. Inst. Brew. 78: 454-458 (1972).
[19] Rose, H.H., and Harrison, J.S. The yeasts. Vol. 3. Academic Press Inc., N.Y.: 149-159 (1968).

جدول(٣) قابلية عزلات الخمائر المحلية وسلالتي المقارنة على تمثيل النترات والنتريت ومقاومة السايكلوهكسيماید

رمز السلالة	تمثيل النترات	تمثيل النتريت	مقاومة السايكلوهكسيماید
أ	−	−	−
ب	−	−	−
٢	+	+	−
١٠	+	+	+
٤٥	+	+	−
٥٠	−	−	−
٧٥	−	−	−
٧٦	+	+	+

جدول (٤) النسب المئوية لتلبد العزلات المحلية وسلالتي المقارنة في اوساط YPD & DM والورث

الوسط	النسبة	المئوية	للتلبد (٪)	
السلالة	YPD	DM	الورث	مدة الحضن
أ	صفر	صفر	صفر	٣ ايام
ب	٥٤,٩	٥٢٠-	٦٤	٣ ايام
٢	٢٨,٢	٢٨٠-	٢٠,٧	٥ اسابيع
١٠	٢١,٩	١٧,٣	١٣,٩	٥ اسابيع
٤٥	٤٢,٢	٤١,٨	٣١,١	٣ ايام
٥٠	٤٤,٤	٤٤,٤	٢٩,١	٣ ايام
٧٥	٦٠	٥٥	٥٣٠-	٣ ايام
٧٦	٩٠,٨	٩٠,٦	٨٨,٦	٣ ايام

جدول(٢) قابلية عزلات الخمائر المحلية على تخمير وتمثيل المركبات الكاربونية

نوع السكر	تخمير(خ) او تمثيل(ث)	رمز السلالة أ	ب	٢	او العزلة ١٠	٤٥	٥٠	٧٥	٧٦
كلوكوز	خ	+	+	+	+	+	+	+	+
	ث	+	+	+	+	+	+	+	+
كالاكتوز	خ	+	+	+	+	−	+	+	−
	ث	+	+	+	+	−	+	+	−
سكروز	خ	+	+	+	+	−	+	+	−
	ث	+	+	−	−	+	+	+	−
مالتوز	خ	+	+	−	−	−	+	+	+
	ث	+	+	−	−	−	+	+	+
سليبايوز	خ	−	−	−	−	−	−	−	−
	ث	−	−	−	−	−	−	−	−
تريهالوز	خ	−	−	−	−	−	−	−	−
	ث	−	−	−	−	−	−	−	−
لاكتوز	خ	−	−	−	−	−	−	−	−
	ث	−	−	−	−	−	−	−	−
رافينور	خ	+	+	+	+	+	+	+	−
	ث	+	+	+	+	+	+	+	−
انيولين	خ	−	−	−	−	−	−	−	−
	ث	−	−	−	−	−	−	−	−
نشأ	خ	−	−	−	−	−	−	−	−
	ث	−	−	−	−	−	−	−	−

فيما اطلق باحثون اخرون(١٥) على هذا النوع بالتلبد الدقيق. اما العزلة رقم ٦٧ فقد كانت نسب تلبدها عالية جداً مقارنة بجميع العزلات والسلالة (أ) عندما بلغت ٩٠,٨٪ و٩٠,٦٪ و ٨٨,٦٪ في اوساط YPD, DM والورث على التوالي، اضافة الى تلبدها السريع الذي حصل بعد ٢٠ ساعة فقط من التنمية على ٢٥°م. وقد عد هذا النوع من التلبد غير مرغوب (١٩) لان التلبد المكر يؤدي الى سرعة فصل الخمائر عن عالق الورث مما ينتج عنه منتوج غير مكمل التخمر. هذا بالاضافة الى ان التلبد المبكر جداً يؤدي الى ترك الوسط غني بالعناصر الغذائية دون استغلال مما يشجع نمو الاحياء المجهرية الاخرى واتلاف المنتوج.

REFERENCES

[1] Brian, L. Miki, A. Hungpoon, N. Allan, P. James and Verneri, L, Seligy. Possible mechanism for flocculation interaction governed by gene F10, in Saccharomyces cervisiae. J.Bacteriol. May: 878-889 (1982).

[2] Beaven, M.J., Delk, D.N. Stewart. G.G. and Rose, A.H. Changes in electrophoretic mobility and lytic enzme activity associated with development of flacculating ability in Saccharomyces cerevisiae. Can. J. Microbiol. 25: 988-895, (1979).

[3] Mill, P.J. The effect of nitrogenous substances on the time of flocculation of Saccaromyces cerevisiae. Journal of General Microbiology, 35: 53-60 (1964).

[4] Day, A.W., Poon, N.H. and Stewart, G.G. Fungal fimbrioe III. The effect on flocculation in Saccharomyces. Can. J. Microbiol. 21: 553-564 (1975).

[5] Lodder, J. The yeasts, a taxonomic study. North Holland Publishing Company, Amsterdam. (1970).

[6] Patel, G.B. Ingledew, W.M. The relationship of acid soluble glycogen to yeast flocculation Can. J.Microiol. 21: 1608-1613 (1975).

جدول (١) تاثير الوسط الزرعي والاس الهيدوجيني ودرجة الحرارة على تلبد السلالة القياسية(أ)

الوسط الزرعي	درجة الحرارة (م)	درجة التلبد: الاس الهيدروجيني ٣,٥	٤,٥	٤,٨	٥,٠	٥,٥	٦,٠	٦,٥
GYSA	8	F_0	F_2	F_2	F_2	F_2	F_1	F_1
	25	F_0	F_1	F_1	F_1	F_1	F_1	F_1
	30	F_0	F_0	F_0	F_0	F_0	F_0	F_0
	35	F_0	F_0	F_0	F_0	F_0	F_0	F_0
YE	8	F_0	F_1	F_1	F_1	F_1	F_0	F_0
	25	F_0	F_1	F_1	F_1	F_1	F_0	F_0
	30	F_0	F_0	F_0	F_0	F_0	F_0	F_0
	35	F_0	F_0	F_0	F_0	F_0	F_0	F_0
ME	8	F_0	F_3	F_3	F_3	F_3	F_1	F_1
	25	F_0	F_2	F_2	F_2	F_2	F_1	F_1
	30	F_0	F_0	F_0	F_0	F_0	F_0	F_0
	35	F_0	F_0	F_0	F_0	F_0	F_0	F_0
YPD	8	F_3	F_3	F_3	F_3	F_3	F_1	F_1
	25	F_2	F_2	F_2	F_2	F_2	F_1	F_1
	30	F_0	F_0	F_0	F_0	F_0	F_0	F_0
	35	F_0	F_0	F_0	F_0	F_0	F_0	F_0
DM	8	F_3	F_3	F_3	F_3	F_3	F_1	F_1
	25	F_2	F_2	F_2	F_2	F_2	F_1	F_1
	30	F_0	F_0	F_0	F_0	F_0	F_0	F_0
	35	F_0	F_0	F_0	F_0	F_0	F_0	F_0

وسط "الورث الصناعي" في اس هايدروجيني ٤،٨ وقدرت نسبة التلبد بعد الحضن على ٢٥م/ ٣-٥ ايام. يبين الجدول (٤) ارتفاع نسبة التلبد في السلالة (أ) عند تنميتها في وسط الورث بدرجة ملحوظة حيث بلغت ٦٤٪ مقارنة بتلبدها في الوسطين YPD, DM التي كانت ٥٢٪ و٥٤,٩٪ عل التوالي. وقد جاءت هذه النتيجة مقاربة لما توصل اليه Stewart et al. (١٧) عندما وجدوا ان ارتفاع نسبة التلبد يعود الى وجود بعض البيتيدات في وسط الورث مما يحفز الخمائر على التلبد. واظهرت العزلتان ١٠،٢ تلبداً ضعيفاً ومتاخراً حيث بلغت نسبة التلبد في الاوساط YPD, DM والورت ٢٨،٢٪ و٢٨٪ و٧، ٢٠٪ للعزلة ٢ و٩، ٢١٪و٣، ١٧٪ و١٣٪ للعزلة ١٠ على التوالي بعد تنميتها لمدة ٥ أيام. ويعد هذا التلبد كامناً وبطيناً وغير مرغوب في الصناعة لانه يترك اعداد كبيرة من الخمائر عالقة في الوسط عند عملية الفصل اضافة الى تسببه في تأخير العمليات التصنيعية مما يغير من صفات المنتوج(٣).

اما العزلتان ٤٥، ٥٠ فقد تلبدت بنسب اعلى لكنها قليلة مقارنة بسلالة المقارنة (أ) في الوسطين YPD, DM. عندما بلغت ٤٢,٢٪ و٤١,٨٪ للعزلة ٤٥ و ٤٤,٤٪ و٤٤,٤٪ للعزلة ٥٠ على التوالي. وكانت تلبد هاتين العزلتين واطئة جداً في وسط الورث الى التراكيز العالية من المركبات التايتروجينية التي مصدرها الاحماض الامينية. وقد كان تلبد العزلة رقم ٧٥ افضل من تلبد العزلات السابقة وسلالة القارنة في وسطي YPDk DM عندما بلغت ٦٠٪ و ٥٥٪ على التوالي لكنها كانت اوطأ (٥٣٪) في وسط الورث من السلالة (أ). وقد اظهر الفحص المجهري ان خلايا هذه العزلة تتكتل بمجموعات مكونة من معدل (١٠) خلايا لا ترى الا بالمجهر. وقد علل Russell et al. (١١) ذلك الى تكوين سلاسل من الخلايا التي لم تكتمل انفصالها بعد التبرعم من خلايا الام في الطور الثابت.

وتجانس عالق الخميرة في الوسط بشكل تجمعات او كتل كبيرة من الخلايا مع ملاحظة سرعة الاتابيب وصفاء الوسط لاختيار المتلبدة منها.

تشخيص العزلات المتلبدة: اتبعت الطرق الواردة في Lodder (٥) لتشخيص جنس الخمائر ونوعها حيث شملت على الفحوصات المظهرية والاختبارات الفسيولوجية التي تضمنت تخمير وتمثيل المركبات الكاربونية وتمثيل المركبات النايتروجينية واختبارات الحساسية لمضاد السايكلوهكسيميد.

طرق الزرع والاوساط المستخدمة: لقحت نقلة بالناقل من المزرعة الاصلية لكل عزلة او سلالة مقارنة (على انفراد) بـ ٢٥ مل من وسط التنمية (YE)، ثم اجريت سلسلة من التخافيف لحساب عدد الخلايا بعدها لقح ١ مل من كل منها في ٩٩ مل من كل من اوساط التنمية(٢)، Yeast Peptone Dextrose (YPD) (٣), Glucose Yeast Extract Salt Ammonium (GYSA) (١١), Malt Extract (ME), Defined Medium (DM) (٦) Yeast Extract (YE) (١٢) ليصبح معدل عدد الخلايا (٥-٦) X ١٠ خلية/١ مل. وبعد الحضن على ٢٥م/ ٣ ايام رسبت الخمائر بالطرد المركزي على ١٥٠٠ دورة/دقيقة لمدة ١٥ دقيقة وغسل العالق مرتين بالماء المقطر .الاس الهايدروجيني ودرجة الحرارة: استخدم الوسطين YPD و DM اضافة الى وسط الى Wort لدراسة تأثير الاس الهايروجيني (٥, ٣ و ٥, ٣ و٤،٨ و٥،٠ و٥،٥ و ٦،٠ و ٦،٥) على تلبد العزلات المحلية المتلبدة وسلالتي المقارنة, فيما استخدمت درجات (٨ و ٢٥ و٣٠ و ٣٥م) لحضن الخمائر لمدة ثلاثة ايام باستثناء درجة ٨م لمدة اسبوعين (٤).

قياس التلبد: استخدمت طريقتي التقدير الظاهري الواردة في (٢) و (١٣) والتي تعتمد اساسا على النظر الى حواف المزرعة السائلة بعد رجها بلطف ثم وصف درجة التلبد حسب حجم الكتل المترسبة ودرجة تعكر العالق او صفائه حيث تعطى الرموز (FO) لعدم التلبد و (F1) تلبد ضعيف و(F2)جيد و (F3) شديدة. اما الطريقة الثانية فهي طريقة النسبة المئوية الواردة في (١٤) والتي تعتمد على النسبة المئوية للخلاياالمتلبدة باستخدام الهيموسايتومتر بعد تعريض الخلايا الى البرج القوي.

النتائج والمناقشة

تبين النتائج في جدول (١) ان الخميرة القياسية (أ) تلبدت في جميع الاوساط الزرعية المستخدمة لكن تلبدها كان ضعيفا في الوسطين YE, GTSA وذلك عند تنميتها في درجتي ٨و ٢٥م. ولم يحصل تلبد في درجتي ٣٠و ٣٥م. وكانت هذه النتيجة مشابهة لحد ما مع ما توصل اليها Day et al. (٤), Amri et al. (٧) (١٠) Kamada and Murata عندما حصلوا على تلبد جيد في درجة ٢١ و ٢٥ و٢٠م على التوالي. ويبدو ان هذا الاختلاف الطفيف يعود الى السلالة المستخدمة وفعاليتها الايضية التي تظهر على مكونات جدار الخلية حيث يعد ذلك من العوامل الاساسية في حدوث التلبد.

كما ويبين الجدول نفسه عدم حدوث تلبد عند الاس الهايدروجيني ٣،٥ فيما كان ضعيفا عند ٦،٠ و٦،٥ . وكان التلبد جيدا عند ٤،٥ و ٤،٨ و ٥،٠ و ٥،٥ في جميع الاوساط باستثناء (YE) عندما كان ضعيفا. ويمكن ان يعزى ذلك الى ارتفاع قطبية جدار الخميرة بانخفاض الاس الهايدروجيني من ٥،٥ الى ٤،٢ (١٠)، فيما بود (١٥) Mill ان اقصى تلبد يحدث عند المدى ٤،٥ – ٥،٥ .

يتضح من خلال تداخل عوامل الوسط الزرعي والاس الهايدروجيني ودرجة الحرارة ان تلبد الخميرة القياسية (أ) كان جيدا في الاوساط DM, ME, YPD باستخدام درجة ٢٥م في اس هايدرتجيني ٤،٨ . ولصعوبة التلبد في الوسط ME (لكونه غير رائق) فقد اختير الوسطين DM, YPD للتجارب اللاحقة.

اما بالنسبة لخميرة الخبز (ب) فانها لم تتلبد في جميع الاوساط والظروف المستخدمة حيث انها استخدمت هنا للمقارنة فقط كونها خميرة غير متلبدة.

عزل الخمائر المحلية وتشخيصها: امكن الحصول على ستة عزلات خميرة متلبدة من اصل (٦٤) عزلة خمائر جمعت من الفواكه المحلية حيث اعطيت الرموز الرقمية ٢ و ١٠و ٤٥و ٥٠ و ٧٥ و ٧٦. وقد اظهرت الفحوصات المظهرية والزرعية للعزلات المحلية وخميرتي المقارنة ان جميع هذه الخمائر كونت الابواغ الكيسية ولون مستعمراتها ابيض الى كريمي وسطوحها ملساء محدبة. وقد تم اجراء الاختبارات الفسيولوجية الاتية لتشخيص العزلات.

تخمير وتمثيل المركبات الكاربونية: تشابهت نتائج اغلب هذه الاختبارات للعزلات المحلية المتلبدة مع سلالتي المقارنة (أ) و(ب) لاسيما العزلتين ٥٠ و٧٠ عندما تطابقت تماما في تخميرهما وتمثيلهما للمصادر الكاربونية المستخدمة مع سلالتي المقارنة, فيما اعطت العزلتان ٢ ,١٠ فحصا موجبا لتخمير وتمثيل الكلوكوز والكالكتوز والرافينوز فقط وسالبا لبقية المركبات. واعتمادا على المرجع رقم (٥) وجد ان العزلات المرقمة ٢ و١٠ و٤٥ و٥٠ و٧٥ تعود الى الجنس Saccharomyces فيما تعود العزلة ٧٦ الى جنس اخر لم يتم تحديده.

تمثيل النترات والنتريت: يظهر من الجدول (٣) ان العزلات ٢ و١٠ و٤٥ و٧٦ قد نمت في الوسط الحاوي على النترات والنتريت كلا على انفراد مما يدل على قابليتها لاستغلالها كمصدر وحيد للنايتروجين. ولم تستطيع العزلتان ٥٠ و ٧٥ من النمو فيها.

مقاومة العزلات للسايكلوهكسيميد: تبين النتائج في جدول (٣) عدم استطاعة العزلات ٢ و ٤٥ و ٥٠ و ٧٥ وسلالتي المقارنة النمو في وسط YE الحاوي على ١٪ سايكلوهكسيميد حيث ان ذلك صفة مهمة للجنس Saccharomyces. اما العزلتان ١٠ و٧٦ فقد قاومت المضاد المذكور. وفي هذا المجال لاحظ Bennet et al (١٦) ان السايكلوهكسيميد يؤثر على صنع الحامض النووي (رنا).

شدة التلبد: اعتماد على النتائج السابقة فقد نميت العزلات المحلية المتلبدة وسلالتي المقارنة في الوسطين DM, YPD اضافة الى

اختيار وسط وظروف التنمية المشجعة على تلبد الخمائر المحلية

*عبد الواحد باقر **مثلى كاظم جواد ***محمد عبد القادر ابراهيم
*قسم علوم الحياة/ كلية العلوم/ الجامعة المستنصرية ** كلية التربية ابن الهيثم *** قسم علوم الحياة/كلية العلوم/ جامعة بغداد، بغداد، العراق
(استلم في ١٩٩٢/١١/٧، قبل للنشر في ١٩٩٣/١/١٩)

ABSTRACT

Two industrially used yeasts, Saccharomyces carlsbergensis (flocculant) and Sacch. cerevisiae (non - floc), were grown in five different media (GYSA, YE, ME, YPD and DM) at various temperatures. (8, 25, 30 and 35°C) and pH (3. 5-6.5). YPD and DM media with pH 4.8 were found to encourage flocculation when yeasts were grown at 25°C/3 days. Same conditions were applied to test the ability of (64) yeast isolates (collected from local fruits) to flocculate six of the isolates were flocculant and the intensity of one of them was very heavy to exceed even the industrial flocculant yeast.

الخلاصة

نميت السلالتين القياسيتين سكارومايسيس كالرلسبرجينسيس (خميرة شديدة التلبد) وسكارومايسيس سيرفيسياي (خميرة عديمة التلبد) في الاوساط الزراعية YPD, DM, ME, YE, GYSA في أس هايدروجيني تراوح بين ٣،٥ - ٦،٥ ودرجات حرارة ٨و٢٥و٣٠و٣٥م لانتخاب الوسط الزرعي والظروف المثلى للتلبد. وقد وجد ان الوسطين YPD, DM وأس هايدروجيني ٤،٨ ودرجة حرارة ٢٥م لمدة ٧٢ ساعة هي افضل الظروف المشجعة على التلبد. بعدها استخدمت هذه الظروف لدراسة قابلية (٦٤) عزلة خميرة جمعت من المصادر الغذائية المحلية على التلبد ومقارنة شدة تلبدها مع السلالة القياسية المتلبدة. وقد ظهر ان (٦) عزلت محلية تلبدت بدرجات متفاوتة وان واحدة منها قد فاقت بتلبدها جميع العزلات وسلالة المقارنة.

المقدمة

يعد التلبد في الخمائر عاملا مهما ومحددا في بعض الصناعات التخميرية مما ادى الى اتجاه الدراسات الحديثة للتركيز على هذه الظاهرة والعوامل البيئية والوراثية المؤثرة عليها. وعرف Brian et al[١] التلبد بقابلية الخلايا على الالتصاق مع بعضها في كتل وترسيبها بسهولة الى القعر. تنتشر ظاهرة التلبد بوضوح بين اجناس من البكتريا والخمائر لا سيما جنس Saccharomyces[٢]. وقسم Mill[٣] الخمائر الصناعية الى متلبدة وغير متلبدة وكامنة التلبد (التي تنفصل ثانية بأبسط التغيرات البيئية وهي تختلف عن المشتتة لاختلاف تركيبها البنائي). ويعزي العديد من الباحثين (٤، ٥، ٦، ٧) ظاهرة التلبد الى تركيب جدار الخميرة ومكوناته والكاربوهيرات التي يحويها هذا الجدار خاصة. ولاحظ Day et al[٤] ان جدران الخلايا المتلبدة مغطاة بشعيرات لا تحتويها غير المتلبدة فيما وجد Stewarrt and Goring[٨] ان شدة التلبد ترتبط مباشرة بعوامل التغذية واطوار النمو. واكد Kamada and Murata [٩] ان تشتت وتلبد الخمائر يعتمد اساسا على تركيز السكر في الوسط والاس الهايروجيني وان الخلايا تتشتت بداية التخمر عندما يكون تركيز السكر عال وعند اس ٥،٥ ثم تتلبد نهاية التخمر عند قلة نسبة السكر وانخفاض الاس الى ٢، ٤. وقد عزت احدى الدراسات [١٠] تلبد الخلايا الى تركيب البوتين على سطحها وان سرعة ترسيب الخمائر تنخفض بارتفاع درجة الحرارة وتزداد بانخفاضها، فيما عزى اخرون ظاهرة التلبد التىالتهوية في المخمر حيث لا يحدث التلبد تحت الظروف اللاهوائية [١]. ولان خاصية التلبد الى التهوية في المخمائر والسلالات التي لها القدرة على الانفصال ذاتيا عن السائل المتخمر قد اصبحت موضع اهتمام العديد من الباحثين والصناعيين لما لذلك من مردود اقتصادي فقد جاءت هذه الدراسة بهدف انتخاب بعض الخمائر من المصادر الغذائية الطبيعية وايجاد الظروف البيئية المشجعة على التلبد ومقارنة ذلك مع السلالات القياسية المعروفة صناعيا.

المواد وطرائق العمل

الخمائر القياسية: استخدمت سلالتين من الخمائر الصناعية Brewer's yeast نوع **Saccharomyces carlsbergensis** (رمز لها بالحرف أ) وهي شديدة التلبد والثانية Baker's yeast نوع **Sacch. cerevisiae** (ب) غير متلبدة.

عزل الخمائر المحلية: جمعت (٦٤) عزلة خميرة من ٨٠ نموذجا من الفواكه التي بدا عليها التخمر في اسواق بغداد والتي شملت على العنب والكمثري والرمان حيث عزلت بتنميتها على ٢٥م لمدة ٣-٥ ايام على الوسط Yeast Extratt (YE) الحاوي على ١١٪ كحول ايثلي، ثم اخذت نقلة واحدة وزرعت بطريقة التخطيط على الوسط Yeast Peptone Dextsose (YPD) تحت الظروف نفسها، اعيد نقلها الى وسط Wort Agar للحصول على مستعمرات نقية. بعدها فحصت مبدئيا لتحديد صفاتها المورعية والمجهرية كونها عزلات خمائر. ثم حفظت على اكار YPD للاختبارات اللاحقة.

اختيار العزلات المتلبدة: لقحت الانابيب الحاوية على وسط YPD بالعزلات المحلية وسلالتي المقارنة كلا على انفراد، وبعد الحضن على ٢٥م/٣ ايام فحصت بالعين المجردة بعد رجها بلطف لملاحظة التعكر

المصابة, غير انها لم تلاحظ في مقاطع الانسجة لاشجار نخيل سليمة حضرت بنفس الطريقة. ولم يلاحظ في كافة المقاطع التي فحصت وجود اي نوع من الفايروسات او الميكوبلازما.

٤ – الاصابة الاصطناعية: لقد سبب الفطر C. radicicola اعراض مرضية على الفسائل الملوثة, تميزت بظهور بقع سوداء اللون داكنة في مناطق التلويث امتدت لتشمل السعف مسببة متنه فتكسره بعد حوالي ٤٠ يوم من موعد التلويث. ورافقت الاصابة بطأ نمو الشجرة وميلان رأسها نحو جهة التلويث وانفصلت منطقة القلب عن جذع الشجرة وصاحبها وجود تعفن جاف في كافة اجزاء النخلة المصابة, وقد امكن اعادة عزل الفطر C. radicicola من الاجزاء المصابة. لم تظهر اية اعراض مرضية على الفسائل الملوثة بالفطريات الاخرى او البكتريا ولا على الفسائل الملوثة بالماء للفطر المعقم.

تطابقت نتائج هذه الدراسة مع النتائج التي تم الحصول عليها في دراسات سابقة (٤-٥, ٦) والتي اشارت الى دور الفطر C. radicicola في تدهور وموت اشجار النخيل في العراق. اما الفطريات الاخرى, خاصة بعض انواع الفطر Fusarium. فقد اشارت دراسة سابقة (١١) بانها من الفطريات المصابة للاشجار الضعيفة او المهملة او الميتة, ما عدا الفطر F. equiseti الذي يحتمل اصابته للاشجار (١٠) والذي لم يلاحظ بالعزل في هذه الدراسة.

٥ – المكافحة الكيمياوية: شوهد تحسن واضح على كافة الاشجار المعاملة بمبيد البنليت بعد حوالي ستة اشهر من موعد الحقن, حيث ظهر السعف الجديد ذو نمو طبيعي واحد رأس النخلة بالاعتدال تدريجيا, ما عدا احد الاقحل المعاملة الذي مات ويحتمل ان تكون اصابته متطورة ولم يتمكن المبيد من مقاومة المسبب, علما بان اقحل النخيل اكثر حساسية للاصابة بهذا المرض من الاناث, اما الاشجار المعاملة بالمبيدات الاخرى فلم يلاحظ وجود اي تحسن عليها, مما يؤكد بان المسبب هو فطر وليس حشرة او بكتريا او ميكوبلازما.

نستنتج من خلال هذه الدراسة والدراسات الاخرى (٤-٥ , ٦, ٩) بان الفطر C. radicicola هو المسؤول الرئيسي عن مرض انحناء الرأس في النخيل (التعفن الجاف), اضافة الى مسؤوليته عن تدهور وموت العديد من اشجار النخيل في المنطقة الوسطى من العراق (٥-٦), وفي بعض مناطق زراعة النخيل بالعالم (٩). ان حفار العذوق O. elegans يلعب دورا مهما في نقل هذا الفطر ودخوله الى الاشجار السليمة, فهي تشابه لما تقوم به بعض الخنافس الناقلة لمسبب مرض تدهور اشجار الدردار الهولندي او تدهور اشجار البلوط (Ceratocystis) وهو الطور الجنسي للفطر C. radicicola (٩), حيث تقوم هذه الخنافس بحمل ابواغ الفطر على اجسامها فتلوث بها الاشجار السليمة اثناء قيامها بحفر الانفاق ووضع البيض, حيث يقوم الفطر بتحلل الانسجة النباتية, مما يوفر لليرقات الفاقسة حديثا تغذية جاهزة يساعدها على النمو والتطور (معيشة تكافئية).

واخيرا فان هناك العديد من الاسئلة التي تحتاج الى دراسات لاحقة للاجابة عليها مثل سبب حساسية بعض الاصناف (سايروبريم) دون غيرها او سبب حساسية الاقحل ضمن الاصناف, اضافة الى العديد من الدراسات المتعلقة بالعوامل البيئية المساعدة لاحداث وتطور المرض.

REFERENCES

[1]
البكر، عبد الجبار، نخلة التمر: ماضيها وحاضرها، والجديد في زراعتها وصناعتها وتجارتها. المشروع الاقليمي لبحوث النخيل والتمور في الشرق الادنى وشمال افريقيا، بغداد، ١٠٨٥ صفحة(١٩٧٢).

[2]
عبد الحسين، علي: النخيل والتمور وافاتهما، وزارة التعليم العالي والبحث العلمي، جامعة البصرة، ٥٧٦ صفحة(١٩٨٥).

[3] Djerbi M. Diseases of the date palm. Reg. Proj. for Palms and Dates Res. Cent. Near East and Norht Africa, Baghdad, 106 gages (1983).

[4]
عباس، عماد حسين ومثنى نوري محي، علاقة الفطر Chalaropsis radicicola والحفار Oryctes elegans بمرض انحناء الرأس على النخيل، المجلة العراقية للاحياء المجهرية ٣(١):١٢١-٢١٩ (١٩٩١).

[5]
البهادلي، علي حسين، جمال طالب الربيعي وهشام محمد جاسم: دراسة ظاهرة موت النخيل، المؤتمر الخامس لمجلس البحث العلمي، بغداد ٧-١١ تشرين اول، ١٩٨٩: ٧١-٧٦(١٩٨٩).

[6]
عباس، عماد حسين، مثنى نوري محي، نزار نومان حمه، جمال طالب الربيعي وعلي حسين البهادلي، تواجد بعض الفطريات المرضية على جذور اشجار النخيل المصابة بالتدهور في العراق. المؤتمر القومي الثالث لافات وامراض الخضر والفواكه في مصر والدول العربية، الاسماعلية، جامعة قناة السويس ٢٤-٢٦ تشرين اول ١٩٨٩، ٣: ٨٨٤-٨٨٩ (١٩٨٩).

[7] Spurr A.R. A low viscosity epoxy resin embedding medium for electron microscopy. J. Ultrast. Res. 26: 31-43 (1969).

[8] Al-Hassan K.K. and Abbas G.V. Out-break of terminal bud*** at date palm caused by Thielaviopsis paradoxa, Date palm J. 5(1): 117-119 (1987).

[9] Nagrai T.R. and Bryce. A monograph of Chalara and allied genera. Wilfrid Laurier University Press, Waterloo, Ontario, Canada, 200 pages. (1975).

[10] Abbas, I.H., Mouhi M.N., Al-Roubaie T.J., Hamma N.N. and El-Behadli A.H. Phomopsis pheonicola and Fusarium equiseti, new pathogens on date palm in Iraq, Mycological Research 95: (April) 509-510 (1991).

[11]
عباس، عماد حسين ومثنى نوري محي : تواجد بعض انواع الفطر Fusarium على اشجار النخيل، المجلة العراقية للاحياء المجهرية ٢(١): ٤٩-٥٦ (١٩٩٠).

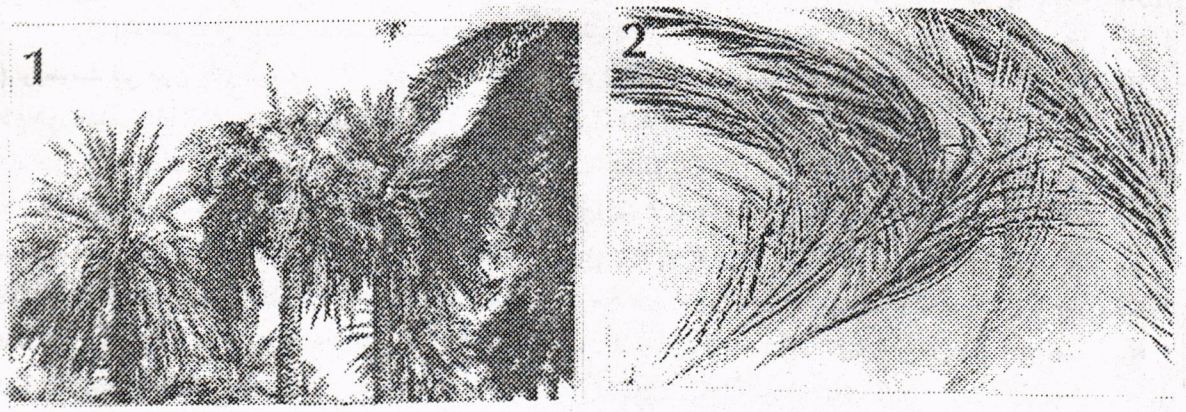

شكل (١) اعراض الاصابة بمرض انحناء الرأس في اشجار النخيل(١)، اعراض الاصابة على السعف(٢)

شكل (٢) ابواغ الفطر Chalaropsis radicola x ٤٠٠(١)، حفارات العذوق Oryctes elegans : اليرقات(٢) والبالغات(٣)

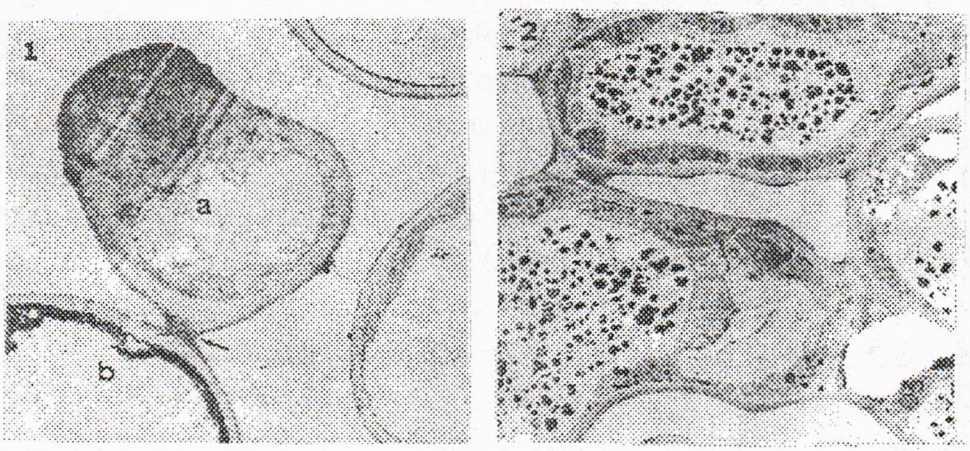

شكل (٣) صورة بالمجهر الالكتروني النافذ لنسيج نخيل مصاب بمرض انحناء الرأس توضح (١) وجود غزل فطر(a) في اتصال مباشر مع الجدار الخلوي للعائل (b)، مواد ذات كثافة الكترونية عالية داخل سايتوبلازم الخلايا المصابة (٢).

في محلول رابع اوكسيد الاوزميوم ٢٪ في نفس محلول المنظم مدة ساعتين للتثبيت النهائي. جففت النماذج باستخدام تراكيز متدرجة من الاسيتون (١٠ - ١٠٠٪) ثم طمرت في مادة البلاستيك حسب طريقة Spurr (٧)، ووضعت في فرن على درجة ٧٠ °م لمدة ١٢ ساعة، قطعت النماذج الى مقاطع رقيقة (٧٠ ميكرون بواسطة جهاز التقطيع الدقيق وحملت على اقراص شبكية نحاسية ٣٠٠ مش. أجريت عملية تصبيغ النماذج بواسطة أسسيتات اليترانيل مدة ١٥ دقيقة ثم بواسطة سترات الرصاص مدة ١٠ دقائق وفحصت بالمجهر الالكتروني النافذ. حضرت مقاطع مماثلة من اشجار سليمة بنفس الطريقة السابقة للمقارنة.

٤ - احداث الاصابة الاصطناعية : اجريت الاصابة الاصطناعية للفطريات المعزولة والبكتريا وذلك بعمل عالق من السبترات تركيز حوالي ١٠^٦ سبور / مل من الفطريات وحوالي ١٠ ٧ خلية / مل من البكتريا تحقنت في قاعدة أساثل من النخيل ناتجة من زراعة البذور صنف بريم بعمر ٥ سنة. أصيبت اصطناعيا ثلاث اشجار لكل نوع من الفطريات والبكتريا المعزولة وبواقع ٥ مل / شجرة تم حقن عدد مماثل من الاشجار بالماء المقطر المعقم للمقارنة.

٥ - اختبار المبيدات الكيمياوية: تم اختيار احدى البساتين الموبوءة بهذا المرض لاجراء تجربة مكافحة باستخدام مبيدات كيمياوية مختلفة، حيث استخدم مبيد فطري هو Benlate (تركيز ٤ غم / لتر)، ومبيد حشري هو Nuvacon - 250 ULV وخليط من Oxytetracyclin و Streptomycin (١ ملغ /لتر). تم حقن هذه المبيدات الى داخل الاشجار بواقع خمسة اشجار لكل مبيد مستخدمين ضعف التراكيز الموصى بها من قبل الشركة المنتجة، وذلك بعمل ثقوب في جذع الشجرة بواسطة مثقب حديدي مجوف حيث تم حقن الشجرة بالمبيد مع تكرار عملية الحقن عدة مرات مستخدمين الكمية ٢-٥ لتر/شجرة، ما عدا مبيد Nuvacron فقد استخدم بواقع ٥٠ مل/شجرة. اختيرت اشجار نخيل صنف ساير بعمر ٤٠ سنة لاجراء هذه التجربة.

النتائج والمناقشة

١ - الاعراض المرضية: لوحظت اعراض الاصابة الطبيعية على اشجار متفرقة داخل البستان الواحد، وتركزت بشكل خاص على الاصناف ساير وبريم، وتميزت الاصابة بميلان رأس النخلة نحو احد الجهات يصاحبها تشوه السعف وانحناءه على هيئة هلال (شكل ١)، فتتطور الاصابة يسقط الرأس تاركا الجذع بعد مرور حوالي شهر من بدأ الاعراض المرضية.

أظهرت المقاطع العرضية في المنطقة العليا من الجذع وجود حلقات بنية اللون داكنة ذات اقطار مختلفة تراوحت ما بين ١-١٠ سم ومحاطة بهالة صفراء اللون، وهي مناطق الاصابة وذات تعفن جاف. لم يلاحظ وجود هذه الحلقات في قلب الشجرة (الجمار) والذي كان سليما من الاصابة، كما لوحظ وجود مناطق مصابة ذات تعفن جاف في بعض السعف المشوه بعد قطعه طوليا ولم يلاحظ وجود اية تعفنات اخرى في مناطق بعيدة عن الرأس بما فيها الجذور والتي كانت سليمة من الاصابة، وقد تركزت مناطق الاصابة في جذع الشجرة المتمرضة لاصابة سابقة بحفار العذوق O. elegans حيث لوحظ في بعض الحالات المرضية وجود مناطق اتصال بين اثر الاصابة بالحفار ومناطق التعفن.

٢- عزل المسببات المرضية:

أ- عزل الفطريات: لقد تم عزل الفطر C. radicicola من اجزاء النخلة المصابة وعلى وجه التحديد في المناطق ذات اللون الداكن(الحلقات)، وتم عزل من الاتفاق واليرقات والبالغات لحفار العذوق O. elegans المتواجدة على الاشجار المريضة، وعزل ايضا من البراز والاحشاء الداخلية لهذه الحشرات، ولم يعزل من المناطق السليمة او قلب الشجرة (الجمار) او من الجذور، على الرغم من عزله من الجذور في دراسة سابقة(٦).

شخص الفطر C. radicicola بالاعتماد على Nag Raj و Bryce (٩) وتم مقارنته باحدى العزلات المشخصة من قبل المعهد الامبراطوري للفطريات (I.M.I316226).

اختلف هذا الفطر عن مسبب مرض المجنونة Thielaviopsis paradoxa كون اباغه تكون مفردة على الحامل الكوني في حين تكون على هيئة سلاسل بالنسبة للفطر T. paradoxa اضافة الى كبر حجم ابواغ الفطر C. radicicola حيث تراوحت ابعاد الابواغ الكبيرة (Macroconidia) ما بين ٢٢-٢٨X١٣-١٧ ميكروميتر، وابعاد الابواغ الصغيرة (Endoconidia) ما بين ١٤-٢٠X٥-٨ ميكروميتر (شكل ٢)ز

لقد رافق عزل الفطر C. radicicola انواع مختلفة من الفطريات كان اهمها:

F. oxysporum ,Fusarium moniliform, F. ,Paecilomyces sp. ،Chaetomium sp. ,F. solani Gilmaniella sp. ,Dendrophoma sp.

كما لم تكشف المزارع المائية عن وجود اي نوع من الفطريات الطحلبية كالفطر Phytophthora او Pythium، بل لوحظ وجود احد الانواع التابعة للفطريات البازيدية وقد تميز بتكوينه مخالب الاتصال (Clamps connection) وامكن عزله وتنميته على الوسط الغذائي PDA وهو ذات نمو سريع وغزل فطري ابيض اللون.

ب - عزل البكتريا: عزلت انواع مختلفة من البكتريا ذات اشكال والوان مختلفة منها الكروية او العصرية ذات الوان خضراء فاتحة، بيضاء، حمراء وصفراء، نقيت هذه العزلات ونميت واستخدمت لاجراء الاختبارات الخاصة باحداث الاصابة الاصطناعية.

٣ - الفحص بالمجهر الالتروني: اظهرت نتائج الفحص بالمجهر الالترقي النافذ وجود غزل فطري في داخل الانسجة المصابة، ولوحظ وجود مناطق اتصال بين الغزل الفطري وجدران الخلايا المصابة، يقابلها تكون مواد ذات كثافة الكترونية عالية بالقرب من جدار الخلية المصابة (شكل ٣). يحتمل ان تكون هذه المواد قد تكونت نتيجة رد فعل العائل لمقاومة المسبب المرضي او قد تكون بداية الاصابة الخلية وموت السايتوبلازم. لوحظت هذه الاشكال بشكل متكرر في الخلايا

عزل وتشخيص المسبب المرضي لانحناء الراس في النخيل

عماد حسين عباس، هادي مهدي عبود، حمود مهيدي صالح
منظمة الطاقة الذرية/ مركز البحوث الزراعية/ بغداد، العراق

(استلم بتاريخ ١٩٩٢/١٢/١٢ ; قبل بتاريخ ١٩٩٣/٥/٨)

ABSTRACT

In 1988, many date palm trees were dying in differents groves located at Baghdad. The mature trees were affected with symptoms of head benging. After dying the crown falls, leaving a bare trunk. Chalaropsis radicicola have consistently been isolated from the dying palm trees. The fungus was also isolated from galleries, larvae, adults of fruit stalk borer Oryctes elegans, associated with this disease. Pathogenicity tests showed that this fungus was capable of causing disease syndrome. Several Fusaria spp. that were isolated from diseased tissue did not infect date palm tree in pathogenicity tests. A study by electro microscopy showed that no mycoplasma or viruses were present in the infected tissue. We concluded that C. radicicola plays a great role in pathogensis of bending head, and O. elegans act as a vector for the fungus, which introduse it into palm trees during breeding attacks.

الخلاصة

في عام ١٩٨٨, لوحظ تدهور وموت عدد كبير من اشجار النخيل في المنطقة الوسطى من العراق وتمثلت الاعراض المرضية بتشوه السعف وانحناء رأس المخلة ثم سقوطه. عزل الفطر Chalaropsis radicicola من كافة اجزاء الشجرة المصابة, كما عزل من انفاق ويرقات وبالغات حفار العذوق Oryctes elegans المتواجدة على الاشجار المريضة. اشارت نتائج العدوى الاصطناعية علهذا الفطر على فسائل نخيل بقدرته على احداث اعراض مرضية بينما لم تظهر بعض انواع الفطر Fusarium وفطريات اخرى وبكتريا معزولة من الاشجار المصابة اية اعراض مرضية على الفسائل الملوثة, كما لم يلاحظ وجود فايروسات او ميكوبلازما في انسجة النخيل المصابة بعد عمل مقاطع رقيقة منها وفحصها بالمجهر الالترتني النافذ. نستنتج من خلال هذه الدراسة على ان الفطر C. radicicola هو المسؤول الرئيسي عن مرض انحناء الرأس في النخيل وان حفار العذوق O. elegans يساعد على نقله ودخوله الى الاشجار السليمة.

المقدمة

يعد مرض انحناء الرأس في النخيل او ما يعرف باسم تحجيم نمو النخلة (التعفن الجاف) من الظواهر المرضية القديمة, حيث لوحظ في موريتانيا, مصر, الجزائر وتونس, غير ان المسبب المرضي لهذه الحالة لم يشخص بعد (١, ٢, ٣).

لوحظت هذه الظاهرة المرضية في بعض البساتين بالمنطقة الوسطى من العراق في عام ١٩٨٨, وقد اشارت دراسة سابقة عن هذه الحالة بمرافقة الفطر Chalaropsis radicicola (Bliss) Moreau للاشجار المريضة اضافة الى انها كانت موبوءة بحفارات العذوق Oryctes elegans Prell (٤), كما اشارت دراسات اخرى الى ان هذا الفطر يساهم بموت وتدهور العديد من اشجار النخيل في العراق (٥-٦).

وبالنظر لعدم وجود دراسة تفصيلية تؤكد سبب هذه الحالة واستكمالا للبحوث المشار اليها في اعلاه, فقد اجري هذا البحث والذي يهدف ايضا الى ايجاد مبيد كيمياوي مناسب لمكافحتها والحد من انتشارها.

المواد وطرق العمل

١ - جمع النماذج: جمعت نماذج من انسجة النخيل المصابة والجذور من بعض البساتين في المنطقة الوسطى من العراق شملت محافظات بغداد, بابل, ديالى وكربلاء. اخذت النماذج من الصنف بريم والصنف ساير (اسطة عمران). كما جمعت بالغات ويرقات حفار العذوق Oryctes elegans المرافقة للاشجار المريضة (شكل ٢).

٢ - عزل المسببات المرضية:

أ - عزل الفطريات: استخدم الوسط الغذائي PDA لعزل الفطريات من النماذج النباتية والحشرات وباتباع الطرق التقليدية. كما استخدمت مزارع مائية للجذور بعد تعقيمها سطحيا وغسلها جيدا بالماء المعقم بواسطة جهاز الهزهاز الكهربائي عدة مرات ثم حضنت لمدة ٤٨ ساعة في درجة حرارة ٢٥°م وفحصت بالمجهر العادي لمشاهدة التراكيب التكارثية للفطريات.

ب - عزل البكتريا: استخدم الوسط الغذائي Nutrient agar لعزل البكتريا من انسجة الاشجار المريضة ومن يرقات وبالغات العذوق الموجودة على تلك الاشجار.

٣ - الفحص بالمجهر الالتروني: تم عمل مقاطع رقيقة من الاجزاء المصابة, حيث قطعت الى قطع صغيرة مساحتها ١ ملم^2 ووضعت في محلول منظم فوسفاتي (٠,٠١ مول فوسفات الصوديوم درجة حموضة ٦,٨). غمرت المقاطع في محلول كلوتزالدهايد ٣٪ لمدة ١٢ ساعة للتثبيت الاولي. غسلت النماذج عدة مرات في المحلول المنظم وغمرت

جدول(١) يوضح كمية ال DNA في المراحل المختلفة من دورة حياة حطلب U. zonata التي تتم قياسها بوحدات (AU) والخطأ القياسي والنسبة بينهما.

المراحل في دورة الحياة	معدل قيمة الـ DNA ± الخطأ القياسي	النسبة
خلايالخيط الخضري	2.5±34.80	2C
الخلايا اللاجنسية	1.7±31.30	2C
الخلايا الجنسية	2.3±30.45	2C
البيوض المخصبة	3.2±64.40	4C

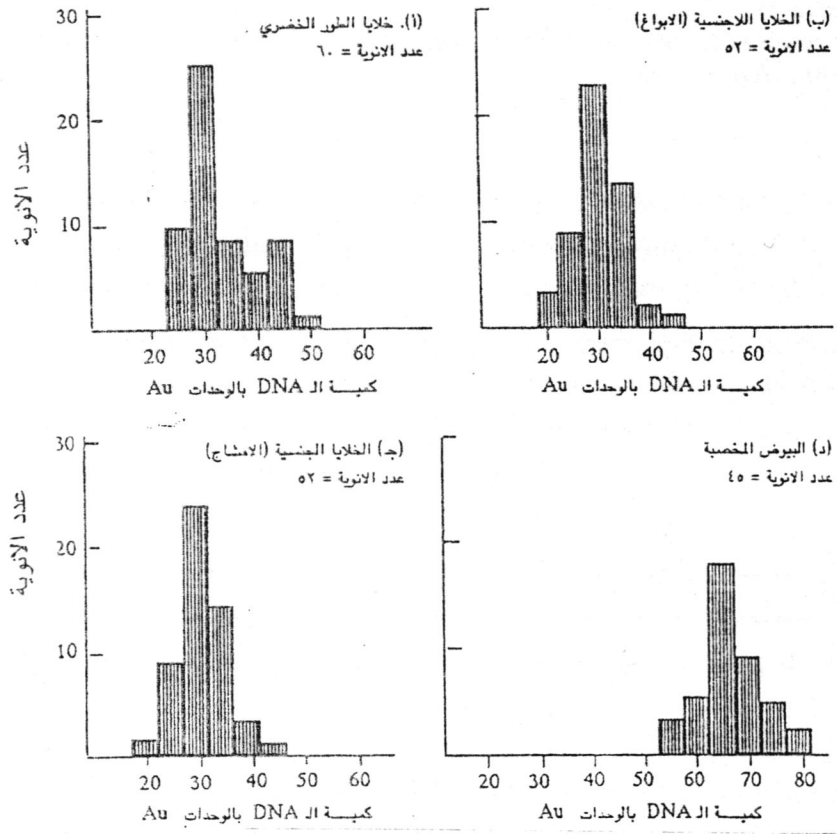

شكل(١) يبين كمية ال DNA (Au) في انوية الخلايا في اربع مراحل مختلفة من دورة الحياة للطحلب U. zonata.

[14] Al-Kubaisy, KH. Untersuchungen Zum Entwichlungskreislaug von Vaucheria Sessilis: M.SC. Thesis. Giessen. W. Germany, (1976).

[15] Trapp, L. Instrumentation for recording microspectrophotometry. In Wied, G.L. Instrumentation to quantitative cytochemi. New York. London. (AP) (1966).

[16] Hale, A.J. Feulgen microspectrophotometry and its correlation with other cytochemical methods. in Wied, G.L. Intriduction to quantitative cytochemistry. New York. London (AP) (1966).

[17] Cavalli - Sforza, L. Biometrie. Stuttgart, (1969).

[18] Swift, H. The constancy of DNA in p;ant nuclei. proc. Nat. Acad. Sci (USA), 36: 643-654, (1950).

[11] Al-Jybaustm KH H O Schwantes and G Seibold Cytophotometrische Untersuchungen Zum Generation swechsel autotropher and heterotropher Organismen Vaucheria sessilis and Saprolegnia ferax. J. cramer 34: 301-316 (in German), (1981).

[12] Koop, H.U. Ueber den Ort dermeiose bei Acetabularia mediterranea. protophlasma, 85: 109-114 (in German) (1975).

[13] Hurdelbrink, L. and H.O. Schwantes: Sur le Cycle de de'veloppement de Batrachospermum. Soc. bot. Fr. Memoires 269-274 (in French), (1972).

تم تعيين كمية الـ DNA تح طول موجي مقداره (٥٦٠ نانوميتر) وهو يطابق اعلى درجة امتصاص بالنسبة لـ Feulgen - DNA) complex) ويطلق على وحدات القياس بالـ (arbitrary units)

للمزيد حول وصف الجهاز لاحظ (١٥) ولمعرفة القياسات الدقيقة يمكن الرجوع الى (١٦).

التحليل الاحصائي للقياسات المتحصل عليها بواسطة جهاز الطيف الخلوي قسمت الى عدة صفوف ورسمت على شكل Histograms وذلك بالاستعانة بالامثلة والجداول الواردة في (١٧).

النتائج والمناقشة

عند فترة طويلة قسمت الطحالب الخضر حسب دورات الحياة الى قسمين فهي اما ان تكون ثنائية المجموعة الكروموسومية اي انها في الطور الخضري من نوع diploid وان الانقسام الاختزالي يحصل عند مرحلة تكوين الامشاج او تكون احادية المجموعة الكروموسومية اي انها في الطور الخضري من نوع haploid حيث يتم الانقسام الاختزالي عند انبات البيضة المخصبة وهذا ما بينته بعض الدراسات الخلوية والوراثية (٥) والتي لا تزال تستخدم نتائجها في العديد من المراجع العلمية (١، ٢، ٣).

الا ان صغر انوية الخلايا في جميع او بعض المراحل من دورات الحياة بحيث تكون عملية تعيين موقع الانقسام الاختزالي على اساس حساب عدد الكروموسومات والفحص تحت المجهر الضوئي ذات صعوبات ولا يعول على نتائجها بشل تام لذلك استخدمت طرق حديثة في البحث لغرض تعيين كمية ال DNA في المراحل المختلفة لدورة الحياة. اذ ان كمية ال DNA توازي عدد الكروموسومات (١٨) وان (1C) تعني Haploid ,(2C) Diploid ,(4C) Tetraploid ولغرض تحديد قيمة المجموعة الكروموسومية وضعت النتائج المتحصل عليها من قياس كميات ال DNA على شكل Histograms شكل (١) وقد اختيرت لهذا الغرض اربع مراحل من دورة حياة حطلب U. zonata وهي كما ياتي:

- انوية خلايا الخيط الخضري وعددها (٦٠) نواة.
- الخلايا التكاثرية اللاجنسية (الابواغ) وعددها (٥٢) نواة.
- انوية الخلايا الجنسية (الامشاج) وعددها (٥٢) نواة.
- انوية البيوض المخصبة وعددها (٤٥) نواة.

وضعت الانوية التي تم قياسها على المحور الصادي وكمية ال DNA على المحور السيني بالوحدات (A.U). لقد حللت احصائيا بتعيين الوسط الحسابي والخطأ القياسي والنسبة بينهما جدول (١) ولتوضيح شكل (١) والجدول (١) للتعرف على توزيع كمية ال DNA في الانوية التي تم قياسها كانت النتائج كما يلي: -

قيمة محتوى الخلايا من ال DNA في خلايا الخيط الخضري (34. 80 ± 2.5 AU) وقيمة ال DNA في الخلايا اللاجنسية (الابواغ) (31.30 ± 1.7 AU) كما ان كمية ال DNA في الخلايا الجنسية (الامشاج) (30.45 ± 2.3 AU) .

اما كمية ال DNA في انوية البيوض المخصبة فكانت (64.40± 3.2AU) . وبما ان كمية ال DNA في الخلايا الخضرية والخلايا اللاجنسية والجنسية هي نصف كمية ال DNA في البيوض المخصبة فان الطحلب يكون من نوع haploid اي احادي المجموعة الكروموسومية في المرحلة الخضرية وان عملية الانقسام الاختزالي تمت عند انبات البيوض المخصبة اي ان الانقسام الاختزالي هو من نوع Zygotic meiosis او ما يسمى بالانقسام الاختزالي الفوري Initial type. وهذا يتطابق مع نتائج الدراسات التي تمت بطرق اخرى خلوية (٥) والتي استخدمت كذلك من قبل (١، ٦، ٧).

ويظهر من الشكل ان خلايا الخيط الخضري تبدو انها تحتوي على كمية من ال DNA اكبر من (2C)وهذا يعود الى ان هناك انوية تكون في مرحلة بناء ال DNA في اثناء الدورة الخلوية والتي تنقسم بعد ذلك ثم تمر بمرحلة G2 وفيها يجب ان تحتوي النواة على ضعف كمية ال DNA قياسا لمرحلة G1 التي تتضمن كمية ال (DNA). (١١، ١٣).

REFERENCES

[1] Bold, H.C. and Wgna, M.J. Introduction to the algae, structure and Reproduction, 2nd Edi. Engle wood calif (1985).

[2] Smith, G. Cryptogamic Botany Algae and Fungi. Vol (1) 2nd Ed. Mcgraw - Hill book comp. Inc. (1983).

[3]
مولود، بهرام ونضال ادريس سليمان وابراهيم البصام: الطحالب والاركيكونيات/ كلية التربية الثانية ابن الهيثم- جامعة بغداد، (١٩٩٠).

[4]
مولود، بهرام ، نضال ادريس سليمان وصباح فرج عبد الاحد: دراسة بيئية مقارنة للطحالب في اليوسفية والراشدية بغداد. مجلة بحوث علوم الحياة عدد ١٧(٢)، ١٣-٣٠.

[5] Gross, I. Ulothrix. Arch. protistenk 73: 206-234, (1931).

[6] Wartenber, A. Systematik der niederen pflanzen. dtv. west germany (1971)

[7] Schwantes, H.O. Pflanzensystematik. Eumycoga. Stuttgart (1975).

[8] Braynt, T.R. and K.L., Howard Meiosis in the Domycetes: A microspectro - Photometeric analysis of DNA in Apodachlya brachynema. Mycologia 63: 58-69 (1971).

[9] Yemman, J. and C.D. Therrien. Quantitative microspectrophotometery of nuclear DNA in selfing strains of the Myxomycete Didymium iridis. Amer. J. Bot. 59 (8): 828-835 (1972).

[10] Peabody, D., J.J. Motta and C.D. Therrien Cytophotometric Evidence for heteroploidy in the life - cycle of Armillaria mellea Mycologia, 70: 487-498, (1987).

تعيين موعد الانقسام الاختزالي في طحلب Ulothrix zonata بقياس كمية (DNA) باستخدام جهاز الطيف الضوئي الدقيق Microspectrophotometer

خالد حمد الكبيسي
قسم علوم الحياة/ كلية العلوم/ الجامعة المستنصرية / بغداد، العراق

(استلم بتاريخ ١٩٩١/١١/٧، قبل للنشر في ١٩٩٢/٢/١٢)

ABSTRACT

Four stages in the nuclear cycle of Ulothrix zonata were stained by the Feulgen - technique and relative DNA - Content per nucleus were measured by microspectro - photometeric analysis. Evidence presented demonstrates DNA - content suggestive of haploid life - cycle.

الخلاصة

تمت معاملة اربعة مراحل في دورة حياة الطحلب Ulothrix zonata باعتماد تقنية فولكن تقيست كمية الـ DNA النسبية للانوية في المراحل المختلفة باستخدام الطيف الضوئي الدقيق. ومن هذه القياسات أعطت الدليل على ان دورة الحياة في هذا الطحلب تكون احادية المجموعة الكروموسومية.

المقدمة

طحلب Ulothrix zonata من الطحالب الخضراء Chlorophyta التي تعيش في المياه العذبة والذي يتميز بكونه خيطي غير متفرع عديد الخلايا, تحتوي خلاياه على بلاستيدة خضراء واحدة حزامية الشكل ونواة واحدة (١, ٢, ٣).

لقد تمت بعض الدراسات على البيئة المائية العراقية وشخصت وجود بعض انواع جنس Ulothrix(٤). اما الدراسات حول المراحل المختلفة لدورة حياة الطحلب وموعد حصول عملية الانقسام الاختزالي قد اشارت الى انه يحدث عند ابنات البويضة المخصبة Zygote وان الطحلب احادي المجموعة الكروموسومية (haploid) في الطور الخضري Vegetative phase[5] . ولا تزال الكثير من المراجع تستخدم هذا المفهوم (١, ٦, ٧), الا أن هذه الدراسة لا يعول عليها لانها لم تتم على اساس حساب عدد الكروموسومات نظرا لصغر حجم النواة في الامشاج والابواغ.

وفي السنوات الاخيرة تمت العديد من الدراسات بتعيين كمية الحامض النووي DNA باستخدام جهاز الطيف الضوئي الدقيق الماسح Scanning microspectrophotometer عند دراسة دورات حياة العديد من الكائنات الحية الواطئة كالفطريات والطحالب (٨, ٩, ١٠, ١١, ١٢, ١٣) لتعيين موعد الانقسام الاختزالي وذلك لمعرفة فيما اذا كان الكائن الحي احادي ام ثنائي المجموعة الكروموسومية.

ولغرض تعيين موقع الانقسام الاختزالي اثناء دورة حياة طحلب ال Ulothrix zonata جددت هذه الدراسة باستخدام طرق بحثية لرفع الالتباس حيث ان عدد الكروموسومات في مثل هذه الحالات يكاد يكون غير واضح.

المواد وطرق العمل

ثم الحصول على طحلب الـ U. zonata من معهد النبات / جامعة كيسن في المانيا الغربية. نمي على درجة حرارة ١٦م في فترات من الضوء / والظلام ١٢/١٢ ساعة يوميا. ومن اجل الحصول على تكوين الابواغ Spores استبدلت فترة الاضاءة الى ٨ ضوء/ ٧٦ ظلام ساعة بعد ذلك تم نقل الطحالب الى اوساط زراعية خالية من عنصر النتروجين لغرض تحويلها الى طور التكاثر الجنسي(١٤).

التصبيغ: استخدام طريقة Feulgen . تمت عملية تثبيت الانسجة النباتية قيد الدراسة في محلول يتكون من الايثانول/ وحامض الخليك الثلجي (٣: ١) لمدة نصف ساعة ثم مررت الشرائح في كحول ٧٠٪ ثلاث مرات (٥ دقائق). نقلت بعد ذلك الى حامض الهيدروكلوريك 5n Hcl ولفترة (٤٥ دقيقة) وبدرجة حرارة الغرفة (٢٥م) بعدها تم تحويلها الى محلول الصبغة Schiff's Reagent (Pararosaniln Parafuchsin, Merck, Darmstadt) في المانيا الغربية ولمدة ساعة ونصف في الظلام, غسلت الشرائح ثلاث مرات في محلول $K_2S_2O_5$ بعد ذلك تمت طمرها.

قياس كمية الـ DNA : تم قياس كمية الحامض النووي DNA في الخلايا في اطوار مختلفة من دورة الحياة باستخدام جهاز الطيف الضوئي الدقيق الماسح نوع (UMSPI) Zeiss والمتصل بجهاز كمبيوتر (PDP 12) حيث وضعت الشرائح تحت قوة تكبير (١٠٠) ومجال القياس (٠,٥ ٠ ميكرون) وبخطوات بالاتجاهين السيني والصادي بمقدار ٠,٥ ٠ ميكرون. ان القياسات المذكورة اعلاه امكننا من تحديد كميات ال DNA ومهما كانت صغيرة وبحدود (10^{-12}-10^{-14} غرام).

شكل رقم (١) مقطع عرضي لسويق ورقة مغمورة لمدة يوم واحد في الماء تظهر أنسجة اللحاء والخشب مرتبة بشكل الكلية والخلايا سليمة

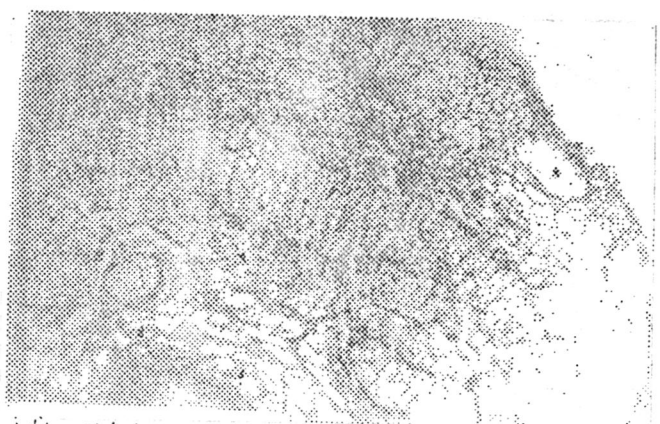

شكل رقم (٢) مقطع مستعرض لسويق ورقة مغمورة لمدة يوم واحد في الراشح الخام. لاحظ تحطم أنسجة البرانكيما والحاء وبقاء اوعية الخشب مفتوحة.

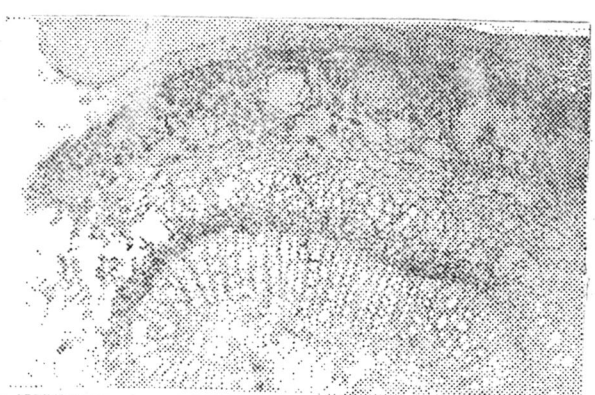

شكل رقم (٣) مقطع مستعرض لسويق ورقة مغمورة لمدة يوم واحد في الراشح المصفى بالفحم. لاحظ بقاء الانسجة سليمة بشكل عام عدا تحطم بعض الخلايا البارانكيمية في نسيج اللحاء وفي القشرة

[8] القصاب، عبد المطلب رضا حيدر، تنقية وتشخيص بعض السموم التي تفرزها الفطر هنتر سونيولا توريولويدي في الوسط الغذائي. رسالة ماجستير قسم علوم الحياة / كلية العلوم/جامعة صلاح الدين /اربيل (١٩٨٦).

[9] Damirdagh, Ihsan S. Interaction between potato viruses X and Y and spectrophotometric assay of PVX. Msc. thesis. Cornell University. ithaca, New York, (1965).

[10] Agrios, G.N. Plant pathology. Third edition. Academic press. (1988).

[11] Van Alfin, N.K. Reassessment of plant wilt toxins. Ann.Rev. Phytopathol. 27: 533-550 (1988).

٤_ صفات المقطع المستعرض لسويق الورقة المغمورة في الراشح المصفى بالفحم:- يوضح الشكل رقم ٣ مقطعا مستعرضا لسويق ورقة اليوكالبتوس المغمورة في الراشح المصفى بالفحم لمزرعة الفطر حيث يلاحظ احتفاظ جميع الانسجة في شكلها الاعيادي تقريبا. وعلى عكس ما احدثه الراشح الخام فقد كان التاثر قليلا على انسجة اللحاء والخلايا البرانكيمية حول اللحاء وكذلك البرانكيما الشعاعية حيث تحطم عدد قليل من الخلايا وكان المظهر العام للمقطع شبيها بمقطع سويق الورقة السليمة.

المناقشة

في البداية يجب ان نوضح ان الراشح الخام لمزرعة الفطر يحتوى على كل الانزيمات والسموم التي ينتجها الفطر ويفرزها الى الوسط الغذائي بما في ذلك انزيم البكتينيز وغيره التي اشار اليها باكستون ووريلسون (٦). اما الراشح المصفى بالفحم فقد اصبح بدون هذه الانزيمات والبروتينات ذلك لان الفحم يزيل كل هذه المركبات (٩). ولهذا وجدنا فروقا اساسية بين تأثير هذين التحضيرين من الراشح على الاعراض المرضية في الاوراق وكذلك على التشريح الداخلي لسويقات الاوراق. وقد كانت النتائج التي حصلنا عليها من حيث الاعراض متفقة تماما مع النتائج المنشورة سابقا (٣, ٧, ٨) فقد ذكر القصاد (٨) ان الجزء الحامضي A أ من سموم الفطر هندرسونيولا توريولويدى يسبب تغييرا في لون الورقة وتهدلا بدون تيبس في حين ان الجزء الكلايكوبروتين ج G من السموم يسبب تيبس الورقة بدون تغيير اللون وان الجزءان معا يسبب تغيير اللون ثم تيبس الورقة. وفي دراستنا الحالية لم نجد علاقة مباشرة بين مظهر الاوعية الخشبية الناقلة للماء ونوع الاعراض المرضية. فقد كانت الاوعية في كل الحالات مفتوحة وسليمة تقريبا (عدا عددا قليل جدا منها) ولكن التغاير النسيجي الواضح كان في الانسجة البرانكيمية وانسجة اللحاء حيث تحطمت هذه الانسجة عند غمر السويق في الراشح الخام وادى ذلك الى تيبس الورقة. ومن الممكن تفسير هذا التحطم بفعل انزيم البكتينيز وقد يكون ذلك ايضا سبب ظهور كتلة سوداء في نهاية السويق المغمور في الراشح الخام وعدم ظهورها في نهاية السويق المغمور في الراشح المصفى بالفحم. ومن جهة اخرى يمكن القول بأن جفاف الورقة حدث بسبب عدم جريان الماء الكافي من خلال اوعية الخشب الناقلة. ويمكن تفسير هذه النتائج على اساس وجود عامل واحد او اكثر للذبول حسبما ذكره اكريوس (١٠) ووجود اكثر من مركب سمي واحد في راشح مزرعة الفطر (٣, ٧, ٨) وعلى ما ورده فان الفن (١١): اذ يناقش الباحث الاخير السموم النباتية المسببة للذبول وكيفية حدوث الذبول فيؤكد ان توقف جريان الماء في الاوعية الخشبية قد يحدث نتيجة لانسداد الفتحات في غشاء النقرة Pit membrame الموجودة بين الاوعية المتجاورة طوليا بسبب فقاعات هوائية Embolism وليس بالضرورة نتيجة لانسداد الاوعية او امتلائها كاملة بمواد ينتجها المسبب المرضي او النبات العائل كما ان الانزيمات الحالة لجدار الخلية في الحالات المرضية تزيد من احتمال حدوث الانسداد بسبب الفقاعات الهوائية. ومن ناحية اخرى فان كميات قليلة جدا (بيكومول) Picomole من السكريات المتعددى او المركبات ذات الاوزان الجزيئية العالية تستطيع سد الثقوب في غشاء النقرة مع بقاء الاوعية ذاتها مفتوحة. وهذا ما حصل فعلا في دراستنا الحالية فأن الاوعية الخشبية ظهرت مفتوحة ولكن حدث تحطم للخلايا المجاورة لها وجدرانها ربما بواسطة انزيم البكتينيز مما نتج عنها مواد سكريه متعددة اضافة الى المواد الكلايكوبروتينية التي ينتجها الفطر (٨) التي تستطيع ان تسد فتحات النقر دون ان تسد المجرى داخل الاوعية الناقلة وبذلك تؤدي الى توقف جريان الماء في سويق الورقة وبالتالي جفاف الورقة. وطبيا لا يمكن اظهار مثل هذه الخلايا في المقاطع المحضرة للفحص المجهري الضوئي. ومما يؤكد هذا المنحى في تفسير النتائج التي حصلنا عليها هو تغيير لون الورقة (تحطم الكلوروفيل) وعدم جفافها بعد غمر السويق في الراشح المصفى بالفحم، وما رافق ذلك من عدم تحطم الخلايا البرانكيمية دلالة على جريان الماء في السويق وتدفق الجزء الحامضي من سموم الفطر هندرسونيولا توريولويدي الى نصل الورقة.

REFERENCES

[1] Wilson, E.E. The branch wilt of percian walnut and its cause. Hilgardia 17: 413-436 (1946).

[2] Al-Hassan, K.K., Al-Hassan, S.A. and Husain, F. Branch wilt of apple in Iraq. F.A.O. Plant protection bulletin 18; 115-118 (1970).

[3] كريم، خالد احمد، احسان شفيق دميرداغ وفياض محمد. ذبول أفرع اليوكالبتوس وسمية راشح مزرعة الفطر المسبب للمرض. المجلة العراقية للعلوم الزراعية. زانكو مجلد (٥) عدد (٣):١٨٣ - ١٩٣(١٩٨٧).

[4] Singh, S.M. and Barde, A.K. Hendersonula toruloidea infection of human skin and nails. Indian J.Dermatol. Venerel. Lepr. 46 (6): 350-355. (1980)

[5] Van Eijk. G.W. and Roeymans, H.J. Further naphthoquinone derivatives from the fungus Hendersonula toruloidea. Experentia 39: 513-514 (1983)

[6] Paxton, J.D. and Wilson, E.E. Analytical and physiological aspects of branch wilt disease pf percian walnut. Phytopathology 55. 21-26 (1965).

[7] القصاب، عبد المطلب رضا حيدر، احسان شفيق دميرداغ ودلاور محمد صابر. ذبول أفرع اليوكالبتوس وسمية راشح مزرعةالفطر المسبب للمرض. الجزء الثاني:- تنقية وتشخيص بعض السموم التي يفرزها الفطر هندرسونيولا. مجلة العلوم الزراعية العراقية مجلد (١٨) عدد (٢):٩٥-١٣٠(١٩٨٧).

ثم وضع مئة مل من المحلوت في كل من الدوارق المخروطية حجم ٢٥٠ مل وتم تلقيح محتويات ثلاث منها بكميات متساوية من نموات الفطر النامي على وسط مستخلص البطاطا بالاكار ولم تلقح ثلاثة اخرى ثم تركت للمقارنة. حضنت الدوارق في ٣٥°م مع الرج احيانا ولمدة عشرين يوما وبعد فترة الحضانة تم تحضير الراشح الخام وهو مزرعة الفطر المرشحة من خلال طبقة من القطن المعقم. اما الراشح المصفى بالفحم فهو مزرعة الفطر المرشحة من خلال مدة قصير من الفحم المنشط, كذلك تم ترشيح الماء المقطر ثم محلول جابكس غير الملقح (المقارنة) من خلال القطن للمقارنة بالراشح الخام وكذلك تم الترشيح من خلال الفحم المنشط للمقارنة مع الراشح المصفى بالفحم.

٣- غمر سويقات الاوراق في الراشح:- اتبعت طريقة كريم واخرون (٣) لملاحظة تأثير الرواشح على الاوراق. فقد تم الحصول على اوراق اليوكالبتوس .Eucalyptus camaldulensis L متساوية الموقع ومن شجرة واحدة وتم غمر سويق ورقة واحدة في احد التحضيرات (الراشح) المبينة في اداناه والموضوع في قنينة صغيرة واستخدمت خمسة مكررات لكل معاملة وهي:-

أ) الراشح الخام لمزرعة الفطر, ب) الراشح المصفى بالفحم لمزرعة الفطر, ج) الراشح الخام لمحلول جابكس الغذائي بدون الفطر, د) الراشح المصفى بالفحم لمحلول جابكس بدون الفطر, ه) الماء المرشح من خلال القطن, و) الماء المرشح والمصفي بالفحم. تركت المعاملات في المختبر حيث تراوحت درجة الحرارة فيه بين ٣٥°م نهارا الى ٢٥°م ليلا ولمدة يومين وخلالها سجلت الاعراض المرضية الظاهرة.

٤- تحضير مقاطع لسويق الاوراق لغرض الفحص المجهري:- اخذت قطع صغيرة من نهايات السريقات المغمورة لمدة ٢٤ ساعة في السوائل المختلفة (التحضيرات أعلاه) وثبتت لمدة يوم واحد في محلول FAA المؤلف من فورمالين ٤٠٪ (٥مل) وحامض الخليك الثلجي (٥ مل) وايثانول ٧٠٪ (٩٠مل). بعدها تم سحب الماء من القطع بواسطة تعريضها الى تراكيز متزايدة بالتدريج من الايثانول ثم طمرت في البرافين ثم قطعت بواسطة المايكروتوم الى شرائح سمكها ١٥ الى ١٧ مايكرومتر ثم استخدمت صبغة السفرانين (١غم في ١٠٠مل ايثانول ٧٠٪) لمدة ربع ساعة ثم صبغة ازرق الاليشيان Alician blue (١غم في ١٠٠مل ايثانول ٧٠٪) لمدة ربع ساعة اخرى. ثم ثبتت على الشرائح الزجاجية لغرض الفحص المجهري. وهذه الشرائح محفوظة لدى الباحث الاول في قسم علوم الحياة / كلية العلوم / الجامعة المستنصرية.

النتائج

١- الاعراض الخارجية في الاوراق:- بعد ٢٤ ساعة من غمر سويق اوراق اليوكالبتوس في الراشح الخام لمزرعة الفطر ذبلت ثم تيبست هذه الاوراق واسودت نهايات السويقات في حين ذبلت وتهدلت (بدون تيبس) الاوراق المغمورة سويقاتها في الراشح المصفي بالفحم مع ظهور احمرار في نصول الاوراق. اما الاوراق المغمورة في السوائل الاخرى (محلول جابكس بدون الفطر المرشح او المصفى بالفحم وكذلك الماء) فلم يحصل فيها اى تغيير ظاهر خلال يومين او اكثر من مدة التجربة.

٢- التشريح الداخلي لسويقات الاوراق المغمورة في الماء او في محلول جابكس الغذائي بدون الفطر:- لم نجد في المصادر المتاحة لنا وصفا او اية صورة للمقطع المستعرض لسويق ورقة اليوكالبتوس ومن خلال الفحص المجهرى تبين لنا ان الانسجة والخلايا الداخلية كانت طبيعية وبدون اي تشويه في كل من الشرائح المحضرة لسويقات الاوراق المغمورة في الماء او في المحلول جابكس بدون الفطر ويوضح الشكل رقم ١ مقطعا مستعرضا لسويق ورقة مغمورة لمدة ٢٤ ساعة في الماء حيث تظهر الخلايا الطبيعية والانسجة مرتبة بشكل كلوى ويمكن تميز طبيقات الانسجة التالية ابتداء من السطح الخارجي وكما يلي: طبقة من الكيوتكل تغطي طبقة البشرة والبشرة المؤلفة من صف واحد من الخلايا مستديرة المقطع. يلي البشرة نسيج كولنكيمي بسمك ٢-٤ خلايا مثخنة في الزوايا. ثم طبقة القشرة بسمك حوالي ١٠ خلايا برانكيمية تتخللها القنوات او الغدد الزيتية المرتبة بشكل صف واحد تحت البشرة. الجزء الاخير من القشرة بسمك ٢-٣ خلايا يتميز بكونه ذو خلايا اصغر من البقية ومضلعة في المقطع وبدون مسافات بينية وشبيهة بالالياف. تحيط طبقة القشرة احاطة كاملة بالانسجة الناقلة (الخشب واللحاء) المرتبة بشكل كلوى في وسط المقطع ويلاحظ ان نسيج اللحاء يحيط من الداخل ومن الخارج بنسيج الخشب ويتخلل نسيجي الخشب واللحاء صفوف من البرانكيما الشعاعية المؤلفة من طبقة واحدة او طبقتين وفي مركز المقطع توجد خلايا برانكيمية اعتيادية ذات مسافات بينية واضحة.

٣- صفات المقطع المستعرض لسويق الاوراق المغمورة في الراشح الخام: يوضح الشكل رقم ٢ مقطعا مستعرضا لسويق ورقة اليوكالبتوس المغمورة في الراشح الخام لمزرعة الفطر.

يوضح هذا المقطع ان خلايا البشرة وطبقات النسيج الكولنكيمي احتفظت بشكلها العام في حين تحطمت معظم الخلايا البرانكيمية في القشرة تحطمت خلايا اللحاء تحطما كاملا بحيث فقد النسيج تنظيمه الخلوى فاصبح طبقة حمراء اللون بتأثير صبغة السفرانين. اما البرانكيما الشعاعية الواقعة بين اوعية الخشب فقد تحطمت فيها بعض الخلايا وبقيت خلايا اخرى سليمة. اما الخلايا الناقلة (اوعية الخشب) في نسيج الخشب فلم تتأثر وبقيت محتفظة بشكلها الاعتيادى. وقد لاحضنا وجود ما يشبه خيوط الفطر (مايسليا) في عدد قليل جدا من هذه الخلايا اضافة الى تراكيب صغيرة شبيهه بالتايلوس Tylose دون ان تسد الوعاء.

التشريح الداخلي لسويق اوراق اليوكالبتوس المغمورة في راشح مزرعة الفطر هندرسونيولا توريولويدي Hendersonula toruloideo

*د. احسان شفيق دميرداغ **و زيدان خليف عمران
*قسم علوم الحياة / كلية العلوم / الجامعة المستنصرية، **قسم علوم الحياة/كلية العلوم/جامعة بابل، العراق
(استلم في ١٩٩٢/١٢/٢٦، قبل للنشر في ١٩٩٣/٥/٨)

ABSTRACT

Petioles of Eucalyptus camaldulensis leaves were immersed in crude culture filtrate of the fungus Hendersonula toruloidea. This treatment caused wilting and drying of the leaves during one day of treatment. Light microscopic examintaion of the cross sections of petioles showed destruction of the phloem and paranchyma tissues, whereas the xylem vessels remained safe except for very few mycelial pieces. On the other hand, tissues of the petiole immersed in charcoal clarified culture filtrate were much less affected and were almost similar to those immersed in water. Such leaves showed some discoloration and wilted slightly but did not dry during the two days of treatment. The problem of water movement in the vessels and wilting of shoots were discussed in the view of the present and other published results. The conclusion is that vessels may remain unharmed but pits may be closed leading to the drought.

الخلاصة

تم غمر سويق اوراق اليوكالبتون Eudalyptus camaldulensing في الراشح الخام لمزرعة الفطر هندرسونيولا Hendersonula toruloidea فسبب ذلك تيبس الاوراق خلال يوم واحد. ومن خلال الفحص المجهري للمقاطع المستعرضة لهذه السويقات تبين تحطم انسجة اللحاء والبرانكيما في حين بقيت الاوعية الخشبية الناقلة للماء سليمة عدا ظهور نموات قليلة جدا من مايسليا الفطر. اما الانسجة في السويق المغمور في الراشح المصفى بالفحم فقد كانت اقل تأثيرا وأشبه ما يكون بالسويق المغمور في الماء كما ان الاوراق المعاملة احمرت وبقيت ذابلة بدون تيبس خلال تعريضها لمدة يومين الى الراشح. تمت مناقشة اسباب توقف جريان الماء في الاوعية الخشبية وذبول الاوراق على ضوء النتائج الحالية والابحاث المنشورة الاخرى. وما توصلنا اليه هو ان الاوعية قد تبقى سليمة ولكن النقر Pits قد تسد فتؤدي الى الجفاف.

المقدمة

يعد الفطر هندرسوليولا توربولويدى Hendersonula toruloidea Nattras من الفطريات الناقصة الذي يصيب عددا كبيرا من العوائل النباتية ويسبب امراض ذبول الافرع في الجوز (١) وفي التفاح (٢) وفي اليوكالبتوس (٣) وبعض سلالات هذا الفطر يصيب الاقدام والاصابع الملوثة في الفلاحين (٤) وان احد هذه السلالات تنتج مشتقات الكوينون (٥) وقد درس باكستون وويسلون (٦) مقاطع تشريحية لاغصان الجوز المصاب المصاب فاوضحا وجود بعض هايفات الفطر داخل الاوعية الناقلة ووجود تضخمات تايلوسية Tylose تسبب انسداد الاوعية تؤدي الى ذبول الافرع كما بين وجود الانزيم الحال للبكتين Pectinase وانزيمات اخرى في راشح مزرعة الفطر ولكنهما لم يكتشفا مواد سامة للنبات. وعلى عكس ذلك اظهرت الدراسات السابقة في العراق (٣، ٧، ٨) ان راشح مزرعة الفطر يحتوي على مركبات سامة للنبات تسبب ذبول الافرع والاوراق المغمورة فيها الا ان هذه الدراسات لم تقدم دراسة تشريحية توضح تأثير راشح مزرعة الفطر او هذه السموم على النسيج الداخلي للاوراق او الافرع الذابلة. لهذا السبب قمنا بهذه الدراسة على امل توضيح هذه العلاقة تتفهم ادق لأسباب حدوث الذبول والتيبس.

المواد وطرائق العمل:-

١- عزل الفطر واثماره:- في موقع جامعة بابل تم تشخيص حالة ذبول الافرع في شجرة مشمش وفيها الاعراض المرضية المألوفة وتم عزل الفطر من طبقة البريدرم في الساق وزرعه على وسط مستخلص البطاطا بالاكار (٢٠٠ غرام بطاطا مقشرة + ٢٠غرام اكار + ٢٠ غم دكركوز في لتر واحد من الماء) وحضنت الاطباق في ٣٤ الى ٣٦ درجة وبعد اسبوع تم فحص الفطر للتأكد من التشخيص اعتمادا على بحث ويلسون (١) وعلى الخبرة السابقة عن هذا الفطر (٣ و٧) وتم تجديد المزرعة [illegible] بانات جديدة من الوسط الغذائي ذاته.

٢- تحضير راشح مزرعة الفطر (الراشح الخام والراشح المصفى بالفحم):- تم تحضير محلول جابكس السائل لأنماء الفطر فيه ومؤلف من المواد الاتية مذابة في لتر من الماء المقطر: سكروكز (٣٠غم) ونترات الصوديوم (٢غم) وكبريتات المغنيسيوم (٠،٥غم) وكلوريد البوتاسيوم ٠،٥غم وفوسفات البوتاسيوم القاعدية K_2HPO_4 (١غم) وكبريتات الحديديك (٠،٠١غم) وتم تصحيح الاس الهيدروجيني بالمحلول الى درجة التعادل PH ٧ بعدها تم التعقيم في الاوتوكليف.

REFERENCES

[1] Al-Zubaidy, B.A. Studies on the biology of the ascarid parasites of dogs and cats. Ph.D. thesis, University of Norht Wales, Bangor. U.K., (1980).

[2] Barriga, O.O. and Myser, W.C. Effects of irradiation on the biology of the larvae of T. canis in the mouse. J.Parasitology, 73, 89-94, (1987).

[3] Beaver, P.C. Toxocariasis (visceral larvae migrans) in retation to tropical eosinophilia. Bulletin de la Societe de Pathologie Exotique, 55, 555-576, (1962), (cited by Al-Zubaidy 1980).

[4] Bilindseel, E. Immunity of Ascaris suum. 2-Investigation of the fate of larvae in immune and non immune mice. Acta Pathologiz Microbiologica Scandinavia, 77, 223-334, (1969), (cited by Al-Zubaidy 1980).

[5] Brambell, M.R. Effects of the age of infestation and the immunity of the host on the distribution of Nippostrongylus brasiliensis in the small intestine of rats. Parasitology, 53,7p., (1963).

[6] Lee, H.F. Effects of super-infection on the behaviour of T.canis larvae in mice. J. of Parasitol., 46, 583-588., (1960).

[7] McCoy, O.R. Artifical immunization of rats against Trichinella spiralis. Am. J. of Hyg., 21, 200., (1935).

[8] Oliver-Ganzales, J. Antigenic analysis of the isolated tissues and body fluids of the round worm Ascaris lumbricoides Var. Suum. Journal of infectiorus Disease, 72, 202-212, (1943).

[9] Olson, L.J. Organ distribution of T. canis in normal mice and mice infected previously with Toxocara, Ascaris of Trichinella. Texas Rep. Biol. Med., 27, 651-657. , (1980).

[10] Sprent, J.F.A. and Chen, H.H. Immunological studies in mice infected with the larvae of A. lumbricoides. 1 Citeria of immunity and immunizing effect of isolated worm tissues. J. Infectious Diseases, 84, 111-123, (1950)

[11] Sprent, J.F.A. The fife history and development of T. cati (Schrank, 1788) in the domestic cat. J. Parasitology 46. 54-78, (1956).

[12] Stoll, N.R. Induction of self-cure and protection, with special reference to experimental vaccination against Haemonchus. Rice Institute Pamphlets, 45, 184, (1958).

[13] Taliaferro, W.H. Antigen-antibody reactions in immunity to metazoan parasites. Proceeding of the institute of Mediciene, Chicago, 14, 358-363, (1943).

[14] Taliaferro, W.H. The inhibition of reproduction of parasites by immune factors. Bactriological Review, 12, 1-17, (1948) (cited by Al Zubaidy 1980).

[15] Tromba, F.G. Immunization of pigs against experimental A. suuminfection by feeding ultra violet-attenuated eggs. J. parasitol., 64, 651-656, (1978).

[16] Urban. J.F. and Tromba, F.G. Development of immune responsiveness to A. suum antigens in pigs vaccinated with ultra violet attenuated eggs. Vet. Immunol. Immunopathol., 3, 399-409, (1982).

الخمج وفي الرئتين 67 يرقة في اليوم الثاني وفي الجسد 71 يرقة في اليوم السابع بعد الخمج. وبلغ المجموع الكلي لليرقات 545 يرقة وقد سجل موت فأرين في هذه التجربة. اما عداد اليرقات في الايام والاعضاء المماثلة في فئران مجموعة السيطرة فكانت في الكبد 154 يرقة والرئتين 134 يرقة والجسد 126 يرقة والمجموع الكلي لليرقات في اعضاء الجسم 957 يرقة وقد لوحظت زيادة في حجم في حجم الطحال والكبد والعقد اللمفاوية الابطية والفخذية مع ظهور اضرار lesions على الكبد والرئتين في الفئران الممنعة وفئران السيطرة الا انها كانت في الفئران الممنعة اقل حجما وعددا. شكل 5، 6، 7، 8 .

المناقشة

لم يظهر ان تمنيع الفئران بالبيوض المشعة بالاشعة فوق البنفسجية عن طريق حقنها تحت الجلد subcutaneous بمستضد مستخلص جسم الديدان whole worms antigen تأثير في تغيير سلوك هجرة يرقات طفيلي T. cati في الاعضاء المختلفة للفئران المخمجة وهذا لا يتفق مع ** : Brambell * حيث ذكر الاول بأن اليرقات والادوار الباغة للطفيليات المختلفة تميل الى الهجرة لمواقع غريبة في المضيف الممنع يختلف عن سلوك هجرتها الطبيعية في المضائف. وذكر الباحث الثاني بأن يرقات T. cati في الفئران الممنعة تغير من سلوك هجرتها بالمقارنة مع مجموعة السيطرة.

من طرق التعبير عن تكوين مناعة ضد اليرقات الطفيلية التي تغزو جسم المضيف الممنع، هي اما منع اليرقات من اختراق مخاطية الامعاء والهجرة داخل الاحشاء وبالنتيجة تطرح مع الغائط، او موت هذه اليرقات داخل انسجة المضيف بعد فترة قصيرة من اختراقها لمخاطية الامعاء، وقد تتأخر اليرقات في هجرتها او يتغير سلوك هجرتها في الفئران الممنعة مقارنة بفئران مجموعة السيطرة الامر الذي يؤدي الى استهلاك اليرقات للخزين الغذائي وبالتالي تسمح لاستجابات المضيف بقتلها او احاطتها بمحفظة capusle.

وقد استخدمنا في هذا البحث مقارنة اعداد اليرقات في اعضاء الفئران الممنعة وغير الممنعة كطريقة للدلالة على ظهور مقاومة للخمج بيرقات طفيلي T. cati وهو نفس المعيار الذي استخدمه كل من Lee (1960) Olson; (1990) في دراستهما على طفيلي اسكارس الكلاب (15) T. canis في دراستهم على طفيلي اسكارس الخنزير A. suum.

توفر النتائج التي تم الحصول عليها في هذه الدراسة دليلا يؤكد ان اعطاء الفئران بيوض ناضجة مشعة بالاشعة فوق البنفسجية ultraviolet عن طريق الفم هي طريقة فعالة في حث جسم المضيف على تكوين استجابة مناعية. كما يظهر ايضا ان مستوى الحماية / الوقاية التي تكونت لها علاقة بعدد البيوض المشعة او بعدد الجرعات المعطاة لها. وهذا يتضح من مقارنة معدل نسب الاختزال (12,21٪، 39,86٪) في الفئران الممنعة بجرعة واحدة او جرعتين على التوالي. وهذا يتفق مع ما وجده (Lee, 1960) حيث بين بأن اعطاء جرعات صغيرة من بيوض T. canis الى الفئران قد حفزها على تكوين مناعة ضد هذه اليرقات وذلك بتأثيرها على عدد اليرقات المستخلصة من انسجة المضيف.

وذكر الباحث Tromba (***) بأن الخنازير الممنعة ببيوض اسكارس الخنزير A. suum المعرضة للاشعة فوق البنفسجية ولدت مستوى عالي من المناعة ضد هذا الطفيلي. واشار Al-Zubaidy (***) بأن بيوض طفيلي T. canis المعرضة للاشعة فوق البنفسجية لمدة (5) دقائق تبقى حية لمدة ايام فقط، وانها قادرة على الفقس في المعي وتبدأ الهجرة لكنها تموت بعد ذلك. ان هذه اليرقات تبقى حية لمدة كافية لتحفز جسم المضيف على تكوين اجسام مضادة antibodies موجهة ضدها او ضد نواتجها الايضية.

وحصل Urban & Tromba (16) على (88٪) اختزال في عدد يرقات A. suum من الرئتين بعد (7) ايام من جرعة التحدي challenge dose ووجد Barriga & Myser (2) بان تشعيع يرقات الدودة T. canis بالاشعة السينية (X-ray) يؤدي الى اختزال امراضيتها، تثبيط هجرتها من الكبد والرئتين.

ان الاستجابة المناعية immune response للمضيف ضد الديدان المدورة Nematoda الطفيلية قد تعمل ضد المراحل اليرقية او البالغة بطرق مختلفة فالديدان البالغة قد يتم طردها من الامعاء او تحطم في الانسجة ولكن في بعض الحالات فان الاستجابة المناعية قد تسبب توقف النمو او التداخل في قدرات وضع البيض.

تشير نتائجنا بأن استعمال مستخلص الديدان البالغة كمستضدات تعطى تحت الجلد subcutaneous تثير استجابة مناعية فعالة تظهر في اختزال عدد اليرقات في الكبد والرئتين والجلد كما يظهر ان اعطاء اكثر من جرعة واحدة يؤدي الى اختزال اكبر في عدد اليرقات.

نتائج مماثلة حصل عليها Blindseil (4) عند دراسته على طفيلي اسكارس الخنزير A. suum حيث بين وجود اختلافات معنوية في اعداد اليرقات المتسخلصة من الكبد والرئتين في الفئران الممنعة بمستضدات الديدان البالغة بالمقارنة مع فئران مجموعة السيطرة.

كما بين Al-Zubaidy (1) ان جرعة تمنيع واحدة في الفئران بمستخلص الدودة البالغة T. canis غير كاف لاثارة المناعة الواقية ضد جرعة التحدي. ومن ناحية اخرى اذا استلمت هذه الفئران جرعتين بينها (14) يوما قبل جرعة التحدي تتكون لديها مناعة واقعية بشكل افضل.

ان درجات الوقاية التي توفرها مستخلصات الديدان في تجارب مختلفة كانت متباينة الى حد كبير. بعض الباحثين لم يجد وقاية (Sprent & Chen, 10, Taliaferror, 1943, 1948; Oliver-Ganzalez, 8) بينما ذكر اخرون ظهور مناعة واقية جزئية (MoCoy, 7, Stoil, 12).

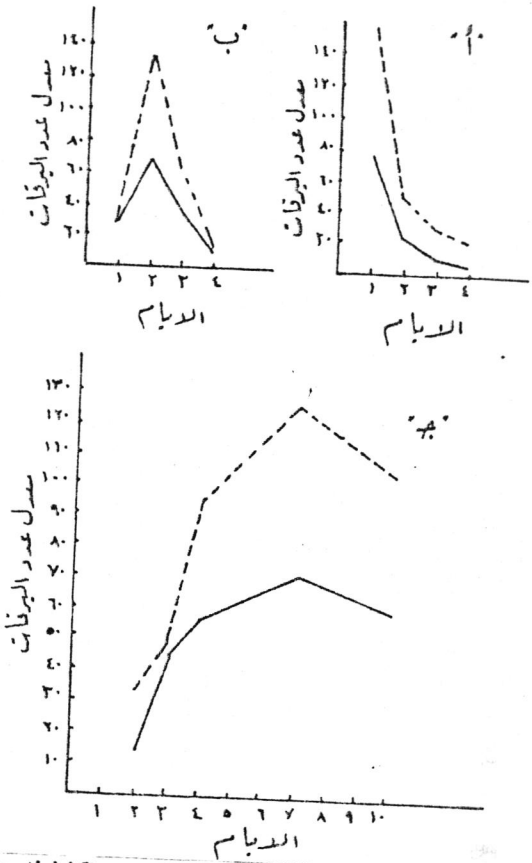

شكل(٥) نمط الهجرة ومعدل عدد يرقات طفيلي اسكارس القطط T. cacti في الفئران الممنعة(—) بجرعة واحدة مقدارها ٢ ملغم من مستخلص الديدان البالغة وفي فئران مجموعة السيطرة(----) في الاعضاء: أ-الكبد ب-الرئتين ج-الجسد

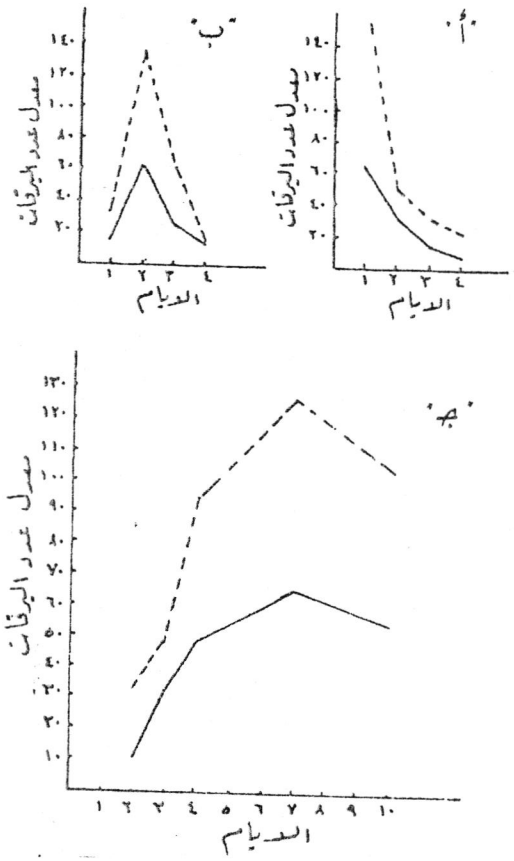

شكل(٧) نمط الهجرة ومعدل عدد يرقات طفيلي اسكارس القطط T. cacti في الفئران الممنعة(—) بجرعتين(٢ +١ملغ) من مستخلص الديدان بالمقارنة مع فئران مجموعة السيطرة(----) في الاعضاء: أ-الكبد ب-الرئتين ج-الجسد

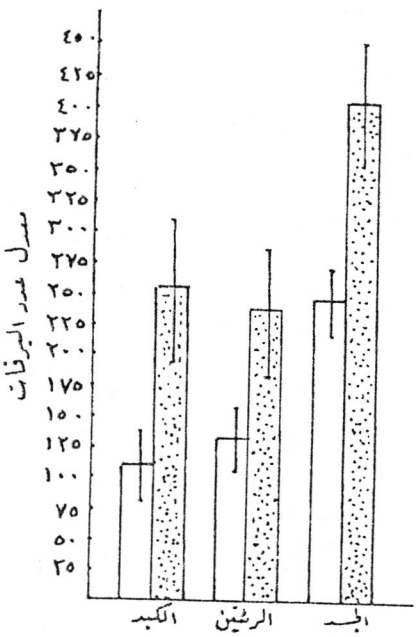

شكل(٦) الاختزال في مجموع معدل اعداد يرقات T. cacti في اعضاء الفئران الممنعة ب ٢ ملغم من مستضد مستخلص جسم الدودة اعلاه مقارنة بفئران مجموعة السيطرة. □المجموعة الممنعة □ مجموعة السيطرة

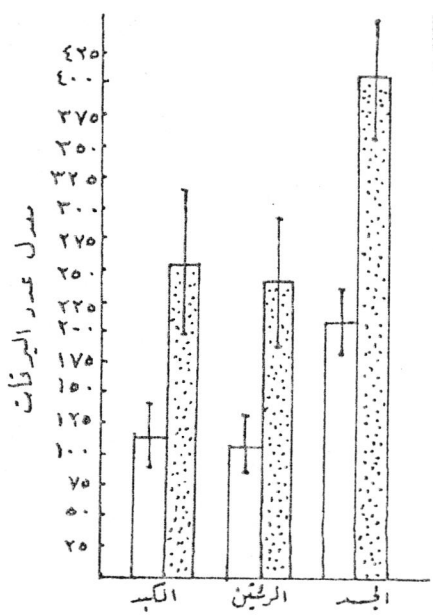

شكل(٨) الاختزال في مجموع معدل اعداد يرقات T. cacti في اعضاء الفئران الممنعة ب ٢ ملغم من مستضد مستخلص جسم الدودة "جرعة اولى" و١ملغم من المستضد"جرعة تقوية"مقارنة بمجموعة السيطرة. □المجموعة الممنعة □مجموعة السيطرة

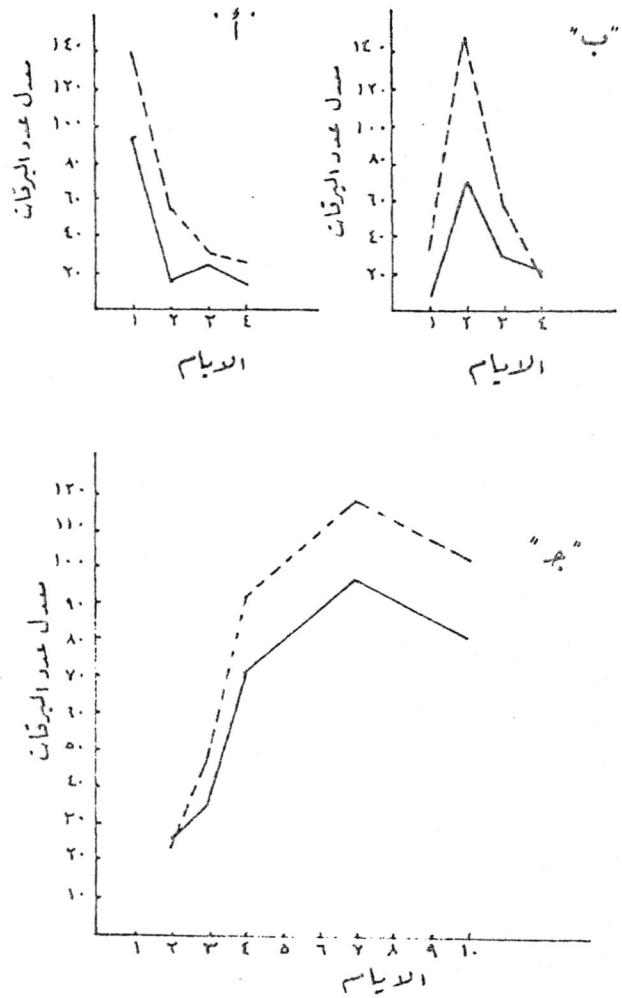

شكل(١) نمط الهجرة ومعدل عدد يرقات طفيلي اسكارس القطط T. cacti في الفنران الممنعة(___) بجرعة واحدة ٢٥٠ بيضة ناضجة مشعة بالاشعة فوق البنفسجية وفي فنران مجموعة السيطرة(----) في الاعضاء: أ-الكبد ب-الرئتين ج-الجسد

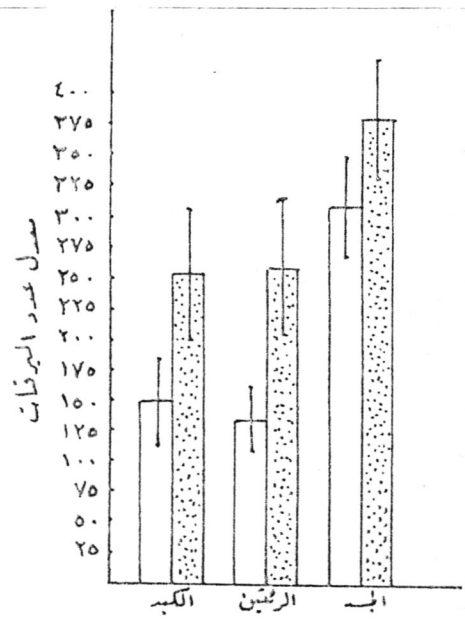

شكل(٢) يوضح الاختزال في مجموع معدل اعداد يرقات T. cacti في اعضاء الفنران الممنعة ب ٢٥٠ بيضة ناضجة مشعة للطفيلي المذكور اعلاه مقارنة مع مجموعة السيطرة. ▯المجموعة الممنعة ▯ مجموعة السيطرة

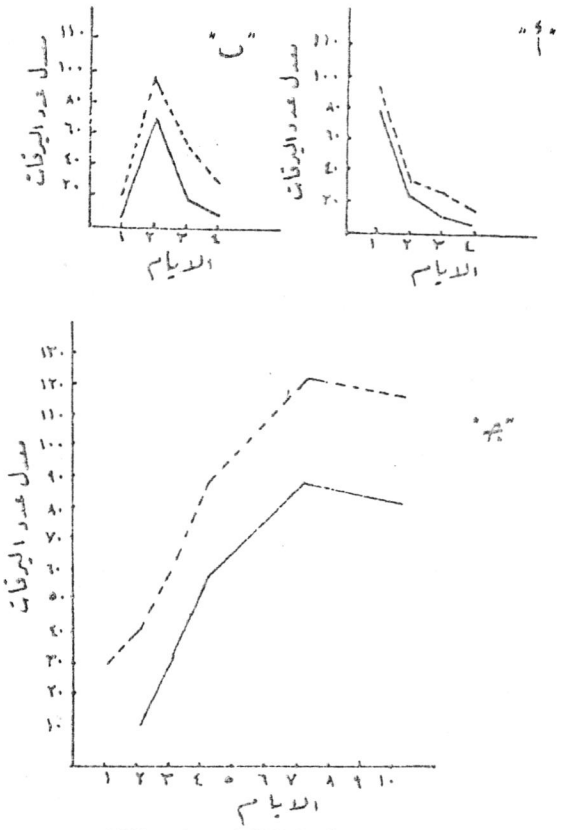

شكل(٣)نمط الهجرة ومعدل عدد يرقات طفيلي اسكارس القطط T. cacti في الفنران الممنعة(___) بجرعتين(٢٥٠ +١٠٠بيضة ناضجة مشعة بالاشعة فوق البنفسجية UV) وفنران مجموعة السيطرة(----) في الاعضاء: أ-الكبد ب-الرئتين ج-الجسد

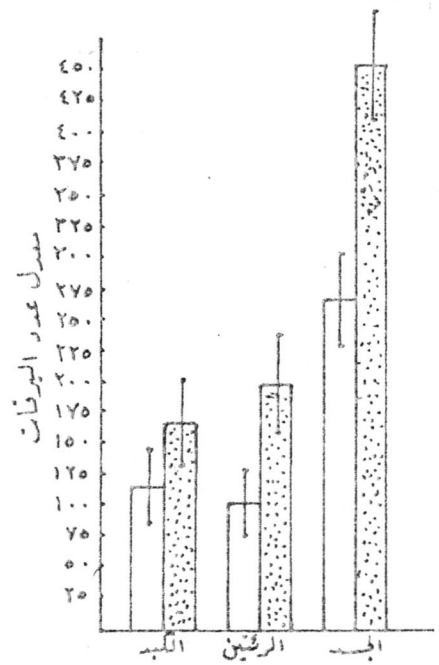

شكل(٤) الاختزال في مجموع معدل اعداد يرقات T. cacti في اعضاء الفنران الممنعة ب ٢٥٠ بيضة ناضجة مشعة "جرعة اولى"ر"١٠٠"بيضة ناضجة مشعة "جرعة تقوية" مقارنة بمجموع معدل اليرقات في مجموعة السيطرة. ▯المجموعة الممنعة ▯ مجموعة السيطرة

من جسم الدودة البالغة او باستخدام بيوض خمجة مضعفه بواسطة الاشعة فوق البنفسجية U.V.

المواد وطرق العمل

تم الحصول على الديدان البالغة من القطط السائبة باعمار مختلفة. ثم استخلصت البيوض من اثاث الديدان. ثم حفظت في محلول حامض الكبريتيك H_2SO_4 عيارية 0.1 N. تنمى البيوض في هذا المحلول بدرجة حرارة ٢٨م لمدة ثلاث اسابيع ثم خمجت الفئران بواسطة حقنة المعدة Stomach tube بعدها قتلت الفئران وتم تشريحها وفي الايام التالية اوحظت الاعضاء التالية, الكبد, الرئتين والعضلات والعظام والتي سميت بالجسد carcass. لقد تم تقطيع هذه الاعضاء الى اجزاء صغيرة, بعدها تم هضمها بواسطة انزيم البيسين الحامض بدرجة حرارة ٣٧م حسب طريقة (11). ثم حسبت اليرقات المهاجرة الى الاعضاء المذكورة.

تم تشعيع البيوض الناضجة (الخمجة) للطفيلي بالاشعة فوق البنفسجية باستخدام جهاز توليد الاشعة فوق البنفسجية اعتمادا على طريقة الزبيدي (١) بطول موجي مقداره ٢٥٤ نانوميتر وعلى مسافة ١٥سم لمدة خمس دقائق.

اما تحضير المستضد فقد استخلص من جسم الدودة البالغة Whole worm antigen التي تم تجفيفها باستخدام جهاز Lyophilizar ثم اذيب المسحوق المجفف في محلول الفوسفيت المنظم Phosphate buffer saline ذات رقم هيدروجيني PH مساو الى (٧،٢) وقد حضر الانتجين بتركيزين هما ١٦ملغم/سم٣ و٨ملغم/سم٣. ولقد صممت تجارب التمنيع وكما يلي:-

١) التجربة الاولى:- لدراسة هجرة اليرقات في الفئران البيضاء الممنعة بالبيوض المشعة بالاشعة فوق البنسفجية ثم استخدام ٨٤ فأرا قسمت الى اربع مجاميع.

المجموعة الاولى (٣٠ فأرا) اعطيت ٢٥٠ بيضة مشعة وبعد مرور ١٤ يوما اعطيت جرعة التحدي المكونة من ١٠٠٠ بيضة خمجة. قتلت الفئران وشرحت وتم هظم اعضائها في الايام ١, ٢, ٣, ٤, ٧ و١٠ بعد اعطاء جرعة التحدي واستخلصت اليرقات وتم دراسة نمط هجرتها وبمعدل ٥ فئران يوميا.

اما المجموعة الثانية فتمثل مجموعة السيطرة وتتكون من ١٢ فأرا. المجموعة الثالثة تتكون من ٣٠ فأرا اعطيت ٢٥٠ بيضة مشعة كجرعة اولى وبعد مرور ٢١ يوما اعيت جرعة التقوية boosterdose وكانت ١٠٠ بيضة مشعة وبعد ٧ ايام اعطيت جرعة التحدي المكونة من ١٠٠٠ بيضة. قتلت الفئران كما مر سابقا وبمعدل ٥ فئران لكل مجموعة. اما مجموعة السيطرة فكانت تتكون من ١٢ فأرا خمجت وذبحت كما مر اعلاه وبمعدل ٢ فأرا يوميا.

٢)) التجربة الثانية:- صممت هذه التجربة لدراسة نمط هجرة يرقات الطقيلي في الفئران الممنعة بمستضد مستخلص من جسم الدودة. تم استخدام ٧٢ فأر ابيض قسمت الى ثلاثة مجاميع:- المجموعة الاولى تتكون من ٣٠ فأرا حقن كل واح منها تحت الجلد جرعة اولى تحتوي على ٢ ملغم من المستضد الممزوج مع محلول Complete fluid adjuvent بنسبة ١:١ وبعد مرور ١٤ يوما اعطيت جرعة التحدي المكونة من ١٠٠٠ بيضة خمجة ثم جرى قتل وتشريح الفئران كما مر سابقا وبمعدل ٥ فئران يوميا. اما المجموعة الثانية فتتكون من ٣٠ فأرا ابيضا حقن كل واحد منها بجرعة حاوية ٢ ملغم من المستضد المستخلص من جسم الدودة ممزوج مع Complete fluid adjuvent بنسبة ١:١ وبعد مرور ٢١ يوما حقنت الفئران تحت الجلد بجرعة التقوية التي تحتوي على ١ملغم من المستضد الممزوج مع محلول Incomplete fluid adjuvect. وبعد مرور ٧ ايام اعطيت جرعة التحدي الحاوية على ١٠٠٠ بيضة خمجة. ثم جرى قتل وتشريح الفئران كما مر سابقا وبمعدل ٥ فئران يوميا.

اما المجموعة الثالثة فتتكون من ١٢ فأرا تمثل مجموعة السيطرة للمجموعتين الاولى والثانية. اعطيت الفئران ١٠٠٠ بيضة خمجة لكل منها وقتلت وشرحت في الايام ١, ٢, ٣, ٤, ٧, ١٠ بعد اعطاء جرعة التحدي لحساب اعداد اليرقات المستخلصة من الاعضاء المختلفة وبمعدل ٢ فأر يوميا.

النتائج

أ- لم يظهر تغيير في نمط هجرة اليرقات في الفئران الممنعة بالبيوض المشعة واعلى عدد من اليرقات سجل في الكبد (٩٣ يرقة) في اليوم الاول وفي الرئتين ٧١ يرقة في اليوم الثاني وفي الجسد (٩٦ يرقة) في اليوم السابع بعد الخمج اما المجموع الكلي لليرقات المستخلصة من كل اعضاء جسم الفأره فكان ٦١١ وسجل هنا موت فأرين بعد اعطاء جرعة التحدي. في مجموعة السيطرة سجل ١٤٠ يرقة في الكبد ١٤٨ يرقة في الرئتين ١١٨ يرقة في الجسد وكان مجموع اليرقات الكلي ٧٥٣ يرقة نسبة الاختزال كانت ١٢،٢١٪ محسوبة ب P_s = Student test ٠،٠٥ شكل ١, ٢

اما في الفئران الممنعة بجرعتين من البيوض المشعة فقد سجل اعلى عدد من اليرقات في الكبد ٧٨ يرقة في اليوم الاول. وفي الرئتين ٦٩ يرقة في اليوم الثاني والجسد ٨٨ يرقة في اليوم السابع بعد الخمج وقد بلغ المجموع الكلي في اعضاء جسم الفأر ٥٣١ وقد سجل موت فأرين في هذه التجربة. اما في مجموعة السيطرة فقد سجل في الكبد ٩٢ يرقة والرئتين ٩٧ يرقة والجسد ١٢١ يرقة واما المجموع الكليلليرقات فقد بلغ ٨٨٣ يرقة. نسبة الاختزال في مجموع اليرقات ٣٩،٨٦٪ بالمقارنة مع مجموعة السيطرة (p = ٠،٠٥) شكل ٣, ٤ .

ب - في الفئران الممنعة بمستضدات مستخلصة من جسم الديدان البالغة.

عند التمنيع بجرعة واحدة لم يظهر تغيير في نمط هجرة اليرقات. اعلى عدد من اليرقات سجل في الكبد ٧٤ يرقة في اليوم الاول بعد

محاولة تمنيع الفئران ضد الاصابة ببرقات دودة Toxocara cati باستعمال بيوض الطفيلي المشعة بالاشعة فوق البنفسجية او انتيجين الدودة البالغة

*برهان عبد اللطيف **، ابراهيم شعبان داود **و صلاح شكر محمود العزاوي
*قسم علوم الحياة / كلية العلوم / الجامعة المستنصرية، **قسم علوم الحياة/كليةالتربية ابن الهيثم، العراق
(استلم في ١٩٩١/٧/١٥، قبل للنشر في ١٩٩٢/٧/٤)

ABSTRACT

The behavior of larvae migration in the UV-immunized mature eggs of mice organs did not change when irradiated through one or two mouth dose for 5 min. Same results were obtained by one or two subcutaneous doses of antigens of the adult worms extract. Comparing with the control groups, total number of the extorted larvae from the immunized mice was reduced. Reduction of 12.2%(p=0.05) was recorded in case of 250 mature eggs immunization, 39,86% when immunized by two doses; first by 250 irradiated mature eggs then after 21 days by 100 irradiated eggs . Percent of 43.05%(p=0.05) was obtained for 2 mg antigen immunization. When immunization was applied by two doses (2 and 1 mg), 50,57% (p=0.05) was obtained. Degree of protection was found to be depending on the type of antigen, method of injection and number of doses

الخلاصة

لم يتغير سلوك هجرة اليرقات في اعضاء الفئران الممنعة بالبيوض الناضجة المشعة بالاشعة فوق البنفسجية لمدة خمس دقائق (بجرعة واحدة او جرعتين) عن طريق الفم وكذلك بالمستضدات من مستخلص الديدان البالغة (الذكور والاناث) بجرعة واحدة او جرعتين عن طريق حقنها تحت الجلد Subcutaneous بالمقارنة مع مجموعة السيطرة في كل حالة. هنالك اختزال في مجموع اليرقات المستخلصة من الفئران الممنعة بالمقارنة مع مجموعات السيطرة وقد بلغ الاختزال (١٢،٢٪) (p = ٠،٠٥) في حالة التمنيع ب ٢٥٠ بيضة ناضجة, (٣٩,٨٦٪) في حالة التمنيع بجرعتين الاولى ٢٥٠ بيضة ناضجة مشعة تليها بعد ٢١ يوما ١٠٠ بيضة مشعة كجرعة تقوية, (p = ٠،٠٥)،(٤٣،٠٥٪) في حالة التمنيع ب ٢ ملغم من مستضد الديدان (p = ٠،٠٥)، (٥٠،٥٧٪)في حالة التمنيع بجرعتين, الاولى ٢ ملغم والثانية ١ ملغم كجرعة تقوية من مستضد مستخلص الديدان (p = ٠،٠٥). ان درجة الوقاية (الحماية) تعتمد على نوع المستضد antigen وطريقة الحقن وعدد الجرعات.

المقدمة

ان دودة Toxocara cati هي دودة اسكارس القطط والعائلة القطية. تعيش اثناء البلوغ في امعاء القطط اما الاطوار اليرقية فقد تصيب عدد كبير من الحيوانات او المضاعف التي تسمى بالمضائف غير الطبيعية Paratenic hosts كالدجاج والاغنام والابقار وحتى الحشرات والانسان وكذلك القوارض والفئران وديدان الارض. تصاب القطط نتيجة لافتراسها الفئران والقوارض المخمجة وغيرها من المضائف العرضية (نفس المصدر). اما الانسان فتنتقل له الاصابة نتيجة لاخذ البيوض الخمجة مع الاكل والشراب الملوث بالبيوض بصورة مباشرة او كيرقات موجودة من خلال سلسلة الغذاء.

بيضة الدودة شبه كروية يبلغ حجمها ٦٥ X ٧٠ مايكرون, تنتج الدودة الانثى حوالي ٢٠٠،٠٠٠ بيضة يوميا. للبيضة القابلية على مقاومة الظروف البيئية كالجفاف ودرجات الحرارة, الا انها حساسة للضوء وخاصة الاشعة فوق البنفسجية.

تنمو في التربة عند توفر الظروف الملائمة من درجة حرارة ورطوبة نسبية الى الطور الخمج وتبقى حية لعدة سنين. وعند ابتلاع البيضة الخمجة تفقس في المعدة والامعاء وتهاجر هجرة جسمية في جسم القطط تعود بعدها الى الامعاء لتنمو لبلوغ الجنسي. اما في المضائف غير الطبيعية ومنها الانسان فانها تهاجر هجرة احشائية تائهة لا تعود اليرقات بعدها الى الامعاء وانما تبقى في انسجة واعضاء الجسم كالكبد والرئتين, الكليتين, الطحال وعضلات الجسم مسببة داء اليرقات الحشوية المهاجرة (Visceral larva migrans, VLM) وتظهر اعراض مرضية مختلفة تبعا لموقعها في اعضاء الجسم وتكون الاصابة اكثر انتشارا في الاطفال الذي تتراوح اعمارهم بين (١-٦) سنوات (3).

في هذا البحث سنحاول التعرف على اهمية التمنيع في الوقاية من الخمج او التخفيف من شدته في المضائف غير الطبيعية (الناقلة) Paratenic hosts متمثلة بالفئران باستخدام مستضدات مستخلصة

مجلة علوم المستنصرية

تعليمات النشر

١. تقوم المجلة بنشر البحوث الرصينة التي لم يسبق نشرها في مكان اخر بعد اخضاعها للتقويم العلمي من قبل مختصين وبأي من اللغتين العربية او الانجليزية.

٢. يقدم الباحث او الباحثون طلبا تحريريا لنشر البحث في المجلة على ان يكون مرفقا بثلاث نسخ من البحث مطبوعة على الالة الكاتبة بترك فراغين (double space) بين سطر واخر على ورق ابيض قياس (A4) من النوع الجيد وتترك مسافة (٢,٥) سم على جانبي كل صفحة.

٣. يطبع عنوان البحث واسماء الباحثين (كاملة) وعناوينهم باللغتين العربية والانجليزية على ورقة منفصلة شرط ان لاتكتب اسماء الباحثين وعناوينهم في اي مكان اخر من البحث وتعاد كتابة عنوان البحث فقط على الصفحة الاولى من البحث.

٤. تكتب اسماء الباحثين كاملة بحروف كبيرة (capital) في حالة استخدام اللغة الانجليزية وكذلك الحروف الاولى فقط من الكلمات (عدا حروف الجر والاضافة) المكونة لعنوان البحث، وتكتب عناوين الباحثين بحروف اعتيادية صغيرة (small letters).

٥. تقدم خلاصتان وافيتان لكل بحث، احداهما بالعربية والاخرى بالانجليزية وتطبع على ورقتين منفصلتين بما لايزيد على (٢٥٠) كلمة لكل خلاصة.

٦. تقدم الرسوم التوضيحية منفصلة عن مسودة البحث، وترسم على ورق شفاف (tracing paper) بالحبر الصيني الاسود، وترفق ثلاث صور لكل رسم وتكتب المعلومات عنها على ورقة منفصلة، ولايجوز تكرار المعلومات ذاتها في الرسوم والجداول في وقت واحد الا اذا اقتضت ضرورة المناقشة ذلك.

٧. يشار الى المصدر برقم يوضع بين قوسين بمستوى السطر نفسه بعد الجملة مباشرة وتطبع المصادر على ورقة منفصلة، ويستخدم الاسلوب الدولي المتعارف عليه عند ذكر مختصرات اسماء المجلات.

٨. يفضل قدر الامكان تسلسل البحث ليتضمن العناوين الرئيسة الاتية: المقدمة، طرائق العمل، النتائج والمناقشة، الاستنتاجات، المصادر، وتوضع هذه العناوين دون ترقيم في وسط الصفحة ولايوضع تحتها خط وتكتب بحروف كبيرة عندما تكون بالانجليزية.

٩. يتبع الاسلوب الاتي عند كتابة المصادر على الصفحة الخاصة بالمصادر، ترقم المصادر حسب تسلسل ورودها في البحث، يكتب الاسم الاخير (اللقب) للباحث او الباحثين ثم مختصر الاسمين الاولين فعنوان البحث، مختصر اسم المجلة، المجلد او الحجم، العدد، الصفحات، (السنة). وفي حالة كون المصدر كتابا يكتب بعد اسم المؤلف و المؤلفين عنوان الكتاب، الطبعة، الصفحات، (السنة)، الشركة الناشرة، مكان الطبع.

مجلد : ٦ سنة : ١٩٩٥

رقم الايداع في دار الكتب والوثائق ببغداد ٢٧٨ لسنة ١٩٩٠

الجامعة المستنصرية
كلية العلوم

مجلة
علوم المستنصرية

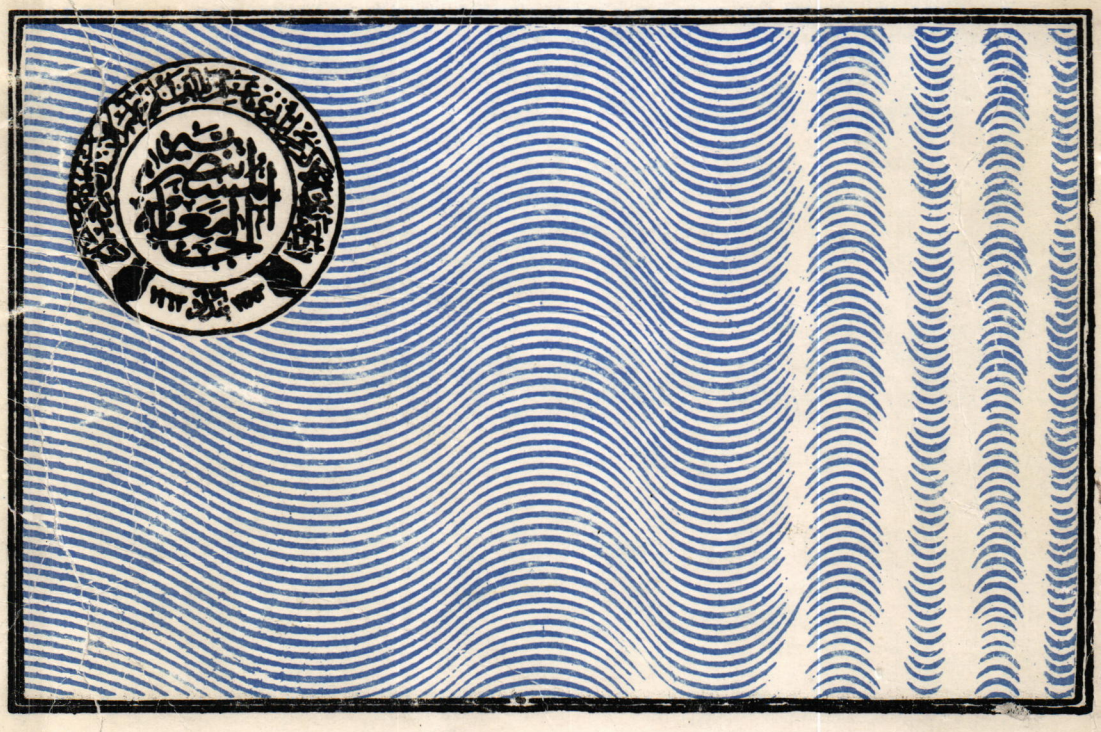

مجلة علمية دورية تصدرها كلية العلوم في الجامعة المستنصرية

تعنون كافة المراسلات الى : سكرتير هيئة تحرير مجلة علوم المستنصرية
كلية العلوم - الجامعة المستنصرية
الوزيرية - بغداد - جمهورية العراق
تلكس : ٢٥٦٦ (مسباد - عراق)
هاتف : ٤١٦٨٤٩١ أو ١-٤١٦٨٥٠٠ (بدالة) خط ٢٧٦